# Mechanisms of cell fate and chromatin plasticity during early mouse embryogenesis

André Eid

# UNIVERSITÉ DE STRASBOURG

*ÉCOLE DOCTORALE des Sciences de la vie et de la santé (ED414)*

**IGBMC - CNRS UMR 7104 - Inserm U 964 - Chromatine et épigénétique dans le développement de l'embryon précoce de souris**

# THÈSE


présenté par :

**André EID**


soutenue le : **15 Avril 2016**

pour obtenir le grade de : **Docteur de l'université de Strasbourg**

Discipline/ Spécialité : Biologie du développement et physiologie

# Mechanisms of cell fate and chromatin plasticity during early mouse embryogenesis

**THÈSE dirigée par :**

**Mme. TORRES-PADILLA Maria-Elena** — Professeur, Université de Strasbourg, France

**RAPPORTEURS :**

**Mme. BOURC'HIS Déborah** — Docteur, Institut Curie, France

**M. DI CROCE Luciano** — Professeur, Center for Genomic Regulation, Espagne

---

**EXAMINATEUR :**

**M. TORA Laszlo** — Professeur, Université de Strasbourg, France

“It is perfectly true, as philosophers say, that life must be understood backwards. But they forget the other proposition, that it must be lived forwards.”

— Søren Kierkegaard

**À mes parents**

# Acknowledgments

I would like to start by thanking the members of the jury committee: Dr. Déborah BOURC'HIS, Pr. Luciano DI CROCE and Pr. Laszlo TORA for taking the time to read and review my thesis.

I also would like to thank my supervisor Pr. Maria-Elena TORRES-PADILLA (first time I call you professor) for her guidance and support. I am grateful for all the scientific and non-scientific discussions that we had and I hope we will continue to have. I am especially thankful for your patience and for finding the right words to make my views more optimistic. I enjoyed my time in the lab and I hope you will keep fostering the same atmosphere and environment that I came to know.

To all the members of the lab (current and previous), I am thankful for your support and your help inside and outside of the lab, it was great to work with you all. I want to especially mention Céline for everything she did (visible and invisible) in the lab, I know that she will be missed in Munich. Adam, thanks for having accepted to take me as a master student, I wonder if I would be writing this had you rejected me as you always claim you should have. Thanks for all your help and most importantly thanks for listening to all the nonsense I come up with (sorry for writing this in American English). Ana and Joanna and Helena (by adoption), thanks for all the fun times and all the jokes (I did not forget the fox thing) during lunch, at breaks and parties. Yusuke, Anas and Takashi thanks for all the discussions we had about everything from Nanog to suchi's to mcdonald's to life decisions (I'm still holding on to that bottle of Sake). Xavier and Julien (X-man and Juju respectively) thanks for accepting to be my flatmates, I am surprised you were not afraid of living with me. By the way thanks for taking care of me (cooking and stuff) during the writing period. Tsune, we had a great sushi last time, please make more, also let's have some coffee please. Maté and Diego (my son), you are both crazy, but in a good way, thank you for all the ethanol fights and bombs, you made feel like a child again. Camille, thank you for doing an amazing job during the lab transition and for all the things you do for the lab. Emily, Andreas and Juana, I am looking forward to working with you guys, it's a shame we didn't get more time to get to know each other.

To the Vermot lab (Emily, Rita, Marina, Francesco and Pedro), thank you all for your friendship and your kindness, for all the tea breaks, for all the cakes, for all the dinners, for the English food, for the pizza nights, for the wedding... Life is much nicer with you around. I wish you all the best and hope to see you as often as possible. To the Pourquié lab thank you for having me in your journal clubs and for all the discussions we've had. I am grateful to Stéphane for always having time to listen and discuss, for all the proof reading I have asked you to make, I know some things I wrote were tough on the eyes, I will compensate with sugary sweets as promised. To the Schneider lab, thank you guys for all the fun times we had at the beer hours, and for always providing me with missing antibodies (Sylvain). To all our collaborators in the IGBMC (animal care takers Hafid, William and Alex; microscopy facility Coralie, Marc and Pascale) thank you all for your professionalism and for making my work much easier.

A big thanks for all my friends Emmy, Lorraine, Mahmoud, Ziad and Ranine for your warm kindness and friendship, for all the time we spent together. To Elias and Yara, come back guys, I miss you a lot, and I miss your cooking also ;). I enjoyed all of our time and holidays together, we should go somewhere after I finish this. Mona, honeybear, a thank you is not enough, you have made my life so much nicer since you became part of it.

A mes frères, Paul et Anthony, je m'excuse pour ma si longue absence, pour l'espace qui s'est créé entre nous. J'espère combler cet espace à l'avenir et réapprendre à vous connaitre, sachez que je suis fière de vous et que je serais toujours là pour vous.

A mes parents, je sais que je vous manque, vous me manquez aussi même si je ne l'avoue que rarement. Vous m'avez soutenu toute ma vie et vous m'avez poussé vers de meilleures routes. Je ne saurais comment vous remercier ou vous repayer pour votre confiance et votre amour. Je vous aime énormément.

# Avant-propos

## Introduction

La fécondation d'un oocyte par un spermatozoïde donne naissance au zygote, une cellule totipotente qui contribue aux tissus embryonnaires et extra-embryonnaires nécessaires au développement. La première phase du développement embryonnaire, entre les stades zygote et blastocyste, est appelée développement préimplantatoire et dure trois jours et demi chez la souris. Juste après la fécondation, le génome du spermatozoïde échange les protamines qui l'ont condensé contre des histones pré-déposées dans l'oocyte. Le matériel génétique, paternel et maternel, est maintenu séparer. Ceci conduit à l'établissement de deux pronoyaux parentaux de volume différent permettant une distinction visuelle puisque le pronoyau paternel est 1,5 fois plus grand que le pronoyau maternel. Cette différence de volume est principalement due à l'échange d'histone qui prend place. Les deux pronoyaux présentent une structure nucléaire particulière, le NLB (*Nucleoli-like body*) qui ressemble à un cercle où se localisent les régions centromériques et péricentromériques qui sont enrichies en éléments répétés. Au stade 2-cellules, les NLB sont maintenus et commencent à être remplacés par les chromocentres qui sont présents dans les cellules somatiques. Ces modifications de l'organisation nucléaire sont un exemple des changements globaux qui prennent lieu durant le développement préimplantatoire.

Dans les cellules eucaryotes, le matériel génétique est enroulé par des histones qui sont des protéines basiques. L'assemblage d'un octamère d'histones autour de 146 à 148 pb (paires de base) de nucléotides constitue un nucléosome qui est l'unité de base de la chromatine. La chromatine est constituée de fibres de 10nm de diamètre et peut se compacter théoriquement en fibres de 30nm et en fibres de 100 et 300nm durant la mitose pour former des structures d'ordre supérieur. Il existe quatre histones de cœur : H2A, H2B, H3 et H4 et qui possèdent plusieurs variantes (par exemple H3.1, H3.2 et H3.3) qui peuvent être remplacées en fonction du cycle ou d'évènement cellulaire. Les histones peuvent être modifiées post-traductionnellement, au niveau du N-terminus, de façon covalente par méthylation, phosphorylation ou acétylation, pour n'en citer que quelques-unes. Ces

modifications (ou marques) post-traductionnelles (MPTs) agissent en tant que signal reconnu par des complexes protéiques qui modulent l'expression génétique positivement ou négativement d'où l'émergence de l'hypothèse d'un code d'histone régulant l'activité génétique.

Dans les cellules somatiques, la chromatine est présente sous deux formes majeures : l'hétérochromatine et l'euchromatine. Cette dernière est une structure relaxée riche en gènes et en histones acétylées (H3K27ac, H3K9ac), ainsi qu'en histones méthylées (H4K4me3 et H3K36me3) corrélant avec une activité transcriptionnelle. L'hétérochromatine est subdivisée en deux groupes : d'une part, l'hétérochromatine constitutive qui est une structure condensée, pauvre en gènes et enrichie en éléments répétés, et qui est marquée par une hypo-acétylation et des MPTs répressives telles que H3K9me3, H4K20me3 et H3K64me3, d'autre part, l'hétérochromatine facultative est marquée par H3K27me3 et H2AK119ub et maintient en particulier le contrôle de l'expression des gènes homéotiques (*Hox*) importants au cours du le développement.

Le pronoyau maternel maintient des marques hétérochromatiques constitutives qui se retrouvent au niveau des NLBs, en contraste avec le pronoyau paternel qui en est dénué. Au stade zygote, H4K20me3 est présente de manière asymétrique uniquement au niveau du pronoyau maternel puis est absente du stade 2-cellules jusqu'à l'implantation de l'embryon. Les méthyl-transférases *Suv4-20h1* et *Suv4-20h2*, catalysant H4K20me2 et H4K20me3, ne sont pas exprimées fortement au cours du développement préimplantatoire et leur élimination par délétion (KO) ne conduit pas à un arrêt du développement préimplantatoire. Dans le but d'étudier l'importance de l'absence de H4K20me3 au cours du développement préimplantatoire, la meilleure stratégie est celle d'une surexpression ectopique des méthyl-transférases *Suv4-20h1* et *Suv4-20h2* au stade zygote dans le but de maintenir H4K20me3 tout au long du développement et d'étudier les effets de cette marque sur le développement préimplantatoire.

**Résultats : première partie**

L'expression ectopique de *Suv4-20h2* conduit au renforcement de la marque H4K20me3 dans le pronoyau maternel et au blocage du développement majoritairement avant le stade 2-cellules. La mutation dans le site catalytique SET de SUV4-20H2 (*Suv4-20h2mut)* bloque l'activité méthyl-transférase et n'augmente pas le niveau de H4K20me3. De plus, la surexpression ectopique de *Suv4-20h2mut* ne provoque pas l'arrêt du développement indiquant que c'est l'augmentation de H4K20me3 et son maintien qui sont responsables de cet arrêt. L'effet de H4K20me3 est également observé suite à la surexpression de *Suv4-20h2* au stade 2-cellules dans l'un des blastomères et indique que le rôle de H4K20me3 dans le blocage du cycle cellulaire n'est pas uniquement spécifique du stage zygote. L'établissement de H4K20me3 n'a pas d'effet sur le niveau de H3K9me3 qui se trouve en amont dans la voie de signalisation de l'hétérochromatine constitutive, mais augmente le niveau de H3K64me3 dont le mécanisme d'établissement n'a pas encore été élucidé. Ces observations indiquent que H4K20me3 et H3K64me3 induisent une hétérochromatinisation de la chromatine maternelle au cours du développement préimplantatoire.

En opposition à l'expression ectopique de *Suv4-20h2*, celle de *Suv4-20h1* ne provoque ni une augmentation de H4K20me3 au stade zygote, ni un blocage du développement préimplantatoire. En revanche, au stade 2-cellules, le niveau de H4K20me3 augmente légèrement et la mutation au niveau du site catalytique SET (*Suv4-20h1mut*) abroge cette augmentation. Ces données montrent que SUV4-20H2 est l'enzyme responsable majoritairement de l'établissement de H4K20me3 au cours du développement préimplantatoire, et que l'activité catalytique de SUV4-20H1 n'est pas suffisante pour activer la voie de blocage de H4K20me3.

Dans le but d'élucider le mécanisme de régulation que H4K20me3 pourrait utiliser pour induire un arrêt du cycle cellulaire, nous avons étudié l'effet de cette marque sur la traduction et la réplication cellulaire. Le niveau d'incorporation d'EU (5-Ethynyl Uridine), au cours de la phase de transcription, dans les embryons micro-injectés par *Suv4-20h2* est réduit en comparaison aux embryons non-injectés et micro-injectés par *Suv4-20h2mut* au stade 2-cellules durant la phase de

transcription embryonnaire. Pour mieux analyser l'effet de *Suv4-20h2* sur l'expression génétique, nous avons analysé l'expression de 48 gènes dans 45 embryons individuellement qui étaient soit non-injectés ou micro-injectés par *Suv4-20h2*, *Suv4-20h2mut* ou *Suv4-20h1*. Ces données montrent une réduction spécifique de l'expression de gènes importants pour la production de ribosomes et de d'ARN polymérase, impliquant H4K20me3 dans la régulation de l'expression génétique et protéique. D'autre part, l'incorporation d'EdU (5-ethynyl-2′-deoxyuridine), dans les embryons micro-injectés par *Suv4-20h2,* au cours de la dernière phase de réplication cellulaire au stade 2-cellules présente une topologie identique à celle des embryons démarrant leur réplication, alors que les embryons non-injectés ou micro-injectés par *Suv4-20h2mut*, présentent un faible taux d'incorporation au niveau des régions hétérochromatiques riches en DAPI. La différence des niveaux d'incorporation d'EdU entre les embryons non-injectés et les embryons micro-injectés par *Suv4-20h2* est également observable au stade zygote durant la dernière phase de réplication, indiquant que l'effet de H4K20me3 n'est pas spécifique à un stade cellulaire et affecte le stade de terminaison de la réplication. Un blocage de la réplication peut avoir des répercussions sur l'expression génétique s'il persiste, surtout au niveau des régions euchromatiques où des évènements de rencontre entre la réplication et la transcription ont été décrits dans la littérature, et ce qui semble être le cas dans les embryons qui expriment ectopiquement *Suv4-20h2*.

La méthylation de H4K20 se fait de manière graduelle avec un premier échelon, H4K20me1, nécessaire pour l'activité méthyl-transférase de *Suv4-20h1* et *Suv4-20h2*. De plus, le niveau de méthylation de H4K20me1 a précédemment été décrit comme étant important pour la réplication cellulaire. En effet, la délétion de PR-Set7, qui catalyse H4K20me1, provoque un blocage du cycle cellulaire. L'expression ectopique de *Suv4-20h1* et *Suv4-20h2* réduit le niveau de H4K20me1 au cours de la phase G2 du cycle cellulaire durant laquelle la marque H4K20me1 est la plus élevée dans les embryons au stade 2-cellules non injectés. Le fait que H4K20me1 est réduite dans les embryons micro-injectés par *Suv4-20h1* et *Suv4-20h2* indique que ces deux enzymes catalysent H4K20me1 vers un degré supérieur de méthylation et suggère que *Suv4-20h1* possède une activité enzymatique spécifique vers H4K20me2 alors que *Suv4-20h2* méthyle spécifiquement H4K20me3. De plus, ces données suggèrent que l'arrêt du développement (préimplantatoire) observé est indépendant des niveaux de H4K20me1. Finalement, le niveau de H3S10p, un

marqueur de la phase G2-M, demeure inchangé dans les embryons analysés validant l'hypothèse que le phénotype de blocage cellulaire est dû principalement à un effet sur la phase S.

Les changements des niveaux de méthylation de H4K20 sont des marqueurs de l'activation de la voie de réparation génomique dans les cellules somatiques avec une accumulation de γH2A.X au niveau des cassures d'ADN. L'expression ectopique de *Suv4-20h2* et de *Suv4-20h2mut* ne modifie pas le niveau de γH2A.X en comparaison avec les embryons non-injectés, suggérant l'absence de l'activation de la voie de réparation de l'ADN. Des études précédentes avaient démontré que les changements du niveau de H4K20me1 activent la voie ATR qui contrôle la progression de la phase S. Nos observations indiquent que les niveaux de CHK1 et CHK1p, deux enzymes en aval d'ATR, augmentent légèrement dans les embryons micro- injectés par *Suv4-20h2* en comparaison avec les embryons non-injectés ou micro- injectés par *Suv4-20h2mut*. Afin de prouver que la voie ATR est impliquée dans le blocage cellulaire nous avons appliqué un inhibiteur spécifique d'ATR. Cet inhibiteur sauve le phénotype et permet à un pourcentage significativement plus important d'embryons d'atteindre le stade 4-cellules. Ce résultat démontre que le phénotype létal au cours du développement préimplantatoire est en partie dû à l'activation de la voie ATR durant la phase S au stade zygote et 2-cellules.

**Résultats : deuxième partie**

Outre l'hétérochromatine constitutive, l'hétérochromatine facultative au travers de la marque H3K27me3 joue aussi un rôle important au cours du développement préimplantatoire et de la reprogrammation de la chromatine paternelle. L'ubiquitylation de H2A sur la Lysine 119 (H2AK119ub) en association avec H3K27me3 marque l'hétérochromatine facultative dans les cellules somatiques. La présence de cette marque n'a pas été étudiée au cours du développement préimplantatoire. Nous avons montré que H2AK119ub est présente tout au long du développement préimplantatoire. Cette marque est présente immédiatement suite à la fécondation dans les deux pronoyaux, mais se retrouve réduite dans le pronoyau paternel au cours de la progression du développement. Au stade blastocyste, H2AK119ub est enrichie dans les cellules du trophectoderme

où elle forme des globules (*foci*) dans 50% des embryons en correspondance avec l'inactivation du chromosome X dans les embryons femelles.

De plus, nous avons analysé la présence de membres du complexe non canoniques de PRC1, afin d'établir leurs fonctions au cours du développement préimplantatoire. RYBP et YAF-2 sont deux homologues qui interagissent avec la protéine RING1, la E3-ubiquityl-ligase du complexe PRC1 qui catalyse H2AK1119ub. La protéine RYBP est présente dans tous les stades du développement préimplantatoire à l'exception du stade zygote. Au stade 2-cellules, RYBP est localisée au niveau des régions DAPI autour des NLBs. La protéine YAF-2 est localisée au niveau des NLBs dans les oocytes et le zygote et enrichie au stade 2-cellules, puis son niveau est réduit à partir du stade 4-cellules.

L3MBTL2 est également membre du complexe non-canonique de PRC1 et se retrouve en complexe avec soit RYBP soit YAF-2. L3MBTL2 possède une activité catalytique qui compacte les nucléosomes et joue un rôle important au cours du développement puisque son inactivation provoque un arrêt du développement durant la gastrulation. Au cours du développement, L3MBTL2 est présente à tous les stades et ne forment pas d'accumulation au stade blastocyste. Par contre, L3MBTL1, un autre membre de la famille des MBTs (*Malignant Brain Tumor*) protéines, présente des accumulations en forme de *foci* au stade morula et blastocyste.

Ces observations indiquent que plusieurs membres du complexe non-canonique de PRC1 sont présents à différents stades du développement préimplantatoire et pourraient jouer un rôle dans la régulation de l'établissement *de novo* de l'hétérochromatine facultative.

**Résultats : troisième partie**

La compaction de l'hétérochromatine a été observée, dans les cellules somatiques, en utilisant la microscopie électronique à transmission (TEM). L'embryon de souris présente une chromatine avec des MPTs différentes de celles des cellules somatiques. Nous avons ainsi voulu observer l'ultrastructure de la chromatine embryonnaire pour comprendre l'effet de l'absence des marques hétérochromatiques telles que H4K20me3. En effet, entre les stades 2-cellules et 8-cellules la proportion de densité électronique mesurée par TEM dans les noyaux augmente significativement en combinaison avec une réduction de la dynamique des histones. L'observation

par TEM de l'augmentation des proportions de régions hétérochromatiques au cours du développement préimplantatoire est en corrélation avec la réduction de la dynamique des histones.

**Conclusion**

Le remodelage des marques hétérochromatiques au cours des premiers stades du développement embryonnaire est un processus structuré important pour la réorganisation de la chromatine parental suite à la fécondation. Ainsi, l'augmentation des niveaux de H4K20me3, marqueuse de l'hétérochromatine constitutive, affecte le processus de réplication et qui semble être différent du rôle que H4K20me3 joue dans le recrutement des protéines ORC dans les cellules somatiques. En outre, des membres du complexe non canonique de PRC1, qui marque l'hétérochromatine facultative, sont exprimés à différents stades du développement préimplantatoire ce qui présage des rôles différents dans le recrutement du complexe PRC1 pour modifier H2AK119ub au cours du développement préimplantatoire. Le rôle de ces protéines pourra être étudié par des techniques d'invalidation. Finalement, l'ultrastructure de la chromatine embryonnaire, qui est affectée par la présence de MPTs, change au cours du développement et reflète la réorganisation nucléaire qui prend lieu entre le stade 2- et 8-cellules. Ces trois résultats reflètent l'importance du remodelage des marques hétérochromatiques pour le développement préimplantatoire

# Table of Contents

# Table of Figures

# Abbreviations

| | |
|---|---|
| 16CS | 16-cell stage |
| 2CS | 2-cell stage |
| 4CS | 4-cell stage |
| 8CS | 8-cell stage |
| ATM | Ataxia-telangiectasia mutated |
| ATR | Ataxia telangiectasia mutated and Rad3-related |
| ATRIP | ATR-interacting protein |
| Bp | base pairs |
| BrdU | 5-Bromo-2′-deoxyuridine |
| CAF-1 | Chromatin-Assembly Factor 1 |
| CBX | chromobox |
| Cdk | Cyclin-dependent kinase |
| cHC | constitutive heterochromatin |
| DSBs | double strand breaks |
| E(var) | Enhancer of variegation |
| EdU | 2′-deoxy-5-ethynyluridine () |
| Eed | Embryonic ectoderm development |
| ESCs | Embryonic stem cells |
| Ezh | Enhancer of zeste homologue |
| fHC | facultative heterochromatin |
| H2Au | H2A ubiquitylation on Lysine119 |
| H2Bu | H2B ubiquitylation on Lysine 123 |
| H3K9me3 | Histone 3 Lysine 9 tri-methylation |
| HMTase | Histone methyl transferase |
| HP1 | Heterochromatin protein 1 |

| | |
|---|---|
| HR | Homologous recombination |
| HU | Hydroxyurea |
| ICM | Inner cell mass |
| IF | Immunostaining |
| KMT | Lysine methyl transferase |
| L3MBTL2 | Lethal(3)malignant brain tumour-like protein 2 |
| MEA | Major embryonic activation |
| MGA | Major genome activation |
| MRN | MRE11-RAD50-NBS1 |
| ncPRC1 | non-canonical PRC1 |
| NHEJ | Non-homologous end joining |
| NLB | Nucleolus-like body |
| NPB | Nucleolus-precursor body |
| nPRC1 | canonical PRC1 |
| ORC | Origin recognition complex |
| PB | Polar body |
| PcG | Polycomb group |
| PCGFs | Polycomb group RING finger proteins |
| PCNA | Proliferating cell nuclear antigen |
| PEV | Position effect variegation |
| PI3K | Phosphoinositide 3-kinase |
| PIKKs | Phosphoinositide 3-kinase-related protein kinases |
| PLK1 | Polo-like kinase-1 |
| PN | ProNuclear stage |
| PRC | Polycomb repressive complex |
| preRC | Pre-replication complex |
| PTMs | Post-translational modifications |
| RPA | Replication protein A |

| | |
|---|---|
| RYBP | RING1 and YY1-binding protein |
| S(var) | Suppressor of variegation |
| SCNT | Somatic cell nuclear transfer |
| SET | Su(var)3-9, E(z), Trx |
| Suz | Suppressor of zeste |
| TE | Trophectoderm |
| vPRC1 | variant PRC1 |
| YAF2 | YY1 associated factor 2 |
| ZGA | Zygotic genome activation |
| γH2AX | Phosphorylation of H2A.X |

# Introduction

# I. Mouse preimplantation development

## 1. Zygotic development

Life, at its onset, begins with an end. Two highly differentiated gametes, the sperm and the egg, fuse together to give rise to the totipotent zygote. The zygote is able to give rise to all embryonic and extra-embryonic tissues. Within the zygote, two nuclei (called pronuclei) are formed containing the maternal and paternal genetic information. The two pronuclei remain physically separated and their genetic material only comes into contact during the first cell division that gives rise to the 2-cell stage (2CS) embryo. The zygotic stage is subdivided into 5 stages called ProNuclear stages or PNs: PN1 is the stage that occurs after fertilization, both pronuclei are still highly condensed, but start undergoing decondensation. Between PN1 and PN2, the paternal genome exchanges the protamines that had packaged the DNA in the sperm with histones that are provided by the oocyte. On the other hand, the oocyte finishes its second meiosis where it was blocked in metaphase 2 before the fertilization occurred. This results in the expulsion of the excess maternal DNA into the second polar body (PB). The first PB is expelled after the end of the first meiosis during oogenesis. Between PN3 and PN4, the zygotic genomes replicate, with the paternal genome starting replication earlier. After replication occurs, between PN4 and PN5, the embryo expresses its own genome in what is called the minor zygotic genome activation (ZGA). Finally, in PN5, the chromatin recondenses before the first mitosis takes place (Figure 1).

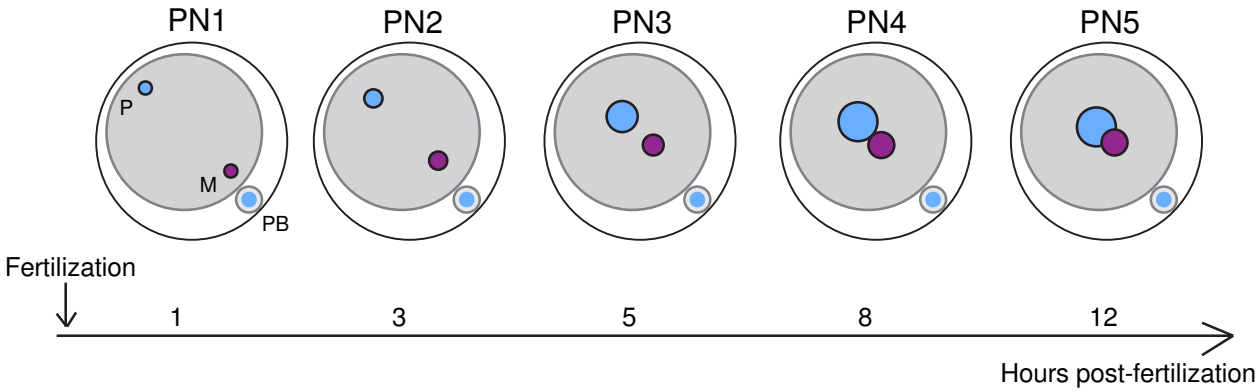


**Figure 1. ProNuclear stages of zygotic development.**
Schematic representation of ProNuclear (PN) stages during zygotic development. The Paternal (P) pronucleus is indicated in blue while the Maternal (M) pronucleus is in violet. PB, Polar Body.

## 2. Development from the 2-cell stage to the blastocyst

The 2CS embryo maintains a certain degree of totipotency and each blastomere can contribute to both embryonic and extra-embryonic tissues. At this stage, the paternal and maternal genetic information still occupy a different space within the same nucleus. At the 4 cell stage (4CS), individual blastomeres lose the capacity to contribute to all embryonic and extra-embryonic tissues and thus totipotency is lost. At the 8CS, the blastomeres start acquiring an identity based on their polarization, as the blastomeres compact, acquire apical basal polarity, in addition to cellular junctions. Blastomere cellular fate is refined at the 16-cell stage (16CS) embryo, or morula, one cleavage round later. The opposing expression of certain marker gens such as *Cdx2* (Outer cells) and Sox2 (Inner cells) at this 16CS lead to the formation of the inner and outer cells. Another round of division leads to the blastocyst stage when two cell lineages are defined as distinct: the trophectoderm (TE) and the Inner Cell Mass (ICM). The trophectoderm is considered multipotent and can give rise to some extra-embryonic tissues, while the ICM is pluripotent, as it contributes to all embryonic tissues and to some extra-embryonic tissues. The ICM cells are not considered as totipotent because of their inability to give rise to all embryonic and extra-embryonic tissues. ICM outgrowths isolated from blastocysts at E3.5 can be expanded in culture and give rise to embryonic stem cells (ESCs) which can be maintained *in vitro* (Evans and Kaufman 1981). These stages of development that have been described occur during the migration of the embryo through the oviduct towards the uterus where the mouse embryo implants at day 4.5 (Figure 2).

## 3. Maternal to zygotic transition

The developmental progression of the embryo requires maternal components, but also to some extent paternal ones as well. Proteins and mRNA are already present in the oocyte and will be used by the zygote. A first phase of expression of the embryonic genome takes place in the zygote between PN3 and PN4. It is followed by a second wave of activation at the 2CS, referred to as the major genome activation (MGA) or major embryonic genome activation (EGA) (Figure 2). By the end of the 2CS, most maternally provided transcripts are degraded. Several studies have reported the importance and necessity of these two cycles of genome activation to the proper development of the embryo, with the EGA thought to be the most important because of the higher gene

expression that results from it. Blocking the MZA or EGA results in embryonic arrest (Aoki, Worrad, and Schultz 1997), underscoring their importance during preimplantation development.

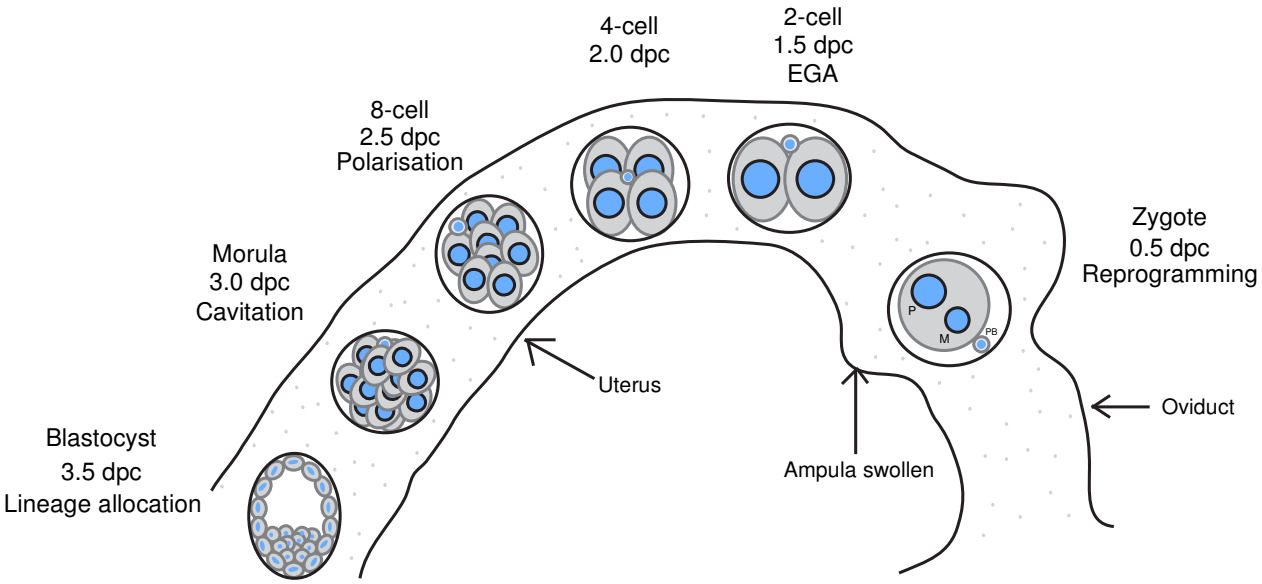


**Figure 2. Preimplantation developmental progression.**
Mouse preimplantation embryos undergo nuclear reprogramming and a small wave of transcription in the zygote, followed by a stronger wave (EGA) at the 2-cell stage. Polarization of the blastomeres takes place during the 8-cell stage and cavitation of the blastocoel during the morula stage. Lineage allocation takes place between the morula and blastocyst stage when the Inner Cell Mass and Trophectoderm lineages are established.

## 4. Timing of replication in mouse embryos

After fertilization, the parental chromatin remains separated in two nuclei and the dynamics of S-phase are different in each nucleus. At the zygote stage, replication is initiated as early as 23h phCG (post human chorionic gonadotropin) and progresses until 30h phCG (Figure 3). The male and female chromatin initiate replication around the same time, but the male pronucleus ends the S phase earlier, most likely because of lack of heterochromatin at this stage. In the 2-cell stage, the nuclei are still synchronized and start replicating at the same time around 34h phCG and finish around 40h phCG (Figure 3).

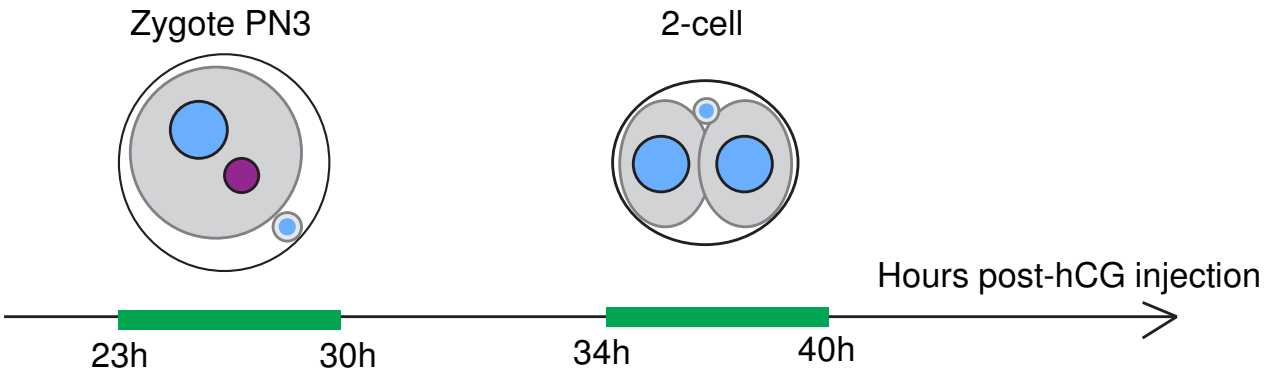


**Figure 3. Replication timing in the zygote and at the 2-cell stage.**
Replication timing (in green) in the zygote initiates at the ProNulear stage 3 at 23h post-hCG (phCG) injection and lasts until 30h phCG. At the 2-cell stage, this event occurs between 34h and 40h phCG.

BrdU incorporation was used to measure the timing of replication in the embryos. The pattern of BrdU that is observed is quite diverse, but could be subdivided into three categories: i) early replication: this is when early origins fire and a burst of dNTP incorporation is observed showing the strongest signal, ii) mid replication: early origins have been replicated and the fork keep progressing, but lower levels of BrdU are detected, supposedly this is the time when facultative heterochromatin is being replicated, iii) late replication: involves replicating constitutive heterochromatin and the BrdU signal becomes weaker and localizes to the repeat rich elements and the nuclear periphery (O'Keefe, Henderson, and Spector 1992) ( Figure 4).

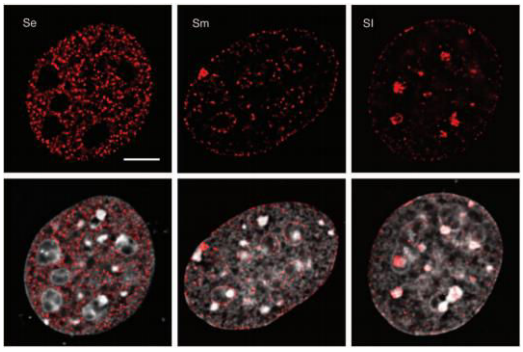


**Figure 4. Spatial-temporal dynamics of DNA replication**
Three HeLa cells exhibiting the characteristic early (Se), mid (Sm) and late (Sl) S-phase patterns are observed by super-resolution microscopy. DNA replication is visualized by short pulse labeling of BrdU (red). Bottom row shows an overlay of the replication staining (red) and DNA staining by DAPI (gray). Scale bar: 5µm. Modified from (Casas-Delucchi and Cardoso 2011) and based on observations by (O'Keefe, Henderson, and Spector 1992)

# II. Chromatin biology

## 1. Chromatin structure and nucleosome organization

After the "revelation" of the DNA double helix structure, and in combination with Mendelian genetics, it was thought that most important "secrets of life" had been discovered. However, genome expression, as important as it is, could not explain on its own certain developmental aberrations and expression patterns, for example, position effect variegation (PEV). This is when chromatin comes into play. The chromatin is a nucleoprotein complex that packages the genetic information. It is composed of the DNA backbone that is wrapped around highly basic proteins, the histones. The first observations of the chromatin structure by electron microscopy (Olins and Olins 1974; Oudet, Grossbellard, and Chambon 1975) revealed the existence of a 10nm fiber (or beads on a string). Two models have proposed how the 10nm fibers can be compacted into 30nm fibers: the solenoidal model (Finch and Klug 1976)and the ribbon (or zig zag) model (Horowitz et al. 1994; Woodcock, Frado, and Rattner 1984) (Figure 5). The 30nm fiber establishment *in vivo* has remained elusive and its existence has been questioned. Furthermore, a higher level of compaction exists in the form of the 100nm and 300nm fibers that are observed during the compaction of mitotic chromosomes (Cook 1995; Belmont 2006).

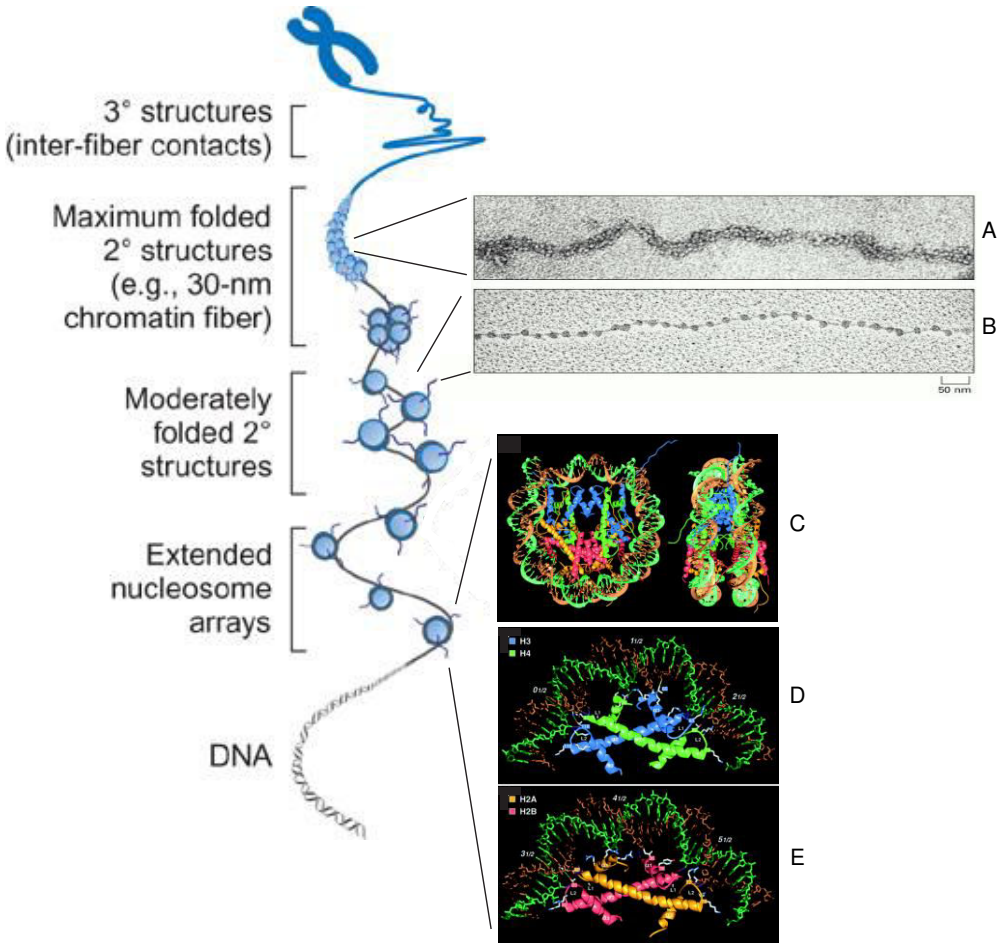


**Figure 5. Chromatin compaction and nucleosome structure.**
Schematic representation of different levels of chromatin organization. Modified from (Caterino and Hayes 2007). A. Isolated chromatin in interphase observed by transmission electron microscopy as 30nm fibers. B. *In vitro* uncondensed chromatin as 10nm fiber. Images from (Alberts B. 2002). C. Nucleosome core particle: ribbon traces for the 146-bp DNA phosphodiester backbones (brown and turquoise) and eight histone protein main chains. D. Representation of H3–H4 histone-fold pair. E. Representation of H2A–H2B histone-fold pair. H3: blue; H4: green, H2A: yellow, H2B: red. Images from (Luger et al. 1997).

The basic repetitive unit of the chromatin is the nucleosome which is composed of 146-148 base pairs (bp) of DNA wrapped around a histone octamer composed of 2 copies of 4 "core" histones: H2A, H2B, H3 and H4 (Luger et al. 1997) (Figure 5). Early experiments had shown that placing a nucleosome on a core promoter could prevent the initiation of transcription *in vitro* (Lorch, LaPointe, and Kornberg 1992) and that histones repress transcription *in vivo*, leading to the

idea that the nucleosome is a general gene repressor (Kayne et al. 1988). It was later shown that histone modifications were also involved in transcriptional activation (Wyrick et al. 1999; Brownell et al. 1996; Durrin et al. 1991).

## 2. Histones and post-translational modifications

Histone proteins are highly conserved proteins in eukaryotes, most likely stemming from their crucial role in chromatin biology. "Core" histones can be divided into 2 groups: replication dependent (or canonical) and replication-independent (or variants). Genes encoding for canonical histones, are located in co-regulated gene clusters (Marzluff et al. 2002) that are highly expressed as non-polyadenylated transcripts during the S-phase and used for newly synthesized DNA strands. In contrast, the variant histones are continuously expressed from outside the histone gene-clusters as poly-adenylated transcripts throughout the cell cycle. Both canonical histones and their variants are deposited and replaced using specific chaperones. The core histones possess a histone fold domain which allows for the interaction between distinct dimers. Core histones also share long unstructured tails at the N-terminus that emerge from the nucleosome structure and are easily accessible. This makes them an easy target for post-translational modifications. Such modifications include citrullination, phosphorylation, SUMOylation, acetylation, ubiquitination, ADP-ribosylation and methylation among others (Kouzarides 2007). These modifications are perceived as a "signaling beacon" that will act in an epigenetic way (maintains a certain state: repressive or permissive). Histone variants also are used in specific cellular contexts, for example CenH3 is the histone variant that replaces the histone H3 in centromeric regions, whereas H2A.X binds to DNA at double strand breaks and activates the DNA repair pathway. Additionally to the core histones, the nucleosome is bound by histone H1 at the entry and exit sites of the DNA, thus stabilizing the structure and allowing for the formation of higher order structure.

The multitude of functions of histone variants and histone modifications later led to the establishment of the idea of the existence of a "histone code" that could act as a regulator of genome activity ((Strahl and Allis 2000). This idea stems from the fact that the DNA is not naked and is wrapped by histones. In turn, histones are modified depending on the cell cycle or on cellular events that require increased or reduced access to the genome. In this way, each cell can have a spatial-temporal control of genome expression and compaction in addition to the information contained

within the genetic sequence itself; this is an epigenetic control. In order for the epigenetic control to take place correctly, the marks or variants that are deposited have to be able to be read, which means that there is a cascade of events that start with the activation of a modifier (be it a protein that will add a modification or erase it) to a reader protein that will interpret this modification (by binding to it or being blocked from accessing it). The concept that each single/individual modification leads to a direct effect on transcriptional activity or compaction state seems to be unrealistic, it is rather more likely that histone modifications act in concert with each other and reinforce each other's "signal" which explains the existence of different domains in the chromatin where marks with similar effect colocalize (for example: H3K4me3 and H4K36me3 are correlated with transcribed genes, while H3K9me3 and H4K20me3 are enriched in silenced and gene poor regions).

## 3. Euchromatin and Heterochromatin

Chromatin states can be roughly subdivided into 2 types: euchromatin and heterochromatin. These two states have been described in 1928 by Emil Heitz, and could also be seen in the sketches made by Walther Flemming in 1882 (Figure 6), while studying mitotic chromosomes, but the definition that he had given to these 2 types of chromatin has since evolved with our increasing understanding. As such, euchromatin, is described as an "open" structure that resembles the 10nm fiber. It is gene rich and permissive to transcription. It is also enriched in chromatin marks and histone variants that are correlated with higher transcription levels. On the other hand, heterochromatin is considered a "closed" structure, which is highly condensed (Passarge 1979; Weintraub and Groudine 1976). It is gene poor and present in repetitive elements such as centromeres, pericentromeres and telomeres. Heterochromatin is enriched in histone marks and variants that correlate with low transcription levels and higher condensation. The last difference that needs to be pointed out is replication timing. It is thought that because euchromatin is easily accessible and contains highly transcribed genes, replication takes place at the beginning of S phase, whereas heterochromatic regions, enriched in repetitive elements, replicate during late S phase. Heterochromatin is itself divided into roughly two functional types: facultative and constitutive, which will be discussed at length in the next paragraphs.

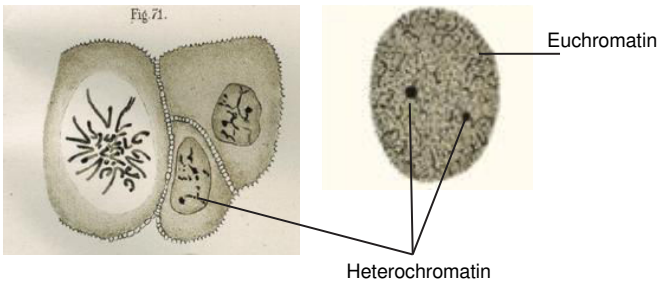


**Figure 6. Schematic representation of nuclear chromatin.**
Sketches made by Walter Flemming (published in 1882) while studying cell division eluded to two types of chromatin.

## 4. Chromatin landscape during preimplantation development

Mouse embryonic development starts by combining the genetic information of the sperm with that of the oocyte. In addition to their genetic material, the gametes also carry epigenetic information. It has been reported that as much as 5% of mouse sperm chromatin, 10% in humans, retains histones which also could retain certain post-translational modifications that could act as epigenetic markers (Hammoud et al. 2009; Hisano et al. 2013; Montellier et al. 2013). That means that they could keep the memory of transcriptional status and carry it over after having undergone cellular divisions. Most sperm chromatin however is packaged with protamines that can also be modified and thus potentially also carry some information to the zygote, however, this hypothesis has not been explored. On the other hand, the oocyte chromatin retains all of its histones and maintains histone modifications, at least globally, as determined by immunofluorescence analyses. Upon fertilization, the sperm protamines are exchanged for histones produced and deposited by the oocyte. Most of the histones are not premodified (except acetylation). The exchange of the protamines, results in an expanded nucleus, between PN3 and PN5, which is larger in volume than the nucleus containing maternal chromatin. Both pronuclei can be distinguished from each other primarily by observing their respective sizes. In comparison, the maternal chromatin is packaged in a pronucleus that has the same size as an oocyte's nucleus. In addition to their differences in volume, other molecular features distinguish the two parental pronuclei. The increase in volume of the paternal pronucleus has been suggested to reflect a state of open chromatin organization, evidenced by the levels of transcription that are 4 to 5 times higher in the paternal pronucleus, during the ZGA, then the output from the maternal chromatin (Bouniol, Nguyen, and Debey 1995).

Furthermore, the increase in accessibility is probably one of the reasons that could explain why the paternal chromatin starts replication slightly earlier than the maternal one. Subsequently, both pronuclei acquire a structure that has a ring-like-shape. This structure is called Nucleolus-Like-Body (NLB, not to be confused with cytoplasmic-NLBs found in certain neurons) or Nucleolus-Precursor-Body (NPB). For coherence, the term NLBs will be used throughout the manuscript. The NLBs are composed mainly of nucleophosmin and are not active in terms of typical nucleolar functionality. Located around the NLBs, in both paternal and maternal pronuclei, are centromeric and pericentromeric regions, rich in repetitive elements (Probst et al. 2007). Histone modifications on these regions around the NLBs, as observed by immunofluorescence (IF) microscopy, show an asymmetry between the maternal chromatin, which is enriched in many histone modifications, in particular those related to heterochromatin, and paternal chromatin, which is largely devoid of them. The presence of the NLBs has been shown to play an important function both during preimplantation development and during reprogramming events upon somatic cell nuclear transfer (SCNT) (Martin et al. 2006). The chromatin landscape in the embryo is very different compared to that of somatic cells, in terms of the global presence of histone modification and compaction.

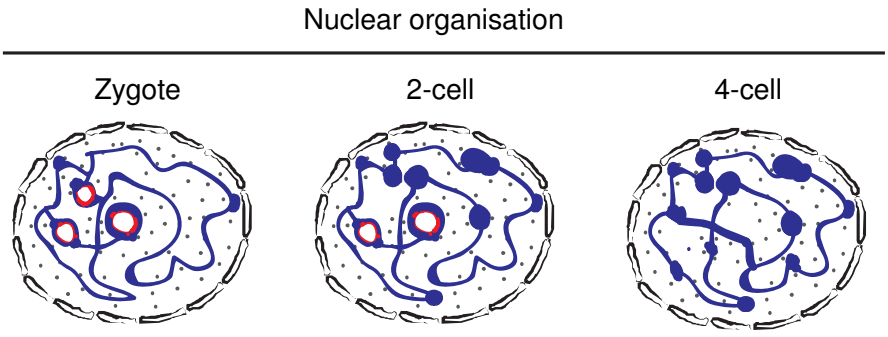


**Figure 7. Nuclear organization in preimplantation embryos.**
Schematic representation of nuclei in the zygote, 2- and 4-cell stages. Nucleoli-Like Bodies (NLBs) are represented in red as ring-like shaped structured at the zygote and 2-cell stage. Chromocenters are represented as foci (in blue) of DAPI rich regions that are observed beyond the 2-cell stage. Peri- and centromeric regions localize to either the NLBs or chromocenters depending on the developmental stage.

## 5. Constitutive heterochromatin

Constitutive heterochromatin (or CH) is one of the two types of heterochromatin. One of the most famous examples of the function that CH can play is in Position Effect Variegation (PEV)

which was initially described in *Drosophila* (Tartof, Hobbs, and Jones 1984). The PEV phenotype was discovered upon the observation that certain cells in the eye change their color, resulting in a red-white mosaic (Patterson and Muller 1930). The gene responsible for eye color in *Drosophila* is called *white* and its locus is located near the mating type locus, on the X chromosome, which itself is close to the centromere that is composed of a heterochromatic domain. Not all the red pigmentation disappears, but a certain percentage of cells lose their red pigmentation and maintain a white color through cellular division (Figure 8). The percentage of cells affected varies from one individual to another and the phenotype is not inherited in a mendelian fashion, indicating that it could not be explained by genetics alone. The PEV phenotype results in a heritable silencing of the *white* gene expression through multiple cell divisions resulting from the translocation of the gene to a position close to heterochromatin. The translocation of the *white* locus with the mating locus and the spreading of the heterochromatic domain results in silencing of the *white* gene in a heritable manner. The PEV phenotype has led to heightened interest in the function that is played by constitutive heterochromatin and the mechanism responsible for its establishment.

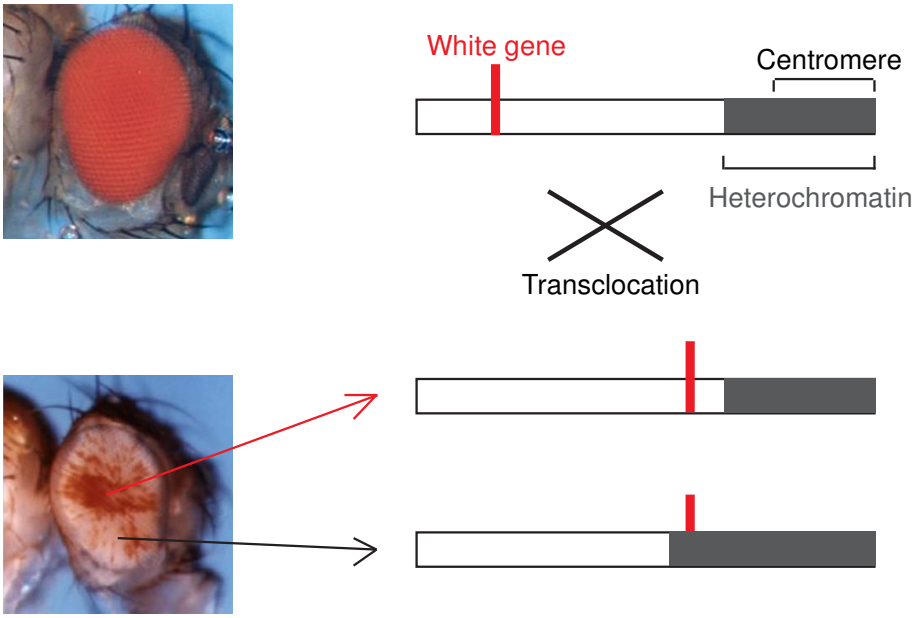


**Figure 8. Schematic representation of Position effect variegation (PEV).**
The White gene (in red) is expressed in the eye of *Drosophila*. The White gene can translocate with the mating-type locus located close to a heterochromatic domain (in grey) present at the centromere on the X chromosome. The heterochromatic spreading can heritably silence the white gene upon translocation in E(var) mutants resulting in a variegated eye color.

Further studies revealed proteins that can act as enhancers "E(var)" or suppressors of variegation "Su(var)". One of the first Su(var) proteins to be studied were SUV39H1/H2 and HP1 (Heterochromatin Protein 1 also known as chromobox or CBX1/3/5 for HP1β/γ/α respectively) (Tschiersch et al. 1994; Rea et al. 2000; Peters et al. 2001; Bannister et al. 2001; Lachner et al. 2001). It was shown that SUV39H proteins had a methyltransferase activity via their SET (Su(var)3-9, E(z), Trx) domains which specifically tri-methylated lysine 9 on the histone 3 (H3K9me3). This heterochromatic histone modification is recognized by the chromodomain of HP1, which in turn can recruit other factors. SUV4-20H1/2 (recently renamed KMT5B/C respectively) are then recruited by the chromoshadow domain of HP1are responsible for the di- and tri-methylation of the lysine 20 on histone 4 (H4K20me2/3) (Schotta et al. 2004; Schotta et al. 2008). These two modifications are considered as markers of constitutive heterochromatin domains. Recently a third modification has been shown to colocalize with them. H3K64me3 seems to also play a role in heterochromatin maintenance, but is present in the core domain of the nucleosome, whereas the other modifications are exposed outside of the core on the N-terminal end of the histone tail (Daujat et al. 2009; Lange et al. 2013).

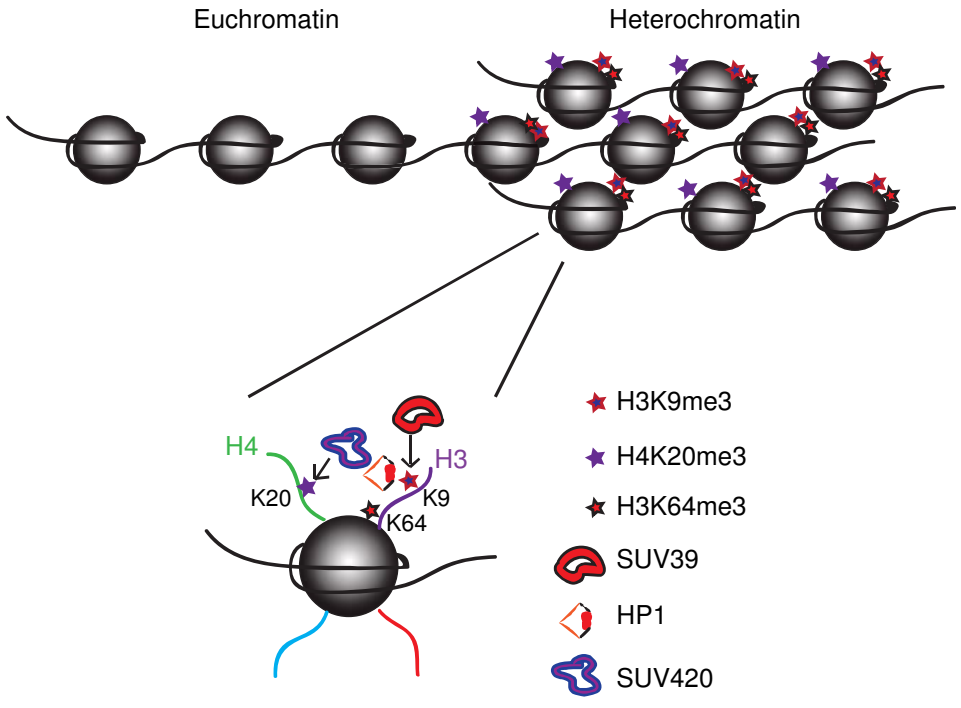


**Figure 9. Constitutive heterochromatin model of establishment in somatic cells.**
Schematic representation of euchromatin and constitutive heterochromatin organization, an inset is showing the current model of heterochromatin establishment and maintenance as explained in the text above.

I recently reviewed the topic on the establishment and maintenance of heterochromatic marks during preimplantation mouse development in (Fadloun, Eid, and Torres-Padilla 2013) to which I have contributed the section on "Heterochromatin in the Early Embryo: A Rather Particular Environment". This section describes the establishment and maintenance mechanisms of heterochromatin in the mouse embryo, as well as strategies and methods that have been used to study heterochromatin in the embryo. This review follows this section, within the Annex 1.

## Annex 1: Mechanisms and Dynamics of Heterochromatin Formation During Mammalian Development: Closed Paths and Open Questions

CHAPTER ONE

# Mechanisms and Dynamics of Heterochromatin Formation During Mammalian Development: Closed Paths and Open Questions

**Anas Fadloun[1], André Eid[1], Maria-Elena Torres-Padilla[2]**
Institut de Génétique et de Biologie Moléculaire et Cellulaire, CNRS/INSERM U964, Université de Strasbourg, Illkirch, France
[1]These authors contributed equally to this work.
[2]Corresponding author: e-mail address: metp@igbmc.fr

## Contents



## Abstract

Early embryonic development in mammals is characterized by major changes in the components of the chromatin and its remodeling. The embryonic chromatin and the nuclear organization in the mouse preimplantation embryo display particular features that are dramatically different from somatic cells. These include the highly specific organization of the pericentromeric heterochromatin within the nucleus and the suggested lack of conventional heterochromatin. We postulate that the plasticity of

*Current Topics in Developmental Biology*, Volume 104
ISSN 0070-2153
http://dx.doi.org/10.1016/B978-0-12-416027-9.00001-2

the cells in the early embryo relies on the distinctive heterochromatin features that prevail during early embryogenesis. Here, we review some of these features and discuss recent findings on the mechanisms driving heterochromatin formation after fertilization, in particular, the emerging role of RNA as a regulator of heterochromatic loci also in mammals. Finally, we believe that there are at least three major avenues that should be addressed in the coming years: (i) Is heterochromatin a driving force in development? (ii) Does it have a role in lineage allocation? (iii) How can heterochromatin "regulate" epigenetic reprogramming?

## 1. INTRODUCTION

Embryonic development is a specificity of metazoans. It starts with the fertilization of the oocyte by a sperm. Following fertilization, the gametes undergo intense chromatin remodeling and epigenetic reprogramming, which is necessary to revert into a totipotent state, essential to start a new developmental program. Importantly, in its natural context, such reprogramming should occur with 100% efficiency in order to sustain development.

In mammals, fertilization is followed by a series of successive divisions during which the embryo generates a higher cell number but maintains the same size overall until the blastocyst stage. The early blastocyst is composed of two lineages: the pluripotent cells of the inner cell mass (ICM), which will give rise to the embryo proper, and the trophectoderm, which will give rise to the placenta and is considered the first differentiated tissue in the embryo. A third lineage, the primitive endoderm, which is extraembryonic, emerges by the late blastocyst stage. After implantation of the blastocyst into the uterine wall, the embryo undergoes gastrulation, during which the three germ layers of the embryo are established and will be complemented by subsequent somitogenesis and organogenesis. During all these developmental processes, the structure of the chromatin is expected to be largely remodeled and modified. The changes to the structure of the chromatin are thought to have a direct effect on gene expression and therefore a key role in the control of developmental gene expression or repression.

In eukaryotic cells, the DNA is organized into chromatin, which regulates the accessibility of the genetic information. The building block of the chromatin is the nucleosome, which consists of two copies of each of the core histones H2A, H2B, H3, and H4 wrapped with ~146 bp of DNA (Luger, Mader, Richmond, Sargent, & Richmond, 1997). The histones are subject to an increasing number of covalent modifications such as methylation and acetylation, which have been shown to regulate chromatin-mediated processes in

multiple ways (Kouzarides, 2007). Variation in what is referred to as the primary structure of the chromatin can be thus achieved as a result of incorporation of an increasing number of histone variants and their accompanying post-translational modifications (Luger, Dechassa, & Tremethick, 2012). This variation has the potential to move the equilibrium to different chromatin states and therefore to impact on chromatin function. Globally, the chromatin is organized in two main functional and structural types or states: euchromatin and heterochromatin (Grewal & Elgin, 2007). The former is considered to be an open structure favorable for transcription and is gene rich, whereas the latter is considered to be in a closed structure that tends to be refractory for transcription and is gene poor. The heterochromatin can be further subdivided into two different types, facultative and constitutive. Facultative heterochromatin is characterized mainly by high levels of trimethylation of the lysine 27 of histone H3 (H3K27me3), a modification which is established by the polycomb repressive complex 2 (PRC2) and which also plays a role in the repression of developmental genes (Cao et al., 2002). However, the constitutive heterochromatin is characterized by strong enrichment of H3K9me3, H4K20me3, and H3K64me3, as well as of high levels of DNA methylation (Daujat et al., 2009; Peters et al., 2001; Schotta et al., 2004). The constitutive heterochromatin assembles mainly on centromeric, pericentromeric, and telomeric regions that are known to harbor repeated sequences such as the major and minor satellites. Constitutive heterochromatin is also present at imprinted genes in an allele-specific fashion and is considered to be a heritable trait that can be passed on to daughter cells and maintained (Regha et al., 2007). Several questions arise on how heterochromatin is established at these specific genomic regions after fertilization and naturally on how they are maintained and propagated through the cell cycle. Another key question that has so far been underinvestigated is whether there is any role for heterochromatin as such, in regulating embryonic development and the restriction of cell fate and plasticity. Indeed, as we propose below, the earliest stages of mammalian embryogenesis are characterized by a lack of a "conventional" heterochromatin.

The period that follows fertilization is particularly interesting in terms of chromatin remodeling due mainly to the genome-wide epigenetic reprogramming that the parental genomes are subject to (reviewed in Burton & Torres-Padilla, 2010). Erasure of most of the epigenetic information carried by the two highly differentiated gametes is thought to be necessary to restore developmental plasticity in the newly formed organism. The formation of the newly fertilized zygote constitutes therefore the climax of totipotency because of the resulting zygote's inherent ability to produce all cell types in a

new organism. However, this amazing capacity of the cells in the mouse embryo to generate all cell types seems to be transient as transplantation experiments have shown that cells from the ICM of a late blastocyst no longer have the potential to form trophectoderm derivatives (Rossant & Lis, 1979). Indeed, the ability of the early embryo to reprogram somatic nuclei decreases as development proceeds (Eckardt, Leu, Kurosaka, & McLaughlin, 2005), suggesting that the capacity to reprogram to totipotency also decreases during time.

What makes the cells in the early embryo capable of supporting such a large degree of plasticity? How is this plastic state achieved after fertilization and how is this state maintained in the early embryo? These questions have remained largely unanswered and are central for our understanding of cell plasticity, development, and reprogramming. We propose that the basis of such plasticity relies—at least partially—on the distinctive heterochromatin features that prevail during early embryogenesis. Here, we will review some of these major features and discuss recent findings that have shed some light on the mechanisms driving heterochromatin formation after fertilization, in particular, in light of what is known in other model systems where we have a more in depth mechanistic knowledge on the formation and maintenance of heterochromatin. Finally, we will put forward some of the questions that in our view represent the major key challenges to address in the field for the coming years.

## 2. HETEROCHROMATIN IN THE EARLY EMBRYO: A RATHER PARTICULAR ENVIRONMENT

Addressing the mechanisms behind the establishment of heterochromatin during the development of preimplantation mouse embryos is particularly relevant because of the huge changes on the chromatin that occur after fertilization. Indeed, most chromatin signatures have to be established *de novo* at the start of development. Because of this, the mouse embryo is one of the few model systems that offer the possibility of dissecting the mechanisms that underlie the establishment of heterochromatin in mammals, as opposed to studying heterochromatin maintenance and/or spreading in somatic cells, where heterochromatin only has to be maintained. Perhaps most interestingly, the question of whether a global rearrangement of heterochromatin and its structure impact on cell potency and development is a very attractive one.

Histones can be posttranslationally modified, and this provides an important level of functionality to the chromatin (Kouzarides, 2007; Strahl & Allis,

2000). The state of the chromatin can control the transcriptional state of a cell and the accessibility to its DNA. As pointed earlier, the two major chromatin states, the euchromatin and the heterochromatin, fluctuate dynamically and it is thought that they are only stabilized once the cells reach their "final" differentiation status. In this sense, the global state of the chromatin could for instance be considered to define the state of potency and plasticity of a cell, through the control of the accessibility to specific sequences of the DNA. In order to dynamically alter nucleosome spacing and/or accessibility, several mechanisms have been described that might in some instances work in a cooperative basis. These include (i) ATP-dependent chromatin remodelers, (ii) DNA methylation (and hydroxymethylation), (iii) histone modifications, (iv) incorporation of specific histone variants, and (v) the nuclear architecture, including the position that a given genomic region occupies within the nucleus.

The constitutive heterochromatin is marked by posttranslational modifications both on the N-terminus of histone tails and in the nucleosomal core region, in particular, by the enrichment of H3K9me3, H3K64me3, and H4K20me3 (Daujat et al., 2009; Peters et al., 2001; Schotta et al., 2004). This state of chromatin is localized to centromeric and pericentromeric regions as well as telomeric regions (the latter only containing H3K9me3) and is also known to be deacetylated (Grewal & Elgin, 2007). Repetitive elements in mammalian genomes are also known to be silenced through the acquisition of a constitutive heterochromatic signature (see Sections 3.5 and 3.6). While the constitutive heterochromatin is considered to assemble mainly at gene poor regions and repetitive elements, the facultative heterochromatin can be present in gene-rich regions that can switch their state between euchromatin and heterochromatin depending on multiple factors (Bernstein et al., 2006). The facultative heterochromatin is characterized by a strong enrichment of H3K27me3 and the related PRC1-catalyzed ubiquitination of H2AK119 (Grewal & Elgin, 2007).

Most posttranslational modifications of histones described to date, including phosphorylation, acetylation, and ubiquitination, are monolayered, which means that they have only one level of modification. In contrast, methylation of lysine residues has been described to occur at three layers: mono-, di-, and trimethylation, each of them with apparent different downstream effects. Indeed, this gives rise to different chromatin landscapes and/or recognition motifs at each layer of modification that can be read or modified by different types of readers and remodelers (Bonasio, Tu, & Reinberg, 2010; Kouzarides, 2007; Santos-Rosa et al., 2002). This has been

very clearly demonstrated through genome-wide analysis of a number of histone modifications using chromatin immunoprecipitation (ChIP)-Seq on native chromatin from resting human CD4 cells (Barski et al., 2007). The results from this analysis showed a different genomic distribution between the monomethylation states of H3K27, H3K9, and H4K20, which are mostly enriched at actively transcribed promoters, compared to the di- and trimethylation states of the three corresponding lysines, which are characteristic of silenced promoters. Thus, we will focus in our review on the function and analysis of the di- and trimethylation of these residues. It is of course unclear whether the results of these analyses, performed in somatic cells, can be applied to ES cells and embryos, where the chromatin seems to be in a slightly atypical configuration and gene expression is considered more dynamic. Therefore, an analysis in mouse embryos is necessary to establish a genome-wide correlation between gene expression and histone modifications or histone variants.

## 2.1. Dynamics of establishment of histone modifications during development and function of their histone methyltransferases

As an immediate response to fertilization by the sperm, the oocyte undergoes its second meiotic division. A totipotent zygote is formed. It is the only cell that contains two separate haploid nuclei within the same cytoplasm, which are therefore referred to as pronuclei. The paternal and maternal genomes remain physically distinct until at least the 2-cell stage and are marked by different chromatin modifications (Mayer, Niveleau, Walter, Fundele, & Haaf, 2000). At the zygote stage, the maternal pronucleus is characterized by the presence of histone trimethylation marks that are specific of constitutive heterochromatin, whereas the paternal genome generally lacks such heterochromatic marks. In particular, H3K9me3, H4K20me3, and H3K64me3 are found to localize to the pericentromeric chromatin in the maternal chromatin, but not in the paternal one (Arney, Bao, Bannister, Kouzarides, & Surani, 2002; Daujat et al., 2009; Kourmouli et al., 2004; Santos, Peters, Otte, Reik, & Dean, 2005). Perhaps the only known exception of a histone mark exclusively associated with the maternal chromatin that is not heterochromatic is H3K36me3, which is transmitted to the embryo on the maternal chromatin and then rapidly remodeled to become undetectable at the 2-cell stage (Boskovic et al., 2012). At around 12–14 h after fertilization, the zygote undergoes the first mitotic division and two daughter cells are formed, each containing a copy of the parental

chromosomes. H3K9me3 can be clearly seen in two-cell nuclei, but it marks asymmetrically half of each nucleus, which corresponds to the maternal chromatin that remains physically segregated from the paternal chromatin within the nucleus (Liu, Kim, & Aoki, 2004; Santenard et al., 2010) (Fig. 1.1). The levels of H4K20me3 are significantly reduced at the 2-cell stage to almost undetectable levels (Kourmouli et al., 2004; van der Heijden et al., 2005; Wongtawan, Taylor, Lawson, Wilmut, & Pennings, 2011), and H3K64me3 is no longer detected at the late 2-cell stage (Daujat et al., 2009). The 4-cell stage is thus characterized by the absence of H3K64me3, H4K20me3, and a marked decrease in H3K9me3 levels. H4K20me3 is not reestablished until after implantation, but the detailed spatiotemporal pattern of *de novo* methylation of H4K20me3 has not been studied. Global levels of H3K9me3 on the other hand continue to be reduced during the 8-cell stage judged from immunofluorescence analysis, and it would appear that H3K9me3 levels start to increase at the 16-cell stage and through the blastocyst stage, and are maintained thereafter (Puschendorf et al., 2008 and our unpublished observations). It should be noted though that most of these analyses are based on immunofluorescence approaches that have not been thoroughly or precisely quantified. It is worth mentioning that reacquisition of H3K9me3 globally seems to coincide with the time when the blastomeres undergo what can be described as the first differentiation step

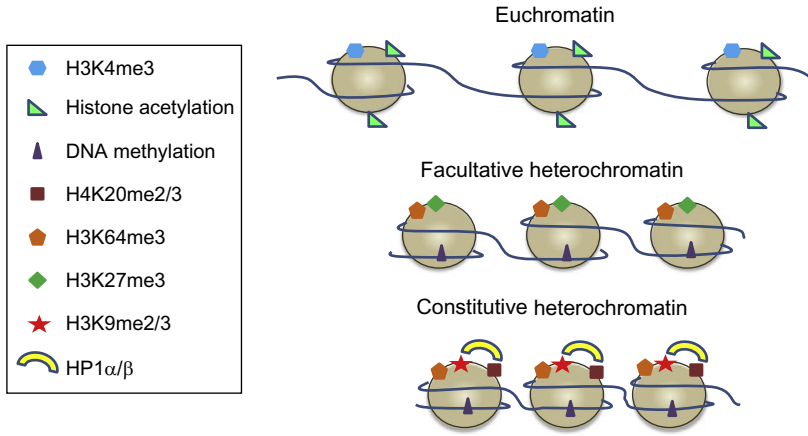


**Figure 1.1** Histone posttranslational modifications and the two chromatin states. Euchromatin is globally marked by H3K4me3 and acetylation of histone tails. However, facultative heterochromatin is marked by H3K27me2/3 and DNA methylation. The latter together with H3K64me3, H3K9me2/3, and H4K20me2/3 are typical of constitutive heterochromatin.

in the embryo, which is referred to as compaction and is achieved through the establishment of E-cadherin junctions at the end of the 8-cell stage.

Regarding the histone methyltransferases that catalyze the methylation of H3K9 and H4K20, many of them have been zygotically knocked-out in the mouse and some of them have early embryonic phenotypes (Table 1.1). In contrast, the methyltransferase(s) responsible for H3K64me3 have not been identified so far. At least eight proteins (Suv39h1, Suv39h2, G9a/Ehmt2, Eset/Setdb1, EuHMTase/GLP, Kmt1d, CLL8, SpClr4) have been described to methylate H3K9 (Kouzarides, 2007), and the list has been recently expanded to 10, as monomethyltransferase activity toward H3K9 has been observed for Prdm3 and Prdm16 (Pinheiro et al., 2012). The first five enzymes are active in mammalian cells (Dodge et al., 2004; Kouzarides, 2007). G9a is responsible for the mono- and dimethylation of H3K9 in euchromatic regions (Rice et al., 2003; Tachibana et al., 2002, 2005). Eset is responsible for the trimethylation of H3K9me3 in euchromatin (Wang et al., 2003; Yang et al., 2002), whereas EuHMTase promotes H3K9 dimethylation of the same regions. In contrast, Suv39h1/h2 can di- and trimethylate H3K9 in pericentric, centromeric, and telomeric regions (Peters et al., 2001; Rea et al., 2000). A key downstream "reader" of H3K9me3 is the heterochromatin protein 1 (HP1) (Bannister et al., 2001; Lachner, O'Carroll, Rea, Mechtler, & Jenuwein, 2001), which specifically recognizes H3K9me3 through its chromodomain. HP1 has been shown in turn to recruit the H4K20 methyltransferase Suv4-20 via its chromoshadow domain (Nielsen et al., 2001; Schotta et al., 2004). Suv4-20 would subsequently establish di- and trimethylation of H4K20me1, the latter being catalyzed by PR-Set7 (Nishioka et al., 2002; Schotta et al., 2004, 2008). These steps have been shown to operate in somatic cells to establish a constitutive heterochromatic configuration over the specific genomic regions (Rea et al., 2000; Schotta et al., 2004, 2008). The presence of H3K9me3 and H4K20me3 is characteristic of maternal centromeric and pericentromeric regions in the zygote, which are organized in a ring-like shape around the nucleolar-like bodies (NLBs). It has been shown recently that another mark is present on these regions: H3K64me3 (Daujat et al., 2009). However, the mechanism of establishment of this modification seems to be independent from the one that we described earlier (Lange et al., submitted for publication). Therefore, more work should be done in order to identify the role and effect of this histone mark during development.

A recent study has shown that a novel methyltransferase, Smyd5, can trimethylate H4K20. It was shown that the trimethylation established by this

**Table 1.1** Embryonic phenotypes of the knock-outs of proteins and complexes involved in heterochromatin establishment and/or maintenance

| Methyltransferase | Domain(s) | Function(s) | Location | Knockout | Phenotype | References |
|---|---|---|---|---|---|---|
| G9a | SET (*Suv3-9*, *E*(z)h, *Trx*) | Catalyzes H3K9me1/2 | Euchromatin | Embryo (full KO) | Lethal between E9.5 and E12.5. Developmental abnormalities. Reduction in H3K9me1/2 | Tachibana et al. (2002) |
| | ANK repeats | Binds H3K9me1/2 | | | | |
| | | | | Germ line (conditional KO) | Defects in meiotic prophase progression and gametogenesis. | Tachibana, Nozaki, Takeda, and Shinkai (2007) |
| | | | | ES (full KO) | Altered DNA methylation in the Prader-Willi imprinted region. | |
| ESET | SET | Catalyzes H3K9me3 | Euchromatin | Embryo (full KO) | KO of the SET domain: lethality at peri-implantation. Defects in ICM formation | Dodge, Kang, Beppu, Lei, and Li (2004) |
| | MBD (methyl-CpG-binding domain) | Binds methylated DNA | | | | |
| | Tudor | Recognizes arginine, H4K20 methylation | | | | |

*Continued*

**Table 1.1** Embryonic phenotypes of the knock-outs of proteins and complexes involved in heterochromatin establishment and/or maintenance—cont'd

| Methyltransferase | Domain(s) | Function(s) | Location | Knockout | Phenotype | References |
|---|---|---|---|---|---|---|
| GLP | SET | Catalyzes H3K9me3 | Euchromatin | Embryo (full KO) | Lethal between 9.5 and 12.5 dpc. Developmental abnormalities | Tachibana et al. (2005) |
| | | Catalyzes H3K27me *in virto* | | | Reduction not only in H3K9me3 but also in H3K9me1 and H3K9me2 | |
| | ANK repeats | Binds to H3K9me1 and H3K9me2 | | | Mislocalization of HP1 | |
| Suv39H1 | SET | Catalyzes H3K9me3 | Centromeric, pericentromeric, and telomeric heterochromatin | Embryo (full KO) | No developmental effect | Peters et al. (2001) |
| | Chromo | Recognizes methylated lysines (H3K9me3) | | | | |
| Suv39H1 | SET | Catalyzes H3K9me3 | Centromeric, pericentromeric, and telomeric heterochromatin | Embryo (full KO) | No developmental effect | Peters et al. (2001) |
| | Chromo | Recognizes methylated sites (H3K9me3) | | | | |

| | | | | | | |
|---|---|---|---|---|---|---|
| Suv39H1/2 | SET | Catalyzes H3K9me3 | Centromeric, pericentromeric, and telomeric heterochromatin | Embryo (full KO) | Prenatal lethality | Peters et al. (2001) |
| | Chromo | Recognizes methylated lysines (e.g., H3K9me3) | | | Replacement of H3K9me3 in heterochromatin with H3K27me3 | |
| | | | | Germ line (conditional KO) | Infertile male mice | |
| | | | | | Increased defects following DNA damage and missegregation during meiosis | Puschendorf et al. (2008) |
| HP1α | Chromo | Recognizes methylated sites (H3K9me3) | Heterochromatin | Embryo (full KO) | No developmental phenotype reported | Aucott et al. (2008) |
| | Chromoshadow | Protein–protein interactions | | | | Brown et al. (2010) |
| | Hinge | RNA/DNA interactions | | | | |

*Continued*

**Table 1.1** Embryonic phenotypes of the knock-outs of proteins and complexes involved in heterochromatin establishment and/or maintenance—cont'd

| Methyltransferase | Domain(s) | Function(s) | Location | Knockout | Phenotype | References |
|---|---|---|---|---|---|---|
| HP1β | Chromo | Recognizes methylated lysines (H3K9me3) | Heterochromatin | Embryo (full KO) | Perinatal lethality | Aucott et al. (2008) |
| | Chromoshadow | Protein–protein interactions | | | Aberrant cerebral cortex development | |
| | Hinge | RNA/DNA interactions | | | | |
| HP1γ | Chromo | Recognize methylated lysines (H3K9me3) | Euchromatin | Embryo (full KO) | Developmental effect? | Takada et al. (2011) |
| | Chromoshadow | Protein–protein interactions | | | Sterility of male mice | Brown et al. (2010) |
| | Hinge | RNA/DNA interactions | | | | Naruse et al. (2007) |
| Suv4-20H1 | SET | Catalyzes H4K20me2/3 | Heterochromatin | Embryo (full KO) | No developmental phenotype reported | Schotta et al. (2008) |
| Suv4-20H2 | SET | Catalyzes H4K20me2/3 | Heterochromatin | Embryo (full KO) | No developmental phenotype reported | Schotta et al. (2008) |

| | | | | | | |
|---|---|---|---|---|---|---|
| Suv4-20H1/2 | SET | Catalyzes H4K20me2/3 | Heterochromatin | Embryo (full KO) | Perinatal lethality | Schotta et al. (2004) |
| | | | | MEFs (conditional KO) | Increase in DNA damage sensitivity<br>Cell cycle defects and chromosomal aberrations | Schotta et al. (2008) |
| EED | WD repeats | Protein–protein interactions and assembly | | Embryo (full KO) | Problems with gastrulation leading to lethality | Shumacher, Faust, and Magnuson (1996) |
| | | | | | Loss of maintenance of the inactive state of the X chromosome in trophoblast cells | Wang et al. (2001) |
| E(z)h2 | SET | Catalyzes H3K27me3 | | Embryo (full KO) | Embryonic lethality caused by problems by implantation, gastrulation and growth defects | O'Carroll et al. (2001) |
| | | | | Germ line (conditional KO) | No effect due to a rescue of the phenotype probably caused by the paternal allele | Erhardt et al. (2003) |
| Suz12 | Zinc finger domain | | | Embryo (full KO) | Lethality around E8.5 with similar phenotype to Eed and E(z)h −/− | Pasini, Bracken, Jensen, Lazzerini Denchi, and Helin (2004) |

enzyme has a repressive effect on gene function, but its function *in vivo* or whether Smyd5 integrates in the heterochromatin feedback loop described earlier has not been addressed (Stender et al., 2012).

Loss-of-function strategies of the corresponding methyltransferases have been used in order to study the function of histone methylation of H3K9 and H4K20. However, in most cases, they have not been deleted specifically in the maternal germ line and therefore the embryos analyzed carry maternal contribution of these methyltransferases, since their mRNAs are present in the oocyte (Hamatani, Carter, Sharov, & Ko, 2004; Wang et al., 2004; Zeng & Schultz, 2005). A role for H3K9 and H4K20 methylation during the earliest stages of preimplantation development has therefore not been addressed directly.

Double null embryos for G9a show high lethality between embryonic day (E) 9.5 and E12.5, with many morphological defects and loss of weight compared to heterozygous littermates. This result showed that G9a is necessary for proper embryonic development and thus that methylation of H3K9 in euchromatic regions is functionally essential for mid-gestation (Tachibana, Sugimoto, Fukushima, & Shinkai, 2001; Tachibana et al., 2002). Furthermore, conditional KO of G9a in the mouse germ line showed that it is essential for meiotic prophase progression and is involved in gametogenesis (Tachibana et al., 2007). Finally, conditional KO of G9a in CD4(+) T cells (Lehnertz et al., 2010) or adult neuronal cells (Schaefer et al., 2009) in adult mice showed a functional role for the reduction of H3K9me2 in immune and cognitive abnormalities. Interestingly, studies have demonstrated that KO of GLP has the same phenotype as $G9a^{-/-}$ during embryogenesis. This is somewhat expected since GLP and G9a can form heterodimeric structures and might positively regulate each other's catalytic activity: indeed, KO of GLP causes a reduction not only in H3K9me3 but also in H3K9me1 and H3K9me2 in euchromatic regions, resulting in relocalization of HP1 (Tachibana et al., 2005). Deletion of the SET domain of ESET results in embryonic death around peri-implantation with defects in ICM formation and inability to derive ES cell lines (Dodge et al., 2004). RNAi-mediated silencing of ESET in murine ES cells causes the differentiation of these cells into trophoblastic lineage, thus demonstrating a potential role in restricting the fate of ICM cells during development (Yuan et al., 2009).

Single KO of either Suv39h1 or Suv39h2 seems not to have an effect on development, but double null mice for Suv39h1 and Suv39h2 show increased prenatal lethality than wild-type mice as well as genome instability upon DNA damage and missegregation during meiosis (Peters et al., 2001).

However, no early embryonic defects have been described. It has also been observed in *dn* Mouse Embryonic Fibroblasts (MEFs) mutant for Suv39h1/2 that the loss of H3K9me3 was accompanied by an increase of H3K27me3 in, for example, pericentromeric repeats (Martens et al., 2005), which seemed to compensate for the lack of Suv3-9 activity on these regions. In the mouse zygote, the Peters lab proposed that there is a hierarchy between the constitutive and facultative heterochromatin at the pericentric and centromeric regions. In case of the incorrect establishment of H3K9me3 mark in the maternal pronucleus, H3K27me3 is established as a fail–safe mechanism to silence these repetitive sequences (Puschendorf et al., 2008). However, the sensing or targeting mechanism for the ability of the PRC2 to deposit H3K27me3 in this context has not been established yet. It was also not reported whether the loss of H3K9me3 on the maternal pericentric chromatin had any effect on the recruitment of Suv420H1/2 and thus if there was any accompanying reduction in H4K20me2/3.

In mammals, there are two genes that code for Suv4-20, *Suv4-20h1* and *Suv4-20h2*, and they that been genetically inactivated both in isolation and in combination. The double KO of Suv4-20h1 and Suv4-20h2 mice also display perinatal lethality, as well as an increase in DNA damage sensitivity, cell cycle defects and chromosomal aberrations (Schotta et al., 2004, 2008). A potential role for *Suv4-20h1/h2* in preimplantation development has not been reported.

The other main component of constitutive heterochromatin is HP1. Mammals have three different HP1 isoforms: HP1α, β, and γ in humans (CBX5, 1 and 3, respectively, in mice). The three HP1s contain the same modular structure: a chromoshadow domain that is involved in protein–protein interactions (Nielsen et al., 2001), a hinge domain that binds ssDNA and RNA (Muchardt et al., 2002), and a chromodomain that recognizes and binds to H3K9me2/me3 (Lachner et al., 2001). An HP1α KO has been reported to have no apparent effect on embryonic development (Aucott et al., 2008; Brown et al., 2010). There seems to be some degree of redundancy among HP1 proteins. Indeed, the HP1γ KO did not show any developmental phenotype, and the authors suggested that the other paralogues of HP1 might compensate for its loss. The absence of HP1γ does result, however, in major defects in chromosome segregation in spermatocytes and leads to severe male sterility (Naruse et al., 2007; Takada et al., 2011). Perhaps surprisingly, in contrast to the KO model, a hypomorphic mutant for HP1γ shows high lethality after birth with only 1% of mice reaching adulthood but with similar effect on spermatogenesis (Brown et al., 2010). Of the three HP1 isoforms, only the HP1β KO mice

show a very strong phenotype, with perinatal lethality and aberrant cerebral cortex development, suggesting a role for HP1β in late stages of development (Aucott et al., 2008). As mentioned earlier, it will be important to probe the function of the HP1 proteins after fertilization by performing, for example, conditional KOs in the maternal germ line. This is particularly relevant in light of the fact that HP1α seems to be absent from embryonic chromatin until the blastocyst stage, whereas HP1β is tethered onto embryonic pericentromeric chromatin as early as in the zygote stage (Arney et al., 2002; Santenard et al., 2010; Santos et al., 2005; Wongtawan et al., 2011). This mirroring temporal expression pattern might suggest different functions of these two HP1 isoforms during epigenetic reprogramming *in vivo*.

Although not strictly a constitutive heterochromatic mark, H3K27me3 has probably a "dual" role during early development. Indeed, it seems to be able to replace functionally the absence of H3K9me3/H4K20me3 on the paternal pericentric heterochromatin (Puschendorf et al., 2008; Santenard et al., 2010). The KOs of several of the components of the PRC2 do show early developmental phenotypes. The catalytic subunit of PRC2, Ezh2, is required for implantation, and mutant embryos for Ezh2 show defective growth, poor implantation rates, and gastrulation defects (O'Carroll et al., 2001). The maternal deletion of Ezh2 has a growth retardation effect on born pups, but the phenotype seems to be rescued by the expression of the paternal allele (Erhardt et al., 2003). The second PRC2 core subunit, Eed, is necessary for gastrulation (Faust, Lawson, Schork, Thiel, & Magnuson, 1998; Shumacher et al., 1996) and for the maintenance of the inactive state of the X chromosome in trophoblast cells (Wang et al., 2001). The KO of the third and last core subunit of PRC2, Suz12, shows a similar phenotype to the *Ezh2* and $Eed^{-/-}$ mice with lethality occurring at E8.5 (Pasini et al., 2004). All these phenotypes are in line with the observation that all three subunits are absolutely required for H3K27me3. Deletion of other Polycomb proteins such as YY1 results in preimplantation lethality and in defective ICM growth (Donohoe et al., 1999). It is therefore very well established that Polycomb proteins play key and essential developmental roles during preimplantation development.

These loss-of-function strategies have established that heterochromatin (through the di- and trimethylation of H4K20, H3K9, and H3K27) is important for developmental processes but do not establish the mechanism by which these modifications confer a cellular effect. Furthermore, several groups have studied the KO of some of these genes in the germ cells and showed an effect on spermatogenesis, but only a few/none of them have

probed the effects on the oocyte development and the maternal contribution to the embryo. Many mRNAs as well as most of the cellular machinery (ribosomes, mitochondria, etc.) are inherited from the oocyte (Poznanski & Calarco, 1991; Smith & Alcivar, 1993; Wagner, 1972). Furthermore, the cytoplasmic components of the oocyte have all the necessary material to reprogram a somatic nucleus (Chan, Smith, Egli, Regev, & Meissner, 2012). Therefore, it would be highly important to directly address the effects of the lack of these methyltransferases from the earliest stages of development. Although with some caveats, the most straightforward way to probe this is probably through the elaboration of conditional KO in the oocyte.

In summary, histone modifications typical of constitutive heterochromatin in somatic cells are exclusively detected on the maternal chromatin at the very beginning of development only. They either become undetectable at the 2-cell stage or are "diluted" upon division until methylation starts to occur *de novo* globally at least three cell divisions later depending on the mark. Indeed, the kinetics of reacquisition of these histone methylation marks seems to be slightly different depending on the histone modification in question (Fig. 1.2). This lack of conventional heterochromatin during the first divisions following fertilization presumably creates a chromatin environment that is permissive for epigenetic reprogramming and a "window of opportunity" for transcription of heterochromatic regions that are normally not transcribed such as retrotransposons (see Section 3.5).

## 2.2. DNA methylation and hydroxymethylation

DNA methylation of cytosines functions in gene silencing (Goll & Bestor, 2005). In spite of being a highly differentiated cell, the sperm shows a promoter DNA methylation landscape that resembles globally that of pluripotent ES cells with a few key exceptions (Farthing et al., 2008). This feature has been suggested to reflect the epigenetic reprogramming of the germ line prior to fertilization and to be important in the transmission of pluripotency to the embryo. The oocyte shows an overall global hypomethylation status and does contribute with a number of specific methylated regions, including differentially methylated regions to the embryo (Smallwood et al., 2011; Smith et al., 2012). Upon fertilization, there is a reduction in global DNA methylation levels that is specific to the paternal genome (Mayer et al., 2000; Rougier et al., 1998). These conclusions were made mainly by using a 5-methylcytosine (5mC) antibody in immunostaining, which clearly reveals a loss of the epitope in the paternal pronucleus. A current emerging notion is, however, that the extent of this demethylation is lesser

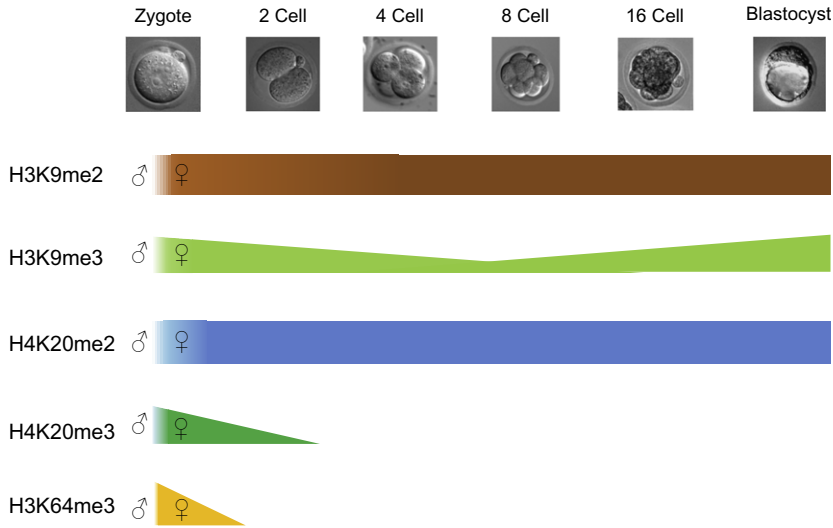


**Figure 1.2** Dynamics of the main constitutive heterochromatic marks during preimplantation development. All heterochromatin marks analysed to date are asymmetrically localized on the maternal chromatin during the zygote stage. The levels of H3K9me2 and H4K20me2 are maintained relatively stable during the early stages of development, whereas global H3K9me3 levels decrease between the 4-cell and the 16-cell stage. H4K20me3 is undetectable on embryonic chromatin by the end of the 2-cell stage and similar kinetics have been described for H3K64me3, which is only present during the zygote stage and is absent afterward.

than what was originally thought and that DNA methylation in the zygote occurs both actively (e.g., before the first round of replication) and passively (concomitant with replication). DNA demethylation has been suggested to be, at least partially, the consequence of the conversion of cytosine methylation to hydroxymethylation by the Tet proteins (Gu et al., 2011; Inoue & Zhang, 2011; Tahiliani et al., 2009; Wossidlo et al., 2011). Together, this results in an asymmetry in DNA modifications between the paternal genome (enriched in DNA hydroxymethylation) and the maternal genome (enriched in DNA methylation) at the zygote stage (Gu et al., 2011; Inoue & Zhang, 2011; Iqbal, Jin, Pfeifer, & Szabo, 2011; Wossidlo et al., 2011). As development progresses, the differences in DNA methylation and hydroxymethylation disappear (Inoue & Zhang, 2011; Iqbal et al., 2011). The overall DNA methylation levels in the embryo decrease during early development and then increase in the epiblast at the blastocyst stage (Mayer et al., 2000; Santos, Hendrich, Reik, & Dean, 2002). On the imprinted genes, however, DNA methylation is not completely lost and

is maintained through development until the formation of the primordial germ cells (PGCs) (Goll & Bestor, 2005). Nevertheless, when looking at single copy genes in detail, the levels of DNA methylation do not seem to obey to a simple kinetic behavior, but there seems to be different waves of re/demethylation in specific regions throughout preimplantation development and even after implantation. It seems more likely that an equilibrium between loss of methylation and *de novo* methylation at different stages of development results in the final methylation landscape of somatic cells (Borgel et al., 2010; Proudhon et al., 2012). Three enzymes catalyze DNA methylation: Dnmt1, Dnmt3A, and Dnmt3B. Dnmt3A and Dnmt3B require for their function another related protein, Dnmt3L (Bourc'his, Xu, Lin, Bollman, & Bestor, 2001; Hata, Okano, Lei, & Li, 2002). The KO of Dnmt1 is lethal at midgestation with growth defects, but Dnmt1 is not required for ES cell maintenance (Li, Beard, & Jaenisch, 1993). The KO of either Dnmt3A or Dnmt3B is also lethal during development, with Dnmt3B specifically required for methylation of centromeric minor satellite repeats (Okano, Bell, Haber, & Li, 1999). Both of these genes are required for *de novo* methylation during development and in ES cells (Okano et al., 1999). Loss of Dnmt3L had the same phenotype as Dnmt3A with loss of imprinting at almost all of the same sites, but not in pericentric regions (Bourc'his & Bestor, 2004; Kaneda et al., 2004). Altogether, these studies would argue that *de novo* DNA methylation *per se* is not required prior to implantation.

Three Tet family enzymes (Tet1/2/3) convert 5mC to 5-hydroxymethylcytosine (5hmC) (reviewed in Tan & Shi, 2012 and Wu & Zhang, 2011). The KO of Tet1 has no effect on development or on pluripotency of ES cells (Dawlaty et al., 2011), although there are conflicting reports concerning the effect of Tet1 silencing using small heterochromatic RNAs (shRNAs) in ES cells (Ito et al., 2010). KO of Tet2 seems also to be dispensable for development (Quivoron et al., 2011). The conditional KO of Tet3 in the oocyte results in loss of conversion of 5hmC to 5mC on the paternal genome in the mouse zygote and in increased incidence of developmental failure as well as reduced fertility (Gu et al., 2011). It has been shown recently that H3K9me2 can be recognized by PGC7/Stella in order to prevent the conversion of 5mC to 5hmC, thus protecting DNA methylation (Nakamura et al., 2012). This might be a mechanism whereby the asymmetry between the paternal and maternal genomes in 5mC and 5hmC is generated, since as we mentioned earlier, H3K9me2 is exclusively present in the maternal chromatin.

## 2.3. Histone variants in heterochromatin in the embryo

The two gametes have a very different landscape of histone variants and chromatin compaction. For instance, the sperm is almost devoid of histones and is instead packed by protamines, a histone-like protein (Nonchev & Tsanev, 1990). This replacement is important physically and physiologically because it will help to package the paternal genome to fit into the sperm head for subsequent transportation through the uterus and ovidcut to reach the oocyte. The DNA bound to protamines reaches 6–20 times more compact packaging compared to the nucleosomal organization (Jenkins & Carrell, 2012; Ward & Coffey, 1991). The protamination of the sperm DNA is tightly regulated and is important for fertility (Aoki, Liu, & Carrell, 2005; Balhorn, Reed, & Tanphaichitr, 1988), but it was also considered to result in the loss of any potential epigenetic information carried through the histones. However, the replacement of histones is not complete and between 5% and 15% of histones depending on the species remains bound to DNA (Jenkins & Carrell, 2012; Wykes & Krawetz, 2003). This retention seems not to be stochastic since developmental gene promoters that are important for embryonic development seem to retain histones specifically (Brykczynska et al., 2010; Hammoud et al., 2009). More interestingly, such promoters, which are silent during preimplantation development, retain H3K27me3 in the sperm (Hammoud et al., 2009). This result suggests that the nucleosomes retained in the sperm might act as transmitters of silencing information for some genes during early development. Additionally, testis-specific histone variants exist (Moss, Challoner, & Groudine, 1989; Trostle-Weige, Meistrich, Brock, & Nishioka, 1984; Witt, Albig, & Doenecke, 1996) and have been described to be posttranslationally modified (Lu et al., 2009), although the function of these modifications has not been addressed in the context of the zygotic reprogramming. Most interestingly, constitutive heterochromatic regions display a distinctive organization in the sperm, with both telomeres and centromeres retaining histones and most likely some of their modifications (Govin et al., 2007; Wykes & Krawetz, 2003). In particular, testis-specific variants of H2A, H2AL1, H2AL2, and TH2B are found in the pericentric chromatin to achieve a DNA packaging structure that protects a ~60 bp DNA fragment (Govin et al., 2007).

The oocyte also contains some specific histone variants but most likely retains the traditional nucleosome packaging of the DNA (Chang et al., 2005). The oocyte is thought to further contain a pool of histones that are to be inherited by the zygote in order to replace the protamines of the paternal genome upon fertilization. The mechanism by which the

replacement takes place is not well understood. The histone H3.3 has been shown to localize preferentially to the paternal chromatin during the zygote stage (Loppin et al., 2005; Santenard et al., 2010; Torres-Padilla, Bannister, Hurd, Kouzarides, & Zernicka-Goetz, 2006; van der Heijden et al., 2005). We have shown in the lab that the mutation of the lysine K27 to alanine of H3.3 results in a missegregation of chromosomes as well as developmental arrest and mislocalization of HP1. The same mutation in H3.1 does not seem to have any effect on either HP1 localization or developmental progression (Santenard et al., 2010). The same work suggested that incorporation of H3.3 in the paternal pericentric heterochromatin is important for the initial establishment of pericentromeric heterochromatin through its lysine 27. It therefore seems that H3.3 has acquired a role in remodeling heterochromatin after fertilization. This is in line with the preferential heterochromatic localization of H3.3 during the first embryonic divisions (Akiyama, Suzuki, Matsuda, & Aoki, 2011; Santenard et al., 2010).

## 2.4. Nuclear architecture in the mammalian embryo

The most astonishing observation that can be made immediately after fertilization is probably the difference in the size of the two pronuclei and the distinctive organization of the heterochromatin in both of them, which is radically different to that of somatic cells (Fig. 1.3).

The paternal pronucleus is almost 25% bigger than the maternal one. This spatial organization reflects the decondensation of the paternal genome that starts with fertilization. This process, which is accompanied by cycles of recondensation and further decondensation (Bouniol-Baly, Nguyen, Besombes, & Debey, 1997; Martin et al., 2006; Probst et al., 2010; Probst, Santos, Reik, Almouzni, & Dean, 2007), might be important for the subsequent establishment of the nuclear compartments and/or characteristic embryonic nuclear architecture. No heterochromatic marks can be detected on the paternal chromatin at this time, but H3K9me1 and H3K27me1 have been observed on the paternal pronucleus as early as during the first decondensation (Santos et al., 2005). This coincidence might reflect some spatiotemporal requirement that needs to be put in place before heterochromatic marking (e.g., H3K27me3) can be added a couple of hours later. Indeed, the changes in decondensation coincide with the emergence of the NLBs. These are ring-like structures around which the centromeric and pericentromeric sequences localize (Probst et al., 2007). The organization of the pericentromeric domains around NLBs is maintained at least until

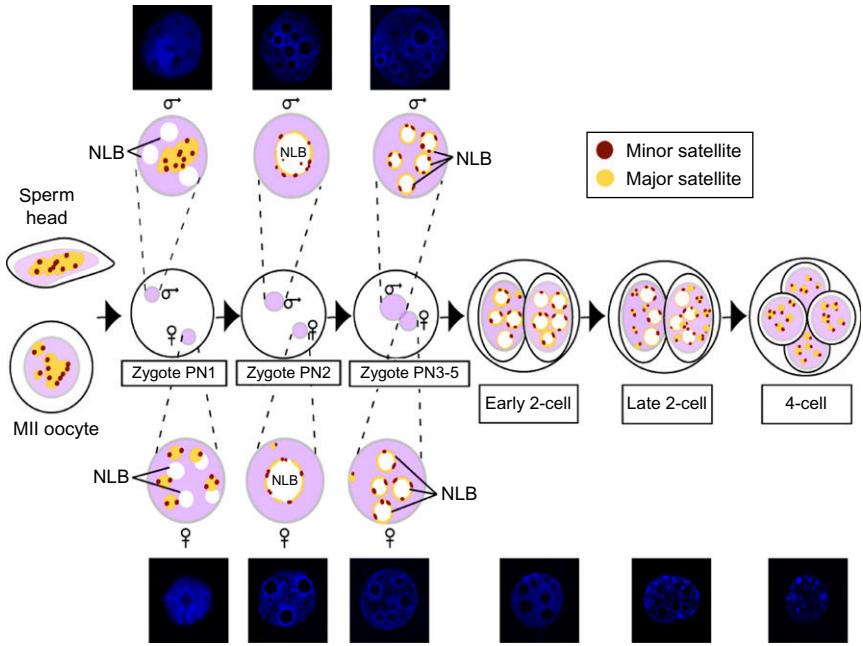


**Figure 1.3** Nuclear architecture changes during preimplantation development in the mouse. The nuclear organization changes dynamically after fertilization. The nucleolar-like bodies (NLBs) are established after fertilization at the pronuclear stage (PN) 1 in the zygote. At the PN2 stage, the minor and major satellites (MMS) reorganize to form a ring-like structure around the NLBs. Between the PN3 and PN5 an increase in the number of NLBs occurs, but the position of the MMS remains the same. At the early 2-cell stage (E2C), the nuclear organization starts to change and by the end of the 2-cell stage (L2C) many MMS start to form new chromocenters independently of the NLBs structure. By the 4-cell stage, most of the NLBs have disappeared and instead the majority of MMS are clustered into "somatic"-like chromocenters. Note that nuclei are not at the same scale.

the 4-cell stage in some nuclei (Martin et al., 2006; Probst et al., 2010, 2007). As development progresses, the NLBs are replaced with chromocenters, which are the clusters of centromeric and pericentromeric regions that appear typically brightly stained by 4′,6-diamidino-2-phenylindole (DAPI) in most somatic cells. The chromocenters are a defining feature of somatic nuclei organization. The disappearance of any reminiscent NLBs in the mouse embryo seems to coincide with the 8-cell stage, which is the stage when cells undertake their first differentiation step (polarization and compaction). It is interesting to note that at this stage, the levels of H3K9me3 seem to be lowest (Fig. 1.2), and H4K20me3 is also absent from embryonic chromatin, suggesting that a loss of heterochromatin might be important for this structural

change in the conformation of pericentromeric chromatin. This is even more important if we take into account the reports, indicating that the establishment of NLBs-like structure after somatic nuclear transfer might increase the probability of success in reprogramming the somatic nucleus (Maalouf et al., 2009; Martin et al., 2006). Functionally, whether this particular spatial nuclear positioning of the heterochromatic and/or its evolution toward a chromocenter configuration is important for development has not been addressed.

From all the above, it is clear that global heterochromatin dynamics seem to be particularly relevant during the earliest stages of development. They most likely impact not only on inheritance but also on the establishment of the embryonic epigenome and the embryo's subsequent differentiation capacities. The dramatically different configuration of embryonic heterochromatin compared to somatic cells is probably linked functionally to the plasticity of the early embryo and to the reprogramming process that occurs during this period. Our understanding of the molecular mechanisms that govern *de novo* establishment of heterochromatin domains after fertilization is, however, still very poor. It is therefore essential to uncover the mechanisms driving heterochromatin formation in mammals in order to fully understand the regulation of epigenetic reprogramming and establishment of pluripotency and plasticity.

Because the paternal genome, due to its packing into protamines, has to acquire a nucleosomal configuration and all the subsequent chromatin signatures for the first time after fertilization, the early mouse embryo constitutes a unique system to address the mechanisms of heterochromatin formation in mammals. However, it is not known how chromatin domains and their epigenetic signatures are established *de novo* in the zygote nor it is the extent to which these domains contribute to the regulation of cell potency. Most of our knowledge on heterochromatin formation and in particular on its establishment comes from work in *Schizosaccharomyces pombe* and *Arabidopsis* (Grewal & Elgin, 2007; Martienssen, Kloc, Slotkin, & Tanurdzic, 2008), but little is known on how heterochromatin is initially established in mammalian cells. This is mainly because in most cells heterochromatin only needs to be maintained as opposed to established *de novo*.

In the next section, we will first discuss extensively the main known mechanisms of establishment and inheritance of heterochromatin in other model systems, in particular, in fission yeast. We will then devote a section to draw parallels and open questions in the mammalian embryo and will discuss how other heterochromatic regions such as retrotransposons could be regulated during early mammalian embryogenesis.

## 3. MECHANISMS OF HETEROCHROMATIN ESTABLISHMENT AND INHERITANCE

### 3.1. Heterochromatin establishment and centromeric chromatin

The histone modification marks that are characteristic of constitutive heterochromatin along with the enzymes that produce these modifications and the proteins that recognize them are highly conserved from fission yeast to human (Kouzarides, 2007). From fission yeast to mammals, methylation of H3K9 is considered to be crucial for heterochromatin assembly (Bannister et al., 2001; Lachner et al., 2001; Rea et al., 2000). As pointed out earlier, in mammals several proteins can methylate H3K9, whereas in fission yeast, Clr4, a single histone H3K9 methyltransferase, directs all methylation of K9 on histone H3 (Yamada, Fischle, Sugiyama, Allis, & Grewal, 2005). Fission yeast lacks the enzymatic machinery for methylation of H3K27 and is also devoid of DNA methylation.

The centromere is a well-known landmark of silent chromatin and a paradigm for epigenetic inheritance. Ultrastructurally, it takes the form of a distinct primary constriction on the condensed metaphase chromosome of higher eukaryotes. The constricted region comprises a different chromatin structure consisting of DNA and protein complexes (the kinetochores) to which microtubules bind to effect proper chromosome movements (Folco, Pidoux, Urano, & Allshire, 2008; Pidoux & Allshire, 2005). The DNA sequence in the centromere is not conserved between organisms, yet the centromere displays similar features across evolution such as the presence of repetitive elements that include the alpha satellite in humans, the minor satellite in mice, the AATAT and TTCTC satellites in *Drosophila* (Cleveland, Mao, & Sullivan, 2003). Consequently, the sequence requirements, if any, for a functional centromere are not established.

In fission yeast, the constitutive heterochromatin regions are linked to centromeres, telomeres, and the mating-type locus. Although there are some variations, the global mechanisms of heterochromatin assembly on all these regions are similar. The centromeres in yeast range from 35 to 110 kb in length, with a central domain on which the kinetochore assembles flanked by outer repeat (*otr*) sequences (consisting of *dg* and *dh* repeats) coated in heterochromatin that resemble the pericentomeric heterochromatin in mammals (Steiner, Hahnenberger, & Clarke, 1993; Wood et al., 2002). Experiments performed with minichromosomes have demonstrated

that DNA sequences from both the *otrs* and the central domain are required for full centromere function (Folco et al., 2008; Wood et al., 2002). Interestingly, the role of the *otr* sequences seems to be purely to provide a functional platform for heterochromatin assembly, since centromeres lacking *otr* sequences become functional when an enzyme that drives heterochromatin assembly is tethered adjacent to the central domain sequences (Kagansky et al., 2009).

It was originally thought that fission yeast centromeres were transcriptionally inert, as a marker gene inserted within centromeric sequence exhibited classical position effect variegation (Allshire, Javerzat, Redhead, & Cranston, 1994; Allshire, Nimmo, Ekwall, Javerzat, & Cranston, 1995). This silencing was thought to reflect spreading of heterochromatin over the inserted gene, thereby blocking access of RNA polymerase II (Pol II). However, it has been demonstrated that centromeres and *otrs* are transcribed in both fission yeast and mammals, and that transcript abundance in yeast is regulated by the RNAi machinery (Lehnertz et al., 2003; Volpe et al., 2002). Most importantly, the transcription of these repeats that triggers the RNAi machinery is an essential part of the heterochromatin assembly pathway. Centromeric transcription occurs during S-phase, during a window of time in which the repressive histone marks at centromeres become diluted upon DNA replication, allowing Pol II access (Chen et al., 2008; Kloc, Zaratiegui, Nora, & Martienssen, 2008).

## 3.2. Establishment and assembly of constitutive heterochromatin

Heterochromatin assembly is a multistep process. Studies from diverse systems suggest that a common set of structural components contribute to the construction of the heterochromatin platform. Initial targeting of heterochromatin to nucleation sites seems to be distinct from the subsequent heterochromatic spreading and maintenance steps. The strategies that are used by the cell to target heterochromatin differ depending on the chromosomal context. Local *cis*-acting sequences can promote the establishment of facultative heterochromatin, as exemplified by retinoblastoma protein and KRAB–KAP1-mediated recruitment of HP1 and SUV39 proteins (Nielsen et al., 2001; Schultz, Ayyanathan, Negorev, Maul, & Rauscher, 2002). The establishment of constitutive heterochromatin is however most often related to the presence of repetitive DNA elements. It is rather the repetitive nature of the genomic regions where heterochromatin assembles and not the DNA sequence itself, which functions as a trigger for

heterochromatin formation (Luff, Pawlowski, & Bender, 1999). These repeats serve as template for the production of noncoding RNA (ncRNA) from both DNA strands, which is often associated with the generation of dsRNA. Although heterochromatin is a silent chromatin structure that blocks transcription, RNA Pol II transcribes these repeats in an exquisitely regulated temporal fashion at particular stages of the cell cycle (Chen et al., 2008; Kloc et al., 2008). Therefore, there seems to be an important and conserved role for both ncRNA and RNAi in this context (Matzke & Birchler, 2005).

The RNAi machinery was originally defined as a regulator of posttranscriptional silencing (Muller et al., 2002), but it is now clear that the RNAi machinery also alters chromatin structure and effects silencing at the transcriptional level. Most importantly, RNAi is central for initiating heterochromatin assembly not only at repetitive DNA in the centromeres and mating-type loci of fission yeast but also at retrotransposons in the *Arabidopsis* germ line (Grewal & Elgin, 2007). In fission yeast, siRNAs derived from heterochromatic repeats are present within the cell and are loaded into the RNA-induced transcriptional silencing (RITS) complex, which is composed of Ago1, Tas3, and the chromodomain-containing protein Chp1(Verdel et al., 2004). RITS is thought to bind to heterochromatic ncRNA using siRNA as a guiding molecule. It further participates in "amplifying" the response since it recruits the RNA-dependent RNA polymerase complex (RDRC), which consists of Rdp1, a poly(A) polymerase (Cid12), and a putative helicase (Hrr1), most likely via physical interactions (Verdel et al., 2004). The RDRC enhances the generation of siRNA by synthesizing dsRNAs from centromeric transcripts as substrates for Dcr1 (Colmenares, Buker, Buhler, Dlakic, & Moazed, 2007; Sugiyama, Cam, Verdel, Moazed, & Grewal, 2005). RITS also recruits Clr4 through the LIM domain protein, Stc1, such that the heterochromatin spreads onto the *dg* and *dh* repeats (Zhang, Mosch, Fischle, & Grewal, 2008). Stc1 associates with RITS on centromeric transcripts and recruits the Clr4-containing complex (CLRC), thereby coupling RNAi to chromatin modification (Bayne et al., 2010). Methylation of H3K9me3 is also recognized by Swi6/HP1, which further reinforces the silencing environment by mediating targeting of HDACs and is also responsible of recruiting the JmjC domain-containing antisilencing factor Epe1 that facilitates the transcription of heterochromatic repeats (see below) (Zofall & Grewal, 2006).

In the RNAi-mediated heterochromatin assembly system, siRNA generation and heterochromatin formation are interdependent, forming a

"self-reinforcing loop." The self-reinforcing as well as the *cis*-acting nature of siRNA during RNAi-mediated heterochromatin formation suggests that the whole process is coupled to the chromatin. This is supported by ChIP experiments, which show the physical association of Ago1 and Rdp1 with chromatin (Cam et al., 2005; Volpe et al., 2002). Recently, DNA adenine methyltransferase identification methods to identify DNA binding sites *in vivo* were used to show that Dcr1 also associates with heterochromatin (Woolcock, Gaidatzis, Punga, & Buhler, 2011). This RNAi-mediated heterochromatin model also applies to the centromere-like repeats in the mating locus and to the subtelomeric regions (Cam et al., 2005).

Whether a similar or related RNAi-dependent mechanism exists in mammals is debatable. For example, there is no direct homolog of Chp1 identified so far in mammalian cells, although it is reasonable to believe that a chromodomain-containing member, like those related to the CBX family, could potentially fulfill a similar role. Furthermore, although the major and minor tandem satellite repeats in the mammalian genome can potentially generate dsRNA (Martens et al., 2005), how and whether these dsRNA molecules are processed has not been addressed.

### 3.3. Maintenance of heterochromatin throughout the cell cycle

During DNA replication, the chromatin is assumed to be drastically perturbed by the passage of the DNA replication machinery. With this, two main questions arise: (i) How is the heterochromatin propagated during S-phase? (ii) How can such a close structure be amenable to remodeling, DNA synthesis, and recondensation? Indeed, constitutive heterochromatin remains silent throughout most of the cell cycle, thanks to the recruitment of a myriad of factors that confer transcriptional silencing RNA Pol II occupancy at heterochromatin is restricted for most of the cell cycle (Chen et al., 2008).

Fission yeast spends most of its time in G2, during which HP1 and Chp2 help in the recruitment and spreading of chromatin modifiers such as SHREC and mediate the assembly of repressive chromatin refractory to RNA Pol II transcription (Grewal & Jia, 2007; Sugiyama et al., 2007). During mitosis, HP1 is lost from H3K9-methylated heterochromatin through the phosphorylation of the neighboring serine 10, which creates a "methyl switch" output (Kloc et al., 2008). H3S10P-mediated decrease in the chromatin association of HP1 proteins during mitosis serves two functions. The first one is to allow for the recruitment of the condensin complex, which is essential for chromosome segregation. The second one is to allow heterochromatic transcripts to accumulate in S-phase by creating a short window

of opportunity in which heterochromatin is relatively accessible to RNA Pol II for transcription of the underlying repeat sequences (Chen et al., 2008; Kloc et al., 2008) (Fig. 1.4). This increased transcription during S-phase coincides temporally with the recruitment of the factors involved in heterochromatin assembly at the repeats. The upregulation of heterochromatin transcripts occurs preferentially on the antisense strand, and these transcripts are believed to attract heterochromatin assembly factors to the nascent transcripts of the repeats in *cis*. Indeed, proteins like Rik1 (a ClrC subunit) and Ago1 (a RITS complex subunit) are preferentially enriched at heterochromatic repeats during S-phase (Chen et al., 2008). At this time, heterochromatic repeats harbor paradoxically marks of active transcription, including H3K36 methylation. Again H3K36 is thought to mediate two functions, one is to promote transcription and the second one is to subsequently recruit HDAC silencing activities to heterochromatic repeats for further heterochromatin reconstitution during G2 to coordinately silence heterochromatic sequences with *cis*-acting posttranscriptional gene silencing by RNAi (Grewal & Jia, 2007; Sugiyama et al., 2007).

Finally, H3K9 methylation stabilizes the chromatin association of RNAi factors and also engages additional ClrC complexes through the Clr4 chromodomain, which is thought in turn to help methylating neighboring, newly incorporated histones. Altogether, this enables the reacquisition of an equivalent parental heterochromatic pattern on the newly formed chromatin after S-phase (Zhang et al., 2008). Importantly, histone chaperones themselves might play their part in this process as CAF1 has been shown to associate with heterochromatin factors (Quivy et al., 2004).

## 3.4. Targetting heterochromatin

A central and prevailing question in chromatin biology is how does a genomic region "know" that it has to be silenced, or in other words, how are chromatin modifiers targeted to the correct region. In the case of heterochromatin formation, this question remains largely unresolved. Recently, it has been shown that heterochromatic ncRNAs can be associated with chromatin through DNA:RNA hybrid formation (Nakama, Kawakami, Kajitani, Urano, & Murakami, 2012), which provides a target for the RITS complex, suggesting that heterochromatic ncRNAs are retained on chromatin via the formation of DNA–RNA hybrids and provide a platform for RNAi-directed heterochromatin assembly. This further suggests that DNA–RNA hybrid formation plays a role in chromatin-related ncRNA functions (Nakama et al., 2012).

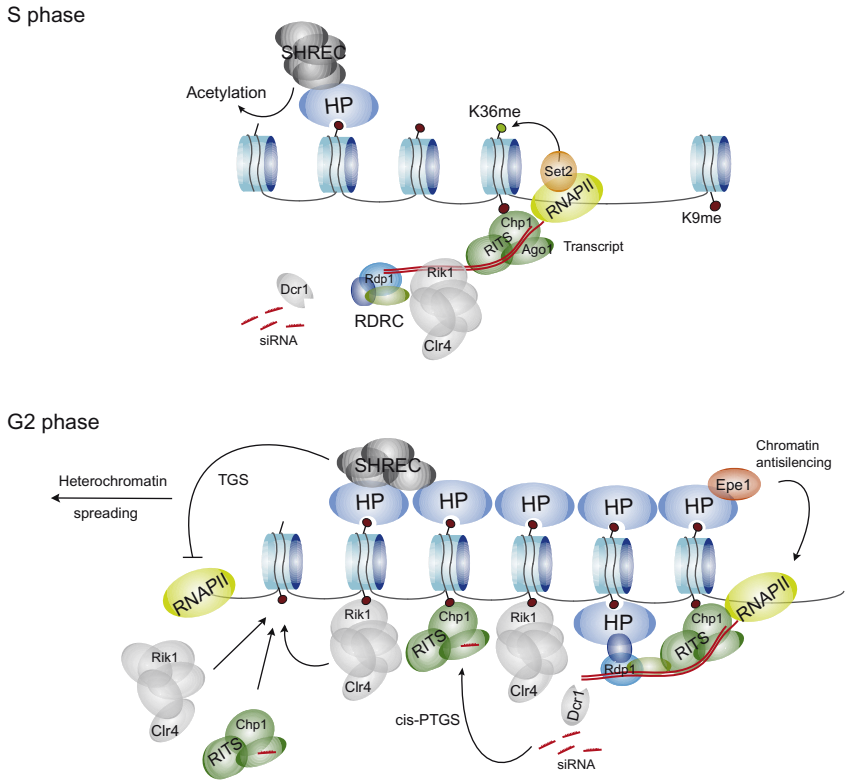


**Figure 1.4** Heterochromatin assembly in fission yeast requires the coordinated action of histone-modifying enzymes and RNAi. During S-phase (top), RNA Pol II activity at centromeric repeats occurs. This, in turn, stimulates the recruitment of heterochromatin assembly factors such as the ClRC subunit Rik1 and the RITS subunit Argonaute 1 (Ago1), as well as histone H3 lysine 36 methylation by the Set2 methyltransferase. Interaction between ClrC and RITS stabilizes their binding to chromatin and facilitates the processing of centromeric repeat RNAs to siRNAs. Recruitment of ClrC may also be mediated by downstream siRNA products such as double-stranded RNAs. Methylation of lysine 9 on histone H3 (H3K9me) by the Clr4 subunit of ClrC not only recruits HP1 proteins but also establishes a positive feedback loop by stabilizing the chromatin association of ClrC (via Clr4 chromodomain) and RNAi components such as RITS (via Chp1 chromodomain). In G2 phase (bottom), HP1 proteins bound to H3K9me recruit not only silencing factors such as the HDAC complex SHREC but also an antisilencing factor, Epe1, that promotes Pol II transcription. Spreading of HP1 proteins and H3K9me from the original nucleation sites allows heterochromatin to serve as a recruiting platform to reinforce its nature, including RITS components. *Adapted from Cam, Chen, & Grewal (2009).*

Studies in *Saccharomyces cerevisiae* and *S. pombe* have provided important insights into the process of assembly. A common theme that has emerged is that heterochromatin assembly is nucleated at specific regulatory sites and then spreads to nearby sequences. This spread typically requires some physical coupling of chromatin modifiers and more structural proteins such as Sir3 and Sir4, and Swi6/HP1 (Grewal & Elgin, 2002; Moazed, 2001).

In *S. cerevisiae*, site-specific DNA-binding proteins bind to nucleation sites (silencers) and then recruit to DNA the Sir2/Sir4 complex (Sir-depending spreading) (Huang, 2002). *S. cerevisiae* lacks H3K9me3, and therefore, the silencing occurs through different mechanisms than in fission yeast. Telomeres and the silent mating-type loci *HML* and *HMR* are packaged in silent chromatin that contains the silent information regulator (SIR) proteins Sir2, Sir3, and Sir4. SIR proteins silence nearby genes at telomeres, a phenomenon known as the telomere position effect. Silent telomeric chromatin is nucleated by the binding of Rap1 (a repressor/activator protein) to the telomeric CAAA repeats. Rap1 then recruits the SIR protein Sir4 (Luo, Vega-Palas, & Grunstein, 2002) which in turn recruits Sir2 and Sir3 (Hoppe et al., 2002; Rusche, Kirchmaier, & Rine, 2002). Silencing at the silent mating-type loci differs from telomere position effect primarily at this nucleation step: silencers contain binding sites for Rap1, the related Abf1 (an ARS binding protein), and Orc1 (an origin recognition complex protein). Sir1 seems to bind Orc1 together with a nearby Sir4 to stabilize nucleation of the SIR complex (Bose et al., 2004). The extending of chromatin, away from the nucleation site, comprises Sir2, Sir3, Sir4, and nucleosomes (Strahl-Bolsinger, Hecht, Luo, & Grunstein, 1997). Sir4 forms a complex with Sir2, a NAD-dependent histone deacetylase that deacetylates lysine 16 (K16) on histone H4 (Liou, Tanny, Kruger, Walz, & Moazed, 2005). Deacetylation of H4K16 allows Sir3 and Sir4 to bind to the H3 and H4 tails (Carmen, Milne, & Grunstein, 2002; Hecht, Laroche, Strahl-Bolsinger, Gasser, & Grunstein, 1995). These observations led to a model in which recurrent rounds of deacetylation by the Sir2–Sir4 complex and subsequent binding of Sir3 and Sir2–Sir4 to deacetylated histone tails propagate silencing (Hoppe et al., 2002; Luo et al., 2002; Rusche et al., 2002).

The SIR complex in budding yeast seems to be unique: of the SIR proteins, only Sir2 has clear orthologues. In most other eukaryotes, silencing relies on a common set of related proteins that make up heterochromatin. As introduced earlier, in *S. pombe*, specialized repetitive sequences and RNAi cooperate to initiate heterochromatin formation (stepwise assembly model). In this case, the shRNAs, generated by RNAi-mediated processing,

provide the specificity for targeting histone-modifying activities to the corresponding genomic location in which they are generated.

In mammals, it has recently been suggested that some transcription factors could act as repressors of heterochromatic pericentromeric repeats and thereby regulate heterochromatic signatures at those repeats (Bulut-Karslioglu et al., 2012). However, it is not yet clear whether this is a generalized mechanism and/or whether the establishment of heterochromatin after fertilization obeys a potential nucleation step that depends upon a transcription factor. In any case, the general agreement suggests that it is the transcripts themselves that are generated from heterochromatic-to-be loci that function as initial nuleators of heterochromatin formation.

## 3.5. Establishment of pericentric heterochromatin in mammals

In mammalian cells, transcription of major satellite repeats occurs during S-phase, and their transcription seems to take place before replication of the heterochromatic sequences (Lu & Gilbert, 2007). Their transcription is induced in response to cell proliferation and may involve H3S10P or dissociation of HP1 proteins triggered by specific signals during the cell cycle. But it has also been reported that gamma-satellite sequences (e.g., major satellite sequences) are repressed upon retinoic acid treatment (Rudert, Bronner, Garnier, & Dolle, 1995). Inducing muscle differentiation using C2C12 cells has also revealed that differentiation is accompanied by a spatial reorganization of constitutive pericentromeric repeats, that is, associated with elevated major and minor satellite transcripts (Terranova, Sauer, Merkenschlager, & Fisher, 2005). Contrasting with these results, ES cell differentiation induced by retinoic acid has been shown to result in increased accumulation or major satellite transcripts (Martens et al., 2005). Thus, although there are a few reports documenting major satellite transcription in mammalian cells, the physiological and differentiation contexts of such reports are varied and it seems difficult to reconcile a potential unique function to those observations. In particular, it is not known whether S-phase transcription facilitates heterochromatin assembly in a manner similar to the process of transcription-coupled establishment of silenced chromatin in fission yeast that we described earlier.

Recent analyses in early mouse embryos have attempted to investigate whether transcription of pericentromeric repeats is functionally linked to heterochromatin formation in mammals. Work by Almouzni and colleagues documented a very precise temporal regulation of major satellite transcription following fertilization (Probst et al., 2010). Transcription from both forward

and reverse strand was detected, but at different degrees and with different temporal dynamics. Interestingly, the paternal pronucleus shows a significantly higher transcriptional rate of major satellites compared to the maternal one (Probst et al., 2010; Puschendorf et al., 2008; Santenard et al., 2010). A burst of transcription of the forward strand correlated temporally with the formation of chromocenters. Importantly, by blocking the effect of major satellite transcription using LNA gapmers, it was shown that there is a strand-specific requirement for the remodeling of heterochromatin into a somatic chromocenter configuration (Probst et al., 2010). These data argue strongly that transcription from the major satellites after fertilization is required for heterochromatin remodeling and developmental progression.

Largely inspired by the work in *S. pombe* and *Arabidopsis*, work from our lab has shown that the transcription of major satellites in the zygote is associated with tethering of HP1β and also with the spatial nuclear localization typical of pericentromeric chromatin around the NLBs in the embryo (Santenard et al., 2010). This further suggests that there might be a functional link between spatial localization and silencing of pericentric domains after fertilization. Although the mechanisms behind are still to be determined, our data suggested that dsRNA from the major satellites can lead to the localization of HP1β to the highly condensed, DAPI-rich regions around the NLBs in the mouse embryo. Interestingly, and in contrast to the *S. pombe* model, it is the hinge region of HP1β rather than its chromodomain that seems to be the main determinant for HP1β localization in embryonic heterochromatin, at least in the zygote and at the 2-cell stage. In agreement with this, mutation of the chromodomain of HP1β does not seem to elicit a major defect in its subnuclear localization (Santenard et al., 2010). This is in line with the fact that the paternal chromatin lacks detectable H3K9me3. In the embryo, silencing of pericentric heterochromatin occurs therefore in the absence of any detectable levels of H3K9me3, and it is instead H3K27me2/3 that seems to be a major player in this process (Puschendorf et al., 2008; Santenard et al., 2010).

Thus, it would seem that transcription of pericentromeric repeats also lies at the heart of the formation of heterochromatic signatures *de novo* in mammals. A number of questions remain, however, unanswered, mainly to determine whether the downstream effectors of such transcription are the components of the RNAi machinery or any related protein(s) and whether the maintenance mechanism throughout the cell cycle depends also on this transcription.

### 3.6. Heterochromatin assembly: A more general RNA-related mechanism also in mammals?

More generally, it is reasonable to say that ncRNA molecules of various sizes appear to play a major role in the regulation of silent chromatin biology. For example, RNAs play an important role in chromosome-specific localization of the activities of chromatin modifiers required for dosage compensation in *Drosophila* and mammals (Park & Kuroda, 2001) and also in some cases of genomic imprinting (Sleutels, Zwart, & Barlow, 2002). In mammals, *Xist* RNA originating from the X-inactivation center is required for initiation but not for the subsequent inheritance of X-inactivation (Avner & Heard, 2001), and silencing is also regulated by *Tsix*, an *Xist* antisense transcript (Cohen & Lee, 2002). Interestingly, it has been recently shown that long interspersed repeated elements (LINEs) that are enriched on the X chromosome compared with autosomes (Boyle, Ballard, & Ward, 1990) participate in creating a silent nuclear compartment into which X-linked genes become recruited. These LINE repeats contain a subset of "young" LINE-1 elements that are therefore relatively active and expressed during X-inactivation, rather than being silenced. Expression of these LINEs requires the specific heterochromatic state induced by *Xist*. These LINEs often lie within escape-prone regions of the X chromosome, but close to the genes that are subject to X-inactivation, and are associated with putative endo-siRNAs. LINEs may thus facilitate X-inactivation at different levels, with silent LINEs participating in assembly of a heterochromatic nuclear compartment induced by *Xist*, and active LINEs participating in local propagation of X-inactivation into regions that would otherwise be prone to escape (Chow et al., 2010).

It is possible that other repetitive elements in the mammalian genome, in particular, retrotransposons, can function as nucleators of silent compartments and/or as spreading or antispreading mechanisms for heterochromatin. In most differentiated cells, such repetitive elements are fully silenced to avoid phenomena such as retrotransposition and recombination that would otherwise compromise DNA integrity (Maksakova, Mager, & Reiss, 2008). As mentioned earlier, the lack of conventional heterochromatic modifications during the earliest stages of embryogenesis has been suggested to provide a window of opportunity for the reactivation of nondesired 'guests' in the genome like retrotransposons. Indeed, transcripts derived from repetitive elements are found in the early embryo (Bachvarova, 1988; Efroni et al., 2008; Evsikov et al., 2004; Packer, Manova, & Bachvarova, 1993; Peaston et al., 2004). We have recently found that the transcriptional activation of these elements decreases at the 8-cell stage after a peak of reactivation

at the 2-cell stage (Fadloun et al, 2013). It is therefore intriguing how retrotransposons are silenced during preimplantation development, since at the time when their transcriptional activity decreases, H4K20me3 and H3K64me3 are undetectable from the embryonic chromatin, and H3K9me3 and DNA methylation seem to decrease, both globally and in LINEs (Santos et al., 2002; Smith et al., 2012). In this sense, the retrotransposons provide actually an excellent model to address how heterochromatic regions other than pericentric domains are silenced during embryogenesis and it will be important to determine how such regions are silenced to start with. LINEs and long terminal repeat retrotransposons (LTRs) are known to be demethylated immediately after fertilization (Lane et al., 2003; Smith et al., 2012; Wossidlo et al., 2010). Most of the data available in the literature, including recent reduced representation bisulfite sequence, suggest that levels of DNA methylation on LTRs and on LINEs do not increase prior to implantation and therefore alternative mechanisms are probably in place to silence retrotransposons in the early embryo (Smith et al., 2012). This is in line with elegant experiments in which deletion of KAP1—which is known to silence endogenous retroviruses through an H3K9me3/DNA methylation pathway—at several developmental times revealed that KAP1-directed DNA methylation is dispensable for the silencing of endogenous retroviruses before E3.5 (Rowe et al., 2010). Although it is well known that retrotransposons are silenced through a piRNA mechanism in the germ line, the piRNA/Dnmt3L pathway seems not to be active in the early embryo (Aravin, Sachidanandam, Girard, Fejes-Toth, & Hannon, 2007; Bourc'his & Bestor, 2004; Carmell et al., 2007; Zamudio & Bourc'his, 2010). It is therefore possible that other RNA-mediated mechanisms also regulate transcription and/or silencing of repetitive loci during early embryogenesis, similar to what it has been shown for pericentromeric repeats. Recent analyses performed in our lab indicating that very short RNAs smaller than 18 nt can regulate expression of LINE elements in the mouse zygote support such a scenario (Fadloun et al., 2013). Thus, it could be that RNA has a more generalized role in regulating transcriptional activity of heterochromatic loci during development.

## 4. CONCLUDING REMARKS

It is clear from all the stated earlier that the organization of the heterochromatin itself as well as its potential role in regulating gene expression will have a key role in imparting epigenetic decisions during early development.

We believe that there are at least three different aspects where future research will have to provide mechanistic insights to these important questions.

The first major question is whether heterochromatin can act as a driving force in development. Although there is a suggestion that plasticity correlates with a more open chromatin configuration in ES cells (Meshorer et al., 2006), a direct causal link between the two has not been established and it is unclear whether the more open configuration is a consequence of pluripotency or the other way around. Second, it will be important to determine whether heterochromatin has a potential role in lineage allocation: Is heterochromatin different in the cells that are destined to become trophectoderm than in the cells that will form the ICM? In support to this hypothesis, it has been shown by electron microscopy that global chromatin architecture differs between the two lineages of the early blastocyst (Ahmed et al., 2010). It will have to be established whether such differences emerge *prior* to lineage segregation and if so, whether they could have an instructive role in cell fate determination. It is known that the dynamics of OCT4 differ between cells of embryos at both 4- and 8-cell stage and that these dynamics are predictive of lineage allocation in the blastocyst (Plachta, Bollenbach, Pease, Fraser, & Pantazis, 2011). The dynamics of OCT4 were suggested to reflect accessibility of OCT4 to its binding sites, and it is therefore possible that a global hetero- versus euchromatin organization impacts on such accessibility. And third, could heterochromatin or the absence of conventional heterochromatin be a regulator of epigenetic reprogramming? Overall, the data we have described earlier are so far correlative, mostly because of the technical difficulties and limited approaches that can be applied to early embryos. Nevertheless, it is clear that there are major chromatin remodeling events after fertilization, in particular, of heterochromatic marks. Importantly, this is paralleled in the germ line during the phase of epigenetic reprogramming (Surani, Hayashi, & Hajkova, 2007), strongly suggesting that absence of heterochromatic marks is necessary for reprogramming. However, there is no formal demonstration that this is indeed the case and that heterochromatin needs to be remodeled in order for reprogramming to take place. One could also envisage another provocative scenario: Could it be that reprogramming is a cause of losing heterochromatin? Or is it that reprogramming can occur because the lack of conventional heterochromatin provides a window of opportunity for it to take place? These are all exciting questions that await further investigation.

## ACKNOWLEDGMENTS

Work in the Torres-Padilla lab is supported by grants from the ANR, ANR-09-Blanc-0114, Epigenesys NoE and ERC-2011-StG 280840 "NuclearPotency." A. F. was supported by a postdoctoral fellowship from the Fondation pour la Recherche Medicale and A. E. is supported by a fellowship from the Ministère de la Recherche et de la Technologie. We thank A. Santenard for providing the template for Fig. 1.3.

## REFERENCES

Ahmed, K., Dehghani, H., Rugg-Gunn, P., Fussner, E., Rossant, J., & Bazett-Jones, D. P. (2010). Global chromatin architecture reflects pluripotency and lineage commitment in the early mouse embryo. *PLoS One*, *5*, e10531.

Akiyama, T., Suzuki, O., Matsuda, J., & Aoki, F. (2011). Dynamic replacement of histone H3 variants reprograms epigenetic marks in early mouse embryos. *PLoS Genetics*, 7, e1002279.

Allshire, R. C., Javerzat, J. P., Redhead, N. J., & Cranston, G. (1994). Position effect variegation at fission yeast centromeres. *Cell*, *76*, 157–169.

Allshire, R. C., Nimmo, E. R., Ekwall, K., Javerzat, J. P., & Cranston, G. (1995). Mutations derepressing silent centromeric domains in fission yeast disrupt chromosome segregation. *Genes & Development*, *9*, 218–233.

Aoki, V. W., Liu, L., & Carrell, D. T. (2005). Identification and evaluation of a novel sperm protamine abnormality in a population of infertile males. *Human Reproduction (Oxford, England)*, *20*, 1298–1306.

Aravin, A. A., Sachidanandam, R., Girard, A., Fejes-Toth, K., & Hannon, G. J. (2007). Developmentally regulated piRNA clusters implicate MILI in transposon control. *Science*, *316*, 744–747.

Arney, K. L., Bao, S., Bannister, A. J., Kouzarides, T., & Surani, M. A. (2002). Histone methylation defines epigenetic asymmetry in the mouse zygote. *The International Journal of Developmental Biology*, *46*, 317–320.

Aucott, R., Bullwinkel, J., Yu, Y., Shi, W., Billur, M., Brown, J., et al. (2008). HP1-beta is required for development of the cerebral neocortex and neuromuscular junctions. *The Journal of Cell Biology*, *183*, 597–606.

Avner, P., & Heard, E. (2001). X-chromosome inactivation: Counting, choice and initiation. *Nature Reviews. Genetics*, *2*, 59–67.

Bachvarova, R. (1988). Small B2 RNAs in mouse oocytes, embryos, and somatic tissues. *Developmental Biology*, *130*, 513–523.

Balhorn, R., Reed, S., & Tanphaichitr, N. (1988). Aberrant protamine 1/protamine 2 ratios in sperm of infertile human males. *Experientia*, *44*, 52–55.

Bannister, A. J., Zegerman, P., Partridge, J. F., Miska, E. A., Thomas, J. O., Allshire, R. C., et al. (2001). Selective recognition of methylated lysine 9 on histone H3 by the HP1 chromo domain. *Nature*, *410*, 120–124.

Barski, A., Cuddapah, S., Cui, K., Roh, T. Y., Schones, D. E., Wang, Z., et al. (2007). High-resolution profiling of histone methylations in the human genome. *Cell*, *129*, 823–837.

Bayne, E. H., White, S. A., Kagansky, A., Bijos, D. A., Sanchez-Pulido, L., Hoe, K. L., et al. (2010). Stc1: A critical link between RNAi and chromatin modification required for heterochromatin integrity. *Cell*, *140*, 666–677.

Bernstein, B. E., Mikkelsen, T. S., Xie, X., Kamal, M., Huebert, D. J., Cuff, J., et al. (2006). A bivalent chromatin structure marks key developmental genes in embryonic stem cells. *Cell*, *125*, 315–326.

Bonasio, R., Tu, S., & Reinberg, D. (2010). Molecular signals of epigenetic states. *Science*, *330*, 612–616.

Borgel, J., Guibert, S., Li, Y., Chiba, H., Schubeler, D., Sasaki, H., et al. (2010). Targets and dynamics of promoter DNA methylation during early mouse development. *Nature Genetics*, *42*, 1093–1100.

Bose, M. E., McConnell, K. H., Gardner-Aukema, K. A., Muller, U., Weinreich, M., Keck, J. L., et al. (2004). The origin recognition complex and Sir4 protein recruit Sir1p to yeast silent chromatin through independent interactions requiring a common Sir1p domain. *Molecular and Cellular Biology*, *24*, 774–786.

Boskovic, A., Bender, A., Gall, L., Ziegler-Birling, C., Beaujean, N., & Torres-Padilla, M. E. (2012). Analysis of active chromatin modifications in early mammalian embryos reveals uncoupling of H2A.Z acetylation and H3K36 trimethylation from embryonic genome activation. *Epigenetics*, 7, 747–757.

Bouniol-Baly, C., Nguyen, E., Besombes, D., & Debey, P. (1997). Dynamic organization of DNA replication in one-cell mouse embryos: Relationship to transcriptional activation. *Experimental Cell Research*, *236*, 201–211.

Bourc'his, D., & Bestor, T. H. (2004). Meiotic catastrophe and retrotransposon reactivation in male germ cells lacking Dnmt3L. *Nature*, *431*, 96–99.

Bourc'his, D., Xu, G. L., Lin, C. S., Bollman, B., & Bestor, T. H. (2001). Dnmt3L and the establishment of maternal genomic imprints. *Science*, *294*, 2536–2539.

Boyle, A. L., Ballard, S. G., & Ward, D. C. (1990). Differential distribution of long and short interspersed element sequences in the mouse genome: Chromosome karyotyping by fluorescence in situ hybridization. *Proceedings of the National Academy of Sciences of the United States of America*, *87*, 7757–7761.

Brown, J., Bullwinkel, J., Baron-Lühr, B., Billur, M., Schneider, P., Winking, H., et al. (2010). HP1gamma function is required for male germ cell survival and spermatogenesis. *Epigenetics & chromatin*, *3*, 9.

Bulut-Karslioglu, A., Perrera, V., Scaranaro, M., de la Rosa-Velazquez, I. A., van de Nobelen, S., Shukeir, N., et al. (2012). A transcription factor-based mechanism for mouse heterochromatin formation. *Nature Structural & Molecular Biology*, *19*, 1023–1030.

Burton, A., & Torres-Padilla, M. E. (2010). Epigenetic reprogramming and development: A unique heterochromatin organization in the preimplantation mouse embryo. *Briefings in Functional Genomics*, *9*, 444–454.

Cam, H. P., Sugiyama, T., Chen, E. S., Chen, X., FitzGerald, P. C., & Grewal, S. I. (2005). Comprehensive analysis of heterochromatin- and RNAi-mediated epigenetic control of the fission yeast genome. *Nature Genetics*, *37*, 809–819.

Cam, H. P., Chen, E. S., & Grewal, S. I. (2009). Transcriptional scaffolds for heterochromatin assembly. *Cell*, *136*(4), 610–614. http://dx.doi.org/10.1016/j.cell.2009.02.004.

Cao, R., Wang, L., Wang, H., Xia, L., Erdjument-Bromage, H., Tempst, P., et al. (2002). Role of histone H3 lysine 27 methylation in Polycomb-group silencing. *Science*, *298*, 1039–1043.

Carmell, M. A., Girard, A., van de Kant, H. J., Bourc'his, D., Bestor, T. H., de Rooij, D. G., et al. (2007). MIWI2 is essential for spermatogenesis and repression of transposons in the mouse male germline. *Developmental Cell*, *12*, 503–514.

Carmen, A. A., Milne, L., & Grunstein, M. (2002). Acetylation of the yeast histone H4 N terminus regulates its binding to heterochromatin protein SIR3. *The Journal of Biological Chemistry*, *277*, 4778–4781.

Chan, M. M., Smith, Z. D., Egli, D., Regev, A., & Meissner, A. (2012). Mouse ooplasm confers context-specific reprogramming capacity. *Nature Genetics*, *44*, 978–980.

Chang, C. C., Ma, Y., Jacobs, S., Tian, X. C., Yang, X., & Rasmussen, T. P. (2005). A maternal store of macroH2A is removed from pronuclei prior to onset of somatic macroH2A expression in preimplantation embryos. *Developmental Biology*, *278*, 367–380.

Chen, E. S., Zhang, K., Nicolas, E., Cam, H. P., Zofall, M., & Grewal, S. I. (2008). Cell cycle control of centromeric repeat transcription and heterochromatin assembly. *Nature*, *451*, 734–737.

Chow, J. C., Ciaudo, C., Fazzari, M. J., Mise, N., Servant, N., Glass, J. L., et al. (2010). LINE-1 activity in facultative heterochromatin formation during X chromosome inactivation. *Cell*, *141*, 956–969.

Cleveland, D. W., Mao, Y., & Sullivan, K. F. (2003). Centromeres and kinetochores: From epigenetics to mitotic checkpoint signaling. *Cell*, *112*, 407–421.

Cohen, D. E., & Lee, J. T. (2002). X-chromosome inactivation and the search for chromosome-wide silencers. *Current Opinion in Genetics & Development*, *12*, 219–224.

Colmenares, S. U., Buker, S. M., Buhler, M., Dlakic, M., & Moazed, D. (2007). Coupling of double-stranded RNA synthesis and siRNA generation in fission yeast RNAi. *Molecular Cell*, *27*, 449–461.

Daujat, S., Weiss, T., Mohn, F., Lange, U. C., Ziegler-Birling, C., Zeissler, U., et al. (2009). H3K64 trimethylation marks heterochromatin and is dynamically remodeled during developmental reprogramming. *Nature Structural & Molecular Biology*, *16*, 777–781.

Dawlaty, M. M., Ganz, K., Powell, B. E., Hu, Y. C., Markoulaki, S., Cheng, A. W., et al. (2011). Tet1 is dispensable for maintaining pluripotency and its loss is compatible with embryonic and postnatal development. *Cell Stem Cell*, *9*, 166–175.

Dodge, J., Kang, Y.-K., Beppu, H., Lei, H., & Li, E. (2004). Histone H3-K9 methyltransferase ESET is essential for early development. *Molecular and Cellular Biology*, *24*, 2478–2486.

Donohoe, M. E., Zhang, X., McGinnis, L., Biggers, J., Li, E., & Shi, Y. (1999). Targeted disruption of mouse Yin Yang 1 transcription factor results in peri-implantation lethality. *Molecular and Cellular Biology*, *19*, 7237–7244.

Eckardt, S., Leu, N. A., Kurosaka, S., & McLaughlin, K. J. (2005). Differential reprogramming of somatic cell nuclei after transfer into mouse cleavage stage blastomeres. *Reproduction*, *129*, 547–556.

Efroni, S., Duttagupta, R., Cheng, J., Dehghani, H., Hoeppner, D. J., Dash, C., et al. (2008). Global transcription in pluripotent embryonic stem cells. *Cell Stem Cell*, *2*, 437–447.

Erhardt, S., Su, I. H., Schneider, R., Barton, S., Bannister, A., Perez-Burgos, L., et al. (2003). Consequences of the depletion of zygotic and embryonic enhancer of zeste 2 during preimplantation mouse development. *Development (Cambridge, England)*, *130*, 4235–4248.

Evsikov, A. V., de Vries, W. N., Peaston, A. E., Radford, E. E., Fancher, K. S., Chen, F. H., et al. (2004). Systems biology of the 2-cell mouse embryo. *Cytogenetic and Genome Research*, *105*, 240–250.

Fadloun, A., Le Gras, S., Jost, B., Ziegler-Birling, C., Takahashi, H., Gorab, E., et al. (2013). Chromatin signatures and retrotransposon profiling in mouse embryos reveal regulation of LINE-1 by RNA. *Nature Structural & Molecular Biology*, http://dx.doi.org/10.1038/nsmb.2495. [Epub ahead of print].

Farthing, C. R., Ficz, G., Ng, R. K., Chan, C. F., Andrews, S., Dean, W., et al. (2008). Global mapping of DNA methylation in mouse promoters reveals epigenetic reprogramming of pluripotency genes. *PLoS Genetics*, *4*, e1000116.

Faust, C., Lawson, K. A., Schork, N. J., Thiel, B., & Magnuson, T. (1998). The Polycomb-group gene eed is required for normal morphogenetic movements during gastrulation in the mouse embryo. *Development (Cambridge, England)*, *125*, 4495–4506.

Folco, H. D., Pidoux, A. L., Urano, T., & Allshire, R. C. (2008). Heterochromatin and RNAi are required to establish CENP-A chromatin at centromeres. *Science*, *319*, 94–97.

Goll, M. G., & Bestor, T. H. (2005). Eukaryotic cytosine methyltransferases. *Annual Review of Biochemistry*, *74*, 481–514.

Govin, J., Escoffier, E., Rousseaux, S., Kuhn, L., Ferro, M., Thevenon, J., et al. (2007). Pericentric heterochromatin reprogramming by new histone variants during mouse spermiogenesis. *The Journal of Cell Biology*, *176*, 283–294.

Grewal, S. I., & Elgin, S. C. (2002). Heterochromatin: New possibilities for the inheritance of structure. *Current Opinion in Genetics & Development*, *12*, 178–187.

Grewal, S. I., & Elgin, S. C. (2007). Transcription and RNA interference in the formation of heterochromatin. *Nature*, *447*, 399–406.

Grewal, S. I., & Jia, S. (2007). Heterochromatin revisited. *Nature Reviews. Genetics*, *8*, 35–46.

Gu, T. P., Guo, F., Yang, H., Wu, H. P., Xu, G. F., Liu, W., et al. (2011). The role of Tet3 DNA dioxygenase in epigenetic reprogramming by oocytes. *Nature*, *477*, 606–610.

Hamatani, T., Carter, M. G., Sharov, A. A., & Ko, M. S. (2004). Dynamics of global gene expression changes during mouse preimplantation development. *Developmental Cell*, *6*, 117–131.

Hammoud, S. S., Nix, D. A., Zhang, H., Purwar, J., Carrell, D. T., & Cairns, B. R. (2009). Distinctive chromatin in human sperm packages genes for embryo development. *Nature*, *460*, 473–478.

Hata, K., Okano, M., Lei, H., & Li, E. (2002). Dnmt3L cooperates with the Dnmt3 family of de novo DNA methyltransferases to establish maternal imprints in mice. *Development (Cambridge, England)*, *129*, 1983–1993.

Hecht, A., Laroche, T., Strahl-Bolsinger, S., Gasser, S. M., & Grunstein, M. (1995). Histone H3 and H4 N-termini interact with SIR3 and SIR4 proteins: A molecular model for the formation of heterochromatin in yeast. *Cell*, *80*, 583–592.

Hoppe, G. J., Tanny, J. C., Rudner, A. D., Gerber, S. A., Danaie, S., Gygi, S. P., et al. (2002). Steps in assembly of silent chromatin in yeast: Sir3-independent binding of a Sir2/Sir4 complex to silencers and role for Sir2-dependent deacetylation. *Molecular and Cellular Biology*, *22*, 4167–4180.

Huang, Y. (2002). Transcriptional silencing in Saccharomyces cerevisiae and Schizosaccharomyces pombe. *Nucleic Acids Research*, *30*, 1465–1482.

Inoue, A., & Zhang, Y. (2011). Replication-dependent loss of 5-hydroxymethylcytosine in mouse preimplantation embryos. *Science*, *334*, 194.

Iqbal, K., Jin, S. G., Pfeifer, G. P., & Szabo, P. E. (2011). Reprogramming of the paternal genome upon fertilization involves genome-wide oxidation of 5-methylcytosine. *Proceedings of the National Academy of Sciences of the United States of America*, *108*, 3642–3647.

Ito, S., D'Alessio, A. C., Taranova, O. V., Hong, K., Sowers, L. C., & Zhang, Y. (2010). Role of Tet proteins in 5mC to 5hmC conversion, ES-cell self-renewal and inner cell mass specification. *Nature*, *466*, 1129–1133.

Jenkins, T. G., & Carrell, D. T. (2012). The sperm epigenome and potential implications for the developing embryo. *Reproduction*, *143*, 727–734.

Kagansky, A., Folco, H. D., Almeida, R., Pidoux, A. L., Boukaba, A., Simmer, F., et al. (2009). Synthetic heterochromatin bypasses RNAi and centromeric repeats to establish functional centromeres. *Science*, *324*, 1716–1719.

Kaneda, M., Okano, M., Hata, K., Sado, T., Tsujimoto, N., Li, E., et al. (2004). Essential role for de novo DNA methyltransferase Dnmt3a in paternal and maternal imprinting. *Nature*, *429*, 900–903.

Kloc, A., Zaratiegui, M., Nora, E., & Martienssen, R. (2008). RNA interference guides histone modification during the S phase of chromosomal replication. *Current Biology: CB*, *18*, 490–495.

Kourmouli, N., Jeppesen, P., Mahadevhaiah, S., Burgoyne, P., Wu, R., Gilbert, D. M., et al. (2004). Heterochromatin and tri-methylated lysine 20 of histone H4 in animals. *Journal of Cell Science*, *117*, 2491–2501.

Kouzarides, T. (2007). Chromatin modifications and their function. *Cell*, *128*, 693–705.

Lachner, M., O'Carroll, D., Rea, S., Mechtler, K., & Jenuwein, T. (2001). Methylation of histone H3 lysine 9 creates a binding site for HP1 proteins. *Nature*, *410*, 116–120.

Lane, N., Dean, W., Erhardt, S., Hajkova, P., Surani, A., Walter, J., et al. (2003). Resistance of IAPs to methylation reprogramming may provide a mechanism for epigenetic inheritance in the mouse. *Genesis*, *35*, 88–93.

Lehnertz, B., Northrop, J. P., Antignano, F., Burrows, K., Hadidi, S., Mullaly, S. C., et al. (2010). Activating and inhibitory functions for the histone lysine methyltransferase G9a in T helper cell differentiation and function. *The Journal of Experimental Medicine*, *207*, 915–922.

Lehnertz, B., Ueda, Y., Derijck, A. A., Braunschweig, U., Perez-Burgos, L., Kubicek, S., et al. (2003). Suv39h-mediated histone H3 lysine 9 methylation directs DNA methylation to major satellite repeats at pericentric heterochromatin. *Current Biology: CB*, *13*, 1192–1200.

Li, E., Beard, C., & Jaenisch, R. (1993). Role for DNA methylation in genomic imprinting. *Nature*, *366*, 362–365.

Liou, G. G., Tanny, J. C., Kruger, R. G., Walz, T., & Moazed, D. (2005). Assembly of the SIR complex and its regulation by O-acetyl-ADP-ribose, a product of NAD-dependent histone deacetylation. *Cell*, *121*, 515–527.

Liu, H., Kim, J.-M., & Aoki, F. (2004). Regulation of histone H3 lysine 9 methylation in oocytes and early pre-implantation embryos. *Development (Cambridge, England)*, *131*, 2269–2280.

Loppin, B., Bonnefoy, E., Anselme, C., Laurencon, A., Karr, T. L., & Couble, P. (2005). The histone H3.3 chaperone HIRA is essential for chromatin assembly in the male pronucleus. *Nature*, *437*, 1386–1390.

Lu, J., & Gilbert, D. M. (2007). Proliferation-dependent and cell cycle regulated transcription of mouse pericentric heterochromatin. *The Journal of Cell Biology*, *179*, 411–421.

Lu, S., Xie, Y. M., Li, X., Luo, J., Shi, X. Q., Hong, X., et al. (2009). Mass spectrometry analysis of dynamic post-translational modifications of TH2B during spermatogenesis. *Molecular Human Reproduction*, *15*, 373–378.

Luff, B., Pawlowski, L., & Bender, J. (1999). An inverted repeat triggers cytosine methylation of identical sequences in Arabidopsis. *Molecular Cell*, *3*, 505–511.

Luger, K., Dechassa, M. L., & Tremethick, D. J. (2012). New insights into nucleosome and chromatin structure: An ordered state or a disordered affair? *Nature Reviews. Molecular Cell Biology*, *13*, 436–447.

Luger, K., Mader, A. W., Richmond, R. K., Sargent, D. F., & Richmond, T. J. (1997). Crystal structure of the nucleosome core particle at 2.8 A resolution. *Nature*, *389*, 251–260.

Luo, K., Vega-Palas, M. A., & Grunstein, M. (2002). Rap1-Sir4 binding independent of other Sir, yKu, or histone interactions initiates the assembly of telomeric heterochromatin in yeast. *Genes & Development*, *16*, 1528–1539.

Maalouf, W. E., Liu, Z., Brochard, V., Renard, J. P., Debey, P., Beaujean, N., et al. (2009). Trichostatin A treatment of cloned mouse embryos improves constitutive heterochromatin remodeling as well as developmental potential to term. *BMC Developmental Biology*, *9*, 11.

Maksakova, I. A., Mager, D. L., & Reiss, D. (2008). Keeping active endogenous retroviral-like elements in check: The epigenetic perspective. *Cellular and Molecular Life Sciences*, *65*, 3329–3347.

Martens, J. H., O'Sullivan, R. J., Braunschweig, U., Opravil, S., Radolf, M., Steinlein, P., et al. (2005). The profile of repeat-associated histone lysine methylation states in the mouse epigenome. *The EMBO Journal*, *24*, 800–812.

Martienssen, R. A., Kloc, A., Slotkin, R. K., & Tanurdzic, M. (2008). Epigenetic inheritance and reprogramming in plants and fission yeast. *Cold Spring Harbor Symposia on Quantitative Biology*, *73*, 265–271.

Martin, C., Beaujean, N., Brochard, V., Audouard, C., Zink, D., & Debey, P. (2006). Genome restructuring in mouse embryos during reprogramming and early development. *Developmental Biology*, *292*, 317–332.

Matzke, M. A., & Birchler, J. A. (2005). RNAi-mediated pathways in the nucleus. *Nature Reviews. Genetics*, *6*, 24–35.

Mayer, W., Niveleau, A., Walter, J., Fundele, R., & Haaf, T. (2000). Demethylation of the zygotic paternal genome. *Nature*, *403*, 501–502.

Meshorer, E., Yellajoshula, D., George, E., Scambler, P. J., Brown, D. T., & Misteli, T. (2006). Hyperdynamic plasticity of chromatin proteins in pluripotent embryonic stem cells. *Developmental Cell*, *10*, 105–116.

Moazed, D. (2001). Common themes in mechanisms of gene silencing. *Molecular Cell*, *8*, 489–498.

Moss, S. B., Challoner, P. B., & Groudine, M. (1989). Expression of a novel histone 2B during mouse spermiogenesis. *Developmental Biology*, *133*, 83–92.

Muchardt, C., Guilleme, M., Seeler, J. S., Trouche, D., Dejean, A., & Yaniv, M. (2002). Coordinated methyl and RNA binding is required for heterochromatin localization of mammalian HP1alpha. *EMBO Reports*, *3*, 975–981.

Muller, J., Hart, C. M., Francis, N. J., Vargas, M. L., Sengupta, A., Wild, B., et al. (2002). Histone methyltransferase activity of a Drosophila Polycomb group repressor complex. *Cell*, *111*, 197–208.

Nakama, M., Kawakami, K., Kajitani, T., Urano, T., & Murakami, Y. (2012). DNA-RNA hybrid formation mediates RNAi-directed heterochromatin formation. *Genes to Cells: Devoted to Molecular & Cellular Mechanisms*, *17*, 218–233.

Nakamura, T., Liu, Y. J., Nakashima, H., Umehara, H., Inoue, K., Matoba, S., et al. (2012). PGC7 binds histone H3K9me2 to protect against conversion of 5mC to 5hmC in early embryos. *Nature*, *486*, 415–419.

Naruse, C., Fukusumi, Y., Kakiuchi, D., & Asano, M. (2007). A novel gene trapping for identifying genes expressed under the control of specific transcription factors. *Biochemical and Biophysical Research Communications*, *361*, 109–115.

Nielsen, A. L., Oulad-Abdelghani, M., Ortiz, J. A., Remboutsika, E., Chambon, P., & Losson, R. (2001). Heterochromatin formation in mammalian cells: Interaction between histones and HP1 proteins. *Molecular Cell*, *7*, 729–739.

Nishioka, K., Rice, J., Sarma, K., Erdjument-Bromage, H., Werner, J., Wang, Y., et al. (2002). PR-Set7 is a nucleosome-specific methyltransferase that modifies lysine 20 of histone H4 and is associated with silent chromatin. *Molecular Cell*, *9*, 1201–1213.

Nonchev, S., & Tsanev, R. (1990). Protamine-histone replacement and DNA replication in the male mouse pronucleus. *Molecular Reproduction and Development*, *25*, 72–76.

O'Carroll, D., Erhardt, S., Pagani, M., Barton, S., Surani, M., & Jenuwein, T. (2001). The polycomb-group gene Ezh2 is required for early mouse development. *Molecular and Cellular Biology*, *21*, 4330–4336.

Okano, M., Bell, D. W., Haber, D. A., & Li, E. (1999). DNA methyltransferases Dnmt3a and Dnmt3b are essential for de novo methylation and mammalian development. *Cell*, *99*, 247–257.

Packer, A. I., Manova, K., & Bachvarova, R. F. (1993). A discrete LINE-1 transcript in mouse blastocysts. *Developmental Biology*, *157*, 281–283.

Park, Y., & Kuroda, M. I. (2001). Epigenetic aspects of X-chromosome dosage compensation. *Science*, *293*, 1083–1085.

Pasini, D., Bracken, A. P., Jensen, M. R., Lazzerini Denchi, E., & Helin, K. (2004). Suz12 is essential for mouse development and for EZH2 histone methyltransferase activity. *The EMBO Journal*, *23*, 4061–4071.

Peaston, A. E., Evsikov, A. V., Graber, J. H., de Vries, W. N., Holbrook, A. E., Solter, D., et al. (2004). Retrotransposons regulate host genes in mouse oocytes and preimplantation embryos. *Developmental Cell*, *7*, 597–606.

Peters, A. H., O'Carroll, D., Scherthan, H., Mechtler, K., Sauer, S., Schofer, C., et al. (2001). Loss of the Suv39h histone methyltransferases impairs mammalian heterochromatin and genome stability. *Cell*, *107*, 323–337.

Pidoux, A. L., & Allshire, R. C. (2005). The role of heterochromatin in centromere function. *Philosophical Transactions of the Royal Society of London. Series B, Biological Sciences*, *360*, 569–579.

Pinheiro, I., Margueron, R., Shukeir, N., Eisold, M., Fritzsch, C., Richter, F. M., et al. (2012). Prdm3 and Prdm16 are H3K9me1 methyltransferases required for mammalian heterochromatin integrity. *Cell*, *150*, 948–960.

Plachta, N., Bollenbach, T., Pease, S., Fraser, S. E., & Pantazis, P. (2011). Oct4 kinetics predict cell lineage patterning in the early mammalian embryo. *Nature Cell Biology*, *13*, 117–123.

Poznanski, A. A., & Calarco, P. G. (1991). The expression of intracisternal A particle genes in the preimplantation mouse embryo. *Developmental Biology*, *143*, 271–281.

Probst, A. V., Okamoto, I., Casanova, M., El Marjou, F., Le Baccon, P., & Almouzni, G. (2010). A strand-specific burst in transcription of pericentric satellites is required for chromocenter formation and early mouse development. *Developmental Cell*, *19*, 625–638.

Probst, A. V., Santos, F., Reik, W., Almouzni, G., & Dean, W. (2007). Structural differences in centromeric heterochromatin are spatially reconciled on fertilisation in the mouse zygote. *Chromosoma*, *116*, 403–415.

Proudhon, C., Duffie, R., Ajjan, S., Cowley, M., Iranzo, J., Carbajosa, G., et al. (2012). Protection against de novo methylation is instrumental in maintaining parent-of-origin methylation inherited from the gametes. *Molecular Cell*, *47*, 909–920.

Puschendorf, M., Terranova, R., Boutsma, E., Mao, X., Isono, K., Brykczynska, U., et al. (2008). PRC1 and Suv39h specify parental asymmetry at constitutive heterochromatin in early mouse embryos. *Nature Genetics*, *40*, 411–420.

Quivoron, C., Couronne, L., Della Valle, V., Lopez, C. K., Plo, I., Wagner-Ballon, O., et al. (2011). TET2 inactivation results in pleiotropic hematopoietic abnormalities in mouse and is a recurrent event during human lymphomagenesis. *Cancer Cell*, *20*, 25–38.

Quivy, J. P., Roche, D., Kirschner, D., Tagami, H., Nakatani, Y., & Almouzni, G. (2004). A CAF-1 dependent pool of HP1 during heterochromatin duplication. *The EMBO Journal*, *23*, 3516–3526.

Rea, S., Eisenhaber, F., O'Carroll, D., Strahl, B. D., Sun, Z. W., Schmid, M., et al. (2000). Regulation of chromatin structure by site-specific histone H3 methyltransferases. *Nature*, *406*, 593–599.

Regha, K., Sloane, M. A., Huang, R., Pauler, F. M., Warczok, K. E., Melikant, B., et al. (2007). Active and repressive chromatin are interspersed without spreading in an imprinted gene cluster in the mammalian genome. *Molecular Cell*, *27*(3), 353–366.

Rice, J., Briggs, S., Ueberheide, B., Barber, C., Shabanowitz, J., Hunt, D., et al. (2003). Histone methyltransferases direct different degrees of methylation to define distinct chromatin domains. *Molecular Cell*, *12*, 1591–1598.

Rossant, J., & Lis, W. T. (1979). Potential of isolated mouse inner cell masses to form trophectoderm derivatives in vivo. *Developmental Biology*, *70*, 255–261.

Rougier, N., Bourc'his, D., Gomes, D. M., Niveleau, A., Plachot, M., Paldi, A., et al. (1998). Chromosome methylation patterns during mammalian preimplantation development. *Genes & Development*, *12*, 2108–2113.

Rowe, H. M., Jakobsson, J., Mesnard, D., Rougemont, J., Reynard, S., Aktas, T., et al. (2010). KAP1 controls endogenous retroviruses in embryonic stem cells. *Nature*, *463*, 237–240.

Rudert, F., Bronner, S., Garnier, J. M., & Dolle, P. (1995). Transcripts from opposite strands of gamma satellite DNA are differentially expressed during mouse development. *Mammalian Genome*, *6*, 76–83.

Rusche, L. N., Kirchmaier, A. L., & Rine, J. (2002). Ordered nucleation and spreading of silenced chromatin in Saccharomyces cerevisiae. *Molecular Biology of the Cell*, *13*, 2207–2222.

Santenard, A., Ziegler-Birling, C., Koch, M., Tora, L., Bannister, A. J., & Torres-Padilla, M. E. (2010). Heterochromatin formation in the mouse embryo requires critical residues of the histone variant H3.3. *Nature Cell Biology*, *12*, 853–862.

Santos, F., Hendrich, B., Reik, W., & Dean, W. (2002). Dynamic reprogramming of DNA methylation in the early mouse embryo. *Developmental Biology*, *241*, 172–182.

Santos, F., Peters, A. H., Otte, A. P., Reik, W., & Dean, W. (2005). Dynamic chromatin modifications characterise the first cell cycle in mouse embryos. *Developmental Biology*, *280*, 225–236.

Santos-Rosa, H., Schneider, R., Bannister, A. J., Sherriff, J., Bernstein, B. E., Emre, N. C., et al. (2002). Active genes are tri-methylated at K4 of histone H3. *Nature*, *419*, 407–411.

Schaefer, A., Sampath, S. C., Intrator, A., Min, A., Gertler, T. S., Surmeier, D. J., et al. (2009). Control of cognition and adaptive behavior by the GLP/G9a epigenetic suppressor complex. *Neuron*, *64*, 678–691.

Schotta, G., Lachner, M., Sarma, K., Ebert, A., Sengupta, R., Reuter, G., et al. (2004). A silencing pathway to induce H3-K9 and H4-K20 trimethylation at constitutive heterochromatin. *Genes & Development*, *18*, 1251–1262.

Schotta, G., Sengupta, R., Kubicek, S., Malin, S., Kauer, M., Callen, E., et al. (2008). A chromatin-wide transition to H4K20 monomethylation impairs genome integrity and programmed DNA rearrangements in the mouse. *Genes & Development*, *22*, 2048–2061.

Schultz, D. C., Ayyanathan, K., Negorev, D., Maul, G. G., & Rauscher, F. J., 3rd. (2002). SETDB1: A novel KAP-1-associated histone H3, lysine 9-specific methyltransferase that contributes to HP1-mediated silencing of euchromatic genes by KRAB zinc-finger proteins. *Genes & Development*, *16*, 919–932.

Shumacher, A., Faust, C., & Magnuson, T. (1996). Positional cloning of a global regulator of anterior-posterior patterning in mice. *Nature*, *383*, 250–253.

Sleutels, F., Zwart, R., & Barlow, D. P. (2002). The non-coding Air RNA is required for silencing autosomal imprinted genes. *Nature*, *415*, 810–813.

Smallwood, S. A., Tomizawa, S., Krueger, F., Ruf, N., Carli, N., Segonds-Pichon, A., et al. (2011). Dynamic CpG island methylation landscape in oocytes and preimplantation embryos. *Nature Genetics*, *43*, 811–814.

Smith, L. C., & Alcivar, A. A. (1993). Cytoplasmic inheritance and its effects on development and performance. *Journal of Reproduction and Fertility. Supplement*, *48*, 31–43.

Smith, Z. D., Chan, M. M., Mikkelsen, T. S., Gu, H., Gnirke, A., Regev, A., et al. (2012). A unique regulatory phase of DNA methylation in the early mammalian embryo. *Nature*, *484*, 339–344.

Steiner, N. C., Hahnenberger, K. M., & Clarke, L. (1993). Centromeres of the fission yeast Schizosaccharomyces pombe are highly variable genetic loci. *Molecular and Cellular Biology*, *13*, 4578–4587.

Stender, J., Pascual, G., Liu, W., Kaikkonen, M., Do, K., Spann, N., et al. (2012). Control of proinflammatory gene programs by regulated trimethylation and demethylation of histone H4K20. *Molecular Cell*, *48*, 28–38.

Strahl, B. D., & Allis, C. D. (2000). The language of covalent histone modifications. *Nature*, *403*, 41–45.

Strahl-Bolsinger, S., Hecht, A., Luo, K., & Grunstein, M. (1997). SIR2 and SIR4 interactions differ in core and extended telomeric heterochromatin in yeast. *Genes & Development*, *11*, 83–93.

Sugiyama, T., Cam, H. P., Sugiyama, R., Noma, K., Zofall, M., Kobayashi, R., et al. (2007). SHREC, an effector complex for heterochromatic transcriptional silencing. *Cell*, *128*, 491–504.

Sugiyama, T., Cam, H., Verdel, A., Moazed, D., & Grewal, S. I. (2005). RNA-dependent RNA polymerase is an essential component of a self-enforcing loop coupling heterochromatin assembly to siRNA production. *Proceedings of the National Academy of Sciences of the United States of America*, *102*, 152–157.

Surani, M. A., Hayashi, K., & Hajkova, P. (2007). Genetic and epigenetic regulators of pluripotency. *Cell*, *128*, 747–762.

Tachibana, M., Nozaki, M., Takeda, N., & Shinkai, Y. (2007). Functional dynamics of H3K9 methylation during meiotic prophase progression. *The EMBO Journal*, *26*, 3346–3359.

Tachibana, M., Sugimoto, K., Fukushima, T., & Shinkai, Y. (2001). Set domain-containing protein, G9a, is a novel lysine-preferring mammalian histone methyltransferase with hyperactivity and specific selectivity to lysines 9 and 27 of histone H3. *The Journal of Biological Chemistry*, *276*, 25309–25317.

Tachibana, M., Sugimoto, K., Nozaki, M., Ueda, J., Ohta, T., Ohki, M., et al. (2002). G9a histone methyltransferase plays a dominant role in euchromatic histone H3 lysine 9 methylation and is essential for early embryogenesis. *Genes & Development*, *16*, 1779–1791.

Tachibana, M., Ueda, J., Fukuda, M., Takeda, N., Ohta, T., Iwanari, H., et al. (2005). Histone methyltransferases G9a and GLP form heteromeric complexes and are both crucial for methylation of euchromatin at H3-K9. *Genes & Development*, *19*, 815–826.

Tahiliani, M., Koh, K. P., Shen, Y., Pastor, W. A., Bandukwala, H., Brudno, Y., et al. (2009). Conversion of 5-methylcytosine to 5-hydroxymethylcytosine in mammalian DNA by MLL partner TET1. *Science*, *324*, 930–935.

Takada, Y., Naruse, C., Costa, Y., Shirakawa, T., Tachibana, M., Sharif, J., et al. (2011). HP1γ links histone methylation marks to meiotic synapsis in mice. *Development (Cambridge, England)*, *138*, 4207–4217.

Tan, L., & Shi, Y. G. (2012). Tet family proteins and 5-hydroxymethylcytosine in development and disease. *Development (Cambridge, England)*, *139*, 1895–1902.

Terranova, R., Sauer, S., Merkenschlager, M., & Fisher, A. G. (2005). The reorganisation of constitutive heterochromatin in differentiating muscle requires HDAC activity. *Experimental Cell Research*, *310*(2), 344–356 [Epub September 21, 2005].

Torres-Padilla, M. E., Bannister, A. J., Hurd, P. J., Kouzarides, T., & Zernicka-Goetz, M. (2006). Dynamic distribution of the replacement histone variant H3.3 in the mouse oocyte and preimplantation embryos. *The International Journal of Developmental Biology*, *50*, 455–461.

Trostle-Weige, P. K., Meistrich, M. L., Brock, W. A., & Nishioka, K. (1984). Isolation and characterization of TH3, a germ cell-specific variant of histone 3 in rat testis. *The Journal of Biological Chemistry*, *259*, 8769–8776.

van der Heijden, G., Dieker, J., Derijck, A. A. H., Muller, S., Berden, J., Braat, D., et al. (2005). Asymmetry in histone H3 variants and lysine methylation between paternal and maternal chromatin of the early mouse zygote. *Mechanisms of Development*, *122*, 1008–1022.

Verdel, A., Jia, S., Gerber, S., Sugiyama, T., Gygi, S., Grewal, S. I., et al. (2004). RNAi-mediated targeting of heterochromatin by the RITS complex. *Science*, *303*, 672–676.

Volpe, T. A., Kidner, C., Hall, I. M., Teng, G., Grewal, S. I., & Martienssen, R. A. (2002). Regulation of heterochromatic silencing and histone H3 lysine-9 methylation by RNAi. *Science*, *297*, 1833–1837.

Wagner, R. P. (1972). The role of maternal effects in animal breeding. II. Mitochondria and animal inheritance. *Journal of Animal Science*, *35*, 1280–1287.

Wang, H., An, W., Cao, R., Xia, L., Erdjument-Bromage, H., Chatton, B., et al. (2003). mAM facilitates conversion by ESET of dimethyl to trimethyl lysine 9 of histone H3 to cause transcriptional repression. *Molecular Cell*, *12*, 475–487.

Wang, H., Huang, Z. Q., Xia, L., Feng, Q., Erdjument-Bromage, H., Strahl, B. D., et al. (2001). Methylation of histone H4 at arginine 3 facilitating transcriptional activation by nuclear hormone receptor. *Science*, *293*, 853–857.

Wang, Q. T., Piotrowska, K., Ciemerych, M. A., Milenkovic, L., Scott, M. P., Davis, R. W., et al. (2004). A genome-wide study of gene activity reveals developmental signaling pathways in the preimplantation mouse embryo. *Developmental Cell*, *6*, 133–144.

Ward, W. S., & Coffey, D. S. (1991). DNA packaging and organization in mammalian spermatozoa: Comparison with somatic cells. *Biology of Reproduction*, *44*, 569–574.

Witt, O., Albig, W., & Doenecke, D. (1996). Testis-specific expression of a novel human H3 histone gene. *Experimental Cell Research*, *229*, 301–306.

Wongtawan, T., Taylor, J. E., Lawson, K. A., Wilmut, I., & Pennings, S. (2011). Histone H4K20me3 and HP1alpha are late heterochromatin markers in development, but present in undifferentiated embryonic stem cells. *Journal of Cell Science*, *124*, 1878–1890.

Wood, V., Gwilliam, R., Rajandream, M. A., Lyne, M., Lyne, R., Stewart, A., et al. (2002). The genome sequence of Schizosaccharomyces pombe. *Nature*, *415*, 871–880.

Woolcock, K. J., Gaidatzis, D., Punga, T., & Buhler, M. (2011). Dicer associates with chromatin to repress genome activity in Schizosaccharomyces pombe. *Nature Structural & Molecular Biology*, *18*, 94–99.

Wossidlo, M., Arand, J., Sebastiano, V., Lepikhov, K., Boiani, M., Reinhardt, R., et al. (2010). Dynamic link of DNA demethylation, DNA strand breaks and repair in mouse zygotes. *The EMBO Journal*, *29*, 1877–1888.

Wossidlo, M., Nakamura, T., Lepikhov, K., Marques, C. J., Zakhartchenko, V., Boiani, M., et al. (2011). 5-Hydroxymethylcytosine in the mammalian zygote is linked with epigenetic reprogramming. *Nature Communications*, *2*, 241.

Wu, H., & Zhang, Y. (2011). Mechanisms and functions of Tet protein-mediated 5-methylcytosine oxidation. *Genes & Development*, *25*, 2436–2452.

Wykes, S. M., & Krawetz, S. A. (2003). The structural organization of sperm chromatin. *The Journal of Biological Chemistry*, *278*, 29471–29477.

Yamada, T., Fischle, W., Sugiyama, T., Allis, C. D., & Grewal, S. I. (2005). The nucleation and maintenance of heterochromatin by a histone deacetylase in fission yeast. *Molecular Cell*, *20*, 173–185.

Yang, L., Xia, L., Wu, D., Wang, H., Chansky, H., Schubach, W., et al. (2002). Molecular cloning of ESET, a novel histone H3-specific methyltransferase that interacts with ERG transcription factor. *Oncogene*, *21*, 148–152.

Yuan, P., Han, J., Guo, G., Orlov, Y. L., Huss, M., Loh, Y. H., et al. (2009). Eset partners with Oct4 to restrict extraembryonic trophoblast lineage potential in embryonic stem cells. *Genes & Development*, *23*, 2507–2520.

Zamudio, N., & Bourc'his, D. (2010). Transposable elements in the mammalian germline: A comfortable niche or a deadly trap? *Heredity*, *105*, 92–104.

Zeng, F., & Schultz, R. M. (2005). RNA transcript profiling during zygotic gene activation in the preimplantation mouse embryo. *Developmental Biology*, *283*, 40–57.

Zhang, K., Mosch, K., Fischle, W., & Grewal, S. I. (2008). Roles of the Clr4 methyltransferase complex in nucleation, spreading and maintenance of heterochromatin. *Nature Structural & Molecular Biology*, *15*, 381–388.

Zofall, M., & Grewal, S. I. (2006). Swi6/HP1 recruits a JmjC domain protein to facilitate transcription of heterochromatic repeats. *Molecular Cell*, *22*, 681–692.

## 6. Facultative heterochromatin

Facultative heterochromatin (fHC) is the second type of heterochromatin that has been recognized and is primarily characterized by the presence of two marks: H3K27me3 and H2Au (H2Au will refer to the H2AK119 mono-ubiquitylation throughout the manuscript). The H3K27me3 mark is the result of the catalytic activity of PRC2 (Polycomb repressive complex 2) mediated via the EZH proteins, while the H2Au activity is mediated by PRC1 via the RING proteins. Initially described by Edward Lewis as regulators of gene expression patterns during the development of *Drosophila*, the term Polycomb (Pc) referred to a *Drosophila* mutant displaying defects in body segmentation. It was thought that Polycomb encoded a repressor of homeotic genes required for segmentation. Nowadays, the PcG (Polycomb Group) refers to a set of genes that provoke a similar phenotype to Pc when mutated. The PcG and Trithorax families exhibit an antagonistic activity in the maintenance and regulation of homeotic gene expression in a spatial-temporal manner during development and in adulthood. PcG proteins have been shown to play a crucial role in development and the establishment of cell differentiation programs, as highlighted by the embryonic lethality in Knockout (KO) mice of the subunits *Eed*, *Ezh2*, *Suz12*, *Ring1b*, among others (detailed below). PcG proteins exist as several multiprotein complexes including the Polycomb Repressive Complexes PRC1 and PRC2. The previously held model was that PRC2 activity takes place prior to and is necessary for the recruitment of PRC1 onto H3K27me3-modified chromatin through the recognition of H3K27me3 by the CBX proteins (Cao et al. 2002). However, recent data has shown that this is not the only means whereby PRC1 can be recruited onto chromatin. The following parts will describe PRC2 composition, function and recruitment, the newly established non-canonical PRC1 complexes, the independent activity of PRC1 from PRC2, the targeting mechanisms, and the functions of PRC1.

## 7. PRC2 composition and function in mammals

The core PRC2 complex is composed of four main subunits: EZH1/2 (Enhancer of zeste homologue), SUZ12 (Suppressor of zeste 12), EED (Embryonic ectoderm development) and RbAp46/48 (known also as RBBP7/4) (Figure 10). This core complex is conserved from *Drosophila* to mammals and is absent in *Schizosaccharomyces pombe* and *Saccharomyces cerevisiae*.

EZH was shown to be involved in the repression of the early-acting segmentation-gap genes (Moazed and O'Farrell 1992; Pelegri and Lehmann 1994), and in influencing chromosome integrity during the rapid nuclear divisions in the first 2h of *Drosophila* development (Jones and Gelbart 1990). Vertebrates have two copies of the enhancer of zeste homologue (Ezh1 and Ezh2). EZH1 is present in dividing and differentiated cells, whereas EZH2 is present in actively dividing cells. In addition, the methyltransferase activity of the PRC2 complex changes depending on the EZH isoform it contains, with EZH2 resulting in higher levels of H3K27me2/3 compared to EZH1 (Margueron et al. 2008). Finally, it seems that the binding affinity to chromatin and the mechanism that leads to the restriction of transcription differ depending on the complex composition. EZH1 is able to bind chromatin independently of methyltransferase activity or presence of histone tails and is thought to lead to silencing primarily via chromatin compaction, as shown *in vitro* and *in vivo* (Margueron et al. 2008; Shen et al. 2008). This mechanism seems to be specific to EZH1. On the other hand, the compaction of chromatin when EZH2 is present seems to be a consequence of the recruitment of PRC1 to H3K27me3. EED acts as a scaffold protein physically linking EZH2 and histone H3 (Tie et al. 2007). SUZ12 stabilizes EZH2 and is necessary for nucleosome detection (Pasini et al. 2004; Nekrasov, Wild, and Muller 2005). RbAp46/48 binds histones and AEBP2 binds EZH2 and enhances its activity *in vitro* (Cao and Zhang 2004).

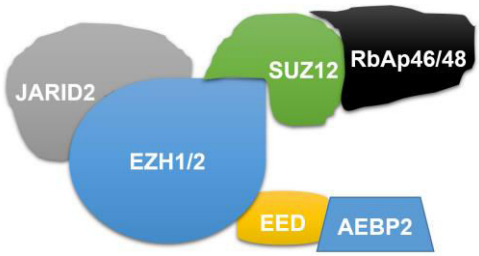


**Figure 10. PRC2 composition**
Schematic representation of the composition of PRC2 as described in the paragraph above. Based on (Margueron and Reinberg 2011a).

After fertilization, the level of PTMs on the paternal chromatin are lower and it gradually acquires *de novo* histone marks during the first cell cycle (Santos et al. 2005; Arney et al. 2002; Santenard et al. 2010). It was shown that the H3K27 residue is required for proper silencing and localization of centromeric repeats in the paternal pronucleus, specifically on the histone H3.3 variant, which is the predominant H3 variant in the paternal pronucleus. Mutating the Lysine 27 to

an Arginine in ectopically expressed H3.3 leads to an arrest of embryonic development before the blastocyst stage (Santenard et al. 2010). Furthermore, PRC2 proteins are important for the *de novo* establishment of fHC in the male pronucleus pronucleus (Arney et al. 2002; Santos et al. 2005; Puschendorf et al. 2008).

Mouse KOs for *Ezh2*, *Eed* and *Suz12* were established to study their functional role during development and show defects in gastrulation only starting at day 7.5 postcoitus although *de novo* fHC is required for preimplantation development, because of maternal contribution that allows embryos to overcome embryonic arrest during preimplantation (Faust et al. 1995; O'Carroll et al. 2001; Pasini et al. 2004). PRC2 is required for many physiological functions during development such as B cell development, imprinted X-inactivation and reprograming of primordial germ cells… (Kalantry et al. 2006; Seki et al. 2007; Su et al. 2003). PRC2 has been shown to be associated with cancer and has been selected as a target for therapy (Valk-Lingbeek, Bruggeman, and van Lohuizen 2004; Varambally et al. 2002). The essential function of PRC2 subunits stem from their regulation/control of genes encoding transcription factors important for development (Boyer et al. 2006). *Eed*$^{-/-}$ ESCs (Embryonic Stem Cells) show a reduction in H3K27me3 and an increase in the expression of transcription factors activated upon lineage commitment (Boyer et al. 2006). Similarly, *Suz12* KD also results a reduction of H3K27me3 in ESCs which fail to differentiate properly (Pasini et al. 2007). On the other hand, *Ezh2*$^{-/-}$ ESCs show a global loss of di- and tri-methylation, but maintain H3K27me3 at a subset of developmental genes (Shen et al. 2008). This has led to speculation that these different members of PRC2 have specific repressive gene targets for ESCs maintenance and differentiation, and that some genes might be targeted specifically or are shared with EZH1 (Martin and Zhang 2005; Pasini et al. 2007; Rajasekhar and Begemann 2007; Schwartz and Pirrotta 2007).

Other proteins have been shown to interact with the core PRC2 components and seem to enhance the activity of the complex. Amongst them, i) PCL1/2/3 (known respectively as PHF1, MTF2 and PHF19) are the mammalian orthologues to *Drosophila*'s Polycomblike (PCL) and interact with EZH2, SUZ12 and RbAp46/48 (Nekrasov et al. 2007); ii) AEBP2 is a zinc finger protein that binds to DNA and was shown to interact with several PRC2 components and enhances the complex's enzymatic activity (Kim, Kang, and Kim 2009), and iii) JARID2, a member of the Jumonji family of proteins, but devoid of the demethylase activity. Deletion of *Jarid2* in mice leads

to the impairment of PRC2 recruitment without strongly affecting H3K27me3 levels (Shen et al. 2009; Landeira et al. 2010) and severely affects cardiovascular, liver development and neural tube formation at day 15.5 post *coitum* (Jung et al. 2005; Takeuchi et al. 1995).

## 8. PRC2 recruitment

PcG proteins are recruited to PREs (Polycomb response elements) in *Drosophila* (Schuettengruber et al. 2014; Schuettengruber et al. 2009; Simon et al. 1993; Brown et al. 1998). In mammals, sequences that are H3K27 tri-methylated are enriched in C and G, most of them classified as CpG islands, however these sequences do not seem to indicate a consensus response element that would be able to recruit PRC2 alone (Ku et al. 2008). However, some reports have suggested the existence of mammalian PREs, using the *Drosophila* PRE recruitment as a model, via the YY1 (Ying Yang 1), a mammalian orthologue to the *Drosophila* PHO DNA binding protein, and an interaction with RYBP and PRC1 (Sing et al. 2009; Woo et al. 2010; Wilkinson, Pratt, and Atchison 2010). However, this is still a matter of debate because of contradictory data resulting from low overlap between PRC2 and YY1 in those studies (Xi et al. 2007; Ku et al. 2008). More recently, it was shown that Minimal DNA sequence elements might be capable of autonomously recruiting PRC2. It was shown that CG islands bind PRC2 if they are devoid of DNA methylation and are not transcriptionally active (Jermann et al. 2014; Riising et al. 2014). The combination of transcription factor binding and DNA sequences showed a better correlation with H3K27me3 than DNA sequence alone, this is indicative of the role transcription factors play in bridging PRC2 recruitment to specific DNA sequences (Benveniste et al. 2014).

The inactive X chromosome provides a useful example when studying chromatin in general and PRC recruitment specifically. The expression of the 17Kb ncRNA, *Xist*, initiates the inactivation of the X chromosome. *Xist* coats the X chromosome in cis and leads to the heterochromatinisation of the X chromosome which becomes methylated with H3K27 (Plath et al. 2003). PRC2 interacts *in vitro* with the stem-loop structures arising from *Xist* RNA (Maenner et al. 2010; Zhao et al. 2008) (Figure 13). Similarly, PRC2 was shown to interact with other ncRNAs such as the ncRNA for *Kcnq1ot1* and *Hotair* leading to the silencing of the ORFs (Pandey et al. 2008; Rinn et al. 2007; Tsai et al. 2010). These observations have led to a proposed model by which ncRNAs might play an important role in the recruitment of PRC2 (Khalil et al. 2009; Margueron

and Reinberg 2011b). More recently, it was shown that JARID2 could also interact with ncRNA to regulate PRC2 recruitment and stabilize its binding to EZH2 (Kaneko, Bonasio, et al. 2014; da Rocha et al. 2014). However, it has also been reported that PRC2 can interact in a nonspecific manner with the 5' region of RNAs from transcriptionally active genes leading to the inactivation of EZH2 HMTase activity, as shown by the absence of H3K27me3 and the accumulation of H3K4me3 and H3K36me3 (Zhao et al. 2010; Kaneko et al. 2013; Kaneko, Son, et al. 2014; Davidovich et al. 2013; Cifuentes-Rojas et al. 2014).

Interplay between histone post-translational modifications can also affect H3K27 methylation state and the recruitment of PRC2. KD of *Setd2*, leads to a loss of H3K36me3, a reduction in H3K27me1 and an increase in H3K27me3 (Ferrari et al. 2014) while the previously described KDs of PRC2 components only leads to a loss of H3K27 methylation. Similar modifications associated with transcriptional activation, such as H3K27ac, H3S28ph, and H3K4me3, also negatively affect PRC2 recruitment and H3K27me3 levels (Xu et al. 2009; Creyghton et al. 2010; Pasini et al. 2010; Yuan et al. 2011; Gehani et al. 2010; Voigt et al. 2012; Sidoli et al. 2014; Schmitges et al. 2011; Lau and Cheung 2011). Recent quantitative mass spectrometry analyses of H2Au interactors identified JARID2 and AEBP2 among the PRC2 subunits with the highest enrichment in *Xenopus* and *Drosophila*. The presence of JARID2 and AEBP2 in PRC2 resulted in stronger activity for H3K27me on unmodified nucleosome templates, and an even stronger increase in H3K27me3 formation when H2Au nucleosomes were used as templates. It was further shown that AEBP2-PRC2 methylated H3K27 on H2Au nucleosomes with a considerably higher efficiency than on unmodified nucleosomes, indicating that AEBP2 is critical for the specific activation of PRC2 by H2Au (Kalb et al. 2014).

## 9. Bivalent domains

The accumulation of PRC2 at CpG islands lead to the realization that these regions, which are enriched near/at the TSS, colocalized in mESCs with H3K4me3, which is a marker of active transcription and of euchromatin (Azuara et al. 2006; Lee et al. 2006; Bernstein, Mikkelsen, et al. 2006; Mikkelsen et al. 2007; Mendenhall et al. 2010; Wachter et al. 2014). H3K4me3 and H3K27me3 are both enriched at the promoters of lineage regulators (Azuara et al. 2006; Bernstein, Mikkelsen, et al. 2006; Rugg-Gunn et al. 2010). This is seemingly in contradiction with the pre-

held conception that H3K27me3 is exclusively localized in heterochromatin domains and that these domains are clearly distinct from euchromatic domains. It is more likely, as evidenced by these reports that the distinction is more dynamic and that certain genes that are dynamically regulated during development or the cell cycle can display both modifications simultaneously. The mechanism by which H3K27me3 and H3K4me3 control genes located in bivalent domains remains to be established. The presence of bivalent domains has been shown *in vivo* in zebrafish (Vastenhouw et al. 2010) and in human and mouse sperm and male PGCs (Hammoud et al. 2009; Mochizuki et al. 2012; Erkek et al. 2013; Lesch et al. 2013; Ng et al. 2013), but it is not known if these domains extend to other species *in vivo* and at which developmental stages they arise. It seems from these reports that the bivalent state is transient and resolves into either an activated or a repressed state depending on the cell fate decision.

## 10. PRC1 composition

The Polycomb repressive complex 1 (PRC1) is composed of four core proteins: i) an E3-ubiquitin ligase, RING that exists in two isoforms: RING1 also called RING1A or RNF1 (RING finger protein 1) and RING2 known as well as RING1B or RNF2. For consistency, RING1A and RING1B will be used in this manuscript. RING1B seems to be more widespread among PRC1 complexes than RING1A. These two proteins are the mammalian homologues to the RING1 protein in *Drosophila* and seem to be interchangeable to some extent. ii) a Polyhomeotic-Like protein, PHC1/2/3 are three homologues to the *Drosophila* Polyhomeotic (Ph-p and Ph-d). iii) a Chromobox protein homologue, CBX2/4/6/7/8, five homologues of *Drosophila*'s Pc. iv) Polycomb group RING finger proteins (PCGFs), with BMI1 (or PCGF4 or RNF51) and MEL18 (or PCGF2) being the only PCGFs with which the CBXs are found (Gao et al. 2012; Wang et al. 2010; Vandamme et al. 2011) (Figure 11). RING1A/B forms a heterodimer with one of the PCGF proteins which creates a scaffold for the other members of the complex. The PRC1 is then formed by the association of one protein of each group described previously. This creates a multitude of potential combinatorial associations which in turn can lead to different functions, localizations, binding affinities and activities.

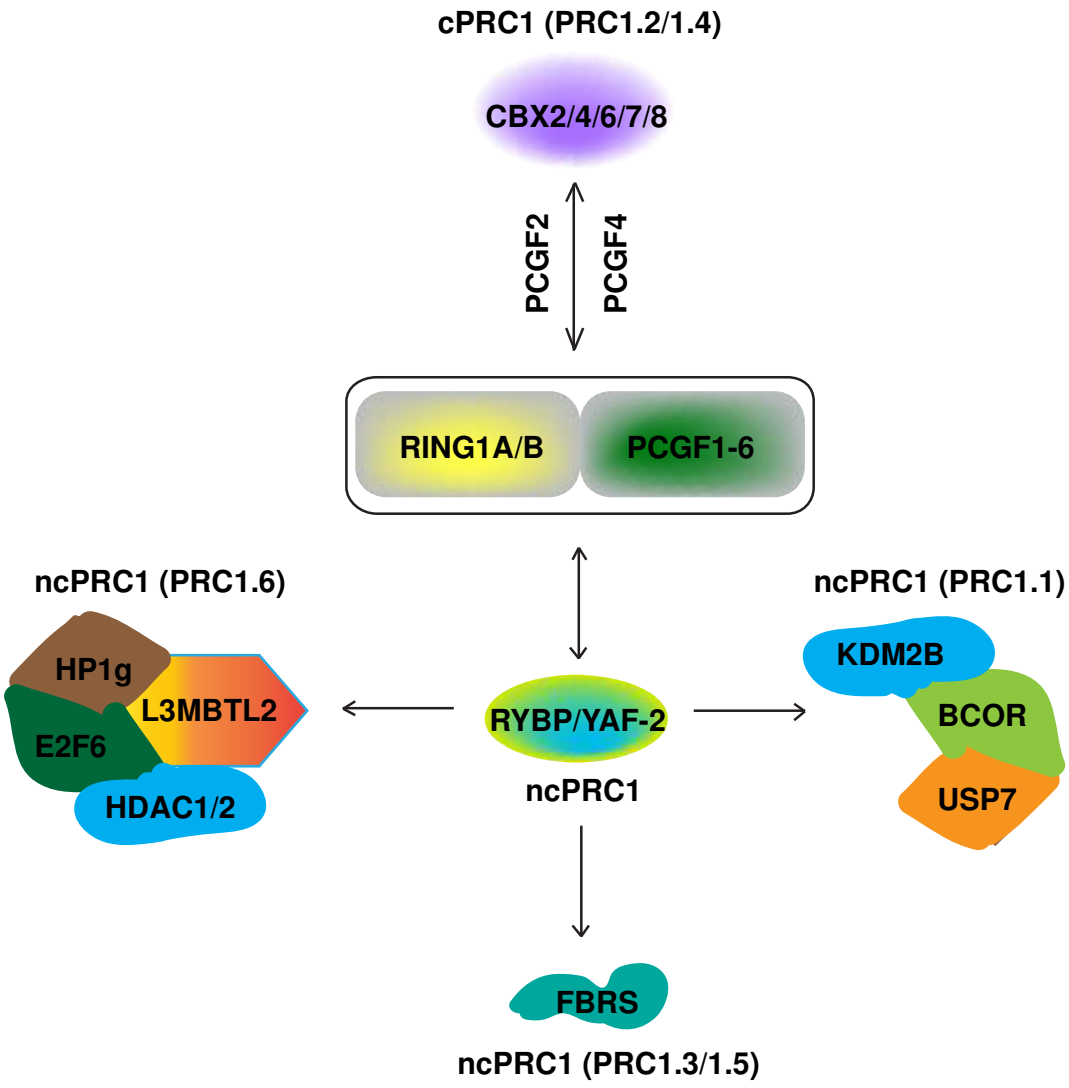


**Figure 11. Canonical and non-canonical PRC1 composition.**
The core complex (RING1A/1B and PCGFs) can associate with distinct proteins, which allows for alternative compositions. PCGF2 and PCGF4 are uniquely present in the cPRC1 complexes (PRC1.2 and PRC1.4, respectively), they are also associated with ncPRC1-containing RYBP or YAF-2, PCGF3/5 are present in the ncPRC1 complexes PRC1.3 and PRC1.5 in association with FBRS, while PCGF1 is present in the ncPRC1 complex PRC1.1 with KDM2B, USP7 and BCOR, and PCGF6 is associated with L3MBTL2, E2F6, HP1γ and HDAC1/2 in the ncPRC1 complex PRC1.6.

The above described form of the complex was until recently the only one that was thought to exist. However, recent data has shown that other proteins can replace canonical subunits within PRC1, thereby generating different PRC1 complexes. The core complex described above will be therefore referred to as the canonical PRC1 (cPRC1), as opposed to ncPRC1 (also called variant

PRC1 or vPRC1), which refers to the non-canonical PRC1 complexes. Another nomenclature exists for PRC1 complexes, in whichPRC1.2 and PRC1.4 are similar to the cPRC1, while PRC1.1/1.3/1.5/1.6 correspond to ncPRC1. Furthermore, to complicate matters, CBX proteins seem to compete with each other to gain access to form cPRC1. CBX2 was initially reported, by RT-PCR, to be the most abundant and important CBX isoform to form cPRC1 in preimplantation development and ESCs, with most other CBXs absent (except CBX8 in the oocyte) (Puschendorf et al. 2008). However, subsequent reports in ESCs have shown that CBX7 is the most abundant CBX protein bound to RING1B and the highest in expression levels (Morey et al. 2012). The effect of CBX7 on cPRC1 recruitment and maintenance of pluripotency in ESCs has been confirmed (O'Loghlen et al. 2012). Inducing differentiation of ES cells leads to a reduction in the levels of CBX7 and an increase in the levels of other CBX proteins (O'Loghlen et al. 2012; Morey et al. 2012). This is in accordance with the fact that PcG genes are targets of CBX7-cPRC1 mediated silencing (Morey et al. 2012) (Figure 12).

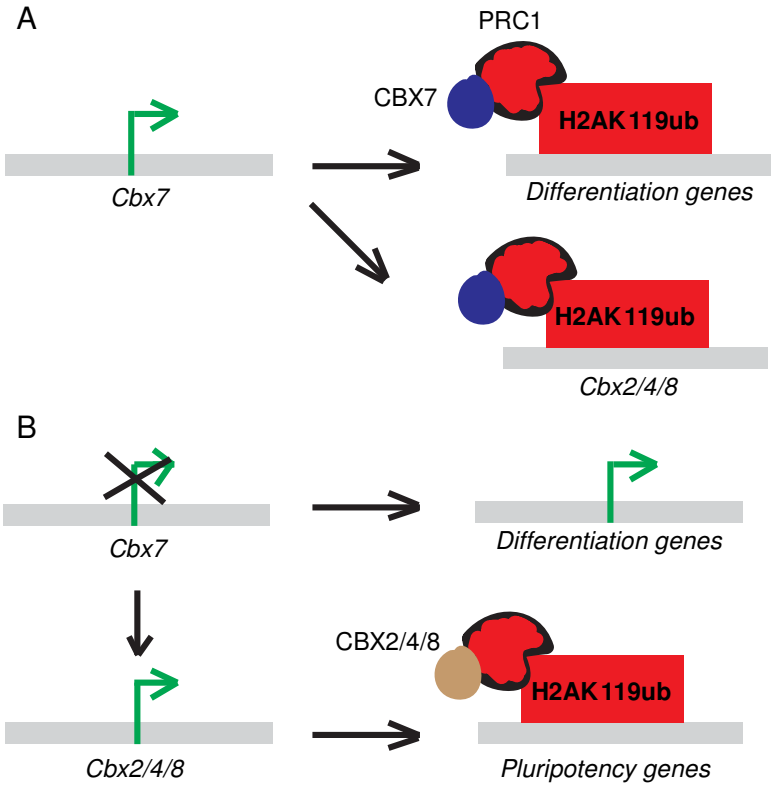


**Figure 12. Role of canonical PRC1 complexes in ESC maintenance and differentiation.**
A. Pluripotent cells express CBX7 (in blue) which recruits cPRC1 (red and black) to silence differentiation genes and *Cbx2/4/8*. B. Once *Cbx7* is silenced, differentiation and developmental genes are expressed and CBX2/4/8 (in brown) target cPRC1 to silence pluripotency genes.

The data regarding CBX2 in mouse preimplantation development is intriguing since KO mice for CBX2 (M33) do not show prenatal lethality, although they exhibit skeletal abnormalities (Core et al. 1997). The fact that *Cbx2* deletion does not affect preimplantation development, in spite of the fact that it is the only CBX protein to be present at this developmental time window (Puschendorf et al. 2008), indicates that there are compensatory complexes at play since *Ring1A/Ring1B*$^{-/-}$ embryos block at the 2-cell stage (Posfai et al. 2012). Thus, further investigations are needed to validate the composition of PRC1 during preimplantation development. Finally, null mice for either of the CBX proteins (2, 4 or 7) do not exhibit prenatal lethality (Core et al. 1997; Forzati et al. 2012; Liu et al. 2013). In contrast, Mel18 and BMI1 double KO embryos die at 9.5 dpc (Akasaka et al. 1996), suggesting that the PCGF proteins are more essential for PRC1 function than CBXs during development, or that compensatory mechanisms among CBX exist and that several CBXs must be knocked-out simultaneously to elicit a potential phenotype.

At the core of the ncPRC1 is RYBP (RING1 and YY1-binding protein) (Garcia et al. 1999) or its close homologue YAF2 (YY1 associated factor 2) in association with RING1A/B and a PCGF protein (Gao et al. 2012; Tavares et al. 2012; Morey et al. 2013). The core ncPRC1 has been found in association with: i) KDM2B, one of the two mammalian homologues of *Drosophila*'s Kdm2, is a demethylase with a zinc-finger-CxxC motif that binds to unmethylated CpG islands and demethylates di- and tri-methylation on H3K36, modifications enriched on actively transcribed genes (Farcas et al. 2012; Wu, Johansen, and Helin 2013; He et al. 2013). KDM2B targets ncPRC1 through its CxxC motif and RYBP/YAF2 improves the activity of RING1B, this complex is called RING1B-KDM2B or PRC1.1 (Wu, Johansen, and Helin 2013). ii) L3MBTL2 (lethal(3)malignant brain tumor-like protein 2), contains Malignant Brain Tumor (MBT) domains which bind histones and compact chromatin, an orthologue of *Drosophila* Sfmbt also known as h-l(3)mbt-like or m4mbt (Guo et al. 2009; Trojer et al. 2007; Trojer et al. 2011). This complex is called RING1B- L3MBTL2 or PRC1.6. iii) FBRS (probable fibrosin-1) forming a complex called RING1B-FBRS or PRC1.3/5 (Figure 11).

## 11. Activity of PRC1 complexes

Because PRC1 composition is more variable than that of PRC2, this has triggered further investigations into its functions. In addition to the ability of the RING proteins to monoubiquitylate H2A on Lysine 119 (Wang et al. 2004; McGinty, Henrici, and Tan 2014), they can also compact chromatin (Levine et al. 2002; Shao et al. 1999; Eskeland et al. 2010). The PCGF protein that is present within PRC1s seems to affect the catalytic activity of RING1B. The presence of PCGF1, 3, and 5, but not 2 or 4, result in a high enrichment of H2Au and recruitment of PRC2 (Blackledge et al. 2014). L3MBTL2 also catalyzes H2AK119 monoubiquitylation and compacts chromatin *in vitro*. Similarly, RYBP was also shown to compact chromatin *in vitro* (Trojer et al. 2011). The Bcor complex, part of the PRC1.1, can also catalyzes H2AK119 monoubiquitylation (Gearhart et al. 2006). Thus, several components of PRC1 can catalytically monoubiquitylate H2AK119 making it difficult to address the redundant activity of these proteins.

Mice KO for *Ring1a* are normal and fertile, the lack of RING1A does not affect the expression of RING1B, which overlaps with RING1A as detected by in situ hybridization in WT mice (del Mar Lorente et al. 2000). The absence of RING1A leads to mild skeletal defects that are attributed to aberrations in HOX gene expression. The presence of RING1B could explain the mild defect as both proteins seem to share the same activity and be interchangeable in PRC1 complexes and could therefore compensate for the absence of RING1A. The same could not be said for the lack of RING1B. Knockout mice for *Ring1b* show an arrest at gastrulation with the epiblast failing to expand, in addition to a defect in anterior migration of the mesoderm. In addition, extraembryonic tissues are also affected, recapitulating a phenotype of $Eed^{-/-}$ and $Ezh2^{-/-}$ mice (Voncken et al. 2003) and indicating that both PRC1-RING1B and PRC2 are likely to regulate genes that play a role in the proliferation or differentiation of extraembryonic tissues. The lack of RING1B does not affect the expression of other PcG proteins (especially EED and EZH1/2). Taken together with other data sets, this indicates that $Ring1b^{-/-}$ phenotype could be a result of an independent upstream action to PRC2. The specific effect on extraembryonic tissues is interesting as it was shown that trophoblast tissue DNA is hypomethylated in comparison to the DNA of embryonic tissues, particularly at repeat elements. This correlates well with the expected presence of PRC1 and PRC2, for silencing, at DNA hypomethylated regions and could explain the observed phenotype. Intriguingly embryos derived by nuclear transfer from ESCs lacking the three active

DNMTs can contribute to extraembryonic tissues if aggregated with wild-type embryos (Sakaue et al. 2010). Unfortunately, the functional role that PRC1 and PRC2 played in establishment of extraembryonic lineage, in the context of triple KO of DNMTs in cells followed by SCNT, was not addressed. Finally, maternal double KO of *Ring1a* and *Ring1b* aggravates the lethal phenotype of single KOs with embryos arresting at the 2-cell stage due to improper regulation of gene expression in the oocyte (Posfai et al. 2012).

Very recently, it was shown that the monoubiquitylation activity of RING1B was not necessary for the repression of target genes in ESCs. The phenotype that was observed in *Ring1B*$^{-/-}$ embryos was rescued by replacing the WT *Ring1b* gene with a mutated form that lacks the monoubiquityl activity (*Ring1BI53A/I53A*), showing that much of the function that PRC1-RING1B plays perhaps, surprisingly is independent of its monoubiquitylation activity and thus most likely dependent on its ability to compact chromatin (Illingworth et al. 2015). Interestingly, H3K27me3 deposition is reduced in *Ring1B*$^{I53A/I53A}$ cells, further confirming the notion that the presence of H2Au is a prerequisite for the placement of H3K27me3 on some genomic regions (Blackledge et al. 2014; Cooper et al. 2014; Kalb et al. 2014). ES cells double null for *Ring1a* and *Ring1b* show a proliferation defect that is stronger than that of PRC2 KOs ESCs and cannot be maintained in culture (Endoh et al. 2008). Deletion of *Ring1b* in the context of *Eed*$^{-/-}$ ES cells increases the differentiation defects (Leeb et al. 2010).

Mice lacking *Rybp* die just before gastrulation at around 6.5 dpc and blastocysts are unable to yield trophectodermal outgrowths *in vitro* (Pirity, Locker, and Schreiber-Agus 2005). Conditional KO of *Rybp* in ES cells leads to a derepression of genes related to preimplantation development during EGA at the 2-cell stage such as *E1f1a*, *Zscan4* and retro-elements. Of special interest is the upregulation of *MuERV* mRNAs among the retro-elements in *Rybp* KO ESCs. Combining *Rybp* KO with KD of *Yaf1* showed no synergistic effects between the two, indicating independent effects on ncPRC1 that have not yet been demonstrated (Hisada et al. 2012).

Mice lacking *L3mbtl2* die before birth, with embryos arresting around day 7.5 post coitus, similarly to the timing of arrest of *Ring1b*$^{-/-}$ embryos (Qin et al. 2012). This phenotype was attributed to a gastrulation failure (Qin et al. 2012). ESCs tend to differentiate more than wild type ESCs upon *L3mbtl3* KO, and show a slower proliferation rate (Qin et al. 2012). These cells led to delayed teratoma formation when injected into adult mice, in comparison to *Ring1b*$^{-/-}$ and *Eed*$^{-/-}$

cells which formed teratomas 3 weeks after injection (Leeb et al. 2010). These *L3mbtl2* KO phenotypes seem to be independent from the ubiquitylation-activity of PRC1 and HMTase activity of PRC2 since H2Au and H3K27me3 are not affected in *L3mbtl2* KO ESCs. Interestingly, H3K9me2 were found to be significantly lower in *L3mbtl2*$^{-/-}$ ESCs, indicating a possible interplay between H3K9me2 and the reported compaction activity (rather than monoubiquityl activity) of L3MBTL2 since H2Au levels are unchanged. Mutations in the ZF and MBT domains of L3MBTL2 affect colony growth indicating that both sites are required for the functional protein. Finally, most genes that are bound by L3MBTL2 in ESCs are unique to ncPRC1 and are not targets of cPRC1 or PRC2 (Qin et al. 2012) suggesting a specific set of targets that are regulated by L3MBTL2-ncPRC1 which may be informative for explaining the gastrulation phenotype of KO mice.

KO of *Scml2*, one of two mammalian homologues (the other being SCML/H1) of *Drosophila*'s Sex Comb on Midleg (SCM) and member of the cPRC1, results in differentiation defects of spermatids and reduced testis size, as well as loss of silencing of Somatic/Progenitor genes and activation of Late-Spermatogenesis Specific genes (Hasegawa et al. 2015). *Scml2*'s silencing, via DNA methylation, on the other hand is important for SynT-I formation in WT trophoblast (Branco et al. 2016). Two isoforms of SCML2 have been reported, SMCL2B lacks the SPM domain and plays a role in cell cycle regulation (Lecona et al. 2013), while SMCL2A (full length protein (Lecona et al. 2013) associates with PRC1.2 (containing PCGF2/MEL18) and PRC1.4 (containing PCGF4/BMI1) which form the cPRC1 (Levine et al. 2002; Gao et al. 2012). SCML2A (an isoform of SMCL2) interacts with the N-terminal region of Ubiquitin-specific protease 7 (USP7), a deubiquitylase that leads to histone H2B deubiquitylation in mammals and flies (van der Knaap 2005, Sarkari 2009) and plays a role in gene silencing since H2Bu is known to colocalize with gene expression, and facilitates the interaction between USP7 and BMI1 (Lecona, Narendra, and Reinberg 2015). USP7 was also shown to play a role in the stabilization of p53 and MDM2 (Li et al. 2004) and is associated with PRC1.1 and PRC1.3 (Sanchez et al. 2007; Gao et al. 2012) and with Mel18 (Maertens et al. 2010). Chemical inhibition of USP7 alters the posttranslational modifications of several PRC1.4 components and results in a reduction of H2Aub levels (Maertens et al. 2010; Lecona, Narendra, and Reinberg 2015).

## 12. Recruitment of PRC1

Recruitment of cPRC1 complexes containing CBX proteins is mediated by H3K27me3-binding via the chromodomain (de Napoles et al. 2004; Wang et al. 2004). H2Au, in turn, acts as a docking site for PRC2, serving as a 'reinforcement loop' (Blackledge et al. 2014; Cooper et al. 2014; Kalb et al. 2014). In addition, analysis of CBXs binding activity (except CBX2) to RNAs demonstrated an interaction between the chromodomain and ss- and dsRNA. Furthermore, CBX7 localization to Xi was disrupted upon RNase treatment indicating that the recruitment of PRC1 here might be directed by Xist ncRNA (Bernstein, Duncan, et al. 2006). Further evidence for the role of RNA in PRC recruitment comes from the fact that CBX7 also interacts with *Anril* ncRNA (Yap et al. 2010) to silence cyclin-dependent kinase inhibitor locus INK4b/ARF/INK4a, a regulator of cellular senescence (Gil et al. 2004). The chromodomain of CBX7 binds *Anril* ncRNA and H3K27me with similar affinities (El Messaoudi-Aubert et al. 2010) (Figure 13). The CBX proteins seem to have specific target genes, for example CBX7 is expressed in ESCs and seems to maintain pluripotency by silencing PRCr (PRC repressed) target genes (Morey et al. 2013; Morey et al. 2012; Brookes et al. 2012), whereas CBX6, does not bind RING1B although it is expressed in ESCs (Morey et al. 2012). The rest of the CBX proteins, part of cPRC1, are expressed upon differentiation and seem to silence lineage-specific genes (Lesch et al. 2013) (Figure 12). Concerning *de novo* recruitment mechanisms, CBX2 targets cPRC1 to the paternal pronucleus in the zygote, which is devoid of constitutive heterochromatin by recognizing AT-rich regions (Tardat et al. 2015).

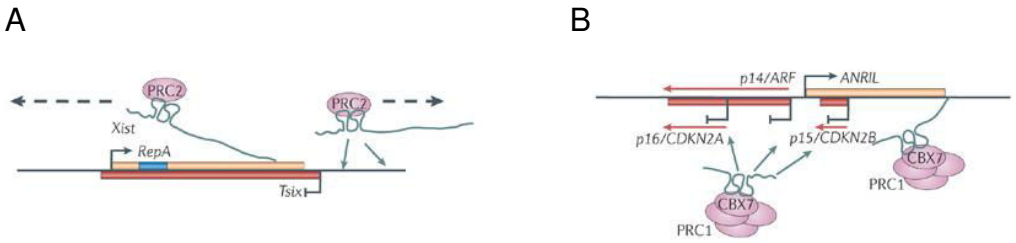


**Figure 13. Examples of PRC1 and PRC2 recruitment by ncRNAs.**
A. Xist non-coding RNA, expressed exclusively by the inactive X chromosome (Xi), contains RepA, a repeat element that is necessary for the recruitment of Polycomb repressive complex 2 (PRC2) (Zhao et al. 2008). Arrows indicate the spreading across Xi. B. ANRIL is a non-coding antisense transcript that binds the CBX7 which is required for the repression of INK4a/ARF tumor-suppressor (Yap et al. 2010). Modified from (Beisel and Paro 2011).

RYBP and YAF2 can interact with YY1, with RYBP playing a role in the ubiquitylation and degradation of YY1 via its interaction with the MDM2 protein (Chen et al. 2009), thus it has been proposed that RYBP and YAF2 might serve as mediators that connect ncPRC1 to YY1 for their recruitment to chromatin (Wilkinson, Pratt, and Atchison 2010; Woo et al. 2010; Garcia et al. 1999; Kalenik et al. 1997). RYBP was also reported to bind DNA and the C-terminus of RING1B and changes its folding upon binding (Neira et al. 2009). Additionally RYBP recognizes ubiquitination through its NZF (Npl4 zinc finger) domain in the N-terminus which is important for its nuclear localization, and also gets monoubiquitylated by RING1B (Arrigoni et al. 2006). Finally, RYBP has a RanBP2-zinc finger, which is a domain that has been shown in other proteins to bind RNA (Loughlin et al. 2009; Nguyen et al. 2011). Although the presence of RYBP increases the ubiquitylation activity of ncPRC1 compared to CBX2-cPRC1 *in vitro* (Gao et al. 2012), it seems that in ESCs, RYBP-ncPRC1 targeted genes (PRCa for PRC active) are not so strongly silenced as CBX7-cPRC1 targeted genes/PRCr (Brookes et al. 2012; Morey et al. 2013) suggesting that CBX7-cPRC1 is the main repressive complex.

SCML2 comprises MBT repeats in the N-terminal region (Montini et al. 1999), which have been shown to bind to monomethylated lysines, a C-terminal SPM domain that mediates interactions with PRC1 (Bornemann, Miller, and Simon 1996), and a RBR (RNA Binding Region) that seems to bind preferentially to ssRNA (Bonasio et al. 2014). The RBR domain was shown to be necessary for the targeting of SCML2A to chromatin but didn't affect its interactions with RING1B and BMI1. The report also suggests that SCML2A can repress gene expression independently of BMI1 recruitment, but doesn't show the mechanism behind it (Bonasio et al. 2014). The discovery of the RBR domain suggests a new mechanism for the recruitment of PRC1 via ncRNA.

KDM2B, member of ncPRC1.1, deficient cells show a reduction in H2Au and SUZ12 recruitment. The loss of the CxxC binding domain of KDM2B results in a mislocalization of RING1B on almost half of CpG islands ESCs. PRC2 components are strongly enriched in mouse ESC nuclear extracts with H2AK119ub, as shown by affinity pull downs (Blackledge et al. 2014). Jarid2–Aebp2-containing PRC2 recognizes H2Au as a docking site and trimethylates H3K27 (Kalb et al. 2014). Targeting a MBD-RING1B/PCGF4 fusion protein (the MBD from KDM2B) to CpG unmethylated DNA resulted in H2Au deposition and was enough to establish H3K27me3 at

pericentric heterochromatin domains in mouse, indicating first, that the activity of PRC1 was affected by DNA methylation, and second, that the demethylase activity of KDM2B was not necessary for the deposition of H3K27me3 when PRC2 is recruited after PRC1 and H2Au establishment (Blackledge et al. 2014; Cooper et al. 2014). Additionally, it was shown that recruitment of PRC2, but not PRC1, to pericentric heterochromatin was blocked by the presence of DNA methylation and other histone marks such as H3K9me3 and H3K36me3 (Cooper et al. 2014). In contrast, H3K9me3 and H2Au showed a strong colocalization *in vivo* (Cooper et al. 2014), owing to the presence of HP1γ (or CBX3) which recognizes H3K9me3 and is part of the RING1B-L3MBTL2 complex (Guo et al. 2009; Farcas et al. 2012).

# III. Replication

The chromatin plays a fundamental role in organizing the genome and *de novo* synthesized histones must be appropriately packaged upon newly replicated DNA. The next chapter of this manuscript will discuss in depth the interplay between replication and chromatin machinery because of their intertwined functions in proliferating cells.

## 1. Origins of replication and initiation of replication

In order to proliferate, cells require a faithful inheritance mechanism to propagate their genome during DNA replication. In *Escherichia coli*, DNA replication is semi-conservative (Meselson and Stahl 1958) and initiates from a single origin of replication (OriC) (Tomizawa and Selzer 1979). However, in eukaryotes several thousands of origins of replication are necessary for an organized, non-random, replication of DNA (Huberman and Riggs 1966; Taylor 1959; Taylor, Woods, and Hughes 1957). No consensus motif has been identified for origins of replication in metazoans, but some evidence suggests that there is a good correlation between replication initiation sites and transcription start sites at efficient promoter-origins (Sequeira-Mendes et al. 2009; Cayrou et al. 2011).

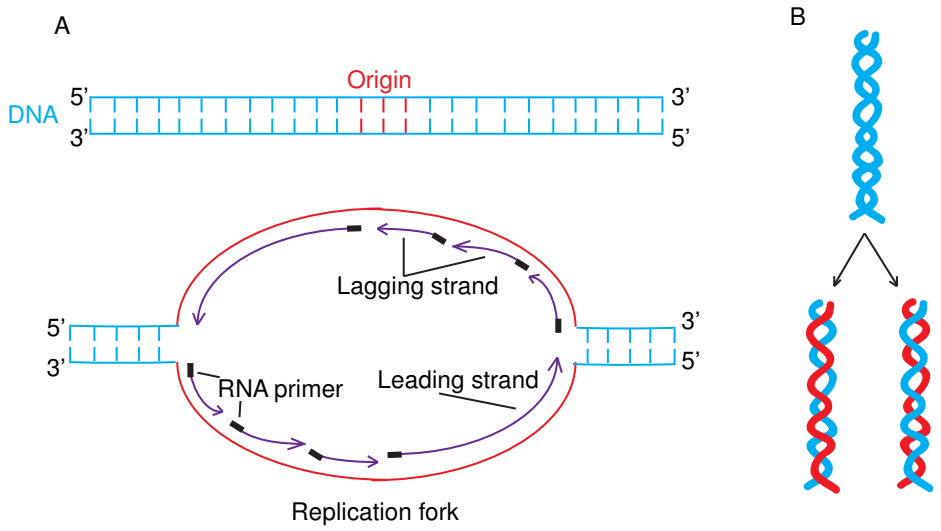


**Figure 14. Basic principles of replication.**
A. DNA replication starts with short RNA primers, synthesized by DNA polymerase-α. Since DNA synthesis always occurs in the 5′ to 3′ direction, one strand of the DNA (the leading strand) will be synthesized continuously, whereas the other strand (the lagging strand) will be synthesized discontinuously. B. DNA replication is semi-conservative; each parental strand serves as template for synthesis of a new strand (Meselson and Stahl 1958).

The origin recognition complex (ORC) directly recognizes such origins and initiates replication. Subsequently, cell division cycle 6 (CDC6), CDT1 and MCM9 are recruited to the origin site to load the minichromosome maintenance (MCM) protein complex MCM2-7 which has an ATPase-dependent DNA helicase activity and forms a ring around the replication origin (Remus et al. 2009; Lutzmann and Mechali 2008). This complex is called the pre-replication complex or preRC, once it is assembled around DNA, the origins are licensed. Additional components associate to the preRC such as: CDC45 and the GINS complex, CDC7–DBF4 and cyclin E–cyclin-dependent kinase 2 (CDK2). Once the scene is set, this enables the association of the DNA polymerase machinery to MCM2-7 to move ahead of the fork to open the double stranded DNA and allow for the synthesis of the complementary strand (Mechali 2010).

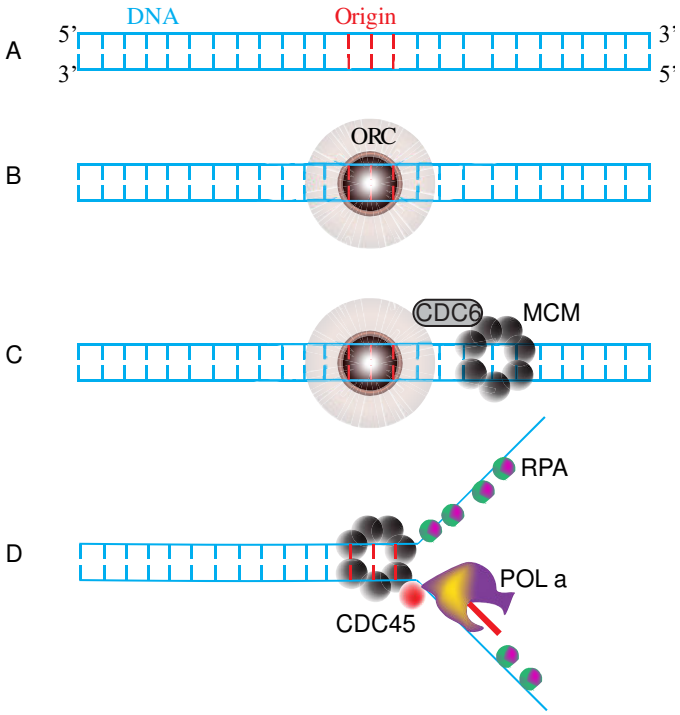


**Figure 15. Schematic representation of replication initiation.**
Proposed model for formation of preinitiation complexes, represented by the binding of MCM, ORC and Cdc6 (C), and subsequent loading of the initiation factors Cdc45, replication protein A (RPA) and DNA polymerase α (Pol α/primase) which synthesizes RNA primers required to prime lagging-strand DNA synthesis (D).

In G1 phase, inactive MCM helicases are preloaded onto the preRCs and are activated depending on: i) the timing of activation. Origins get activated asynchronously during S-phase and are classified into three groups (early, mid or late-replicating origins), ii) the stress response (DNA damage for example) or iii) growth conditions which could lead to the activation of origins in order to complete replication in a timely fashion (Taylor 1977; Gilbert 2007). The selection of which origin to initiate seems to be set during G1 of each cell cycle (Sasaki et al. 2006) and varies depending on stress or even developmental program (Norio et al. 2005). It seems in *S. pombe* and in human cells that active origins seem to cluster (initiation zone) and be separate by large numbers of silent origins (Pasero and Gasser 2002; Lebofsky et al. 2006). Some memory of replication seems to exist in the form of replicon clusters, but not at specific origins (Jackson and Pombo 1998; Takebayashi et al. 2001). In conclusion, three timings of origin replication exist (early, mid and late), additionally different types of origins exist (flexible, dormant/inactive and constitutive).

Intriguingly many replication clusters have been shown to localize to heterochromatic areas that are late replicating regions, which seem to be controlled by CHK2 in yeast (Hayashi et al. 2007), indicating that a chromatin context is also at play in determining replication timing.

## 2. Mediators of Replication Stress

Several sources of stress can affect replication. Among them, the i) lack of components (dNTP, histone, chaperones…) that are necessary for the synthesis and incorporation into chromatin of DNA (Poli et al. 2012; Bester et al. 2011; Anglana et al. 2003), ii) unrepaired DNA lesions (dsDNA) that lead to fork collapse (reviewed by (Ciccia and Elledge 2010)), iii) excessive ssDNA resulting from continuous unwinding of the parental DNA by the replicative helicase after the polymerase stalling (Pacek and Walter 2004; Sogo, Lopes, and Foiani 2002), iv) nicks and gaps in the DNA, v) errors caused by misincorporated desoxynucleotides (summarized in (Dalgaard 2012)), vi) collisions between replication and transcription complexes (Helmrich et al. 2013; Bermejo, Lai, and Foiani 2012; Bermejo et al. 2011), vii) secondary structure of DNA (G-quadruplexes, triplexes, hairpins…) that promote replication slippage (McMurray 2010), viii) 'early replicating fragile sites' that replicate early in the S-phase and are found in highly transcribed regions (Barlow et al. 2013), ix) 'common fragile sites' harbor few active replication origins and are susceptible to polymerase stalling (Letessier et al. 2011) x) chromatin compaction and accessibility (Khurana and Oberdoerffer 2015).

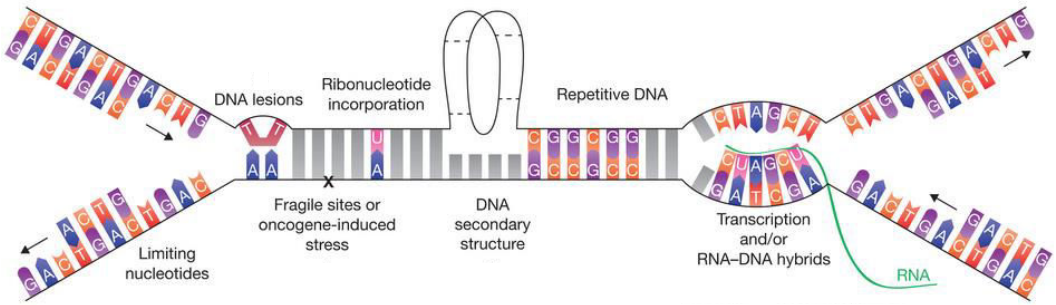


**Figure 16. Examples of sources of replication stress**
Schematic representation of potential sources that can slow or stall DNA replication, including limiting nucleotides, DNA lesions, ribonucleotide incorporation, repetitive DNA elements, transcription complexes and/or RNA–DNA hybrids, DNA secondary structure and fragile sites. Modified from (Zeman and Cimprich 2014).

## 3. Cellular response to replication stress

Phosphoinositide 3-kinase (PI3K)-related protein kinases (PIKKs) are major regulators of DNA-damage response, among them the ataxia-telangiectasia mutated (ATM) and RAD3-related (ATR) are the most studied. They are homologous proteins that share a Ser/Thr kinase activity and target an overlapping set of substrates to mediate cell-cycle arrest and DNA repair. ATM is activated in response to double-strand breaks (DSBs), in contrast ATR seems to be activated during S-phase in order to regulate origin firing and repair stalled forks (Cimprich and Cortez 2008). ATR has been shown to be essential for the viability of replicating human and mouse cells (Cortez et al. 2001; de Klein et al. 2000; Brown and Baltimore 2000), whereas mutations in ATM are known to predispose the ataxia-telangiectasia disorder (Savitsky et al. 1995). One of the earliest events that occur during replication stress is the phosphorylation of H2A.X (or γH2AX), which can be promoted by both ATR and ATM (Celeste et al. 2002; Celeste et al. 2003; Ward and Chen 2001; Szilard et al. 2010; Petermann, Woodcock, and Helleday 2010; Ozeri-Galai et al. 2008), but requires ATM for maintenance (Sirbu et al. 2011).

## 4. Activation of the ATR pathway

Once a replication fork is stalled, it can lead to DNA damage causing ssDNA or dsDNA lesions. RPA (replication protein A) recognizes and binds to ssDNA (Bochkarev et al. 1997) which triggers the recruitment of replication-stress response proteins, and mainly ATR via ATRIP (ATR-interacting protein) (Cortez et al. 2001; Zou and Elledge 2003; Fanning, Klimovich, and Nager 2006) that binds directly to RPA (Ball 2007). For ATR recruitment, the ssDNA has been shown to require a 5' double-stranded primer junction (Ellison and Stillman 2003; Majka, Niedziela-Majka, and Burgers 2006; MacDougall et al. 2007). However, there are no specific markers or modifications that can be used to certify that ATR is itself activated or not (Cimprich and Cortez 2008). To become activated ATR also requires the RAD9-RAD1-HUS1 complex (also known as 9-1-1) (Stokes et al. 2002; Byun et al. 2005; MacDougall et al. 2007) to bring TopBP1 into close proximity to activate it (Kumagai et al. 2006). ATR then phosphorylates CHK1 at Serine 317 and 345 (Liu et al. 2000; Guo et al. 2000; Zhao and Piwnica-Worms 2001) which subsequently becomes activated and autophosphorylated at Serine 296 (Clarke and Clarke 2005; Kasahara et al.

2010), leading to the dissociation of CHK1 from chromatin (Smits, Reaper, and Jackson 2006; Zhang et al. 2005). Several others proteins are also phosphorylated by ATR including some of the MCM proteins(Cortez, Glick, and Elledge 2004). Intriguingly, ATR has also been shown to become activated upon: stalled transcription (Buchmann, Skaar, and DeCaprio 2004; Derheimer et al. 2007), collisions between DNA and RNA polymerases (Bermejo 2011) and at common fragile sites (Casper et al. 2002).

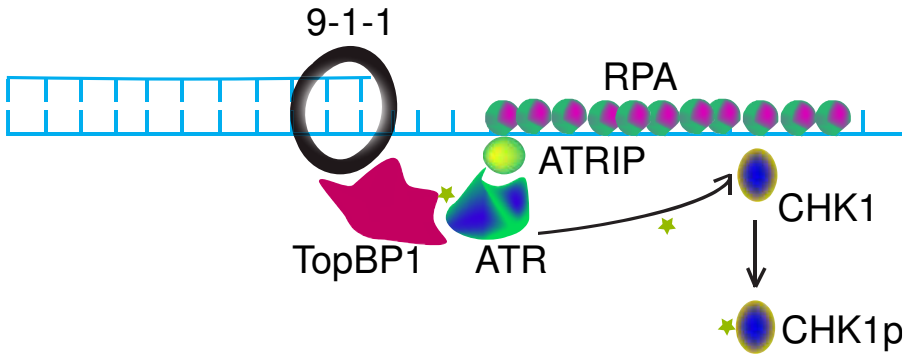


**Figure 17. Activation of the ATR pathway.**
Exposed ssDNA is rapidly coated by RPA, which directly binds ATRIP and recruits the ATRIP/ATR complex. Meanwhile, the 9-1-1 clamp is loaded to the fork and recruits TopBP1 in proximity of ATR activating its kinase activity. ATR, in turn, phosphorylates Chk1 to release it from the chromatin and activate the inter-S phase replication stress checkpoint.

As previously mentioned, following phosphorylation by ATR, CHK1 is in turn activated through phosphorylation. In fission yeast, for example, CHK1 phosphorylation is required for cell cycle arrest upon DNA damage (Capasso et al. 2002). CHK1's effect on the cell cycle is probably due to its phosphorylating activity on WEE1 and CDC25 (O'Connell et al. 1997; Lee, Kumagai, and Dunphy 2001; Peng et al. 1997). CHK1 can activate: i) the G2-M checkpoint by phosphorylating CDC25C resulting in its cytoplasmic localization (Peng et al. 1997; Matsuoka, Huang, and Elledge 1998; Sanchez et al. 1997), ii) S and G2 checkpoints by phosphorylating CDC25A and triggering its proteasome-mediated degradation (Hassepass, Voit, and Hoffmann 2003; Molinari et al. 2000; Sorensen et al. 2003; Zhao, Watkins, and Piwnica-Worms 2002). However, CHK1 can also regulate CDC25A activity in the absence of DNA damage (Zhao, Watkins, and Piwnica-Worms 2002; Sorensen et al. 2003; Chen, Ryan, and Piwnica-Worms 2003),

as well as CDC25B phosphorylation at the centrosome during unperturbed cell division (Schmitt et al. 2006). Additionally, CHK1 plays an important role in fork speed progression by controlling excess origin firing and its absence reduces the incorporation of dNTPs and stalls replication forks (Petermann et al. 2006; Petermann, Woodcock, and Helleday 2010). The ATR-mediated activation of CHK1 results in increased origin firings and reduced replication fork speeds (Petermann et al. 2006; Petermann, Woodcock, and Helleday 2010; Wilsker et al. 2008; Maya-Mendoza et al. 2007). However, the activation of dormant origins is not directed by CHK1, but by polo-like kinase-1 (PLK1) which is recruited (Trenz, Errico, and Costanzo 2008) following the phosphorylation of MCM2 by ATR (Cortez, Glick, and Elledge 2004; Yoo et al. 2004). This mechanism could be a way for the cell to catch up while it repairs the stress induced (Taylor 1977; Gilbert 2007), but at the same time it puts pressure on the cellular system because the increasing number of origins will mean more competition for cellular components (more dNTPs, helicases, polymerases…) which in turn leads to a global reduction in the speed of the forks. It might seem that, upon DNA damage, the increase in origin forks (dormant forks activation) (McIntosh and Blow 2012; Ge, Jackson, and Blow 2007; Woodward et al. 2006) is counterintuitive, but as it leads to the reduction of the speed of all the forks, it gives the cellular machinery time to resolve errors.

## 5. Activation of the ATM and DNA-PK pathways

Double strand breaks (DSBs) will arise in the case of persistent stress that leads to unresolved forks and collapse and thus to the recruitment of ATM and DNA-PK (members of the PIKKs family) (Hanada et al. 2007; Sirbu et al. 2011). Two hypotheses for how a stalled replication fork can lead to DSBs are presented in Zeman 2014 and will not be discussed here. More importantly for this discussion are the ATM and DNA-PK pathways. In the case of DNA-PK, double-strand breaks are bound rapidly by the Ku heterodimer (Ku70 and Ku80), which loads and activates the catalytic subunit of DNA-PK (DNA-PKcs) to initiate NHEJ (Non-homologous end joining) (Mahaney, Meek, and Lees-Miller 2009; Roberts et al. 2010). Upon activation DNA-PKcs get autophosphorylated on the six-residue ABCDE cluster (or T2609 cluster) which destabilizes its interaction with DNA ends and provides access to end processing enzymes (Meek, Dang, and Lees-Miller 2008). (Shrivastav, De Haro, and Nickoloff 2008). ATM on the other hand is activated by the MRE11-RAD50-NBS1 (MRN) complex to set up Homologous Recombination (Williams,

Williams, and Tainer 2007). ATM in turn activates CHK2 (by dimerization and autophosphorylation) which, in contrast to CHK1, is largely inactive in the absence of DNA damage (Lukas et al. 2001). CHK1 and CHK2 share many downstream substrates that play an important role in cellular homeostasis (Bartek and Lukas 2003). However, in contrast to CHK1$^{-/-}$ mice, CHK2 deficient mice are viable (Takai et al. 2002), suggesting that CHK2 activity can be compensated by another mechanism.

## 6. Role of chromatin during DNA replication

The chromatin landscape affects the process of DNA replication progression, which can be slowed down by tightly organized chromatin. However, chromatin is not merely obstructive to replication as problems with fork replication require changes in the chromatin environment in order to get resolved.

As replication initiates, the need to open the chromatin structure and access DNA sequences is primordial. What happens to the parental nucleosomes? And how are new histones incorporated during replication? Current data suggests that the parental histones are evicted ahead of the replication fork and are disrupted into two H2A-H2B dimers and one H3-H4 tetramer. It is thought that this eviction happens via ATP-dependent chromatin-remodeling enzymes, such as ISWI or ACF1, as reported by (Collins et al. 2002; Poot et al. 2004; Groth et al. 2007). Histone chaperones are also implicated in the eviction process and might act as acceptors of evicted histones, for example: FACT, a H2A-H2B chaperone, has been found in complex with MCM (Tan et al. 2006; Gambus et al. 2006). Nucleosomes are reformed as soon as there are 225 (±145) nucleotides on the leading strand and 285(±120) nucleotides using simian virus 40 (SV40) minichromosomes (Sogo et al. 1986). The parental nucleosomes maintain their PTMs (Benson et al. 2006), theoretically carrying over “epigenetic” information, and are deposited either on the leading or lagging strand (Sogo et al. 1986; Jackson 1988). Synthesis of new histones is vital for cell viability (Kim 1998) and the incorporation of these histones is critical to restore nucleosome occupancy. Newly synthesized H3-H4 are deposited, onto replicating DNA, by CAF-1 (or Chromatin-Assembly Factor 1), a conserved three-subunit protein, and targeted by PCNA (proliferating cell nuclear antigen) (Shibahara and Stillman 1999). Histones H3.1 and H3.2 are known to be deposited by CAF-1 in a DNA-replication-dependent manner whereas H3.3 deposition is DNA-replication-

independent via HIRA (Tagami et al. 2004; Latreille et al. 2014) or DAXX and ATRX (Lewis et al. 2010). Depletion of CAF-1 in HeLa cells led to the phosphorylation of CHK1 and accumulation of cells in S phase (Hoek and Stillman 2003) Of note also, is the presence of PTMs (mainly acetylation) on histones prior to their *de-novo* incorporation (Sobel et al. 1995; Ma et al. 1998). Interestingly, H3K9me1 and me2 were also found among the PTMs (Loyola et al. 2006).

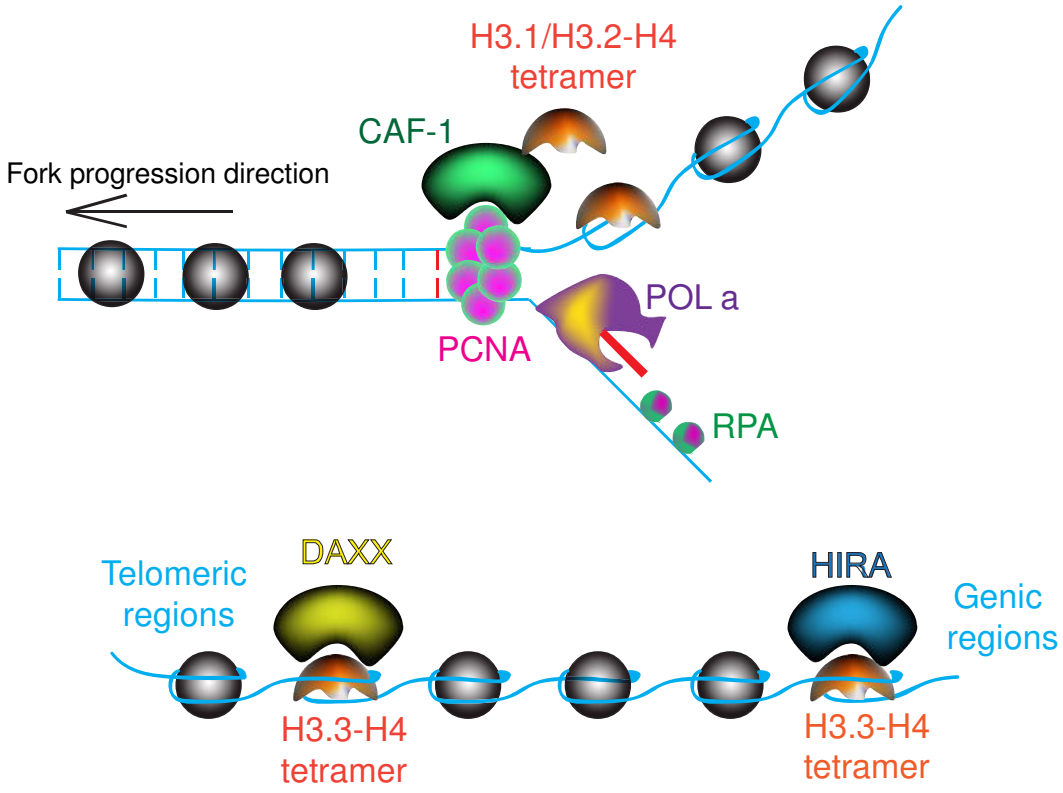


**Figure 18. Replication dependent and independent deposition of H3-H4 tetramer.**
Deposition of histones onto newly synthesized DNA is regulated by histone chaperones. On one hand, deposition of H3.1 and H3.2 is replication dependent and (H3.1/2–H4) tetramers are deposited by CAF-1 in coordination with PCNA. On the other hand, HIRA and DAXX mediate replication-independent nucleosome assembly of (H3.3–H4) tetramers at genic and telomeric regions respectively.

"Silent" chromatin, enriched with heterochromatic marks, is known to replicate later than "accessible" euchromatic regions (reviewed by (Mechali et al. 2013)). Reduction of H3K9me3 in response to overexpression of KDM4A demethylase, in mammalian cells and *C. elegans,* promoted chromatin accessibility and accelerated cell cycle progression and replication timing, after cells where synchronized at G1/S and S with hydroxyurea (HU) arrest and release in comparison to cells

in G2/M (by nocodazole arrest). Conversely, the loss of catalytic activity of KDM4A led to an increase in the amount of ssDNA, but did not change replication duration, and depletion of KDM4A induced DNA-damage associated with replication-stress and resulted in ATR/p53-dependent apoptosis (Black et al. 2010). Interestingly, it was reported that KDM4A overexpression resulted in copy number gains at certain loci, that required the cell to re-replicate these areas, providing a framework for explaining how copy number gains can take place *in vivo* during tumorigenesis (Black et al. 2013). These events can be suppressed by the overexpression of Suv39h1 or HP1γ (Black et al. 2010; Black et al. 2013). This suppression could be a result of the interaction that can take place between HP1 and ORC (Pak et al. 1997; Murzina et al. 1999). Another histone PTM that is important for stable replication is H2B ubiquitination on Lysine 123 (H2Bu) which facilitates the establishment of newly formed nucleosomes following DNA replication. Loss of H2Bu slowed replication fork progression, but didn't affect pre-RC formation in *S. pombe* (Trujillo and Osley 2012).

## 7. Role of H4K20 methylation during replication and damage response

H4K20me1 is mediated by PR-Set7 at the nucleosome (Nishioka et al. 2002; Oda et al. 2009). Initial reports suggested that PR-Set7 was important for S-phase progression (Jorgensen et al. 2007; Tardat et al. 2007). PR-Set7 and H4K20me1 were later shown to increase in G2-M, to be reduced in G1 and to start increasing afterwards in S phase, indicating a fluctuation during the cell cycle (Oda et al. 2009; Sirbu et al. 2011). H4K20me2, on the other hand, showed a decrease during S-phase and then increased in G2-M. PR-Set7$^{-/-}$ mice exhibited decondensation of mitotic chromosomes that could be potentially explained by the reduction in H4K20me3 levels, and PR-Set7 null ESCs accumulated in G2-M (Oda et al. 2009). Notably, lack of PR-Set7 (or Set8) activated the ATR pathway and led to cell cycle arrest while inhibition of ATR or CHK1 rescued this phenotype suggesting that H4K20 methylation levels could be important for replication initiation (Jorgensen et al. 2007), since it was shown that LRWD1 (Leucine-Rich Repeats and WD Repeat Domain Containing 1 or ORCA for Origin Recognition Complex-Associated Protein), which associates to ORC, binds to H4K20me3 *in vitro* (Shen et al. 2010; Vermeulen et al. 2010). Importantly, H4K20me1/2/3 are bound by the BAH (bromo adjacent homology) domain of *Mus musculus* ORC1 *in vitro*, linking H4K20 methylation to DNA replication licensing and DNA

damage repair pathways (Kuo et al. 2012). Alternatively, H4K20 methylation can disrupt replication by recruiting CRB2, or its mammalian homologue 53bp1, via a Tudor domain to DNA damage sites (Sanders et al. 2004; Botuyan et al. 2006; Pei et al. 2011).

# Results: first part

## Annex 2: Remodeling of Suv420 activity in the pre-implantation embryo is essential for the timely control of replication

# Remodeling of Suv420 activity in the pre-implantation embryo is essential for the timely control of replication.

André Eid[1]

Adam Burton[1,2]

Maria-Elena Torres-Padilla[1,2]*

[1] *Institut de Génétique et de Biologie Moléculaire et Cellulaire, CNRS/INSERM U964, U de S, F-67404 Illkirch, CU de Strasbourg, France.*

[2] *Institute of Epigenetics and Stem Cells, Helmholtz Zentrum München D-81377 München, Germany.*

* torres-padilla@helmholtz-muenchen.de

Tel. + 49(0) 89-3187-3317

Fax. + 49(0) 89-3187-3389

**Key Words:** mouse embryo, Suv420, heterochromatin, replication stress

Extensive chromatin remodeling after fertilization is thought to take place to allow for a new developmental program to start. This includes dynamic changes in histone methylation (such as H4K20) and in particular, the remodeling of heterochromatic marks such as H4K20me3. While the essential function of H4K20me1 in pre-implantation embryos has been well-established, the role of the additional methylation states through the action of the Suv420 methyltransferases has not been addressed. Here we show that Suv420h1/h2 are mostly absent in the mouse embryo before implantation, correlating with a rapid decrease of H4K20me3 from the 2-cell stage onwards. Ectopic expression of Suv4-20h2 leads to sustained levels of H4K20me3, developmental arrest and defects in

S-phase progression. The developmental phenotype can be partially overcome through inhibition of the ATR pathway, suggesting that the main function for the remodeling of H4K20me3 after fertilization is to allow the timely and coordinated progression of replication. This contrasts with the replication program in somatic cells, where H4K20me3 has been shown to promote replication origin licensing, and anticipates a different regulation of replication during this developmental time window.

## Introduction

The fertilization of the oocyte by the sperm results in the formation of a totipotent zygote that has the ability to provide all extra- and embryonic tissues necessary for embryonic development. The earliest stage of development before implantation is of critical importance for setting up the first embryonic lineages in the blastocyst. Therefore, how the organization of the chromatin and its architecture are defined during the first cell divisions to enable such changes in cellular plasticity and fate remains a central question in biology.

In the mouse, pre-implantation development is characterized by a distinctive, atypical state of chromatin signatures, since many histone post-translational modifications (PTMs) are reduced or absent after fertilization. In addition, the paternal and maternal chromatin remain physically segregated in two separate pronuclei that maintain distinctive chromatin marks, with the maternal chromatin containing many constitutive heterochromatin histone modifications, while the paternal chromatin is rather enriched with facultative heterochromatin ones, which are thought to substitute for the absence of constitutive heterochromatin (reviewed (Burton and Torres-Padilla 2014)). The histone H4 Lysine 20 di- and tri-methylation (H4K20me2/3) are known marks of constitutive heterochromatin in somatic cells. H4K20me3 localizes primarily at centromere, pericentromeres and telomeres that are enriched in repetitive sequences and are gene poor (reviewed (Fadloun, Eid, and Torres-Padilla 2013)). This is in contrast to H4K20me1, which is one of the most abundant modifications on H4 and localizes to a wide variety of genomic regions in a cell-cycle dependent manner (Houston et al. 2008; Barski et al. 2007; Jorgensen et al. 2007; Oda et al. 2010). While in yeast one single enzyme catalyzes the three methylation states, in mammals H4K20me1 is catalyzed by PR-Set7 and H4K20me2 and H4K20me3 are both catalyzed by the histone methyltransferases SUV420H1 and SUV420H2 (Kmt5b and Kmt5c, respectively) (Schotta et al. 2004; Schotta et al. 2008; Rice et al. 2002; Nishioka et al. 2002). Immediately after fertilization, in the zygote, H4K20me3 is only detected on the maternal pronucleus, where it appears mostly distributed around ring-like structures formed by the nucleoli precursors (Nucleolar-Like

bodies) which harbor the peri- and centromeric regions (Wongtawan et al. 2011; Probst et al. 2007). Importantly, H4K20me3 is undetectable from the 2-cell stage onwards, and remains so until the peri-implantation period (Wongtawan et al. 2011).

This transient loss of H4K20me3 is perplexing and raises two important questions. Firstly, the only other cell types displaying absence of H4K20me3 seem to be cancer cells with increased pluripotent capacity and proliferation activity, resulting in poor prognosis for patients (Fraga et al. 2005; Schneider et al. 2011; Yokoyama et al. 2014) It is thus essential to understand how fluctuations on H4K20me3 levels impact cell proliferation and cellular potency. Secondly, the lack of conventional constitutive heterochromatin in zygotes and 2-cell stage embryos has been linked to their characteristic nuclear organization and high chromatin dynamics, which is believed to support a higher developmental plasticity. However, whether changes in this atypical heterochromatin configuration play a functionally role in developmental plasticity beyond a mere correlation has not been addressed. As such, the question thus arises of whether forced maintenance of H4K20me3 during pre-implantation could restrict developmental capacity.

The observation that the absence of H4K20me3 in pre-implantation development correlates with the highest cellular potency prompted us to ask whether this absence is required for zygotic reprogramming to take place and to investigate how H4K20me3 relates to cellular proliferation *in vivo*. To address this, we first profiled systematically the two methyltransferases responsible for H4K20 tri-methylation, *Suv4-20h1* and *Suv4-20h2,* and found that they are only weakly expressed after fertilization. Accordingly, in order to achieve sustained maintenance of H4K20me3 throughout pre-implantation development, we ectopically expressed *Suv4-20h1* and *Suv4-20h2* from the zygote stage. Our results show that ectopic expression of *Suv4-20h2* is sufficient to restore global levels of H4K20me3. *Suv4-20h2* displayed a markedly higher ability to restore H4K20me3 than *Suv4-20h1*. Embryos expressing ectopically *Suv4-20h2* – but not *Suv4-20h1* – did not develop beyond the 2-cell stage, indicating that the remodeling of H4K20me3 is required for pre-implantation development completion. *Suv4-20h2* expression led to a proliferation defect accompanied by replication abnormalities. Importantly, the developmental phenotype was partially rescued by inhibition of the ATR pathway, suggesting that

H4K20me3 induces replication stress and S-phase arrest. Our results shed light into the functional role of the absence of H4K20me3 during pre-implantation development and suggest that, in contrast to somatic cells, H4K20me3 is incompatible with timely progression of DNA replication of the embryonic chromatin.

## Results

### Expression of H4K20 modifiers during pre-implantation development

SUV4-20H1 and SUV4-20H2 are the two mammalian homologues of *Drosophila*'s Set8. The combined knock-out of *Suv4-20h1/h2* completely abolishes H4K20me3, with slightly different contributions from SUV4-20H1 and SUV4-20H2 (Schotta et al. 2004; Schotta et al. 2008), indicating that they are the major H4K20me3 methyltransferases in mammalian cells. We thus addressed the expression of both genes by RT-qPCR in all stages of pre-implantation development. The pattern of expression of *Suv4-20h1* resembles that of maternally inherited genes with stable levels between the zygote and 2-cell stage, followed by a sharp reduction to non-detectable levels at the 4-cell stage to be subsequently re-expressed at the 8-cell stage; *Suv4-20h1* remains expressed at the morula and blastocyst stage although to a lower extent compared to *Actinb* (Fig. S1). In contrast, *Suv4-20h2* mRNA levels are drastically lower than *Suv4-20h1* throughout pre-implantation development (Fig. S1). A third enzyme, *Smyd5*, was reported to methylate H4K20 *in vitro* (Stender et al. 2012), although the contribution of SMYD5 to global H4K20me3 levels is unclear. We find that, in contrast to the two SUV4-20 enzymes, the expression of SMYD5 is strongly induced from the 2-cell stage onwards, and is expressed throughout all the stages analyzed (Fig. S1). Given the strong expression of SMYD5 during these developmental time periods, when H4K20me3 is undetectable on embryonic chromatin, it is unlikely that SMYD5 contributes to the global remodeling of H4K20me3 after fertilization. Note that there are no specific antibodies available for SUV4-20H1, SUV4-20H2 or SMYD5 (our unpublished observations), and therefore our analysis for these three enzymes focuses on mRNA exclusively. To date, only one demethylase has

been shown to be able to act on H4K20me3 *in vitro*, *Phf2* (Stender et al. 2012). Thus. we next investigated the expression of *Phf2* in pre-implantation embryos. RT-qPCR showed that the mRNA for *Phf2* is abundant in the zygote, in comparison with later stages, where it is practically absent from the 8-cell stage onwards, suggesting that *Phf2* mRNA is inherited maternally and is quickly degraded after fertilization. Immunostaining confirmed that PHF-2 is present throughout all stages of pre-implantation development concomitantly with absence of H4K20me3 (data not shown).

Although we cannot formally exclude a contribution of demethylation towards keeping H4K20me3 practically absent from the embryonic chromatin, the results above suggest that low H4K20me3 levels throughout the cleavage stages may be due to low expression of SUV420 methyltransferases, in particular of SUV4-20H2, rather than to active demethylation.

**Ectopic expression of *Suv4-20h2* results in accumulation of H4K20me3**

Given the above results, in order to maintain sustained H4K20me3 during pre-implantation development, we chose to ectopically express *Suv4-20h2* in zygotes. Zygotes were microinjected at 17h post-hCG with mRNA for HA-tagged *Suv4-20h2* in combination with mRNA for *GFP* as a positive control for injection (Fig. 1A). Control groups included embryos injected with mRNA for *GFP* alone as well as non-injected embryos. After microinjection, embryos were cultured until the late zygote stage and analyzed by immunofluorescence using an HA-antibody, which revealed that SUV4-20H2 was efficiently translated, and localized throughout the nucleoplasm of both maternal and paternal pronuclei (Fig. 1A). In wild-type embryos, H4K20me3 is only detected around the NLBs and nuclear periphery at DAPI-rich regions in the maternal pronucleus and it is absent from the paternal pronucleus, creating an asymmetric pattern at this stage (Fig. 1A, non-injected) (Kourmouli et al. 2004; Wongtawan et al. 2011). Expression of *Suv4-20h2* resulted in a clear increase in H4K20me3 levels in the maternal pronucleus, but not in the paternal pronucleus (Fig. 1A). This observation was surprising considering that SUV4-20H2 was distributed equally between both pronuclei, and suggests that SUV4-

20H2 is unable to modify the levels of H4K20me3 on the paternal chromatin in the zygote. The levels of H4K20me3 remained elevated at later stages of development upon ectopic expression of SUV4-20H2. At the 2-cell stage, SUV4-20H2 was readily detected in the nucleus of both blastomeres, as well as H4K20me3 (Fig. 1B). This was in contrast to non-injected embryos, where there were no detectable levels of H4K20me3, in agreement with earlier findings (Fig. 1B). The distribution of H4K20me3 throughout 2-cell stage nuclei, as opposed to only half of the nucleus, indicates that SUV4-20H2 can methylate both paternal and maternal chromosomes at this stage, suggesting that methylation on the paternal chromatin is delayed in comparison to the maternal one, which takes place in the zygote.

To test for specific effects of the methyltransferase activity of SUV4-20H2, we generated a mutant in the SET domain. The SET domain is shared across several other histone methyltransferases, including SUV3-9H1 in which a mutation in the amino acid sequence (NHSCD) abrogates its catalytic activity (Rea et al. 2000; Lachner et al. 2001). We therefore generated a SUV4-20H2 construct where the corresponding NHDC motif was replaced by AAAG within the SET domain of SUV4-20H2. The resulting mutant protein will be referred throughout this manuscript as SUV4-20H2mut, while the wild type will be referred to as SUV4-20H2WT. We microinjected early zygotes as above, with mRNA for *Suv4-20h2mut* and *GFP*, and analyzed embryos at the late zygote stage. The AAAG mutation did not affect the localization of SUV4-20H2mut, which remained evenly distributed in both pronuclei, but it efficiently abolished the methyltransferase activity of SUV4-20H2, since expression of SUV4-20H2mut did not lead to an increase in H4K20me3 levels in either the maternal or the paternal pronucleus (Fig. 1A). Likewise, levels of H4K20me3 remained low in 2-cell stage embryos expressing SUV4-20H2mut, similarly to control embryos (Fig. 1B).

Therefore, our results show that SUV4-20H2WT increases H4K20me3 levels *in vivo* and that our approach can be used to study the effect of maintaining H4K20me3 levels during pre-implantation development.

**H4K20me3 maintenance blocks pre-implantation development**

We next addressed whether embryos displaying sustained H4K20me3 can develop normally. Embryos were microinjected with mRNA for *Suv4-20h2WT* as above at 17h phCG and cultured for 3 days until the blastocyst stage. Embryos were monitored daily, with embryos failing to reach the morula/blastocyst stage being considered as arrested or blocked. As controls we used non-injected (ni) embryos, embryos microinjected with *GFP* mRNA alone, and embryos microinjected with mRNA for *Suv4-20h2mut* in combination with *GFP*. Control embryos showed robust development, with 95.5%, 83.3% and 82.5% developing to the morula stage for the non-injected embryos (n=131) or embryos expressing GFP (n=176) and SUV4-20H2mut (n=73), respectively (Fig.1C). These percentages reflect typical developmental rates obtained in these assays (Santenard et al. 2010; Jachowicz et al. 2013). In contrast, embryos expressing SUV4-20H2WT displayed a strikingly lower developmental rate (38%; n=98) (Fig. 1C). SUV4-20H2mut embryos resulted in the same developmental rate as GFP embryos, indicating that the presence of the SUV4-20H2 protein *per se* does not result in embryonic lethality, but its histone methyltransferase activity does. Thus, we conclude that the embryonic arrest observed for SUV4-20h2WT embryos is most likely due to the resultant increase in H4K20me3, suggesting that the complete removal of this heterochromatic mark is required during pre-implantation development.

We next addressed whether the developmental phenotype upon expression of SUV4-20H2WT at the zygote stage is specific to that stage exclusively. For this, we asked whether microinjection of mRNA for *Suv4-20h2WT* at a different stage results in a similar cellular arrest. We microinjected a single 2-cell stage blastomere with mRNA for *Suv4-20h2wt* in combination with *GFP* or with mRNA for *GFP* alone as a negative control (Fig. S2A). As in the zygote, SUV4-20H2WT increased the levels of H4K20me3 in the injected cell in 2-cell embryos (Fig. S2B). Counting the number of cells derived from the SUV4-20H2WT-expressing blastomeres versus those derived from the GFP-only or the non-injected sister blastomere revealed a reduced cell progeny in SUV420H2WT-expressing blastomeres (Fig. S2C), indicating that expression of SUV4-20H2WT in 2-cell embryos leads to cellular arrest. Immunostaining of these embryos showed that cell arrest was

often accompanied by nuclear fragmentation (Fig. S2D). In conclusion, SUV4-20H2-mediated H4K20me3 leads to cell proliferation arrest in pre-implantation embryos independently of the stage of development.

**Sustained H4K20me3 blocks embryos prior to the 2-cell stage and modifies heterochromatin signatures**

To understand the mechanism behind the developmental arrest in *Suv4-20h2WT*–expressing embryos, we dissected the developmental stages at which the embryos blocked. Most embryos arrested at the zygote and 2-cell stage; 45% and 32% respectively. Eighteen percent blocked at the 4-cell and 5% at the 8-cell stage (Fig 1D). The distribution of arrested embryos across pre-implantation development suggests that H4K20me3 affects the earlier stages of development during which epigenetic reprogramming is taking place. Thus, we wondered whether the maintenance of H4K20me3 at the zygote and 2-cell stage could perturb other heterochromatic marks. Analysis of H3K9me3 revealed no global differences between non-injected, *GFP* or *Suv4-20h2WT*-expressing embryos (Fig. 1E). This result is in line with the suggested model for heterochromatin establishment where SUV39H1/H2 activity is upstream of SUV4-20H1/H2 (Schotta et al. 2004). Thus, increased H4K20me3 occurred without global changes in H3K9me3, allowing us to distinguish phenotypic effects between the typical full 'H3K9me3-directed' heterochromatin versus those effects specific to changes in H4K20me3.

H3K64me3 is an additional constitutive heterochromatin histone modification, and its distribution during pre-implantation development strongly resembles that of H4K20me3 (Daujat et al. 2009): H3K64me3 is present in the maternal pronucleus but is undetectable from the 2-cell stage onwards. In agreement, H3K64me3 was undetectable in non-injected embryos at the 2-cell stage (Fig. 1F). In contrast, SUV4-20H2WT embryos showed a marked increase in H3K64me3 in 2-cell stage nuclei, but not in SUV4-20H2mut embryos (Fig. 1F). This observation is surprising considering that MEFs double KO for *Suv4-20h1* and *Suv4-20h2* retain H3K64me3, which had suggested that H3K64me3 was independent of SUV420 activity (Lange et al. 2013). Thus, the interplay between

H4K20me3 and H3K64me3 in the embryo may obey different regulatory mechanisms than in somatic cells.

**The H4K20me3 developmental block is mediated by SUV4-20H2 at the zygote and 2-cell stage**

*Suv4-20h1* is the second mammalian homolog of Set8 and is only weakly expressed in the early embryo (Fig. S1). To address whether the embryonic block observed following H4K20me3 maintenance is specific to the histone methyltransferase activity of SUV4-20H2, we undertook the same experimental design as above with SUV4-20H1. Ectopically expressed SUV4-20H1 displayed a similar nuclear localization as SUV4-20H2 at the zygote stage. However, SUV4-20H1 did not detectably increase levels of H4K20me3 at the zygote stage (Fig. 2A), and only weakly did H4K20me3 levels increase at the 2-cell stage (Fig. 2B), indicating that *in vivo*, the catalytic activity towards H4K20me3 establishment is higher for SUV4-20H2 than for SUV4-20H1. This is in agreement with previous suggestions from crystallography work (Southall, Cronin, and Wilson 2014). The low histone methyltransferase activity of SUV4-20H1 was lost upon mutating the NHDC sequence of its SET domain into AAAG, similarly to SUV4-20H2 (Fig. 2B, SUV4-20H1mut). Next, we performed a developmental potential assay with embryos expressing SUV4-20H1 similarly to that of SUV4-20H2 (Fig. 2C). We microinjected early zygotes with either *Suv4-20h1WT* or *Suv4-20h1mut* mRNA in combination with mRNA for *GFP,* or with mRNA for *GFP* alone. Ninety-eight percent of non-injected embryos reached the morula/blastocyst stage (n=127) (Fig. 2B). *GFP*– and *Suv4-20h1mut*– embryos developed at a similar rate, with 78% (n=80) and 80% (n=54) of them reaching the morula/blastocyst stage respectively (Fig. 2B). In spite of a slightly lower developmental rate in these embryos, this difference is not statistically significant and most likely results from the micromanipulation of the embryos. Similarly, embryos expressing ectopically *Suv4-20h1WT* did not show a significant change in developmental progression, with 65.9% of embryos developing beyond the morula stage (n=78) (Fig. 2C). This observation indicates that the H4K20me3 increase from the zygote to the 2-cell stage is a primary

cause of the embryonic arrest and is primarily mediated by SUV4-20H2 histone methyltransferase activity.

**Changes in transcriptional activity in embryos expressing SUV4-20H2 are limited**

In the mouse, the first wave of embryonic gene expression takes place in the zygote and the second wave, with a higher transcriptional activity, takes place at the 2-cell stage (Aoki, Worrad, and Schultz 1997; Bensaude et al. 1983; Flach et al. 1982). Deposition of H4K20me3 through SUV4-20H2 can cause RNA Pol II pausing and repress gene expression in transformed cell lines by blocking H4K16ac (Kapoor-Vazirani, Kagey, and Vertino 2011). Given that most SUV4-20H2 embryos arrested at the zygote and 2-cell stage, we thus investigated whether the increase in H4K20me3 resulted in suppression of transcriptional activation in these embryos. To evaluate global levels of gene expression, we pulsed embryos in culture with EU (5-Ethynyl Uridine) for one hour at the late 2-cell stage, corresponding to the late phase of transcription during genome activation (Fig. 3A). Non-injected and SUV4-20H2mut embryos showed a similar distribution of EU pattern, indicating that SUV4-20H2mut does not compromise EGA with 84.6% (n=13) and 94.4% (n=18) of embryos displaying active transcription, respectively (Fig. 3A-B). A significant proportion of 2-cell stage embryos expressing SUV4-20H2WT (61.1 %, n=18) also displayed active transcription (Fig. 3B). Nevertheless, it seems that most embryos displayed lower transcriptional activity, since only 22 % of SUV4-20H2 embryos showed high levels of EU incorporation, in comparison with more than 50% for the non-injected and SUV4-20H2mut groups (Fig. 3B). This suggests that sustained H4K20me3 impacts on global levels of transcription at the 2-cell stage and could partly explain the developmental block. However, because most SUV4-20H2WT embryos displayed transcriptional activity, albeit at reduced rates, these observations could also suggest a delay in the onset of transcriptional activation. Because the timing of transcriptional activation in the embryo is closely related to that of replication, it remains possible that the reduced transcriptional activity in SUV4-20H2WT embryos reflects a delay and/or a defect in S-phase progression.

**H4K20me3 disturbs developmental progression through replication in the zygote and the 2-cell stage embryo.**

Previous reports have indicated that H4K20 methylation levels may play a role in the control of replication timing and origin licensing (Tardat et al. 2007; Tardat et al. 2010; Oda et al. 2009; Oda et al. 2010; Vermeulen et al. 2010; Beck et al. 2012). Thus, we wondered whether the developmental arrest observed upon expression of SUV4-20H2WT could be due to a misregulation of S-phase. To address this hypothesis, embryos were subjected to an EdU (5-ethynyl-2'-deoxyuridine) pulse of one hour at the late 2-cell stage, at which most embryos are expected to be in late S-phase (Bolton, Oades, and Johnson 1984). Because it is known that replication does not proceed synchronously across embryos, we further scored replication patterns as 'late' or 'early' according to whether they reflect a late S-phase (with low levels of EdU detected at the NLBs or the nuclear periphery) or an early-mid S-phase (where replication foci are visible and evenly distributed in the nucleus) respectively. As expected, most non-injected embryos displayed a late replication pattern at this time point (21 out of 25) (Fig. 3D-E). Similarly, albeit with some delay presumably due to the microinjection procedure, most SUV4-20H2mut embryos also displayed a late replication pattern (12 out of 20) (Fig 3D-E). SUV4-20H2WT embryos instead mostly showed an early replication pattern with 85% of embryos displaying high levels of EdU incorporation (n=13) (Fig. 3D-E). This observation points towards a misregulation of S-phase progression in SUV4-20H2WT embryos, and prompted us to further investigate the timings of S-phase initiation and completion.

We thus performed EdU labeling at four different time points that correspond to the onset and completion of S-phase in zygotes and in 2-cell stage embryos. Because of the limited number of embryos available per experiment, in these experiments we only used non-injected embryos as negative controls. At the onset of replication in the zygote stage, all control embryos had started replication and showed stable levels of EdU incorporation (Fig. 3F), and 80% of embryos had finished replication by 29h post-hCG injection (Fig. 3G). In contrast, while most SUV4-20H2WT embryos started timely replication (90%; n=20), the majority of them (68%) showed significantly higher levels of EdU incorporation

than non-injected embryos in both pronuclei (Fig.3F), and all embryos maintained robust levels of EdU incorporation at 29h phCG (Fig. 3G). These experiments suggest that while SUV4-20H2WT embryos enter S-phase at a similar time to the controls, S-phase progression is delayed. Likewise, at the 2-cell stage control and SUV4-20H2WT embryos displayed similar levels of replication foci at the start of S-phase (35h phCG; Fig. 3H). However, SUV4-20H2WT embryos showed high levels of EdU incorporation at 39h phCG, while non-injected embryos had mostly completed S-phase at this time (Fig. 3I). These observations indicate a clear effect on S-phase progression in embryos with sustained H4K20me3 levels at the zygote and 2-cell stage. This phenotype correlates well with the timing and distribution of the embryonic arrest elicited upon ectopic expression of SUV4-20H2 (Fig. 1D).

**Misregulation of S-phase is independent of changes in H4K20me1 in *Suv4-20h2*–expressing embryos**

Previous reports have shown that changes in the levels of H4K20me1 and the expression of PR-Set7 lead to an intra S-phase checkpoint activation and cell cycle arrest (Houston et al. 2008; Oda et al. 2009; Tardat et al. 2007). Since H4K20 methylation is processive (Sims et al. 2006; Congdon et al. 2010) it is possible that the increased H4K20me3 levels upon ectopic expression of SUV4-20H2WT have repercussions on the levels of H4K20me1, and thus the developmental phenotypes/ misregulation of S-phase may be due to changes in H4K20me1 rather than to an increase in H4K20me3. To address this, we analyzed levels of H4K20me1 in non-injected embryos as well as embryos expressing SUV4-20H2mut or SUV4-20H2WT at the 2-cell stage during G2 phase, when H4K20me1 levels are highest (Fig. 4A). Expression of SUV4-20H2WT led to a reduction in H4K20me1 levels, suggesting that H4K20me1 is indeed used as a substrate for the higher methylation state (Fig. 4A). Surprisingly, expression of SUV4-20H1WT showed a stronger reduction of H4K20me1 (Fig. 4B), even though it did not lead to an increase in H4K20me3 (Fig. 2B). This suggests that SUV420H1WT converts H4K20me1 to dimethylation. Indeed, the reduction in H4K20me1 upon expression of SUV4-20H1WT was dependent on its methyltransferase activity (Fig. 4B). However, in spite of our multiple attempts to identify

a specific H4K20me2 antibody, we were unable to perform immunostaining for H4K20me2 (not shown).

Importantly, even though SUV4-20H1WT embryos show a reduction in H4K20me1 levels, they do not exhibit embryonic lethality or cell cycle arrest (Fig. 2C), in contrast to SUV4-20H2WT embryos that show both reduction of H4K20me1 and developmental arrest (Fig. 1C). This observation leads us to conclude that the developmental arrest in SUV4-20H2WT embryos is mostly independent of changes in H4K20me1 levels. Indeed, while PR-Set7 loss leads to a G2/M arrest (Oda et al. 2009; Tardat et al. 2010), we did not detect changes in H3S10p in SUV4-20H2WT embryos compared to non-injected or SUV4-20H2mut controls (Fig. 4C).

**The SUV4-20H2-mediated embryonic arrest is partially rescued by inhibition of ATR**

All of our observations together suggest that the phenotypic arrest of embryos expressing SUV4-20H2WT is a result of a misregulation of DNA replication. H4K20 methylation can be a marker of DNA damage and increased levels of H4K20me2/3 have been linked to the activation of the ATR pathway in cancer cells (Botuyan et al. 2006; Hajdu et al. 2011; Pei et al. 2011). We therefore hypothesized that sustained H4K20me3 could trigger DNA damage checkpoint activation during S-phase in the embryo. We thus investigated the levels of γH2A.X, an indicator of DNA damage and replication stress and CHK1p/CHK1, a downstream effector kinase of the ATR pathway and marker of S-phase checkpoint activation (Mechali et al. 2013). Immunostaining of 2-cell stage embryos in the late S-phase with a γH2A.X antibody revealed diffuse nuclear accumulation of γH2A.X with a few foci in control, non-injected embryos, in agreement with previous observations (Ziegler-Birling et al. 2009)(Fig. 4D). We did not detect changes in the global levels of γH2A.X in embryos expressing either SUV4-20H2WT or SUV4-20H2mut (Fig. 4D), suggesting that sustained H4K20me3 levels do not cause DNA damage and that γH2A.X is not involved in the embryonic arrest observed.

SUV4-20H2WT embryos showed higher levels of CHK1 in comparison with non-injected and SUV4-20H2mut embryos (Fig. 4E). In addition, CHK1p was undetectable in non-

injected embryos, but displayed a weak signal in SUV4-20H2WT embryos (Fig. 4F). The observation that CHK1 and CHK1p levels appeared higher in SUV4-20H2WT embryos suggested a checkpoint activation during S-phase. We reasoned that if embryos with sustained H4K20me3 levels upon expression of SUV4-20H2 arrest because of an S-phase checkpoint activation, we should be able to release the developmental arrest, at least partially, through inhibition of the ATR pathway. To address this, embryos were injected as above with mRNA for *Suv4-20h2WT* and cultured in the presence of an ATR inhibitor (ATRi) from the late zygote stage (Fig. 4G). Since longer inhibition of ATR is known to block developmental progression (Brown and Baltimore 2000; Nakatani et al. 2015), we focused specifically on assessing the developmental block beyond the 2-cell stage (that accounts for 74% of the phenotype) by scoring embryos that reached the 4- to 8-cell stage transition. As shown in figure 4G, all non-injected embryos cultured in the presence of the ATRi reached the 4-cell stage in a similar rate to non-injected embryos cultured without inhibitor. SUV4-20H2WT embryos treated with ATRi developed at significantly higher rates than SUV4-20H2WT embryos cultured without the inhibitor ($p<0.05$; $n=32$) (Fig. 4G). Although not all embryos overcame the 2-cell stage block upon inhibition of the ATR pathway, our results suggest that the developmental defects elicited from sustaining H4K20me3 levels are partially alleviated by inhibiting S-phase checkpoint activation. This leads us to conclude that the primary function of H4K20me3 remodeling after fertilization is to allow swift and ordered replication. This contrasts with the replication program in somatic cells, where H4K20me3 has been shown to promote ORC (Origin Replication Complex) binding, and anticipates a different regulation of replication during this developmental time window.

## Discussion

Embryonic development requires a unique reprogramming mechanism to wipe the slate clean for the developmental program to initiate. Zygote and 2-cell stage embryos exhibit a particular nuclear structure with distinctive and asymmetric chromatin signatures

thought to be necessary for epigenetic reprogramming. Heterochromatic marks are unique identifiers of parental chromatin that accumulate asymmetrically on the maternal chromatin and are absent from the paternal chromatin. To address the requirement for such a chromatin environment *in vivo*, we undertook the strategy of ectopic expression of two H4K20me3 histone methyltransferases, *Suv4-20h1* and *Suv4-20h2*. Indeed, ectopic expression of such chromatin modifiers can be used to interrogate the system to shed light into the regulatory mechanisms of the early embryo by studying how these mechanisms react to such perturbations. The ectopic expression of *Suv4-20h2* modifies H4K20 methylation levels by reducing H4K20me1 and increasing H4K20me3 and leads to embryonic arrest, mostly before the 2-cell stage. This embryonic arrest is dependent on the histone methyltransferase activity of SUV4-20H2. In addition, the developmental block seems to derive from the specific activity of SUV4-20H2 and the sustained H4K20me3 levels, since expression of SUV4-20H1 does neither result in developmental arrest nor affect H4K20me3 levels markedly. While it is likely that the developmental arrest observed is mainly due to the H4K20me3 increase, the changes in H3K64me3 levels could also potentially contribute to the developmental phenotype observed upon *Suv4-20h2WT* ectopic expression.

The expression of SUV4-20H2 also leads to a misregulation of S-phase with increased replication sites, concomitant with activation of the ATR pathway. We postulate that the subsequent activation of the intra-S phase checkpoint is the cause of the cell cycle block. It is known that activation of ATR leads to a block of replication forks that exhibit ssDNA, but in order to compensate for the delayed stalled forks undergoing repair, several dormant origins initiate replication (Gilbert 2007), which could explain the continuous EdU incorporation observed in the late S-phase in zygotes and 2-cell stage embryos expressing SUV4-20H2WT. Chemical inhibition of ATR partially rescues the S-phase block and developmental capacity. The persistent embryonic arrest in a proportion of embryos could result from misregulation of gene expression independently of the cell cycle/S phase progression at the 2-cell stage which might not be overcome by ATR inhibition. However, we cannot at this stage distinguish effects on gene expression caused by developmental arrest or not.

Our results showcase the necessity for an asymmetric chromatin signature in zygote and 2-cell stage embryos that is devoid of H4K20me3 and heterochromatin domains, and anticipates a functional difference in the organization of the replication program between the early embryo and somatic cells.

## Methods

### Embryo collection, microinjection and culture

Embryos were collected from 5-7 week old F1 (C57BL/6J × CBA/H) super-ovulated females crossed with F1 males. Superovulation was induced by intraperitoneal injection of pregnant mare serum gonadotropin (PMSG, Intervet, 5 IU) and human chorionic gonadotropin (hCG, Intervet, 7.5 IU) 46-48 hours later. Zygotes were collected between 17-19h post-hCG (phCG) injection. mRNAs were transcribed in vitro from the pRN3P plasmid using the mMESSAGE mMACHINE kit (Ambion). All cDNAs were subcloned to include identical 5'-cap and untranslated region (UTR) (including Kozak) and a poly-T 3'-UTR tail to ensure equivalent expression levels after micro-injectionn. *Suv4-20h1* and *Suv4-20h2* cDNA was obtained through a generous gift from G. Schotta (LMU, Munich) and *Suv4-20h1mut* through a generous gift from D. Beck (New York University,New York). *Suv4-20h2mut* was prepared by site-directed mutagenesis of Suv4-20h2 at Asparagine 273 to Cysteine 276 (NHDC) into AAAG (wild type sequence: CAACCATGACTG to mutated sequence: CGCCGCTGCCGG) (Rea et al. 2000). Zygotes were microinjected with 1-2 pl of the indicated mRNAs (700 ng/ul for *Suv4-20h1*/*Suv4-20h1mut*/*Suv4-20h2*/*Suv4-20h2mut* or 250 ng/ul for *Gfp*) and allocated to the experimental groups at random. Embryos were cultured in KSOM (K-modified simplex optimized medium) microdrops under oil at 37°C, 5% $CO_2$ until they were fixed. Micro-injections at the 2-cell stage were performed in one of the blastomeres at random after embryo collection at 41-43h phCG. Rescue experiments of the developmental block where performed by adding KSOM containing 10µM of an ATR inhibitor (Millipore) after injection and renewing the medium daily for two days. Embryos were scored once daily to determine developmental progression. For statistical analysis of embryonic development, N-1 Two Proportion test for comparing independent proportions for small and large sample sizes was used, it is

based on the N-1 Chi-Square test originally proposed by Pearson, 1900 and recommended by Campbell, 2007. All experiments were performed after approval of the Ethics Committee of the Université de Strasbourg and according to French and European legislation on animal experimentation.

**EU and EdU incorporation**

Embryos were incubated with 50 µM 5-Ethinyl Uridine (EU) for 1 hour at 48 hours post-hCG treatment and then visualized by Click-iT chemistry (Life Technologies) as described in the manufacturer's instructions. Quantifications were performed as described in quantification of fluorescence intensity. Embryos were incubated with 50 µM 5-ethynyl-2'-deoxyuridine (EdU) for 1h at times indicated in the figure legends and in figure schemes and then viusalised by Click-iT chemistry (Life Technologies) as described in the manufacturer's instructions.

**Immunostaining and Confocal Microscopy**

Fixation of freshly collected embryos from F1 superovulated, microinjected and cultured embryos was performed as described (Torres-Padilla et al. 2006). Briefly, the zona pellucida was removed with Acid Tyrode solution, followed by two washes in PBS and fixation in 4% paraformaldehyde, 0.04% triton, 0.3% tween-20, 0.2% sucrose at 37°C to ensure preservation of nuclear architecture. After permeabilization with 0.5% Triton in PBS, embryos were washed 3x in PBSt (0.1% Tween20 in PBS), quenched in 2.6 mg/ml freshly prepared ammonium chloride, washed 2x in PBSt and blocked for 3-4 hours or ON (overnight) at 4°C in blocking solution (BS: 3% BSA in PBSt) and incubated with primary antibodies in BS. Antibodies used were as follows: anti-HA (abcam 16B12), anti-H3K9me3 (Millipore 07-442), anti-H4K20me3 (Millipore 07-463), anti-H3K9me3 (Millipore 07-442), anti-H3K64me3 (generous gift from S. Daujat IGBMC, Illkirch), anti-H3K20me1 (abcam ab9051), anti-H3S10p (abcam ab5176), anti-γH2A.X (Millipore 05-636), anti-CHK1 (Cell Signaling 2G1D5) and anti-CHK1p (Cell Signaling S345 133D3). After overnight incubation at 4°C, embryos were washed 3x in PBSt, blocked for 20 minutes in BS and incubated for 3h at RT in BS containing secondary antibodies labelled with Alexa fluorophores (Invitrogen). After washing 2x in PBSt and 1x in PBS, embryos were mounted

in Vectashield (Vector Laboratories) containing 4'-6-Diamidino-2-phenylindole (DAPI) for visualizing DNA. Confocal microscopy was performed on a 63x oil objective in a TCS SP5 inverted confocal microscope (Leica). Z-sections were taken every 0.5-1 µm. Image analysis was performed using the software LAS-AF (Leica) and Imaris (Bitplane).

**Quantification of Fluorescence Intensity**

Confocal z-series stacks were reconstructed in 3D using Imaris software (Bitplane) and the pronuclei (zygote) or nuclei (2-cell stage) were segmented based on the DAPI channel. The average fluorescence intensity for the channel of interest within the segmented region was calculated after uniform background subtraction with a 95% confidence. The fluorescence intensity for each embryo was normalized to the average of the non-injected control group. The data was tested for normality using the Kolmogorov-Smirnov test. If the data was found not to be normally distributed, the Mann-Whitney U-test, a non-parametric test was used.

## Figures and Figure Legends

Figure 1

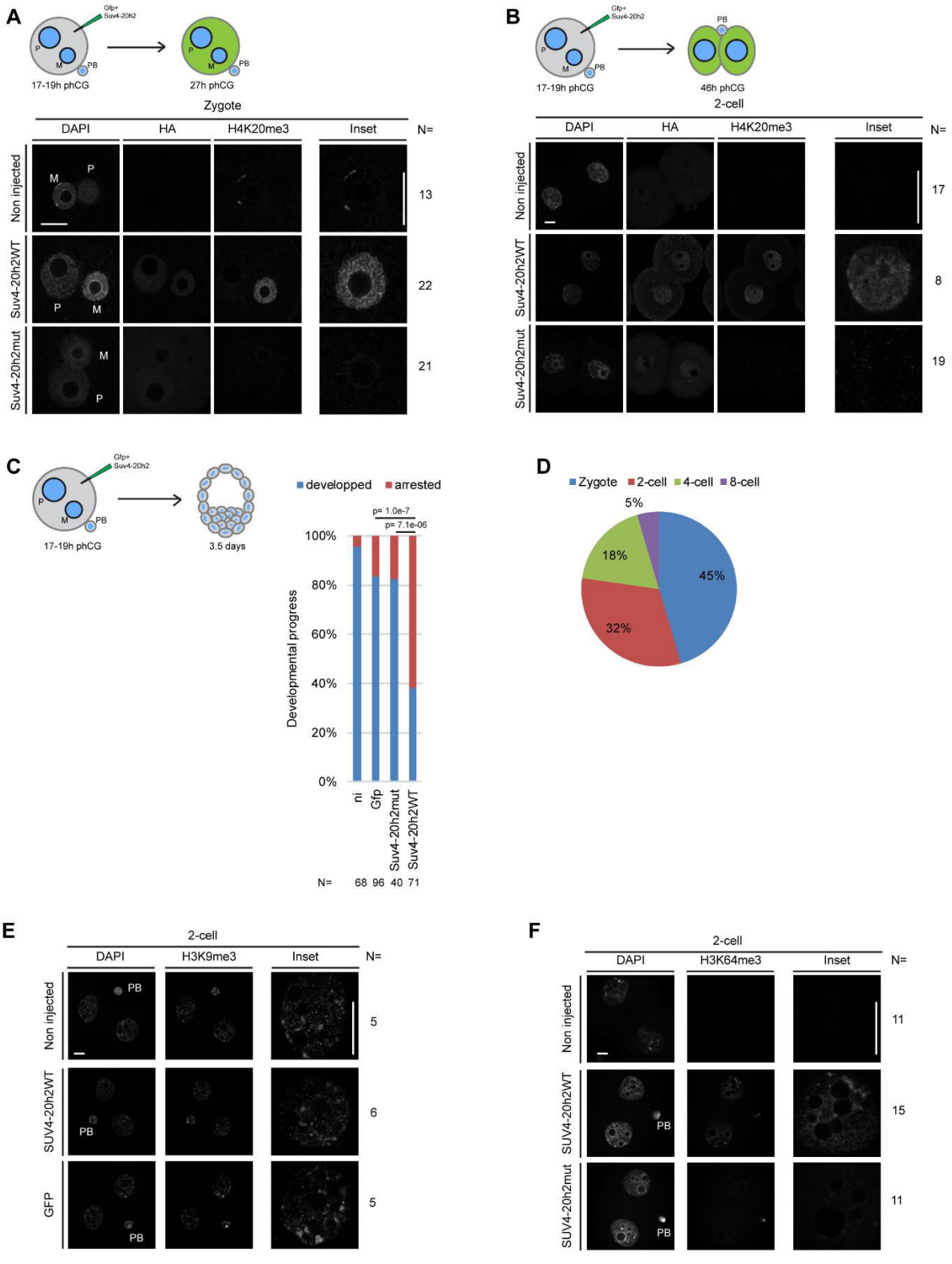

**Figure 1: Maintenance of H4K20me3 through Suv4-20h2 ectopic expression blocks embryonic development prior to the 2-cell stage.**

**A**. Schematic representation of the experimental design is shown at the top of the figure. Zygotes between 17-19h post-hCG (phCG) were micro-injected with mRNA *Suv4-20h2WT* or *Suv4-20h2mut*, in addition to *GFP*, cultured in KSOM media and then fixed in 4% formaldehyde (as indicated in the material and methods) at 27h phCG. Representative images showing single Z-projections of confocal sections of non-injected, *Suv4-20h2WT*- and *Suv4-20h2mut*-injected zygotes stained with DAPI, HA and H4K20me3 antibodies. An inset of the maternal pronucleus is shown on the right panels. N numbers are indicated on the right. M: maternal, P: paternal. Scale bar is 10µm, except in the inset where it is 5µm.

**B**. Microinjections were performed as in A, except that embryos were fixed at 46h phCG. Representative images showing single Z-projections of confocal sections of non-injected, *Suv4-20h2WT*- and *Suv4-20h2mut*-injected 2-cell stage embryos stained with DAPI, HA and H4K20me3 antibodies. An inset of one of the two nuclei is shown in the right panels. N numbers are indicated on the right. Scale bar is 10µm, except in the inset where it corresponds to 5µm.

**C**. Zygotes were microinjected as in A and cultured until the blastocyst stage. The number of embryos reaching the blastocyst stage (developed) was quantified for non-injected (ni), *GFP* alone-*, Suv4-20h2mut*- and *Suv4-20h2WT*-injected embryos. Total numbers of embryos are indicated below the plot. Statistical testing was performed using the N-1 Two Proportion test for comparing independent proportions.

**D**. Pie chart with the distribution of arrested *Suv4-20h2WT*-injected embryos by stage.

**E-F**. Zygotes were microinjected as in A and analyzed with an H3K9me3 (E) or an H3K64me3 (F) antibody at the 2-cell stage. Representative images showing single Z-projections of confocal sections of non-injected, *Suv4-20h2WT*- and *GFP*-injected embryos. An inset of one of the two nuclei is shown in the right panels. N numbers are indicated. Scale bar is 10µm, except in the inset where it corresponds to 5µm. PB, Polar Body.

Figure 2

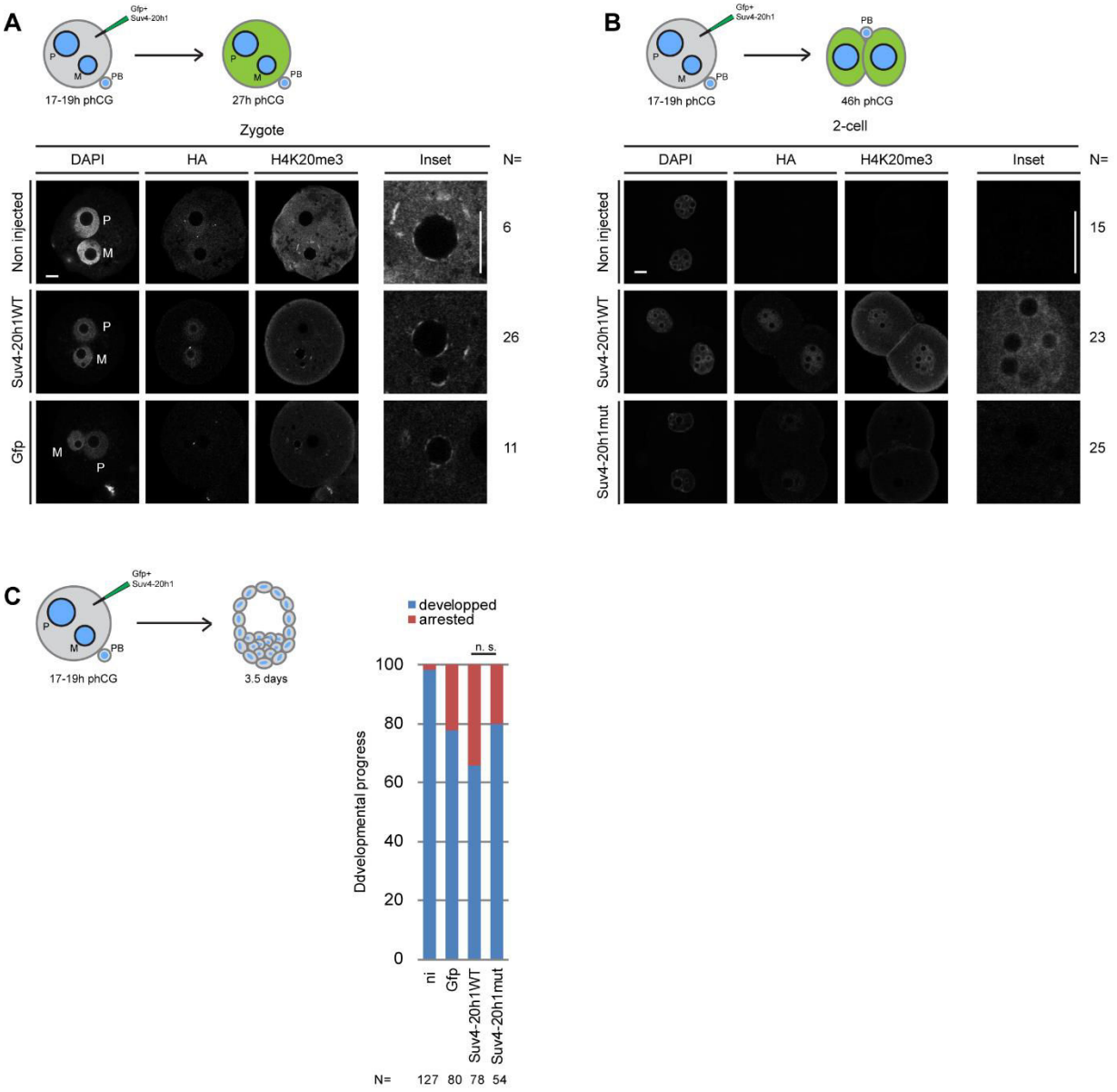


**Figure 2. Ectopic expression of *Suv4-20h1* does not arrest embryonic development or increase H4K20me3 levels in the zygote.**

**A**. Schematic representation of the experimental design. Zygotes microinjected with mRNA for *Suv4-20h1WT* or *Suv4-20h1mut*, cultured and fixed for immunostaining using HA or H4K20me3 antibodies at 27h phCG. Representative images showing single Z-projections of confocal sections of non-injected, *Suv4-20h1WT*- and *GFP*-injected zygotes are shown. An inset of the maternal pronucleus is shown on the right panels. N numbers

are indicated. M: maternal, P: paternal. Scale bar is 10µm, except in the inset where it is 5µm.

**B**. Zygotes were micro-injected with mRNA for *Suv4-20h1WT* or *Suv4-20h1mut* as in A, cultured and analyzed at the 2-cell stage. Representative images showing single Z-projections of confocal sections of non-injected, *Suv4-20h1WT*- and *Suv4-20h1mut*-injected embryos stained with DAPI, HA and H4K20me3 antibodies. An inset of one of the two nuclei is shown in the right panels. N numbers are indicated. Scale bar is 10µm, except in the inset where it is 5µm.

**C**. Zygotes were micro-injected with mRNA *Suv4-20h1WT* or *Suv4-20h1mut*, in combination with *GFP* and cultured until the blastocyst stage. The percentage of embryos that reached the blastocyst stage (developed) is plotted for non-injected (ni), Gfp-*, Suv4-20h1mut*- and *Suv4-20h1WT*-injected embryos. The total number of embryos analyzed is indicated. Statistical testing was performed using the N-1 Two Proportion test for comparing independent proportions.

Figure 3

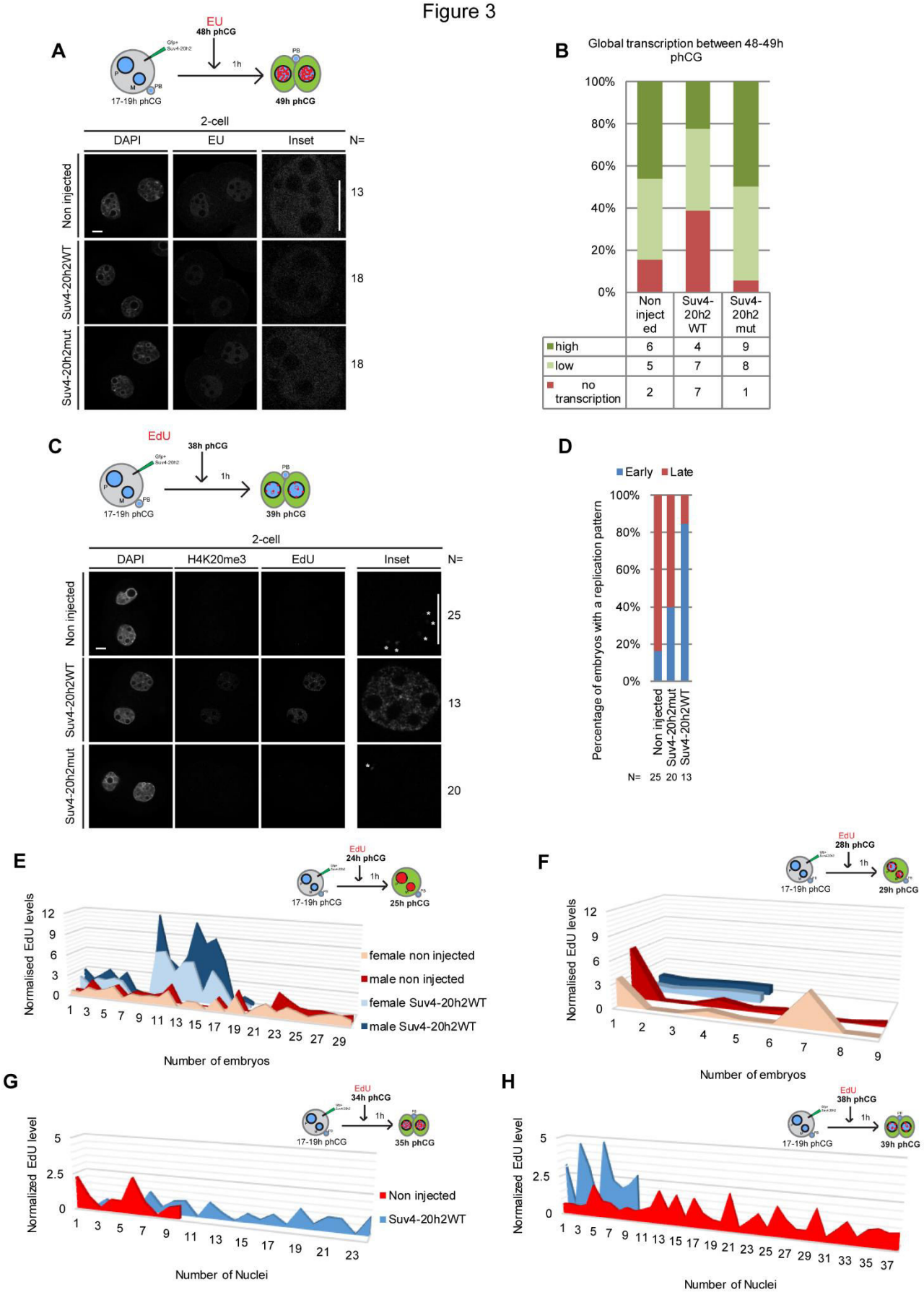
A
EU
48h phCG
1h
17-19h phCG
49h phCG
2-cell
DAPI
EU
Inset
N=
Non injected
Suv4-20h2WT
Suv4-20h2mut
13
18
18
B
Global transcription between 48-49h phCG
100%
80%
60%
40%
20%
0%
Non injected
Suv4-20h2 WT
Suv4-20h2 mut
high 6 4 9
low 5 7 8
no transcription 2 7 1
C
EdU
38h phCG
1h
17-19h phCG
39h phCG
2-cell
DAPI
H4K20me3
EdU
Inset
N=
Non injected
Suv4-20h2WT
Suv4-20h2mut
25
13
20
D
Early
Late
Percentage of embryos with a replication pattern
100%
80%
60%
40%
20%
0%
Non injected
Suv4-20h2mut
Suv4-20h2WT
N= 25 20 13
E
EdU
24h phCG
1h
17-19h phCG
25h phCG
Normalised EdU levels
12
9
6
3
0
1 3 5 7 9 11 13 15 17 19 21 23 25 27 29
Number of embryos
female non injected
male non injected
female Suv4-20h2WT
male Suv4-20h2WT
F
EdU
28h phCG
1h
17-19h phCG
29h phCG
Normalised EdU levels
12
9
6
3
0
1 2 3 4 5 6 7 8 9
Number of embryos
G
EdU
34h phCG
1h
17-19h phCG
35h phCG
Normalized EdU level
5
2.5
0
1 3 5 7 9 11 13 15 17 19 21 23
Number of Nuclei
Non injected
Suv4-20h2WT
H
EdU
38h phCG
1h
17-19h phCG
39h phCG
Normalized EdU level
5
2.5
0
1 3 5 7 9 11 13 15 17 19 21 23 25 27 29 31 33 35 37
Number of Nuclei

**Figure 3: H4K20me3 affects replication progression and global gene expression.**

**A**. Zygotes were micro-injected with mRNA *Suv4-20h2WT* or *Suv4-20h2mut*, cultured until the 2-cell stage and pulsed with EU for 1h at 48h phCG. Shown are representative images showing single Z-projections of confocal sections of non-njected, *Suv4-20h2WT*- and *Suv4-20h2mut*-injected embryos stained with DAPI and EU visualized by Click-iT reaction. An inset of one of the two nuclei is shown on the right. N numbers are indicated. Scale bar is 10µm, except in the inset where it is 5µm.
**B**. Distribution of EU patterns in late 2-cell stage embryos. Embryos were divided into three groups based on their EU pattern: i) no transcription (no EU detected), ii) low levels of transcription and iii) high levels of transcription.

**C**. Zygotes micro-injected with mRNA for *Suv4-20h2WT* or *Suv4-20h2mut* were cultured until the 2-cell stage, pulsed with EdU for 1h at 38h phCG 1h, fixed and analyzed for EdU incorporation. Representative images showing single Z-projections of confocal sections of Non injected, *Suv4-20h2WT*- and *Suv4-20h2mut*-injected embryos. An inset of one of the two nuclei is shown on the right. White asterisks indicate EdU labelling in non-injected and *Suv4-20h2mut*-injected embryos. N numbers are indicated. Scale bar is 10µm, except in the inset where it is 5µm.
**D**. Distribution of the replication patterns based on EdU labelling at 38-39h phCG as shown in panel D.
**E-F**. Normalized EdU levels measured in each pronucleus of non-injected and *Suv4-20h2WT*-injected zygotes at 24-25h phCG (E) and 35-34h phCG (F).
**G-H**. Normalized EdU levels measured in each nucleus of non-injected and *Suv4-20h2WT*-injected 2-cell stage embryos at 24-25h phCG (G) and 35-34h phCG (H).

Figure 4

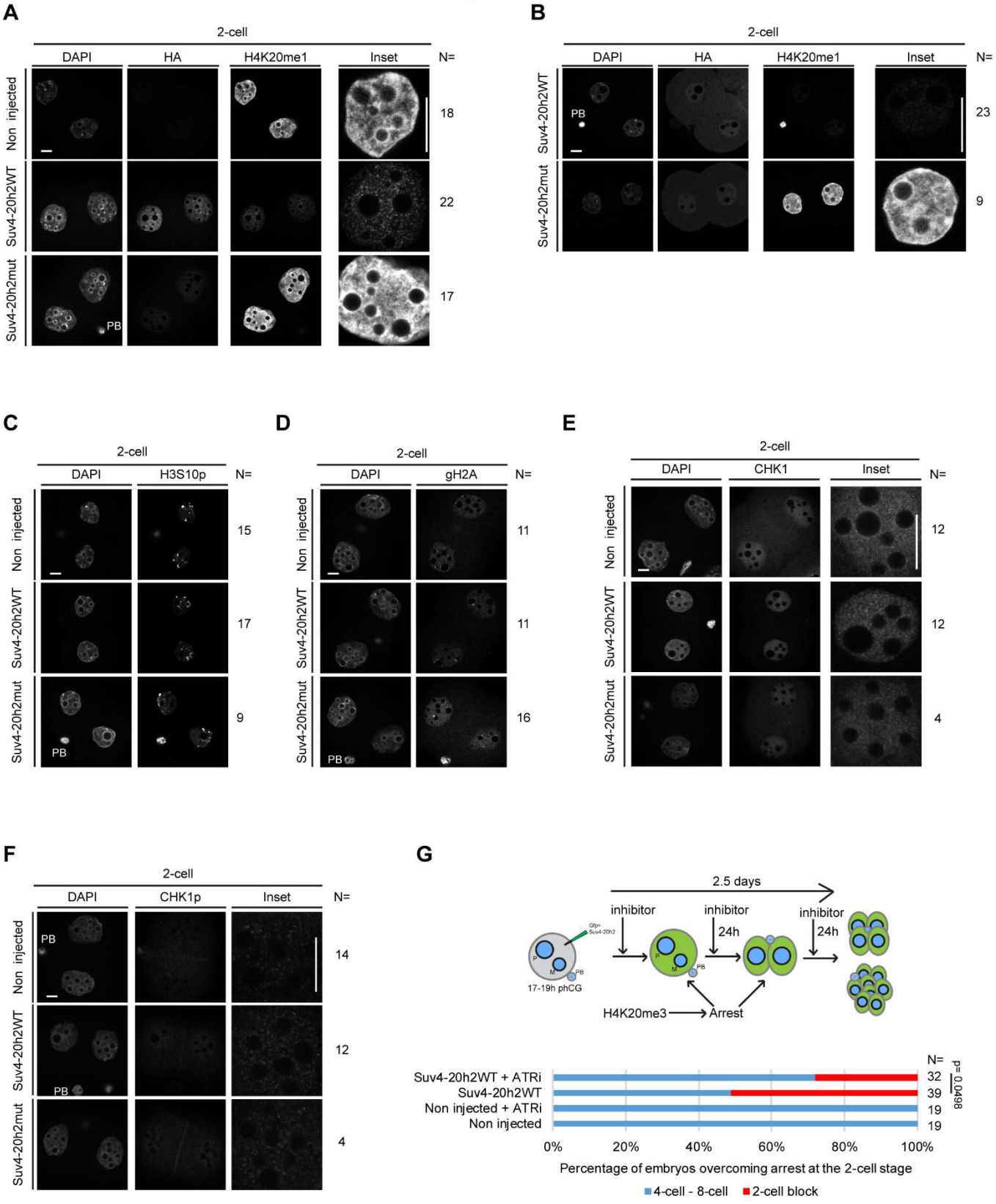
A
2-cell
DAPI
HA
H4K20me1
Inset
N=
Non injected
Suv4-20h2WT
Suv4-20h2mut
PB
18
22
17
B
2-cell
DAPI
HA
H4K20me1
Inset
N=
Suv4-20h2WT
Suv4-20h2mut
PB
23
9
C
2-cell
DAPI
H3S10p
N=
Non injected
Suv4-20h2WT
Suv4-20h2mut
PB
15
17
9
D
2-cell
DAPI
gH2A
N=
Non injected
Suv4-20h2WT
Suv4-20h2mut
PB
11
11
16
E
2-cell
DAPI
CHK1
Inset
N=
Non injected
Suv4-20h2WT
Suv4-20h2mut
12
12
4
F
2-cell
DAPI
CHK1p
Inset
N=
Non injected
Suv4-20h2WT
Suv4-20h2mut
PB
14
12
4
G
2.5 days
inhibitor
inhibitor
24h
inhibitor
24h
17-19h phCG
H4K20me3
Arrest
N=
Suv4-20h2WT + ATRi
Suv4-20h2WT
Non injected + ATRi
Non injected
32
39
19
19
p=0.0498
0%
20%
40%
60%
80%
100%
Percentage of embryos overcoming arrest at the 2-cell stage
4-cell - 8-cell
2-cell block

**Figure 4: Embryonic arrest is partially rescued by inhibition of ATR**

**A**. Representative images of 2-cell stage embryos analyzed at 46h phCG with DAPI, HA and H4K20me1 antibodies. Single Z-projections of confocal sections are shown. An inset of one of the two nuclei is shown on the right. N numbers are indicated. Scale bar is 10µm, except in the inset where it is 5µm. PB, Polar Body.

**B**. Representative single Z-projections of confocal sections of *Suv4-20h1WT*- and *Suv4-20h1mut*-injected 2-cell stage embryos stained at 46h phCG with DAPI, HA and H4K20me1 antibodies. An inset of one of the two nuclei is shown in the right panels. N numbers are indicated. Scale bar corresponds to 10µm, except in the inset where it corresponds to 5µm. PB, Polar Body.

**C**. Representative 2-cell stage embryos acquired at 46h phCG stained with DAPI and H3S10p antibodies, showing confocal single Z-projections of non-injected, *Suv4-20h2WT*- and *Suv4-20h2mut*-injected embryos. An inset of one of the two nuclei is shown on the right. N numbers are indicated. Scale bar corresponds to 10µm, except in the inset where it corresponds to 5µm. PB, Polar Body.

**D**. Representative confocal single Z-projections of non-injected, *Suv4-20h2WT*- and *Suv4-20h2mut*-injected 2-cell stage embryos stained at 46h phCG with DAPI and γH2A.X antibodies. An inset of one of the two nuclei is shown in the right panels. N numbers are indicated. Scale bar corresponds to 10µm, except in the inset where it corresponds to 5µm. PB, Polar Body.

**E**. Representative 2-cell stage embryos stained at 39h phCG stained with DAPI and CHK1 antibodies showing single confocal Z-projections of Non injected, *Suv4-20h2WT*- and *Suv4-20h2mut*-injected embryos. An inset of one of the two nuclei is shown on the right. N numbers are indicated. Scale bar corresponds to 10µm, except in the inset where it corresponds to 5µm.

**F**. Confocal single Z-projections of Non injected, *Suv4-20h2WT*- and *Suv4-20h2mut*-injected 2-cell stage embryos acquired at 39h phCG with DAPI and CHK1p antibodies. An inset of one of the two nuclei is shown in the right panels. N numbers are indicated. Scale bar corresponds to 10µm, except in the inset where it corresponds to 5µm. PB, Polar Body.

**G**. A schematic representation of the experimental design is shown at the top of the figure. Zygotes between 17-19h post-hCG (phCG) are micro-injected with mRNA *Suv4-20h2WT* and *GFP*, cultured in the presence or absence of an ATR inhibitor (ATRi) until the 8-cell stage. A bar chart of the developmental progression until the 4-cell stage is shown in the bottom. Statistic test was performed using the N-1 Two Proportion test for comparing independent proportions.

## Supplementary Figure and Figure Legends

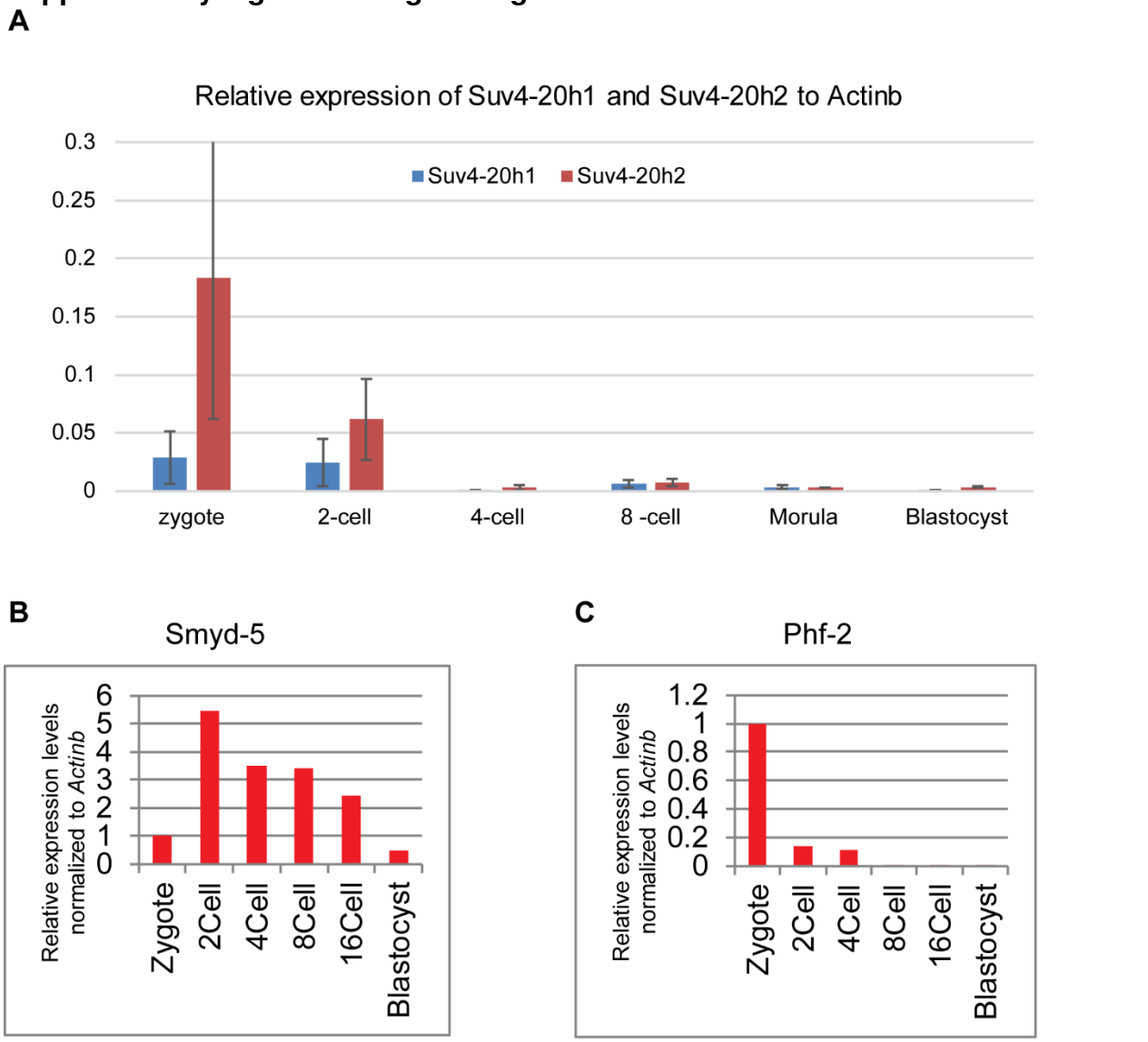


**Figure S1. Expression levels of H4K20me3 methyl- and dimethyl-transferases during pre-implantation development.**

Relative expression level of Suv4-20h1 (A), Suv4-20h2 (A), Smyd-5 (C) and Phf-2 (D) at all stages of pre-implantation development normalized to *Actinb*. Shown are means ± s.d. of two independent experiments performed in technical replicates.

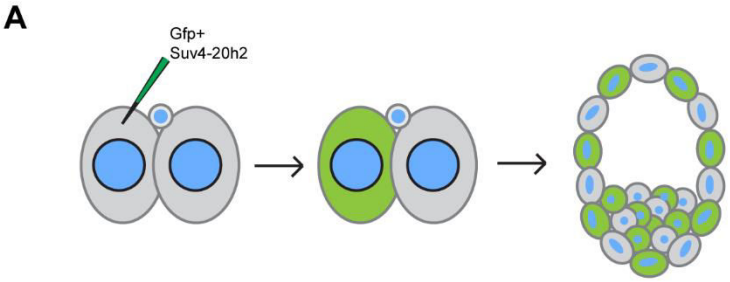
A
Gfp+
Suv4-20h2

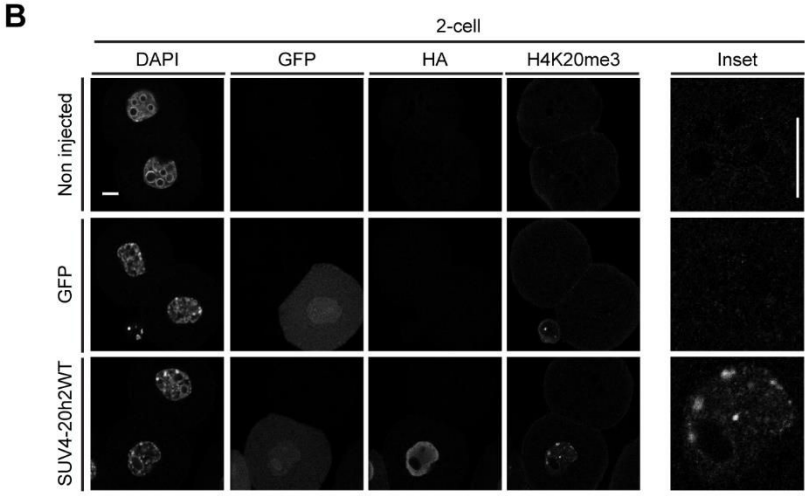
B
2-cell
DAPI
GFP
HA
H4K20me3
Inset
Non injected
GFP
SUV4-20h2WT

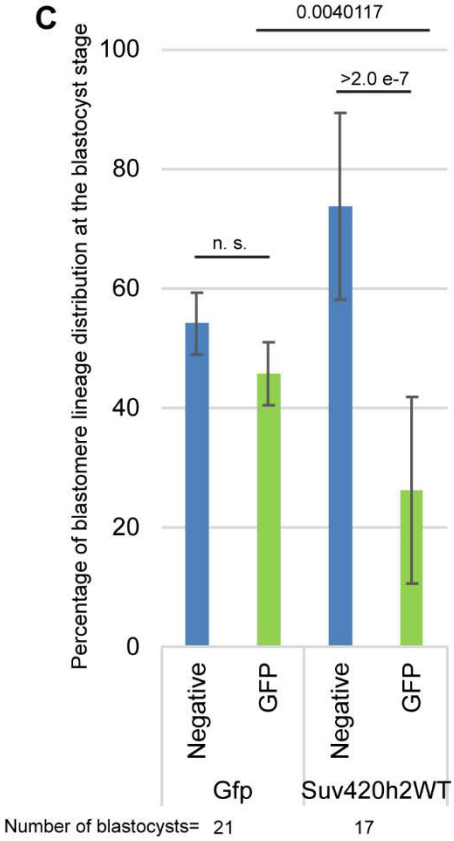
C
0.0040117
>2.0 e-7
n. s.
Percentage of blastomere lineage distribution at the blastocyst stage
100
80
60
40
20
0
Negative
GFP
Negative
GFP
Gfp
Suv420h2WT
Number of blastocysts= 21 17

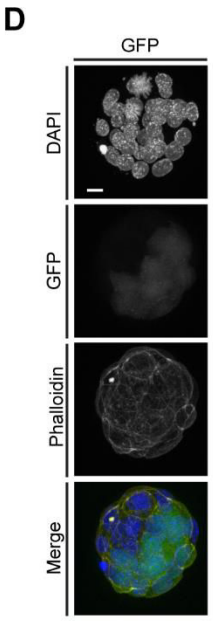
D
GFP
DAPI
GFP
Phalloidin
Merge

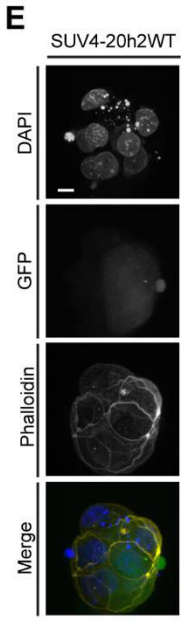
E
SUV4-20h2WT
DAPI
GFP
Phalloidin
Merge

**Figure S2. Expression of SUV4-20H2 at the 2-cell stage results in a cell proliferation arrest.**

**A**. Experimental design: a random blastomere of a 2-cell stage embryo (41-43h phCG) was micro-injected with mRNA for *Suv4-20h2WT* and *GFP*.

**B**. Representative confocal single Z-projections of Non injected, *Suv4-20h2WT*- and *Gfp*-injected 2-cell stage embryos stained at 48h phCG with DAPI, GFP; HA and H4K20me3 antibodies. An inset of one H4K20me3 of the two nuclei is shown on the right panels. Scale bar corresponds to 10µm, except in the inset where it corresponds to 5µm. PB, Polar Body.

**C**. Bar chart distribution of the number of GFP negative and positive blastomeres at the blastocyst stage in *Gfp*- or *Suv4-20h2WT*- injected 2-cell stage embryos. The number of blastocysts analyzed is indicated at the bottom of the chart.

**D-E**. Representative full Z-projections of confocal sections of blastocysts injected with *Suv4-20h2WT*- and *GFP* acquired with DAPI, GFP, and phalloidin. A merged channel of the three signals is shown at the bottom. Scale bar corresponds to 10µm.

**Acknowledgments**

We are grateful to Gunnar Schotta (LMU) for providing antibodies, wild-type Suv4-20h1 and Suv4-20h2 constructs and helpful discussions, as well as David Beck (NYU) for providing Suv4-20h1mut construct. M.E.T.-P. acknowledges funding from EpiGeneSys NoE, ERC-Stg 'NuclearPotency', EMBO Young Investigator Programme and the Schlumberger Foundation for Research and Education. A.E is a recipient of a doctoral fellowship from the Ministère de l'Enseignement Supérieur et de la Recherche and from the Fondation pour la Recherche Médicale (FDT20150532012).

# Results: second part

# Annex 3: Characterization of non-canonical Polycomb Repressive Complex 1 subunits during early mouse embryogenesis

# Characterization of non-canonical Polycomb Repressive Complex 1 subunits during early mouse embryogenesis

André Eid[1] & Maria-Elena Torres-Padilla[1,2]*

[1] *Institut de Génétique et de Biologie Moléculaire et Cellulaire, CNRS/INSERM U964, U de S, F-67404 Illkirch, CU de Strasbourg, France.*

[2] *Institute of Epigenetics and Stem Cells, Helmholtz Zentrum München D-81377 München, Germany.*

* metp@igbmc.fr

Tel. + 49(0) 89-3187-3317

Fax. + 49(0) 89-3187-3389

**Key Words:** mouse embryo, PRC1, histone modification, epigenetic reprogramming

**Running title:** non-canonical PRC1 in early mouse embryos

## Abstract

An intense period of chromatin remodelling takes place after fertilisation in mammals, which is thought necessary for epigenetic reprogramming to start a new developmental programme. While much attention has been given to the role of Polycomb Repressive Complex 2 (PRC2) and to canonical PRC1 complexes during this process, little is known as to whether there is any contribution of non-canonical PRC1 in shaping the chromatin landscape after fertilisation. Here, we first describe in detail the temporal dynamics and abundance of H2A ubiquitylation (H2AK119ub), a histone modification catalysed by PRC1, during pre-implantation mouse development. In addition, we have analysed the presence of the two characteristic subunits of non-canonical PRC1 complexes, RYBP and its homolog YAF-2. Our results show that H2AK119ub is inherited from the sperm, rapidly removed from the paternal chromatin after fertilisation, but detected again prior to the first mitosis, suggesting that PRC1 activity occurs as early as the zygotic stage. RYBP and YAF-2, together with the non-canonical subunit L3MBTL2, are all present during pre-implantation development but show different temporal dynamics. While RYBP is absent in the zygote, it is strongly induced from the 4-cell stage onwards. YAF-2 is inherited maternally and localises to the pericentromeric regions in the zygote, is strongly induced between the 2- and 4-cell stages but then remains weak to undetectable subsequently. Altogether, our data suggest that non-canonical PRC1 is active during pre-implantation development and should be regarded as an additional component during epigenetic reprogramming and in the establishment of cellular plasticity of the early embryo.

## Introduction

Fertilisation is the first step of embryonic development, whereby the paternal and the maternal genomic material get together to form a new organism. By implication, the process of fertilisation triggers a number of molecular events on the parental genomes, including major chromatin remodelling. One of the main purposes of such remodelling is epigenetic reprogramming itself, which allows the reversion from a highly differentiated state in the gametes to a totipotent state in the zygote (Surani, Hayashi, and Hajkova 2007). The molecular mechanisms behind epigenetic reprogramming include histone variant exchange, changes in nuclear organisation and DNA methylation, the activation of a large fraction of transposable elements, but also rapid and drastic changes in histone modifications (Hemberger, Dean, and Reik 2009; Burton and Torres-Padilla 2014).

Amongst them, H3K27me3, catalysed by the Polycomb Repressive Complex 2 (PRC2) and, in general, polycomb group (PcG) proteins have been shown to play important roles from the earliest stages of development (Puschendorf et al. 2008; Erhardt et al. 2003; Santenard et al. 2010). At large, PcG repression is achieved through two major types of complexes that mediate various biochemical functions including histone modifying activities, recognition of covalent modifications and physical compaction of chromatin. PRC2 displays its main catalytic activity towards H3K27me3 while the main catalytic activity of PRC1 is monoubiquitylation of H2A at lysine 119 (K119), although PRC1 has also been shown to be able to compact chromatin independently of H2AK119ub *in vitro* and *in vivo* (Illingworth et al. 2015; Eskeland et al. 2010; Francis, Kingston, and Woodcock 2004). Genetically and biochemically, a role for PRC1 in transcriptional repression has been clearly demonstrated (Simon and Kingston 2009). The initial model for PcG repression posited that PRC1 recruitment depends upon previously established H3K27me3 domains by the action of PRC2. Subsequent recruitment of PRC1 then leads to H2AK119ub on those domains through the enzymatic activity of RING1A/RING1B, and to increased chromatin compaction. However, recent evidence supports an emerging view whereby PRC1 is indeed recruited to genomic regions occupied by PRC2 and in a manner dependent on H3K27, but additionally, PRC1 can be recruited onto chromatin independently of H3K27me3, presumably through alternative protein-protein interactions, via the Mel18 subunit for example (Tavares et al. 2012), or through ncRNAs recruitment, such as the interaction between CBX7 and

ANRIL (Yap et al. 2010; El Messaoudi-Aubert et al. 2010). Thus, both PRC2 and PRC1 can mediate repression independently of each other.

In addition to RING1A/RING1B, the core subunits of canonical PRC1 include a CBX protein (2, 4, 6, 7 or 8) homologue of *Polycomb*, PHC proteins (1 to 3) and BMI1/PCGF4 or MEL18/PCGF2 (Francis, Kingston, and Woodcock 2004; Levine et al. 2002). However, a systematic proteomics approach in human cells identified additional non-canonical PRC1 complexes, revealing a greater complexity than previously anticipated (Gao et al. 2012). While RING1A/1B is a common theme for all PRC1 complexes, CBX and PHC proteins are replaced by either RYBP or YAF-2 in non-canonical PRC1 complexes. The incorporation of either RYBP or YAF-2 into PRC1 is presumably of functional relevance since -at least *in vitro*- RYBP can stimulate the ubiquitylation activity of PRC1 but YAF-2 does not (Gao et al. 2012). A further subdivision into functionally distinct families is provided by the presence of one of the 6 PCGF homologues (Gao et al. 2012). The high heterogeneity of PRC1 complexes is thought to allow a combinatorial assembly of multiple subunits to integrate additional biochemical activities including readers for other histone modifications -such as HP1s or the MBT (Malignant Brain Tumor) family members (Qin et al. 2012) –as well as histone modifiers - such as HDACs (Farcas et al. 2012).

In the mouse embryo, PcG proteins support 'facultative' heterochromatin establishment in the male pronucleus (Santos et al. 2005; Arney et al. 2002; Puschendorf et al. 2008), and a mutation in K27 within H3.3, the main histone variant incorporated in the male pronucleus, results in developmental arrest and heterochromatin defects (Santenard et al. 2010). In addition, the combined deletion of both RING1 subunits, RING1A and RING1B, results in developmental arrest before the 2-cell stage due to defective regulation of the transcriptional programme of the oocyte (Posfai et al. 2012). Most studies addressing the function or the expression of PcG subunits in the early mammalian embryo have focused on PRC2 or on canonical PRC1 complexes, for example, the expression of most CBX proteins has been characterised in the early embryo (Tardat et al. 2015; Puschendorf et al. 2008). However, we still do not know whether non-canonical PRC1 can potentially contribute to the changes in chromatin remodeling that take place after fertilisation. Indeed, the heterogeneous nature of PRC1 complexes makes it difficult to pinpoint the contribution of a specific complex and/or subunit to cellular plasticity and cell fate decisions. Here, we have first thoroughly analysed the dynamic changes of the main catalytic activity of PRC1, H2AK119ub, during pre-implantation

development. In addition, we have systematically characterised the main defining subunits of non-canonical PRC1 complexes, RYBP and YAF-2 and of additional non-canonical polycomb related proteins L3MBTL1 and L3MBTL2. Our results suggest that PRC1 activity is dynamic and takes place from the earliest stages of mouse development and suggest that non-canonical PRC1 activity contributes to the changes in chromatin remodeling that take place after fertilisation.

## Results

### H2AK119 mono-ubiquitination is abundant during preimplantation development.

We first analysed the activity of the PRC1 complex by examining H2A monoubiquitylation on lysine 119 (H2AK119ub). We detected H2AK119ub throughout preimplantation development at all stages analysed (Fig. 1A). At the zygote stage H2AK119ub was present in both female and male pronuclei and in the polar body (PB), which was thereafter used as an internal control for subsequent stages of development. Subsequently, H2AK119ub was abundant throughout development, in 2-cell, 4-cell, 8-cell and morula stages (Fig. 1A). However, the pattern of distribution of H2AK119ub varied along these developmental times. H2AK119ub localised at the DAPI (4', 6-diamidino-2-phenylindole)-dense regions surrounding the NLBs (Nulceolar Like Bodies) in zygotes at PN4 stage (ProNuclear4) (Fig. 1C) and in 2-cell stage embryos (Fig. 1A). The pattern of localisation of H2AK119ub changed at the 4-cell stage, which corresponds to the time when chromocenters are being established and the NLBs are lost (Probst et al. 2007). After the 4-cell stage, H2AK119ub did not colocalise anymore with the DAPI-dense regions (Fig. 1A and 1B), and showed instead a disperse distribution throughout the nucleoplasm. This localisation persisted in the 8-cell stage, except that most blastomeres exhibited one large (arrows), single focus (n= 5/7). One cell division later, H2AK119ub became localized in a more ‘dotty’ like pattern (Fig. 1A), reminiscent of polycomb bodies observed in other cell types (Saurin et al. 1998). Thus, H2AK119ub displays three different global patterns in the early embryo: i) an initial localisation to DAPI-rich pericentromeric regions in the zygote and 2-cell stage embryos, ii) a more disperse pattern in 4- and 8-cell embryos and a iii) foci-like distribution in the morula.

At the blastocyst stage we observed two types of patterns for H2AK119ub (Fig. 1B). Half of the embryos analysed (n=9) displayed intense foci labeled with H2AK119ub (Fig. 1B), similarly to the

appearance of foci of RING1B/RNF2 during X inactivation (de Napoles et al, 2004). Furthermore, these foci were not detected in the ICM (Inner Cell Mass), but were detected exclusively in the trophectoderm (Fig. 1B). This pattern is reminiscent of previous observations of colocalisation between H2AK119ub, RING1 (RING1A and RING1B/RNF2) and the inactive X that have been shown to occur in TS (Trophoblast Stem) and ES (Embryonic Stem) cells (de Napoles et al. 2004; Fang et al. 2004). Thus, we conclude that H2AK119ub marks sites of imprinted X chromosome inactivation in mouse blastocyst *in vivo*. While this pattern may be set at an earlier developmental time, we did not find a correlation with the foci of H2AK119ub that we observed e.g. at the morula stage (Fig. 1A). Indeed, while we observed foci in morula stage embryos, we observed this pattern in more than half of the embryos, and therefore it is likely not to be related to embryonic X inactivation.

Next, to better understand the establishment of H2AK119ub after fertilisation, we carefully analysed the presence of H2AK119ub at different stages of zygotic development (PN1 to PN5) (Fig. 1C). We first detected H2AK119ub in both pronuclei immediately after fertilisation (PN1) (Fig. 1C), suggesting that the sperm chromatin already contains H2AK119ub. H2AK119ub retained the same pattern until PN2, where it was enriched in the central part of the decondensing male pronucleus, which corresponds to the region where pericentromeric chromatin localizes at these stages (Probst et al. 2007; Jachowicz et al. 2013). Thereafter H2AK119ub levels were significantly reduced in the male pronucleus at PN3 (Fig. 1C). At PN4, H2AK119ub became detectable again, and localized at the NLBs on both pronuclei, in agreement with a previous report (Tardat et al. 2015). H2AK119ub levels were further reduced as the embryo reached PN5 and approached the first mitotic division (Fig. 1C). Thus, H2AK119ub is detected in both, oocyte and sperm chromatin at fertilisation, but is transiently absent from the male pronucleus at mid-zygotic stages, suggesting that PRC1 activity is dynamic and takes place from the earliest stages of mouse development.

## RYBP is expressed in preimplantation mouse embryos.

PRC1 complexes can mediate H2AK119ub independently of H3K27me3 and PRC2 proteins (Pasini et al. 2007; Trojer et al. 2011). The dynamics and localisation pattern of H3K27me3 in

conjunction with that of PRC2 components have been well studied in the mouse embryo (Santos et al. 2005; Santenard et al. 2010; Puschendorf et al. 2008). Therefore, having established that H2AK119ub was present in preimplantation development, we wondered whether non-canonical PRC1 complexes contribute also to H2AK119 ubiquitylation. We thus next analysed the expression of members of the non-canonical PRC1 complexes that can mediate H2AK119ub independently of PRC2 activity. When assembled with RYBP, non-canonical PRC1 mediates H2AK119ub without the need of pre-existing H3K27me3 (Tavares 2012). We first examined the localisation of RYBP (RING1 and YY1 Binding Protein). Albeit weakly, in the oocyte RYBP was distributed both in the nucleus and the cytoplasm. This observation was surprising given the expected nuclear localisation of RYBP based on findings in other cell types (Tavares et al. 2012; Hisada et al. 2012). However, immediately after fertilisation, we did not detect RYBP at the zygote stage, neither in the cytoplasm nor in the nucleoplasm of any of the two pronuclei (Fig. 2A). At the 2-cell stage, RYBP was weakly detected in the nuclei of both blastomeres, where it showed a slight accumulation around the NLBs at DAPI dense regions (Fig. 2A, arrows). Although the immunofluorescence signal for RYBP was weak, RYBP remained present at all stages analysed until the blastocyst stage (Fig. 2A). Apart from the slight accumulation around the NLBs in 2-cell stage embryos, we did not observe any particular nuclear accumulation when the protein was detected. However, we noticed that, besides the nuclear localisation, RYBP also was present in the mid-body after nuclear division (Fig. 2A). We also observed that RYBP was present during mitosis and localized to the spindle (data not shown). These observations indicate that RYBP may not play a role in H2AK119ub establishment or maintenance at the zygote stage, but could do so after the 2-cell stage.

## The RYBP homologue YAF-2 is inherited maternally and its levels decrease during preimplantation development.

YAF-2 (YY1 Associated Factor 2), an RYBP homologue, is another component of non-canonical PRC1 complexes. The presence of YAF-2 is mutually exclusive with that of RYBP, and therefore defines different complexes (Gao et al. 2012). Thus, we next addressed whether YAF-2 could potentially play a role in mediating H2AK119ub establishment and maintenance in early mouse development. We detected YAF-2, albeit weakly, in GV oocytes around the NLB and nuclear

periphery (Fig 2B). However, YAF-2 was below the detection limit immediately after fertilisation (data not shown) and it only starts getting detected at PN4 in the zygote (Fig. 2B, arrows) where it shows some association to the NLBs. YAF-2 was present in the 2-cell embryos, where it showed some enrichment around the NLBs, but its localisation appeared rather punctuate throughout the nucleoplasm, without exclusive localisation with DAPI-rich regions (Fig. 2B). Subsequently, the levels of YAF-2 were reduced throughout preimplantation development after the 4-cell and till the blastocyst stage, but remained visible albeit weak (Fig. 2B). This data leads us to conclude that YAF-2 is present in the early mouse embryo and that it could potentially contribute the ubiquitylation of H2A via a non-canonical form of PRC1 in which YAF-2 is part of. However, the patterns of YAF-2 at the morula and blastocyst stages do not indicate a specific accumulation at foci (Fig. 2B) like H2AK119ub does (Fig. 1A-B), suggesting that YAF-2 may globally not be involved in the subsequent establishment of H2AK119ub on the X-chromosome.

## L3MBTL2, a specific subunit of non-canonical PRC1.6 complex is expressed in preimplantation embryos.

Considering the diversity of non-canonical PRC1 complexes, we next focused more specifically on one of them, PRC1.6. Our reasoning behind this choice was two-fold. Firstly, PRC1.6 is the only PRC1 complex that, in addition to catalytic activity towards H2AK119, possesses histone deacetylation activity (Gao et al. 2012) and therefore could also contribute to the rapid changes in histone acetylation that characterise pre-implantation development (Aoki, Worrad, and Schultz 1997; Adenot et al. 1997; Burton and Torres-Padilla 2014). Secondly, PRC1.6 contains a recognition module, through L3MBTL2, for H4K20me1, which is essential for pre-implantation development, as deletion of PR-Set7 results in lethality by the 8-cell stage (Oda et al. 2009; Gao et al. 2012). Since L3MBTL2 is a defining, unique feature of PRC1.6, we therefore assessed its localisation through pre-implantation development. L3MBTL2 was readily detected in the mature GV oocyte, where it exhibited a rather uniform nuclear localisation, but was excluded from the DAPI-rich regions (Fig. 3A). After fertilisation, L3MBTL2 was present on both pronuclei at the zygote stage. The levels of L3MBTL2 decreased significantly at the 2-cell stage, and gradually increased between the 4-cell and morula stages (Fig. 3A). In blastocysts, L3MBTL2 displayed a more diffuse signal, with high background. However, some weak accumulation was visible across the nuclei of both the ICM and the trophectoderm. Thus, L3MBTL2 is inherited maternally but

strongly reduced at the 2-cell stage, becoming then present again after the 4-cell stage. It is possible that the low levels of L3MBTL2 between the zygote and 2-cell stage help to relieve a repressive chromatin state globally, thereby helping to promote zygotic genome activation.

In addition to L3MBTL2, another MBT family member and polycomb-related protein, L3MBTL1, can also bind to methyl-lysines, including H4K20me1/2 (Trojer et al. 2011; Stielow et al. 2014). Thus, we finally addressed the protein levels of L3MBTL1, the mouse homologue of the *Drosophila* PcG protein l(3)mbt (Wismar et al. 1995; Koga et al. 1999). The fully grown GV oocyte displayed a clear nuclear localisation of L3MBTL1, which appeared dispersed, without any obvious enrichment in either DAPI-rich foci or the regions surrounding the NLB (Fig. 3B). We detected L3MBTL1 at all stages of preimplantation development that we analysed, from the zygote to the blastocyst stage (Fig. 3B). In the zygote, L3MBTL1 localised to both pronuclei and had no particular enrichment in DAPI-dense regions. L3MBTL1 retained the same localisation pattern until the morula stage, where all nuclei analysed displayed L3MBTL1 foci in association with the nucleoli, but excluded from DAPI-rich regions (Fig. 3B, arrows). In all the blastocysts analysed, L3MBTL1 was present in both the ICM and the TE lineages (Fig. 3B). Like in the morula stage, L3MBTL1 displayed condensed foci in proximity to the nucleoli in the blastocyst (Fig. 3B). Because this localisation was detected in all blastocysts analysed, it suggests that these foci may not be linked to X inactivation, as in the case of H2AK119ub (de Napoles et al. 2004). Thus, while L3MBTL2 shows temporal changes in its expression pattern during pre-implantation development, L3MBTL1 remained present throughout all stages analysed.

## Discussion

Our observations above suggest that different types of PRC1 complexes (Schwartz and Pirrotta 2013) might be at play during early mouse development. Given the temporal changes in the expression of the subunits that we analysed, it is likely that different complexes play different functions during this period, but also that their activities and assembly change dynamically during these first divisions. For example, CBX2, a member of the canonical PRC1, is expressed between

the zygote and 8-cell stages and later at the blastocyst stage (Puschendorf et al. 2008). Thus, one could postulate that CBX2 is involved in the targeting of canonical PRC1 activity at these stages. While we did not detect RYBP in zygotes, we detected YAF-2 enriched around the NLBs, suggesting that CBX-2 directed PRC1 activity is not alone in promoting H2AK119ub at these regions. Indeed, *Ring1a/Ring1b* double knock-out results in derepression of major satellites transcription from the paternal chromatin (Puschendorf et al. 2008). Since the *Ring1a/Ring1b* double knockout abolishes PRC1 activity as a whole, additional experiments will be necessary to address whether there is a differential contribution between those two potential PRC1 complexes in mediating heterochromatin silencing. This can be further assessed by the depletion of YAF-2 in the zygote or a complete YAF-2 knock-out model to study the different roles that the non-canonical mediated H2AK119ub compared to the canonical ones during early mouse development.

Interestingly, all three YAF-2, RYBP (this work) and CBX2 (Tardat et al. 2015) are expressed in 2-cell stage embryos, suggesting that at this stage, at least three types of PRC1 complexes could potentially form to enable widespread PRC1 activity. This is supported by the strong H2AK119ub signal observed at this stage, where H2AK119ub is not only restricted to the heterochromatic regions surrounding the NLBs where RYBP is enriched, but clearly extends to the nucleoplasm. Indeed, RYBP containing PRC1 exhibit stronger H2AK119Ub activity than those containing CBX2/CBX8 *in vitro* (Gao et al. 2012). The 2-cell stage coincides with EGA (Embryonic Genome activation), which also corresponds to the structural changes that start to take shape between the 2-cell and 4-cell stages when the NLBs are replaced by the chromocenters as the organizing centers of chromatin structure. Thus, the 2-cell stage may require a large deal of chromatin remodeling and changes, to which increased PRC1 activity may contribute. Conditional knock-out of *Rybp* in ES cells leads to derepression of genes related to preimplantation development during EGA, such as *Eif1a*, *Zscan4* and some retrotransposons. Of special interest is the upregulation of MuERVs among the retrotransposons upon *Rybp* deletion. Double knock-out of *Rybp* and *Yaf2* in ES cells showed no synergistic effects, suggesting potential independent effects for these two forms of non-canonical PRC1 complexes (Hisada et al. 2012).

At later stages of development, at the blastocyst stage, previous data suggested a lack of enrichment of CBX2 at RING1B/RNF2 foci in the blastocyst (Puschendorf et al. 2008). We observed foci of H2AK119ub at this stage, which are presumably linked to X inactivation (de Napoles et al. 2004).

However, neither RYBP nor YAF-2 displays a strictly similar pattern to that of H2AK119ub at this stage. Thus, a different PRC1 complex might be at play when RING1 is recruited by Xist to the X inactivation center (Schoeftner et al. 2006). One should keep in mind, however, that mechanisms other than H2A ubiquitylation could also contribute to PRC1 function. This has been clearly demonstrated for the case of L3MBTL2, which does not seem to stimulate RING1A/RING1B activity in vitro, and was therefore suggested to act as a recruiter exclusively (Trojer et al. 2011). Because L3MBTL2 has its own biochemical activities by which it can compact chromatin in vitro (Trojer et al. 2011), recruitment of L3MBTL2 and PRC1 could facilitate local chromatin compaction in a histone modification independent manner. Indeed, our observations that both L3MBTL2 and L3MBTL1 are expressed throughout pre-implantation development, could provide more versatile actions of polycomb-related function at specific genome locations at a given developmental time. While it is known that the catalytic, ubiquitylation activity of PRC1 is not necessary to compact chromatin at the time of gastrulation *in vivo* (Illingworth et al. 2015; Eskeland et al. 2010)whether catalytic activity *per se* of PRC1 is necessary after fertilisation, has not been addressed.

In sum, our work contributes to the molecular characterisation of the embryonic chromatin after fertilisation, and places non-canonical PRC1 activity as a potential important player to consider when understanding the molecular definition of epigenetic reprogramming *in vivo*.

## Materials & Methods

### Embryo collection.

Mice were bred in a 12 h light cycle. Embryos were collected as described (Hogan et al. 1994) from CD1 X CD1 natural mating. Zygotes and cleavage stage embryos were collected at the indicated developmental stages upon puncturing of the *ampullaswollen* and the oviduct. Blastocysts were obtained by flushing the uterus with M2 medium (Sigma). All embryos were fixed immediately after collection. Pronuclear stages (PN) were classified according to Adenot et al. (Adenot et al. 1997). Experiments with animals were carried out according to valid legislation in France and under the authorization of the Com'eth ethical committee.

### Immunostaining.

After removal of the *zona pellucida* with acid Tyrode's solution (Sigma), embryos were washed three times in PBS and fixed as described (Torres-Padilla et al. 2006). Embryos were permeabilised, washed with PBS-T (0.1% Tween in PBS), blocked and incubated with the primary antibodies. The primary antibodies were: H2AK119ub (Cell Signaling D27C4, rabbit monoclonal), YAF-2 (ThermoFisher Scientific PA5-30359, rabbit polyclonal), RYBP (Abcam ab5976, rabbit polyclonal), L3MBTL1 and L3MBTL2 (from D. Reinberg, rabbit polyclonal; (Trojer et al. 2011). A dilution of 1/250 was used for all the primary antibodies. After O.N. incubation in the primary antibody, embryos were washed twice in PBS-T, blocked for additional 20 minutes and incubated for 3 h with the corresponding secondary antibodies at RT. The secondary antibody used in this work is AlexaFluor 488 (Life Technologies, goat anti-rabbit). After washing, embryos were mounted in Vectashield (Vector Laboratories) supplemented with 4'-6-Diamidino-2-phenylindole (DAPI) for visualisation of the DNA.

### Confocal analysis.

Confocal microscopy was performed using a 63x oil objective in a Leica SP5 or SP8 inverted microscope. Confocal sections were acquired every 0.5µm and images were analysed using Lecica

LAS AF Lite 2.6.3 build 8173. Images for this manuscript were formatted using Adobe Illustrator CS6. The number of embryos analysed in this work are shown in the table S1 as follows: A) Number of embryos collected per stage for each antibodies; B) Number of zygotes stained with H2AK119ub at the different ProNuclear stage (PN), and C) Number of blastocysts stained with H2AK119ub and pattern of foci. Each staining was repeated at least in 2 independent biological replicates.

## Figures and Figure Legends

Figure 1

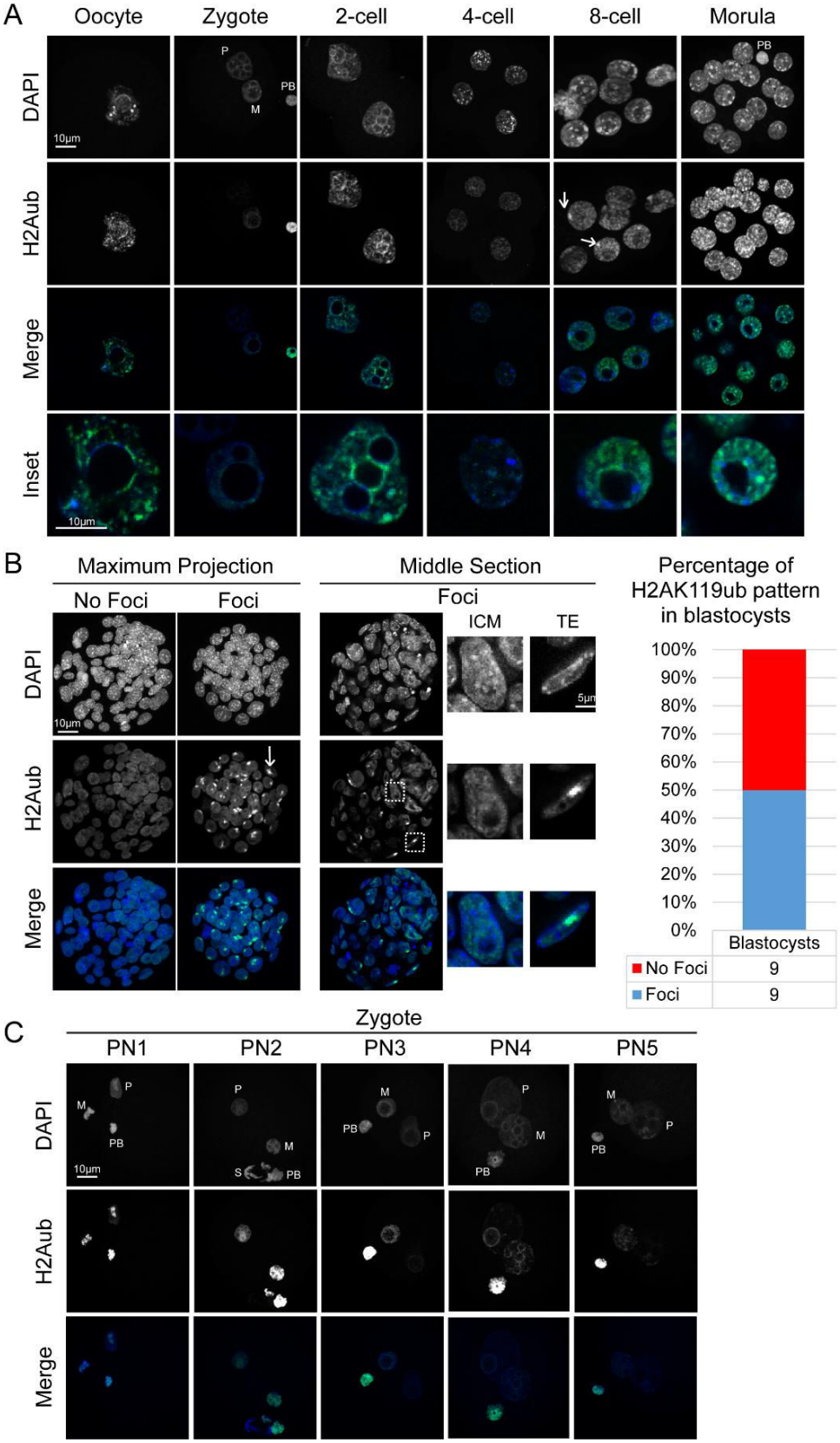

**Figure 1. Dynamic establishment of H2AK119ub during mouse pre-implantation development.**

A) Representative images showing full Z-projections of confocal sections of oocytes and embryos from the zygote to the morula stage stained with DAPI and H2AK119ub antibodies. White arrows at the 8-cell stage indicate accumulation of H2AK119ub at foci. Bottom panels are merged images of single sections showing insets of nuclei from the embryos above at a higher magnification.

B) Representative images of full Z-projections of confocal sections of blastocysts stained with DAPI and H2AK119ub antibody. A representative projection of a blastocyst showing H2AK119ub accumulation in foci is shown with two insets depicting one Inner Cell Mass (ICM) nucleus and a tropherctoderm (TE) nucleus. On the right, the percentage of embryos showing or not H2AK119ub foci, N=18.

C) Full projection of confocal Z-sections of H2AK119ub and DAPI at five different pronuclear (PN) stages in the zygote. Abbreviations: M: maternal, P: paternal, PB: polar body, S: sperm. Scale bars correspond to 10μm

Figure 2

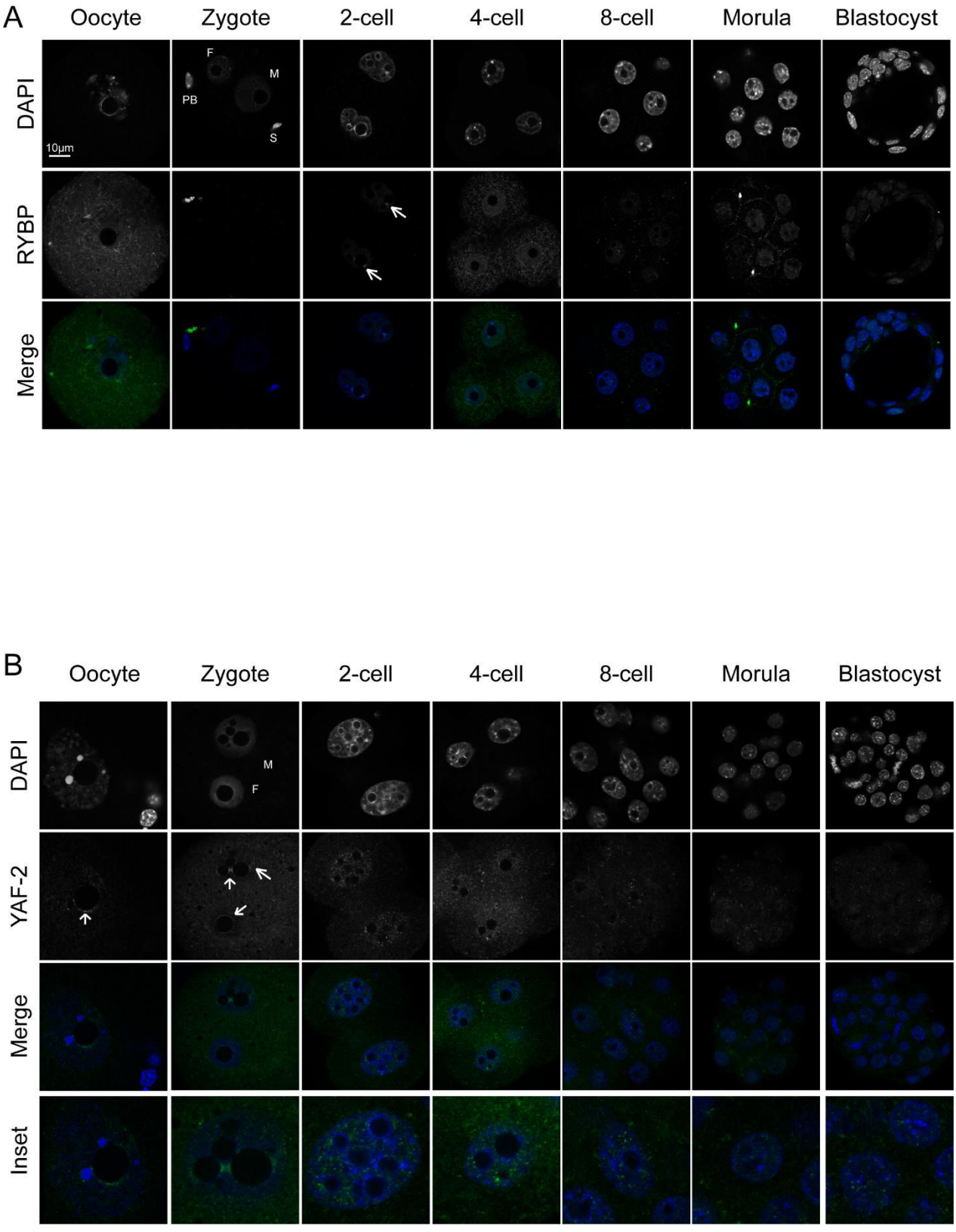
A
Oocyte
Zygote
2-cell
4-cell
8-cell
Morula
Blastocyst
DAPI
RYBP
Merge
F
M
PB
S
10µm
B
Oocyte
Zygote
2-cell
4-cell
8-cell
Morula
Blastocyst
DAPI
YAF-2
Merge
Inset
M
F

**Figure 2. Changes in non-canonical PRC1 components during pre-implantation development.**

A –B. Confocal single projection images of DAPI and RYBP (A), or YAF-2 (B), are shown. White arrows indicate the accumulation of the protein. Merge insets of nuclei are shown for YAF-2 at the bottom. Abbreviations: M: maternal, P: paternal, PB: polar body, S: sperm. Scale bar is shown in white and corresponds to 10μm for both stainings.

Figure 3

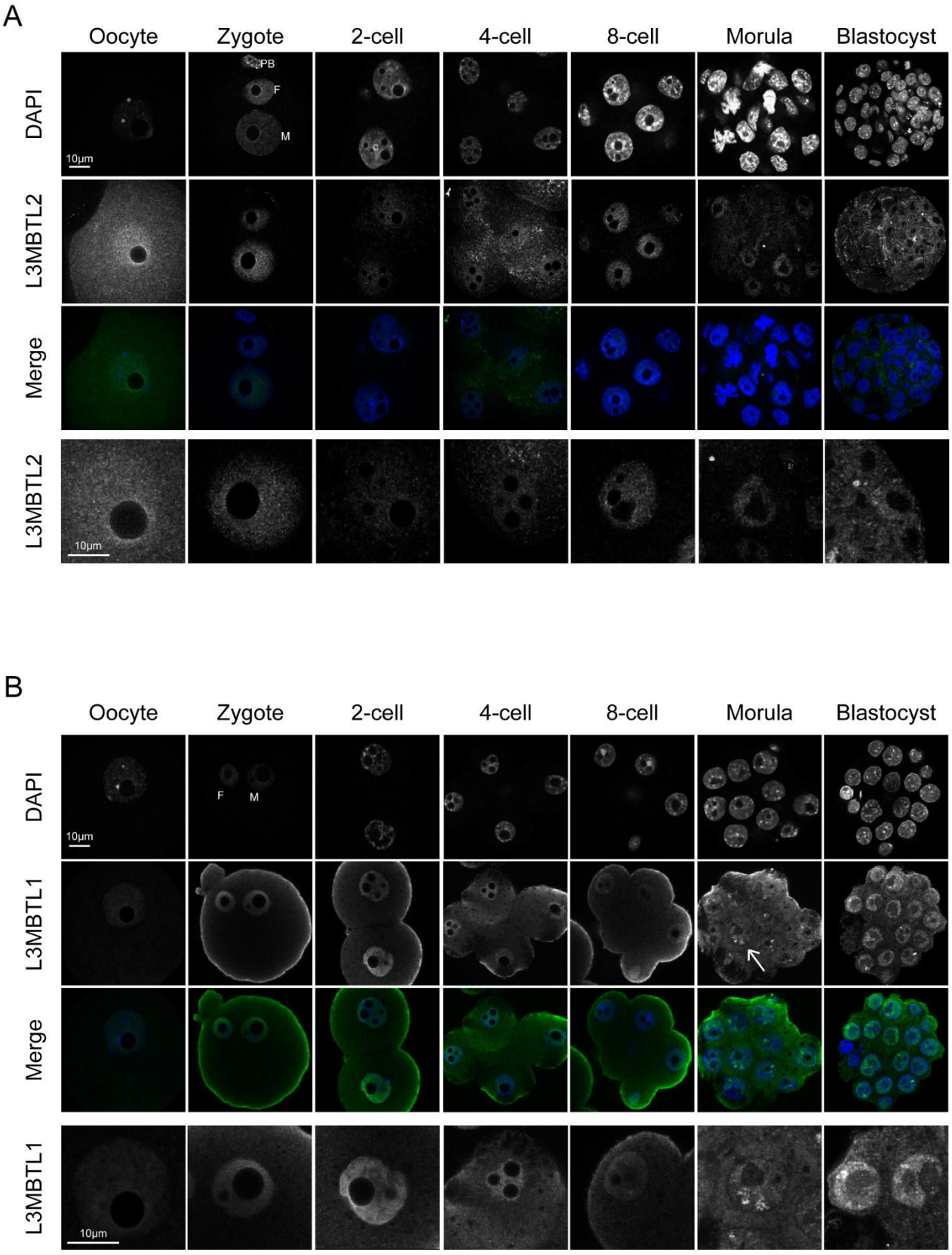
A
Oocyte
Zygote
2-cell
4-cell
8-cell
Morula
Blastocyst
DAPI
L3MBTL2
Merge
L3MBTL2
PB
F
M
10μm
B
Oocyte
Zygote
2-cell
4-cell
8-cell
Morula
Blastocyst
DAPI
L3MBTL1
Merge
L3MBTL1
F
M
10μm

**Figure 3. MBT family proteins are present in early mammalian development.**

A) Representative confocal sections of immunofluorescence analysis of oocytes and embryos at the indicated stages of development analysed with the L3MBTL2 antibody. DNA was stained with DAPI (top panel). A merged, single section is also shown (L3MBTL2 in green, DAPI in blue). Insets showing a higher magnification of nuclei from the same embryos, but with the L3MBTL2 signal in grayscale are shown at the bottom.

B) Representative single confocal sections of oocytes or embryos stained with the L3MBTL1 antibody, as indicated. The DAPI (top panel) and the L3MBTL1 channels are shown in grayscale. In the merge image L3MBTL1 is shown in green and DAPI in blue. The bottom panel shows higher magnifications of nuclei of the same representative embryos, with the L3MBTL1 staining is depicted in grayscale. M: maternal, P: paternal, PB: polar body. Note that the L3MBTL1 antibody used gave some non-specific staining around the cell membrane in some of the embryos analysed. Scale bar as indicated.

## Acknowledgments

We are grateful to Zhonghua Gao and Danny Reinberg for providing the L3MBTL1 and 2 antibodies and to Celine Ziegler-Birling for support with mouse handling and collection. M.E.T.-P. acknowledges funding from EpiGeneSys NoE, ERC-Stg 'NuclearPotency', EMBO Young Investigator Programme and the Schlumberger Foundation for Research and Education. A.E is a recipient of a doctoral fellowship from the Ministère de l'Enseignement Supérieur et de la Recherche and from the Fondation pour la Recherche Médicale (FDT20150532012).

# Results: third part

In addition to studying heterochromatin modifications during preimplantation development, I was interested in studying the ultrastructure of chromatin *in vivo*. The link between chromatin modifications and chromatin compaction has been studied extensively *in vitro* by electron microscopy and eluded to in studies of nucleosome accessibility using MNase treatments. I was interested in showing a direct link between heterochromatin marks *de novo* establishment and their effect on chromatin compaction. To study this relation, experimental conditions had to be set up using mouse embryos as a model. Our objectives were threefold:

- What does the chromatin ultrastructure look like in the embryo and does it change similarly to nuclear dynamics observed using fluorescence microscopy and which were described in the introduction of this manuscript?
- Do heterochromatin marks positively correlate with chromatin compaction *in vivo*?
- Can chromatin compaction be modified *in vivo* by ectopic expression of histone post-translational modifiers?

The best method that both has high resolution and shows chromatin compaction in preimplantation embryos is electron microscopy (EM), assuming that the observed electron density is indicative of chromatin compaction, and as a result transmission EM (TEM) was used to observe embryonic chromatin.

The initial experimental design was supposed to use correlative-EM, in which fluorescence microscopy can be combined with TEM to study chromatin ultrastructure. To this end, embryos had to be fixed by being subjected to liquid nitrogen freezing (similar to cryo-EM methods) in order to fix the chromatin structure as fast as possible and avoid artifacts that might arise from chemical fixation. The technical difficulty in using this method is that the freezing of the embryo has to be homogeneous to avoid ice crystals which would disrupt the structure of organelles. Further complicating the task, is the fact that the nucleus is located centrally inside the cytoplasm which means that it will be the last organelle to be fixed within the embryo. Additionally, lipids and water carried inside the embryos increased the freezing duration and can lead to ice crystal formation. Regardless of these challenges, we managed to freeze the embryos and obtained

preserved organelle structures in the cytoplasm, but not in the nucleus where we could not avoid ice crystal formation. To overcome this problem, several cryo-protectants were applied (dextran, BSA 20%) during the cryo-fixation, but to no avail as we did not manage to avoid ice crystals in the nucleus. Therefore, we resorted to using chemical fixation to stain the embryos and established a protocol using glutaraldehyde and formaldehyde. This protocol allowed us to observe the ultrastructure of chromatin in the embryos, but blocked the possibility of studying correlation between heterochromatin marks and chromatin compaction, because glutaraldehyde made epitopes inaccessible to immune-gold labelling strategies (loss of antigenicity). Thus we could only achieve one of our objectives which is to study the chromatin ultrastructure in embryos and describe the dynamics of this structure across several stages of development. This work has led to the discovery that electron density significantly increases between the 2-cell and 8-cell stages concomitant with changes in histone dynamics and nuclear structure and has been published in Bosckovic et al. and can be found in Annex 4 on the following page.

## Annex 4: Higher chromatin mobility supports totipotency and precedes pluripotency *in vivo*

RESEARCH COMMUNICATION

# Higher chromatin mobility supports totipotency and precedes pluripotency in vivo

**Ana Bošković,[1] André Eid,[1] Julien Pontabry,[1] Takashi Ishiuchi,[1] Coralie Spiegelhalter,[1] Edupuganti V.S. Raghu Ram,[2] Eran Meshorer,[2] and Maria-Elena Torres-Padilla[1,3]**

[1]CNRS/INSERM U964, Université de Strasbourg, Institut de Génétique et de Biologie Moléculaire et Cellulaire, F-67404 Illkirch, France; [2]Department of Genetics, The Alexander Silberman Institute of Life Sciences, The Hebrew University of Jerusalem, Jerusalem 91904, Israel

**The fusion of the gametes upon fertilization results in the formation of a totipotent cell. Embryonic chromatin is expected to be able to support a large degree of plasticity. However, whether this plasticity relies on a particular conformation of the embryonic chromatin is unknown. Moreover, whether chromatin plasticity is functionally linked to cellular potency has not been addressed. Here, we adapted fluorescence recovery after photobleaching (FRAP) in the developing mouse embryo and show that mobility of the core histones H2A, H3.1, and H3.2 is unusually high in two-cell stage embryos and decreases as development proceeds. The transition toward pluripotency is accompanied by a decrease in histone mobility, and, upon lineage allocation, pluripotent cells retain higher mobility than the differentiated trophectoderm. Importantly, totipotent two-cell-like embryonic stem cells also display high core histone mobility, implying that reprogramming toward totipotency entails changes in chromatin mobility. Our data suggest that changes in chromatin dynamics underlie the transitions in cellular plasticity and that higher chromatin mobility is at the nuclear foundations of totipotency.**

Supplemental material is available for this article.

Received January 25, 2014; revised version accepted April 16, 2014.

Embryonic cells are characterized by a large degree of plasticity, which is the ability to generate different cell types upon differentiation and is necessary to start a full developmental program. After fertilization, the mouse embryo has the transient capacity to generate both embryonic and extraembryonic cell types, a feature that is referred to as totipotency (Tarkowski 1959; Ishiuchi and Torres-Padilla 2013). This is in contrast to pluripotent cells, which contribute to all three germ layers of the embryo proper, but not to extraembryonic lineages, and therefore have a more restricted potential than totipotent cells. In mice, only the zygote and two-cell stage blastomeres are, strictly speaking, totipotent, since they have the ability to develop into a full organism without the need of carrier cells (Tarkowski 1959; Tarkowski and Wroblewska 1967; Kelly et al. 1978; Ishiuchi and Torres-Padilla 2013). As development progresses, pluripotent cells form in the inner cell mass (ICM) of the blastocyst, accompanied by the activation of pluripotency-associated transcription factors like *Nanog* and *Pou5f1/Oct4* (Nichols et al. 1998; Chambers et al. 2003). The first differentiated embryonic tissue, the trophectoderm (TE), appears morphologically distinguishable and surrounds the ICM in the blastocyst. Thus, during the early stages of development, the mouse embryo undergoes dramatic changes in cellular plasticity.

Upon fertilization, embryonic chromatin undergoes intense chromatin remodeling. Indeed, this epigenetic reprogramming of the gametes is thought to be essential to gain totipotency (Sado and Ferguson-Smith 2005; Surani et al. 2007; Hemberger et al. 2009). However, the precise conformation of embryonic chromatin and the way it is remodeled to sustain totipotency and subsequent pluripotency remain largely unknown. In particular, whether and which changes in chromatin dynamics and organization underlie the transitions in cellular plasticity have not been established. It is generally assumed that a more plastic chromatin is present in pluripotent cells. Although this has been analyzed to some extent in pluripotent stem (embryonic stem [ES]) cells in culture (Meshorer et al. 2006; Melcer et al. 2012), it has not been addressed in vivo, and the molecular and epigenetic features of totipotent cells are scarce. Moreover, whether chromatin plasticity is functionally linked to cellular potency and fate has not been addressed experimentally.

## Results and Discussion

To address whether chromatin plasticity parallels cellular potency in vivo, we first examined chromatin mobility. For this, we set up fluorescence recovery after photobleaching (FRAP) of chromatin proteins in embryos. Although FRAP is an approach routinely used in cultured cells, it has not yet been used to track chromatin dynamics in the developing mammalian embryo. We therefore first established conditions for FRAP of chromatin proteins that are compatible with normal embryonic development (Supplemental Fig. S1) We injected mRNA for GFP-tagged histones into zygotes at the fertilization cone stage before pronuclei formation based on previously titrated histone mRNA concentrations (Santenard et al. 2010). We then cultured these embryos and performed FRAP on individual two-cell or eight-cell stage nuclei (Fig. 1A). To ensure that the GFP signal that we observed derives from histones in chromatin, we first verified incorporation of exogenously expressed histones by analyzing mitotic chromosomes, which revealed a strong GFP signal on chromatin (Supplemental Fig. S2). Second, we also imaged interphase nuclei

[*Keywords*: pluripotency; chromatin dynamics; reprogramming; cell fate; totipotent cells]
**[3]Corresponding author**
**E-mail metp@igbmc.fr**
Article is online at http://www.genesdev.org/cgi/doi/10.1101/gad.238881.114.

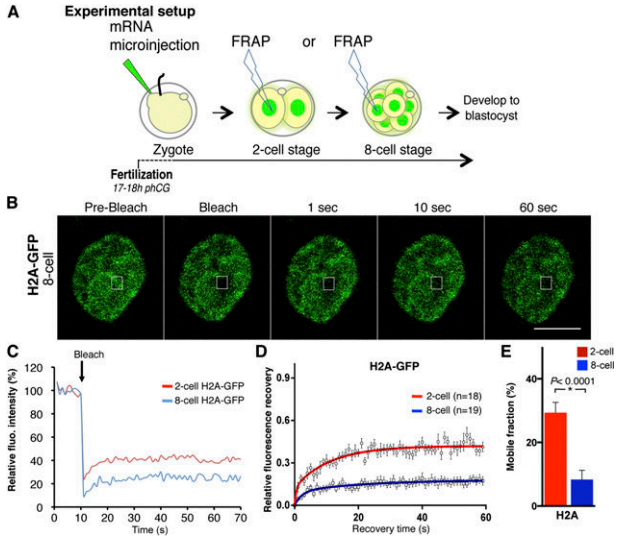


**Figure 1.** FRAP analysis of chromatin components in the developing mouse embryo reveals a decrease in chromatin mobility of H2A-GFP. (*A*) Experimental setup for FRAP in embryos. Zygotes were collected and microinjected with in vitro transcribed mRNA and cultured until the indicated developmental stages, when they were subjected to FRAP. After imaging acquisition, embryos were cultured until the blastocyst stage, and their development was scored. (*B*) A representative nucleus of an eight-cell stage embryo expressing H2A-GFP during a FRAP experiment is shown. The bleached region is represented by a rectangle. Bar, 10 μm. (*C*) Representative single FRAP curves of H2A-GFP at the two-cell (red) and eight-cell (blue) stages. The bleach time point is indicated by an arrow. Recovery of H2A-GFP is significantly faster at the two-cell stage compared with the eight-cell stage. (*D*) Recovery curves of H2A-GFP at the two-cell (red) and eight-cell (blue) stages. Recovery was quantified in the bleached area over a 60-sec period, and the curves were normalized to zero to account for differences in bleach depth between experiments. Individual points are mean ± SEM, and mean values were fit into an exponential curve. (*E*) Estimated mobile fractions (±SEM) of H2A-GFP in two-cell and eight-cell stage embryos.

after treatment with Triton X-100, which releases non-bound chromatin proteins. Triton pre-extraction did not detectably alter the GFP signal in the nucleoplasm. Together, this suggests that under the experimental conditions that we established, GFP-tagged histones are efficiently incorporated into embryonic chromatin (Supplemental Fig. S2). We initially analyzed chromatin mobility of histone H2A, carefully avoiding the nucleoli precursors. A representative nucleus of an eight-cell stage embryo during FRAP acquisition for H2A and single typical FRAP curves of two-cell and eight-cell stage nuclei are shown in Figure 1, B and C, respectively. H2A-GFP showed a striking, reproducible high mobility in two-cell stage embryos, with relatively fast recovery kinetics and an ~29% mobile fraction (Fig. 1D,E; Supplemental Table S1). Interestingly, H2A-GFP mobility was significantly reduced at the eight-cell stage compared with the two-cell stage ($P < 0.0001$) (Fig. 1D,E; Supplemental Tables S3), suggesting that chromatin dynamics decrease as development proceeds. Importantly, the mobility of H2A-GFP and its changes during development were independent of the amount of mRNA injected or the timing of microinjection (Supplemental Fig. S4).

Upon chromatin remodeling, H2A/H2B dimers are known to be released prior to H3 and H4 tetramers (Groth et al. 2007; Xu et al. 2010; Winkler et al. 2012). To address whether the above observations are specific for H2A or reflect a general property of embryonic chromatin, we expanded our analysis to histone H3. We used the same experimental design as above and verified chromatin incorporation of the three H3 variants H3.1, H3.2, and H3.3 fused to GFP (Supplemental Figs. S2, S3; Santenard et al. 2010). Similarly to H2A-GFP, GFP-tagged H3.1 and H3.2 displayed a remarkable high mobility in two-cell stage embryos (Fig. 2A–C), with a mobile fraction of 24% ± 5% ($n = 20$) and 25% ± 5% ($n = 17$), respectively, which was independent of the amount of mRNA injected (Supplemental Fig. S4). Importantly, the mobility of both H3.1-GFP and H3.2-GFP decreased significantly as development proceeded to the eight-cell stage, reaching a mobile fraction of ~5% for both histones ($P = 0.01$ for H3.1-GFP and $P < 0.0001$ for H3.2-GFP) (Fig. 2B,C,E; Supplemental Tables S1, S3, S4). Thus, globally, canonical

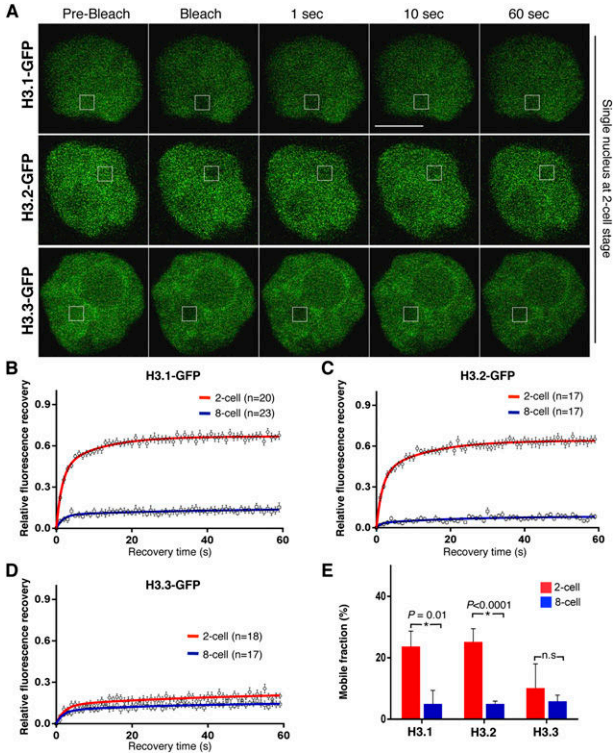


**Figure 2.** Mobility of core histones H3.1-GFP and H3.2-GFP decreases between the two-cell and the eight-cell stages, but H3.3-GFP mobility remains unchanged. (*A*) Nuclei of two-cell stage embryos expressing either H3.1-GFP (*top*), H3.2-GFP (*middle*), or H3.3-GFP (*bottom*) at the indicated time points during representative FRAP experiments. The bleached region is indicated by a rectangle. (*B*) FRAP curves for H3.1-GFP in two-cell and eight-cell stage embryos reveal higher mobility of H3.1-GFP at the earlier developmental stage. (*C*) H3.2-GFP FRAP curves at the two-cell and eight-cell stages. Two-cell stage embryos show an unusual, high mobility behavior of H3.2-GFP, which is dramatically decreased with developmental progression. (*D*) FRAP curves for H3.3-GFP at the two-cell and eight-cell stages show no significant change in H3.3 dynamics between the two stages. (*E*) Calculated mobile fractions (±SEM) of H3 variants at the two-cell and eight-cell stages. (*B–D*) Values represent mean ± SEM of multiple embryos, where *n* indicates the number of nuclei analyzed. FRAP was performed in only one nucleus per embryo. The mean values were fit into an exponential curve. *P*-values were calculated using unpaired *t*-test between each two groups.

core histones display a remarkably high mobility at the beginning of embryogenesis, as measured by FRAP, which diminishes as development proceeds, suggesting that chromatin mobility might be linked to cellular potency. Next, we analyzed the replacement histone variant H3.3. In contrast to H3.1 and H3.2, H3.3-GFP showed much lower mobility in two-cell stage embryos, with an estimated mobile fraction of 10% ± 7.8% ($n$ = 18), which did not change significantly in eight-cell embryos (6% ± 2%; $n$ = 17; $P$ = 0.59) (Fig. 2D,E; Supplemental Table S3), suggesting that some chromatin components may not change their mobility between the two-cell and eight-cell stages.

To investigate whether the decreased mobility of canonical core histones at the eight-cell stage is regulated through the action of histone modifiers, we performed FRAP for H2A-GFP and H3.1-GFP in the presence of chemical inhibitors. Incubation of eight-cell stage embryos with TSA, a global HDAC inhibitor known to affect H1e mobility in ES cells (Melcer et al. 2012), did not seem to alter the mobility of H2A-GFP or H3.1-GFP compared with control embryos ($P$ = 0.92 and $P$ = 0.67, respectively) (Supplemental Fig. S5; Supplemental Table S5). We also asked whether decreasing global H3K9me2 levels through the action of BIX-01294, a compound reported to inhibit the G9a methyltransferase (Kubicek et al. 2007), would impact histone mobility in eight-cell stage embryos. Culturing eight-cell stage embryos with BIX-01294 led to a reduction in global H3K9me2 levels. While H3.1-GFP mobility remained virtually unchanged upon BIX-01294 treatment, H2A-GFP displayed a slightly higher mobility in the presence of BIX-01294 (Supplemental Fig. S5). However, this difference was not statistically significant under the experimental conditions used (Supplemental Table S5). Although not statistically significant, the trend change in H2A-GFP dynamics in the presence of BIX-01294 may suggest that global changes in H3K9 methylation might potentially be involved in the changes in histone mobility from the two-cell to the eight-cell stage. Indeed, it is known that global H3K9me3 levels increase from the eight-cell stage onward, when embryonic constitutive heterochromatin state is replaced by the canonical *Suv39h*-mediated state (Puschendorf et al. 2008). The sharp down-regulation of the H3K9me2/me3 demethylase *Kdm4b* at the eight-cell stage is also in line with this suggestion (Burton et al. 2013). Since BIX-01294 is reported to inhibit specifically G9a (Kubicek et al. 2007), it will be important to manipulate additional H3K9me pathways to address this in full.

To further explore the hypothesis that chromatin dynamics might be linked to cellular potency, we next investigated chromatin mobility in the two lineages of the early blastocyst, the ICM and the TE, which are characterized by different degrees of cellular potency. We devised an experimental setup to perform FRAP in individual nuclei of ICM and TE cells (Fig. 3A). FRAP analysis revealed that H3.1-GFP displays higher mobility in pluripotent cells of the ICM compared with the differentiated TE counterpart (Fig. 3B). Remarkably, the recovery kinetics between the ICM and TE differed drastically, by an order of magnitude higher (Fig. 3B, inset; Supplemental Table S2), and the H3.1-GFP mobile fraction was approximately twofold higher in ICM cells compared with the TE (Fig. 3B), suggesting that pluripotent cells retain high chromatin mobility, while TE cells do not.

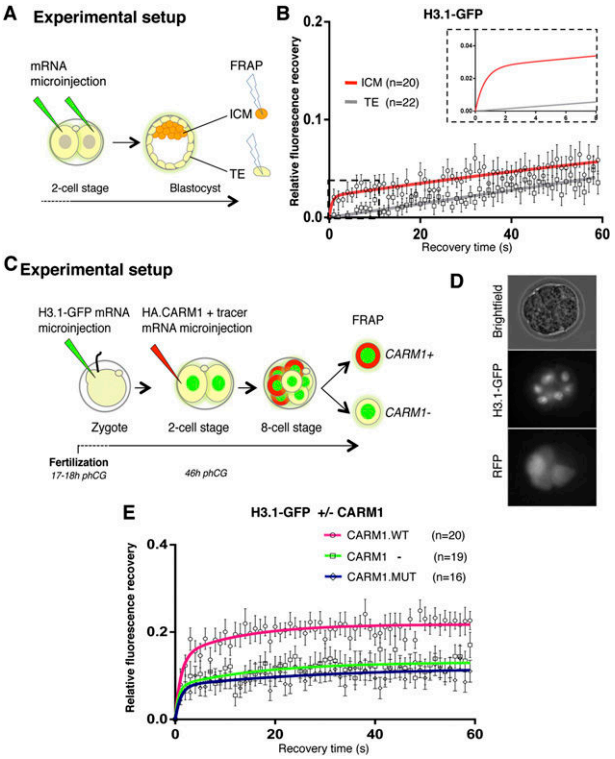


**Figure 3.** Pluripotent cells retain high chromatin mobility upon lineage allocation. (*A*) The two blastomeres of a two-cell stage embryo were microinjected with equal amounts of H3.1-GFP mRNA, and embryos were developed to the blastocyst stage. At embryonic day 3.5 (E3.5), a single nucleus of the ICM and in the TE was subjected to FRAP as in Figure 1. (*B*) Mean FRAP values for H3.1-GFP in the ICM (red line) and TE (gray line) over 60-sec period of recovery immediately after bleaching. The smaller graph in the *top right* corner represents a zoom of the dashed rectangle, which includes the first 8 sec post-bleach, in which data points are omitted for clarity. (*C*) Schematic representation of FRAP experiments to address chromatin mobility during lineage allocation. Zygotes were microinjected with H3.1-GFP mRNA as in Figure 1 and cultured until the late two-cell stage, when one blastomere was microinjected with HA.CARM1 mRNA and mRFP mRNA as tracer. Microinjection of HA.CARM1 mRNA at this stage allocates the progeny of the injected cell to the ICM (Torres-Padilla et al. 2007). (*D*) Representative eight-cell stage embryo after double microinjection. (*Middle* image) While all nuclei are H3.1-GFP-positive, only four blastomeres are RFP-positive (and HA.CARM1-positive). (*E*) FRAP curves for H3.1-GFP in HA.CARM1 wild-type-positive (pink line), HA.CARM1-negative (green line), and CARM1 catalytic death-positive (dark blue line) blastomeres at the eight-cell stage. In each embryo, one RFP-positive and one RFP-negative cell were analyzed by FRAP. Allocation of ICM fate through CARM1 expression increases H3.1-GFP mobility at the eight-cell stage. Under the same experimental conditions, the CARM1 catalytic mutant does not alter H3.1-GFP mobility.

The difference in H3.1-GFP mobility between ICM versus TE that we observed and the fact that ICM cells display higher mobility further prompted us to ask whether chromatin mobility is functionally linked to lineage allocation. To directly address this possibility, we sought to determine chromatin mobility in embryonic cells immediately before the segregation of these two lineages, which first occurs upon the formation of outer and inner cells during the division of the eight-cell to the 16-cell stage (Kelly et al. 1978; Johnson and Ziomek

1981). In the ideal experimental setup, tracking chromatin mobility in eight-cell stage blastomeres that are destined to become ICM should be performed. However, because the cells in the mammalian embryo are not predetermined but are subject to regulative development (Rossant and Tam 2004), performing this is technically not feasible without perturbing development. We therefore took advantage of earlier findings showing that expression of PRMT4/CARM1 in a late two-cell stage blastomere drives the progeny of this cell to the ICM (Torres-Padilla et al. 2007). We microinjected H3.1-GFP mRNA in zygotes as before and performed a second microinjection of *Carm1* mRNA together with RFP mRNA as a lineage tracer (Fig. 3C). We then conducted FRAP in CARM1-positive and CARM1-negative cells at the eight-cell stage, which were distinguishable by the presence of the RFP tracer (Fig. 3C,D). Notably, while the CARM1-negative cells displayed the H3.1-GFP mobility of eight-cell blastomeres described above, CARM1-expressing cells showed a significantly higher H3.1-GFP mobility and a mobile fraction of approximately twofold (14% ± 3% compared with 7.7% ± 2% for the fast fraction and 7.3% ± 2.9% compared with 5.4% ± 1.7% for the slower fraction; $P < 0.01$) (Fig. 3E; Supplemental Table S6). Importantly, cells expressing a CARM1 catalytic mutant that is unable to direct cells toward the ICM (Torres-Padilla et al. 2007) displayed an H3.1-GFP mobility similar to noninjected cells ($P = 0.97$) (Fig. 3E; Supplemental Table S6), suggesting that cells destined to become pluripotent ICM retain higher histone mobility than future TE cells.

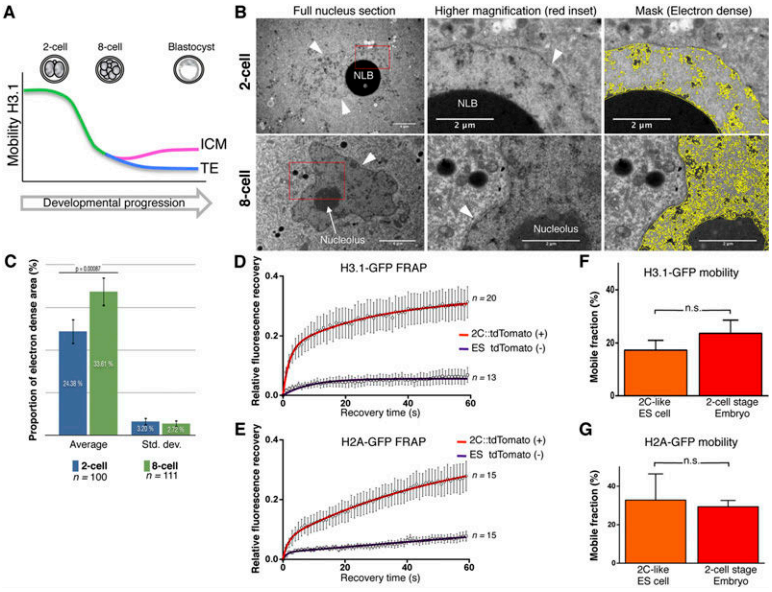


**Figure 4.** Totipotent cells display unusually high chromatin mobility and loose chromatin ultrastructure. (*A*) Schematic summary of H3.1-GFP mobility throughout development. (*B*) Electron micrographs of two-cell (*top*) and eight-cell (*bottom*) stage nuclei. Nucleolar-like bodies (NLBs) and nucleoli are indicated; arrowheads point to the nuclear membrane. The higher magnification corresponds to the red *inset*. The *right* column shows the mask to segment electron-dense regions for quantification (see Supplemental Fig. S8 for details). Note that the NLBs are very electron-dense, presumably due to the presence of negatively charged proteins such as nucleoplasmin (Inoue and Aoki 2010). (*C*) Quantification of the relative electron-dense area in two-cell and eight-cell stage nuclei reveals an increase of chromatin compaction. The average and SD of the indicated number of sections analyzed are shown. (*D*,*E*) Mean FRAP values of H3.1-GFP (*D*) and H2A-GFP (*E*) in tdTomato-positive two-cell-like (2C) ES cells (red curve) compared with tdTomato-negative ES cells (purple curve) grown in LIF+2i medium. The number of cells analyzed is shown at the side of each curve. ES cells with 2C properties are characterized by dramatically higher H3.1 mobility compared with non-2C, pluripotent ES cells within the same population. (*F*,*G*) Mobile fractions (±SEM) of H3.1-GFP (*F*) and H2A-GFP (*G*) in 2C ES cells and two-cell stage embryos. While the variability is higher in the in vitro totipotent cells (2C-like), the high mobility of H3.1-GFP is comparable between in vitro 2C cells and in vivo in two-cell embryos. (n.s.) Non-significant (unpaired *t*-test).

The above results together suggest that, in totipotent cells in the early embryo, the core histones H3.1-GFP, H3.2-GFP, and H2A-GFP display a very high mobility and that their mobility decreases as development proceeds, with pluripotent cells maintaining higher histone mobility than the TE upon lineage allocation (Fig. 4A). Given the unusually high mobility that we observed in two-cell stage nuclei, we next wondered whether any particular conformational or organizational feature of embryonic chromatin could be the basis for this. We thus established conditions to analyze embryonic chromatin ultrastructurally using transmission electron microscopy (TEM). Analysis of two-cell stage nuclei with TEM revealed a rather dispersed nucleoplasm largely devoid of the typical heterochromatic, electron-dense regions found in differentiated cells (Supplemental Fig. S6; Davies 1967), with a prominent nucleolar-like body (NLB) (Fig. 4B). Instead, only few electron-dense foci were visible throughout the nucleus, with no obvious enrichment of electron-dense heterochromatin in the vicinity of the nuclear membrane, a known feature of somatic cells (Cremer and Cremer 2001; Towbin et al. 2013), in agreement with reported electron spectroscopic imaging (Ahmed et al. 2010). Eight-cell stage chromatin appeared slightly more compacted than in two-cell nuclei, with larger electron-dense areas and stronger accumulation of compacted chromatin regions around the nuclear membrane and the nucleolus (Fig. 4B). Indeed, quantification of the electron-dense area across >100 TEM sections for each stage revealed a significant increase in the proportion of the electron-dense area between the two-cell and the eight-cell stage ($P = 0.0008$) (Fig. 4C), suggesting progressive compaction of a significant part of the chromatin between these two stages. Furthermore, the global increase in the proportion of electron-dense regions correlates with the decrease in histone mobility from the two-cell to the eight-cell stage that we observed. Thus, early embryonic chromatin displays an "atypical" loose chromatin ultrastructure, in line with the high chromatin protein mobility that we report.

Interestingly, the eight-cell stage changes in histone mobility correlate with global changes in chromatin organization and in the developmental program. Namely, major changes in heterochromatin organization, including formation of chomocenters (Probst et al. 2007), the global repression of retrotransposons (Peaston et al. 2004; Fadloun et al. 2013), and a significant increase in the electron-dense regions in the nuclei (this study), take place by the eight-cell stage. Also, these changes in histone mobility coincide with the time when individ-

ual cells develop polarity (Johnson and Ziomek 1981), which we previously suggested to co-occur with major changes in the expression of chromatin modifiers at the eight-cell stage (Burton et al. 2013).

Totipotent "two-cell-like" (2C) cells have recently been shown to emerge stochastically in ES cell cultures in vitro and can be identified by the activation of a specific endogenous retroelement of the ERVL family, MuERVL (Macfarlan et al. 2012). We reasoned that if high chromatin mobility is indeed an inherent property of totipotent cells, 2C ES cells should display equally high chromatin mobility as two-cell stage embryos. To address this, we generated ES cells stably expressing tdTomato under the control of MuERVL regulatory sequences, as previously described (Macfarlan et al. 2012). We confirmed that tdTomato expression occurs in a rather low percentage of the ES cell population (<0.5%) and that these ES cells are devoid of detectable levels of OCT4 protein (Supplemental Fig. S7; Macfarlan et al. 2012; data not shown). We then transfected plasmids harboring the same H3.1-GFP and H2A-GFP cDNAs as above and performed FRAP in 2C ES cells as well as in "normal" ES cells within the same colonies (tdTomato-positive and tdTomato-negative, respectively). Remarkably, 2C ES cells displayed a much higher mobility for both H3.1-GFP and H2A-GFP in tdTomato-positive compared with tdTomato-negative ES cells (Fig. 4D,E). The average mobile fraction of both proteins, albeit more variable, was similar to that in two-cell stage blastomeres (Fig. 4F,G). Thus, totipotent cells in vivo and in vitro are characterized by a very mobile chromatin configuration, suggesting that induction of totipotency entails changes in chromatin mobility.

Our results suggest that, globally, embryonic chromatin is extremely dynamic, more than in ES cells, which, although pluripotent, have a more restricted developmental potential than the totipotent cells in the early embryo. A loose chromatin conformation in the early embryo, in terms of both its dynamics and ultrastructure, might be permissive for the large-scale remodeling underlying epigenetic reprogramming after fertilization. While all core histones assayed were highly mobile, the replacement histone variant H3.3-GFP was the least mobile of the histones analyzed. Because H3.3 has been shown to be the major H3 variant deposited after fertilization (Torres-Padilla et al. 2006; Santenard et al. 2010; Akiyama et a. 2011), this initial incorporation of H3.3 may serve as a "placeholder" mechanism prior to the subsequent incorporation of the replication-dependent histones H3.1 and H3.2. It is possible that the high dynamics observed for H3.2 and H3.1 might be the result of this global wave of incorporation of H3.1/H3.2 and/or the transition toward a more "mature chromatin" where H3.3 is no longer the major histone variant. This is in agreement with the known dynamics of incorporation of H3 variants after fertilization as well as with the proposed model of H3.3 as a "placeholder" (Akiyama et al. 2011; Dunleavy et al. 2011) and as protective nucleosome gap filling (Ray-Gallet et al. 2011).

Our data suggest that increased chromatin mobility in vitro and in vivo is a key feature of totipotent cells and distinguishes them from pluripotent cells. Whether altering chromatin mobility is sufficient to induce totipotency and modulate cellular plasticity is an attractive possibility that remains to be addressed.

## Materials and methods

### *Embryo collection and microinjection*

Embryos were collected from F1 (C57BL/6 × CBA/H) crosses on superovulation. Human H3.1 (Santenard et al. 2010), H3.2, H3.3 (Santenard et al. 2010), and H2A (HIST1H2AK) cDNAs were subcloned into pRN3P plasmid, and corresponding mRNAs were transcribed in vitro, as described previously (Santenard et al. 2010). All fusions were cloned with EGFP in the C terminus, and all plasmids have identical 3′ and 5′ untranslated regions (UTRs). For the FRAP analysis in blastocysts, the levels of GFP in the blastocyst were too noisy when microinjection was performed in the zygote. Thus, to overcome this limitation, both blastomeres of two-cell stage embryos, collected at 45 h after administration of human chorionic gonadotropin (hphCG), were injected with identical concentrations of mRNA. We previously determined that recovery rates are independent of protein levels (see Supplemental Fig. S4). We verified incorporation of histones into chromatin (see the Supplemental Material).

### *FRAP microscopy*

FRAP was performed using a Leica SP2 confocal microscope and at 37°C using a 63.0 × 1.4 oil objective. Embryos were placed in drops of M2 medium on a glass-bottomed dish. A rectangular region of interest of 2.28 $\mu m^2$ was chosen randomly within a nucleus, avoiding the NLBs, and was subjected to FRAP. Ten prebleach frames were acquired followed by two bleach pulses without acquisition. Recovery of fluorescence was followed during 60 sec, with 1 frame per second. The raw data were processed with Fiji software (ImageJ). All analysis was done on background-subtracted values using EasyFRAP (see the Supplemental Material for a thorough description). The obtained curves were normalized using the full-scale normalization method so that the first post-bleach frame was set to 0. Normalized curves were then subjected to curve fitting.

### *Curve fitting and statistical analysis*

Experimentally obtained and normalized recovery curves were fit using Prism6 software (GraphPad Software). A two-phase exponential association equation, $Y = \mathrm{Ymax1} \times [1 - e(-\mathrm{K1} \times X)] + \mathrm{Ymax2} \times [1 - e(-\mathrm{K2} \times X)]$, was used to obtain mobile fractions and reaction rates, as this has been previously described to be appropriate for nuclear proteins (Phair and Misteli 2000). Unpaired *t*-tests were used for comparing two groups. Throughout the study, Ymax1 values are used for mobile fraction estimation, as they reflect the steady-state protein pool, unless otherwise stated.

### *Electron microscopy*

Embryos at the two-cell ($n = 3$) and eight-cell ($n = 3$) stages were collected after natural matings of B6CBAF1/J mice, fixed, and contrasted with osmium tetroxide and 1% uranyl acetate for 1 h. Samples were observed with a transmission electron microscope using an Orius 1000 CCD camera. Quantification of electron-dense regions was performed with a dedicated analysis pipeline implemented in ImageJ and MatLab (Supplemental Fig. S8).

## Acknowledgments

We thank members of the M.E.T.-P. laboratory for discussions, and P. Kessler and M. Koch of the IGBMC-ICS imaging facility. M.E.T.-P. acknowledges funding from EpiGeneSys, ERC-Stg "NuclearPotency," and FP7 Marie-Curie Actions ITN Nucleosome4D. E.M. acknowledges funding from ERC-Stg "ExprES" (281781), Nucleosome4D ITN, and the Israel Ministry of Science. A.B. was a Nucleosome4D and Association pour la Recherche contre le Cancer fellow. T.I. holds a post-doctoral HFSP fellowship, and A.E. holds a fellowship from the Ministère de l'Enseignement Supérieur et de la Recherche. E.V.S.R.R. was a Nucleosome4D ITN fellow and a Lady Davis Fellow.

## References


Ahmed K, Dehghani H, Rugg-Gunn P, Fussner E, Rossant J, Bazett-Jones DP. 2010. Global chromatin architecture reflects pluripotency and lineage commitment in the early mouse embryo. *PLoS ONE* **5:** e10531.

Akiyama T, Suzuki O, Matsuda J, Aoki F. 2011. Dynamic replacement of histone H3 variants reprograms epigenetic marks in early mouse embryos. *PLoS Genet* **7:** e1002279.

Burton A, Muller J, Tu S, Padilla-Longoria P, Guccione E, Torres-Padilla ME. 2013. Single-cell profiling of epigenetic modifiers identifies PRDM14 as an inducer of cell fate in the mammalian embryo. *Cell Rep* **5:** 687–701.

Chambers I, Colby D, Robertson M, Nichols J, Lee S, Tweedie S, Smith A. 2003. Functional expression cloning of Nanog, a pluripotency sustaining factor in embryonic stem cells. *Cell* **113:** 643–655.

Cremer T, Cremer C. 2001. Chromosome territories, nuclear architecture and gene regulation in mammalian cells. *Nat Rev Genet* **2:** 292–301.

Davies HG. 1967. Fine structure of heterochromatin in certain cell nuclei. *Nature* **214:** 208–210.

Dunleavy EM, Almouzni G, Karpen GH. 2011. H3.3 is deposited at centromeres in S phase as a placeholder for newly assembled CENP-A in G(1) phase. *Nucleus* **2:** 146–157.

Fadloun A, Le Gras S, Jost B, Ziegler-Birling C, Takahashi H, Gorab E, Carninci P, Torres-Padilla ME. 2013. Chromatin signatures and retrotransposon profiling in mouse embryos reveal regulation of LINE-1 by RNA. *Nat Struct Mol Biol* **20:** 332–338.

Groth A, Rocha W, Verreault A, Almouzni G. 2007. Chromatin challenges during DNA replication and repair. *Cell* **128:** 721–733.

Hemberger M, Dean W, Reik W. 2009. Epigenetic dynamics of stem cells and cell lineage commitment: digging Waddington's canal. *Nat Rev Mol Cell Biol* **10:** 526–537.

Inoue A, Aoki F. 2010. Role of the nucleoplasmin 2 C-terminal domain in the formation of nucleolus-like bodies in mouse oocytes. *FASEB J* **24:** 485–494.

Ishiuchi T, Torres-Padilla ME. 2013. Towards an understanding of the regulatory mechanisms of totipotency. *Curr Opin Genet Dev* **23:** 512–518.

Johnson MH, Ziomek CA. 1981. The foundation of two distinct cell lineages within the mouse morula. *Cell* **24:** 71–80.

Kelly SJ, Mulnard JG, Graham CF. 1978. Cell division and cell allocation in early mouse development. *J Embryol Exp Morphol* **48:** 37–51.

Kubicek S, O'Sullivan RJ, August EM, Hickey ER, Zhang Q, Teodoro ML, Rea S, Mechtler K, Kowalski JA, Homon CA, et al. 2007. Reversal of H3K9me2 by a small-molecule inhibitor for the G9a histone methyltransferase. *Mol Cell* **25:** 473–481.

Macfarlan TS, Gifford WD, Driscoll S, Lettieri K, Rowe HM, Bonanomi D, Firth A, Singer O, Trono D, Pfaff SL. 2012. Embryonic stem cell potency fluctuates with endogenous retrovirus activity. *Nature* **487:** 57–63.

Melcer S, Hezroni H, Rand E, Nissim-Rafinia M, Skoultchi A, Stewart CL, Bustin M, Meshorer E. 2012. Histone modifications and lamin A regulate chromatin protein dynamics in early embryonic stem cell differentiation. *Nat Commun* **3:** 910.

Meshorer E, Yellajoshula D, George E, Scambler PJ, Brown DT, Misteli T. 2006. Hyperdynamic plasticity of chromatin proteins in pluripotent embryonic stem cells. *Dev Cell* **10:** 105–116.

Nichols J, Zevnik B, Anastassiadis K, Niwa H, Klewe-Nebenius D, Chambers I, Scholer H, Smith A. 1998. Formation of pluripotent stem cells in the mammalian embryo depends on the POU transcription factor Oct4. *Cell* **95:** 379–391.

Peaston AE, Evsikov AV, Graber JH, de Vries WN, Holbrook AE, Solter D, Knowles BB. 2004. Retrotransposons regulate host genes in mouse oocytes and preimplantation embryos. *Dev Cell* **7:** 597–606.

Phair RD, Misteli T. 2000. High mobility of proteins in the mammalian cell nucleus. *Nature* **404:** 604–609.

Probst AV, Santos F, Reik W, Almouzni G, Dean W. 2007. Structural differences in centromeric heterochromatin are spatially reconciled on fertilisation in the mouse zygote. *Chromosoma* **116:** 403–415.

Puschendorf M, Terranova R, Boutsma E, Mao X, Isono K, Brykczynska U, Kolb C, Otte AP, Koseki H, Orkin SH, et al. 2008. PRC1 and Suv39h specify parental asymmetry at constitutive heterochromatin in early mouse embryos. *Nat Genet* **40:** 411–420.

Ray-Gallet D, Woolfe A, Vassias I, Pellentz C, Lacoste N, Puri A, Schultz DC, Pchelintsev NA, Adams PD, Jansen LE, et al. 2011. Dynamics of histone H3 deposition in vivo reveal a nucleosome gap-filling mechanism for H3.3 to maintain chromatin integrity. *Mol Cell* **44:** 928–941.

Rossant J, Tam PP. 2004. Emerging asymmetry and embryonic patterning in early mouse development. *Dev Cell* **7:** 155–164.

Sado T, Ferguson-Smith AC. 2005. Imprinted X inactivation and reprogramming in the preimplantation mouse embryo. *Hum Mol Genet* **14:** R59–R64.

Santenard A, Ziegler-Birling C, Koch M, Tora L, Bannister AJ, Torres-Padilla ME. 2010. Heterochromatin formation in the mouse embryo requires critical residues of the histone variant H3.3. *Nat Cell Biol* **12:** 853–862.

Surani MA, Hayashi K, Hajkova P. 2007. Genetic and epigenetic regulators of pluripotency. *Cell* **128:** 747–762.

Tarkowski AK. 1959. Experiments on the development of isolated blastomers of mouse eggs. *Nature* **184:** 1286–1287.

Tarkowski AK, Wroblewska J. 1967. Development of blastomeres of mouse eggs isolated at the 4- and 8-cell stage. *J Embryol Exp Morphol* **18:** 155–180.

Torres-Padilla ME, Bannister AJ, Hurd PJ, Kouzarides T, Zernicka-Goetz M. 2006. Dynamic distribution of the replacement histone variant H3.3 in the mouse oocyte and preimplantation embryos. *Int J Dev Biol* **50:** 455–461.

Torres-Padilla ME, Parfitt DE, Kouzarides T, Zernicka-Goetz M. 2007. Histone arginine methylation regulates pluripotency in the early mouse embryo. *Nature* **445:** 214–218.

Towbin BD, Gonzalez-Sandoval A, Gasser SM. 2013. Mechanisms of heterochromatin subnuclear localization. *Trends Biochem Sci* **38:** 356–363.

Winkler DD, Zhou H, Dar MA, Zhang Z, Luger K. 2012. Yeast CAF-1 assembles histone (H3–H4)2 tetramers prior to DNA deposition. *Nucleic Acids Res* **40:** 10139–10149.

Xu M, Long C, Chen X, Huang C, Chen S, Zhu B. 2010. Partitioning of histone H3–H4 tetramers during DNA replication-dependent chromatin assembly. *Science* **328:** 94–98.

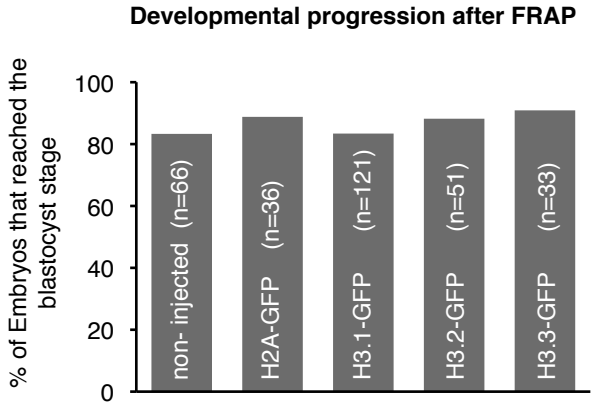


**Supplementary Figure 1.**
Experimental conditions used for FRAP experiments do not affect normal embryonic development. Developmental progression after FRAP analysis of 2- and 8-cell stage embryos. After mRNA microinjection in the zygote as in Figure 1, embryos were subject to FRAP at the 2- or 8-cell stage and were returned to the incubator for culture. Their subsequent development was monitored daily until the blastocyst stage and was plotted in percentage (bars). The number of embryos analysed for each construct is indicated. Non-injected embryos were used as control. Figure shows that FRAP experiments did not affect embryonic development to the blastocyst stage and embryos were morphologically indistinguishable from control embryos.

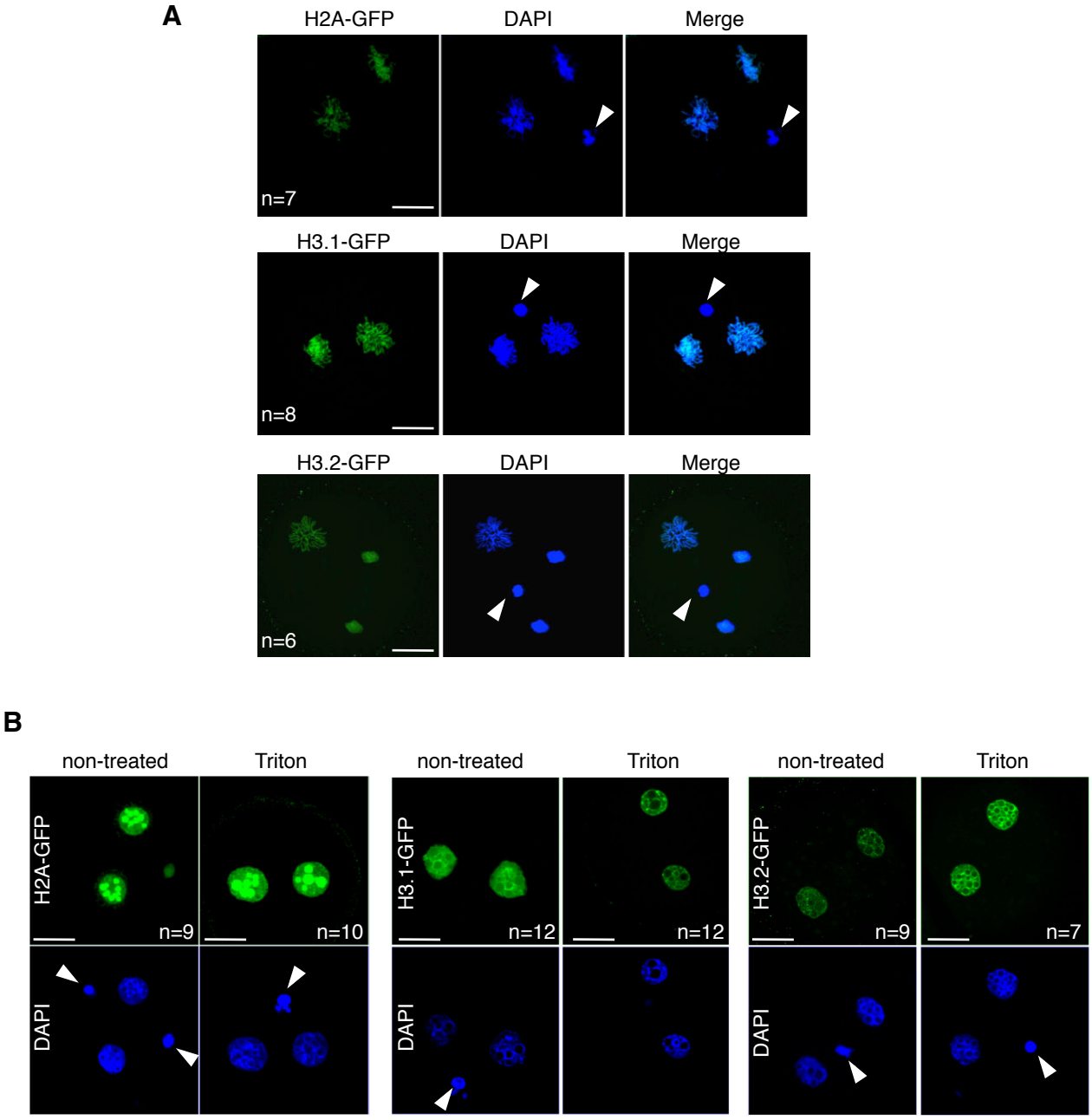


**Supplementary Figure 2.**
GFP-tagged histones are efficiently incorporated into embryonic chromatin.
A. Embryos microinjected with H2A-GFP (top), H3.1-GFP (middle) and H3.2-GFP (bottom) mRNAs were fixed during mitosis from 2-cell to 4-cell stage (~ 48h post-hCG) and the GFP signal was analysed using confocal microscopy. DNA was stained with DAPI upon mounting (blue). Full Z-series projections of images acquired every 1μm are shown. Merge between green and blue chanels shows a clear signal of GFP in mitotic chromatin for the three histones. Polar bodies are indicated by an arrowhead.
B. Two-cell stage embryos expressing H2A-GFP, H3.1-GFP or H3.2-GFP were treated with Triton X-100 for 10 min immediately before fixing at 46 h post-hCG as described in Hajkova et al. (2011). Control non-treated embryos were exposed to the vehicule only. Embryos were then fixed, mounted in Vectashield with DAPI, and images were acquired on an inverted confocal microscope. Full Z-series projections of confocal sections of 2-cell embryos taken every 1 μm are shown. Note that there is no significant difference in GFP signal in the nucleoplasm in Triton-treated versus control embryos. DNA was stained with DAPI (blue). Where visible, polar bodies are indicated by an arrowhead.
The number of embryos analysed for each condition (n) is indicated on the corresponding panel. Note that H3.3-GFP incorporation occurs efficiently under identical experimental conditions (Santenard et al., 2010). Scale bar is 25 μm.

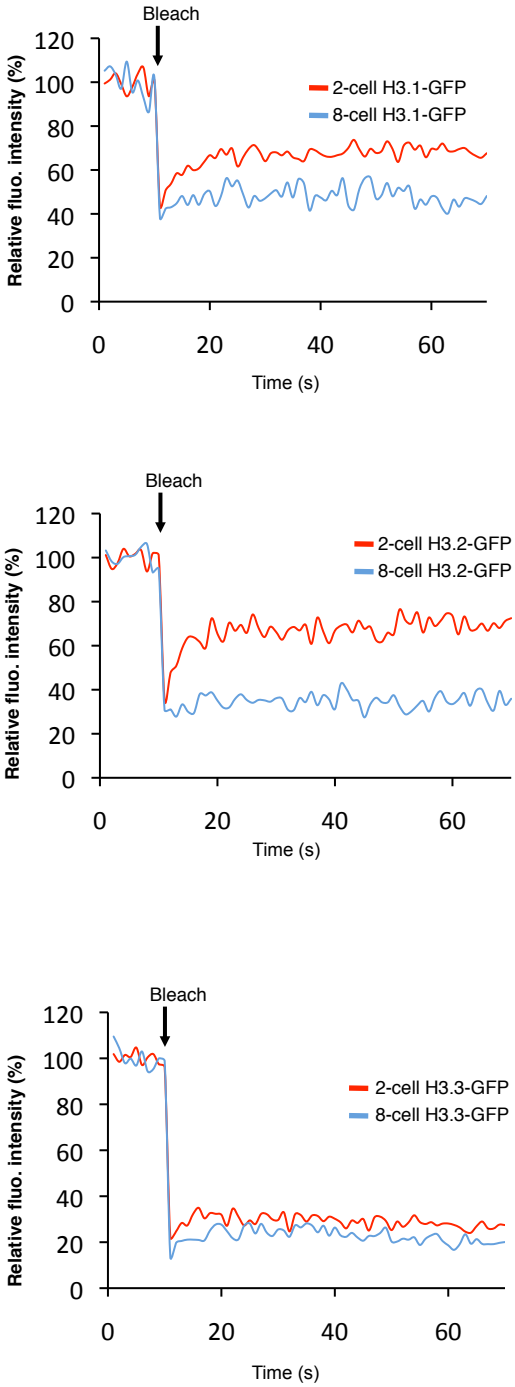


**Supplementary Figure 3.**
Representative FRAP raw data curves from a single nucleus at indicated developmental stage with bleach depth and recovery for H3.1-GFP, H3.2-GFP and H3.3-GFP. Experimental conditions were as in Figure 1 and 2.

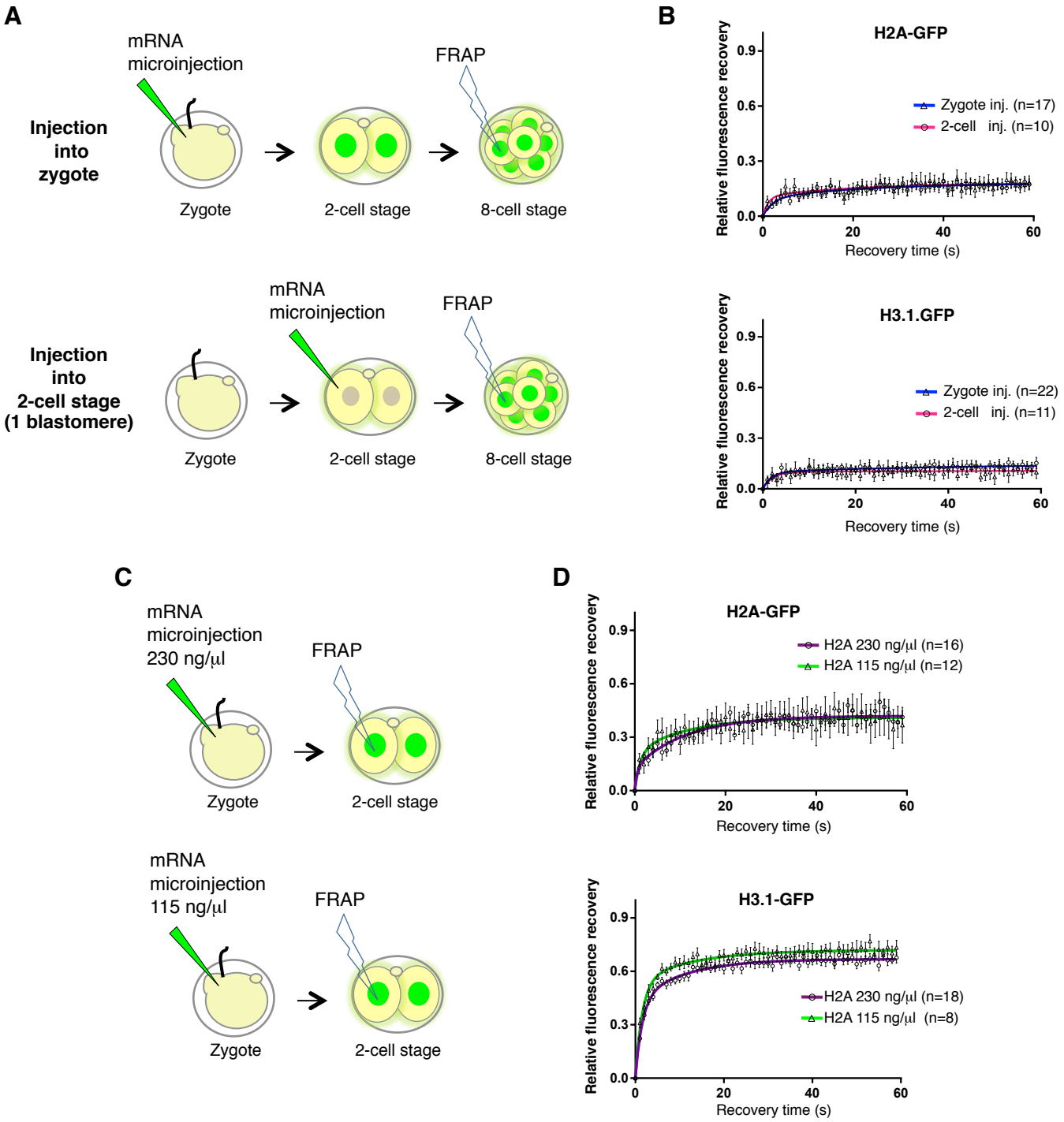


**Supplementary Figure 4.**

Histone mobility in the early embryo is independent of protein amount.

A. Schematic experimental setup to investigate if histone-GFP recovery rates are dependent on protein concentrations. In the first series of experiments, mRNAs coding for H2A-GFP or H3.1-GFP were microinjected at fertilization cone stage, as in Figure 1 at 230 ng/µl. Additionally, mRNA at same concentration was microinjected into 1 blastomere at the late 2-cell stage (~46 h post-hCG), 2 replication cycles later than in the the first series of experiments. n indicates the number of nuclei analysed for each condition.

B. FRAP curves for H2A-GFP and H3.1-GFP at the 8-cell stage were obtained for both conditions using identical parameters. For both histones tested, we observed no significant difference in recovery kinetics and mobility between the two experimental conditions, indicating that histone-GFP mobility is a stage-dependent property.

C. Zygotes were microinjected with 230 ng/µl of H2A-GFP and H3.1-GFP mRNA or with half of the mRNA concentration (115 ng/µl) at the fertilisation cone stage as in Figure 1 and FRAP was conducted at the 2-cell stage.

D. Under both mRNA concentrations, H2A- and H3.1-GFP showed virtually identical FRAP curves at the 2-cell stage. This finding strongly suggests that histone mobility does not depend on protein amounts, but is instead an intrinsic feature of the embryonic stage analysed. n indicates the number of nuclei analysed for each condition.

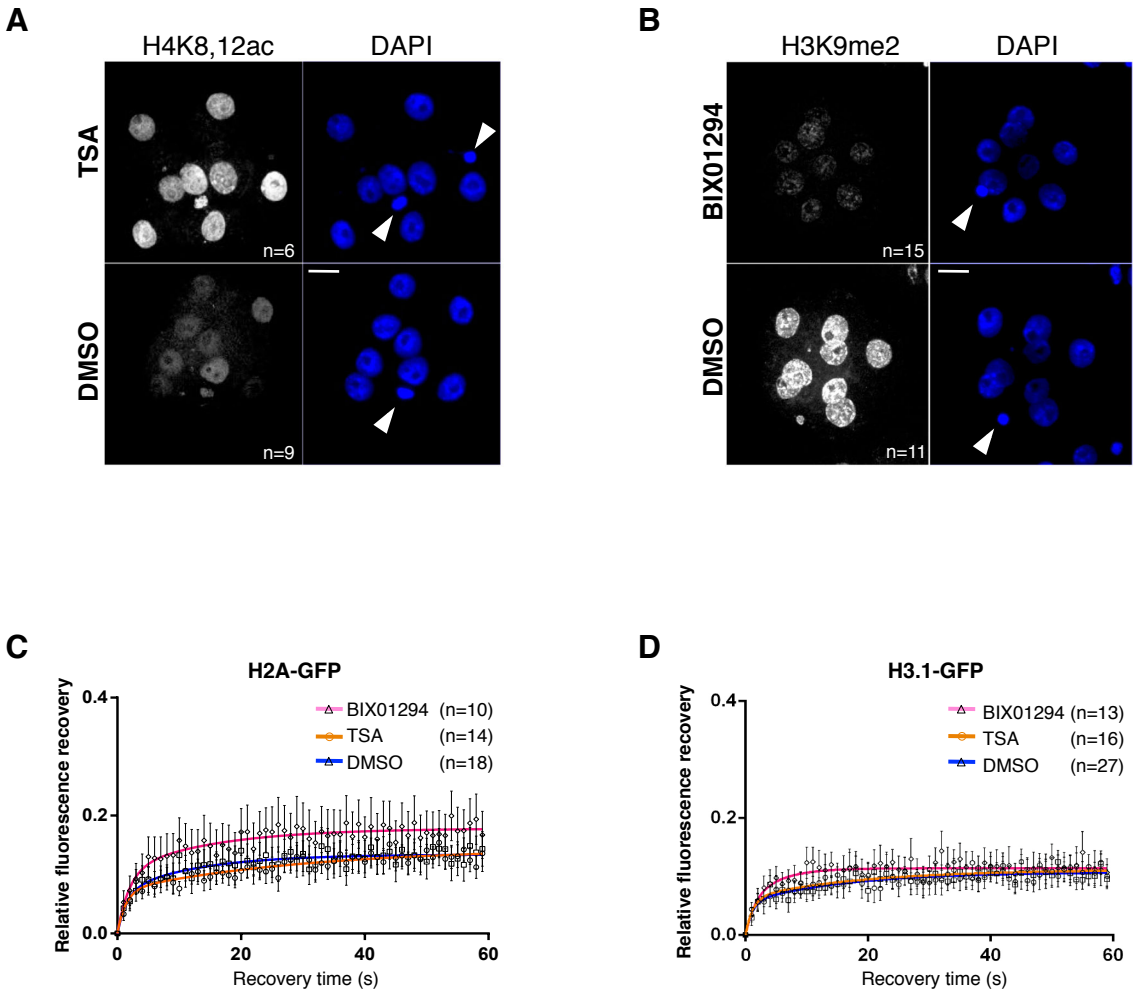


**Supplementary Figure 5.**

Effect of chemical inhibitors of histone modifying enzymes on chromatin mobility.

A-B. Embryos were microinjected at the fertilization cone stage as depicted in Fig. 1A and cultured until the 8-cell stage. Eight-cell stage embryos were treated with 100 nM TSA (A) or 4.1 uM BIX-01294 (B). Embryos were then either analyzed by immunofluorescence (A,B) or by FRAP (C, D). After fixation, TSA-treated embryos were stained with an H4K8,12ac antibody (A) and BIX-01294-treated embryos were stained against H3K9me2 (B). Control embryos were treated with the vehicule (DMSO). Images from representative control and treated embryos acquired at the same time under identical microscope settings are shown. Scale bar is 15 μm; the arrowheads indicate the polar body in the DAPI channel.

C. H2A-GFP mobility in 8-cell stage TSA-treated (orange line), BIX-01294-treated (pink) or control (blue) embryos. FRAP curves calculated as described in Supplementary Methods and double normalized are shown with mean ± S.E. of the indicated amount of embryos analyzed per group.

D. H3.1-GFP mobility in 8-cell stage TSA-treated (orange line), BIX-01294-treated (pink) or control (blue) embryos. FRAP curves calculated as described in Supplementary Methods and double normalized are shown with mean ± S.E. of the indicated amount of embryos analyzed per group.

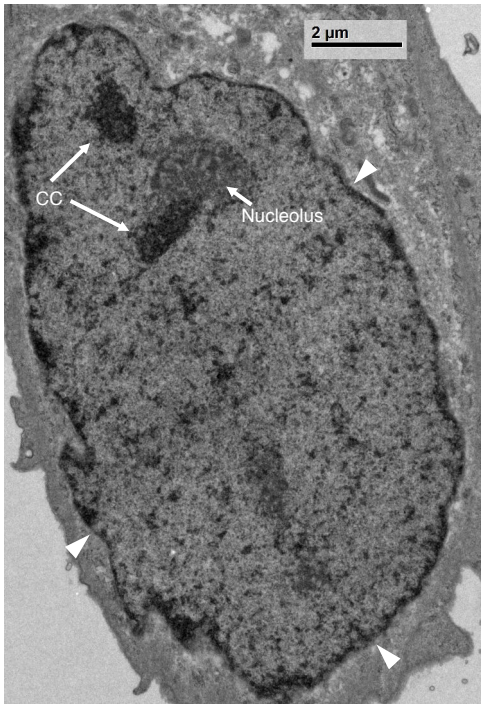


**Supplementary Figure 6.**
Micrograph obtained by tranmission electron microscopy of fibroblast performed in identical conditions and at the same time as in 2- and 8-cell stage embryos. Primary MEFs cultured in DMEM 1g/ml + 10% FCS + gentamycin were fixed and treated with the same solutions as embryos (as described). A representative nuclear section of n > 40 is shown. Arrows point to chromocentres (CC) formed from highly compacted heterochromatin regions and the nucleolus. Arrowheads point to the nuclear membrane.

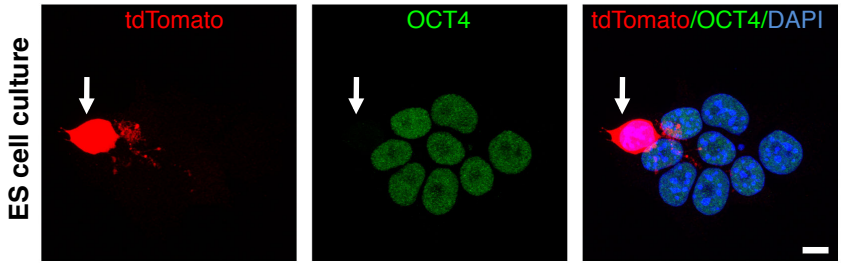


**Supplementary Figure 7.**
Characterisation of 2-cell (2C)-like ES cells. ES cells were stably transfected with the 2C::tdTomato plasmid. Shown are representative confocal images of ES cells processed for immunostaining with OCT4. The expression of tdTomato, indicative of 2C-like ES cells, corresponds with OCT4-negative cells (arrow). Scale bar is 10 μm.

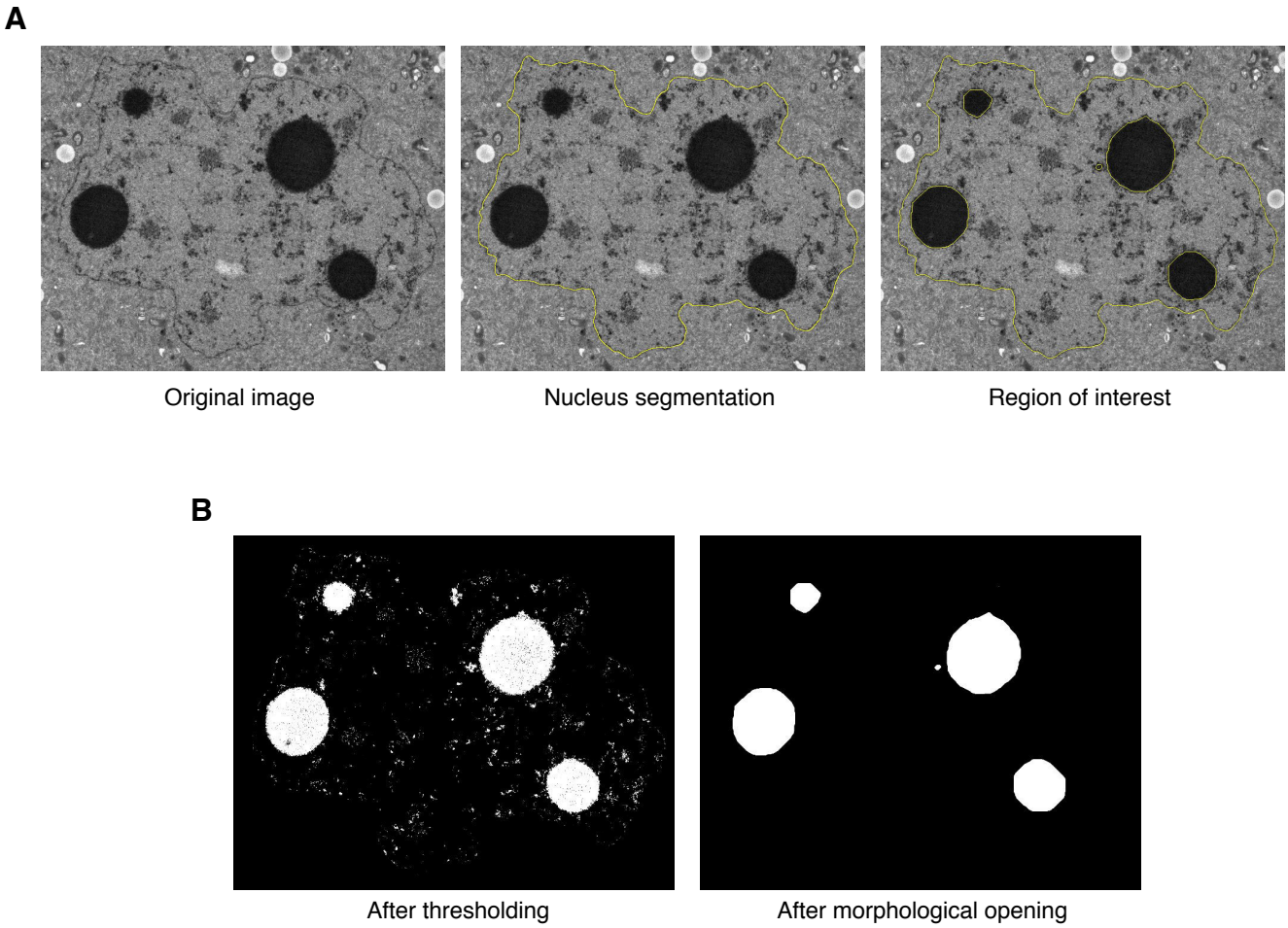


**Supplementary Figure 8.**
Method implemented for the quantification of electron dense regions over the nucleus in transmission electron micrographs.
A. Example for the segmentation of the ROI (nucleus – nucleolar-like bodies) of a section of a 2-cell stage nucleus. The left panel shows the original image. The middle panel shows the resulting segmentation of the nuclear membrane in yellow and the right panel shows the resulting ROI after extraction of the NLB area (surrounded by a yellow line).
B. The procedure used for segmentation of the NLBs is shown as an example before (left) and after thresholding and morphological opening (right). The nucleoli are assumed to be large electron-dense (ED) regions with smooth edges. Thus, after thresholding, the remaining small parts can be removed by using a morphological opening.

## Supplementary Materials and Methods

### Embryo collection and microinjection

Zygotes and 2-cell stage embryos were collected at 17-18 h post-hCG and 46 h post-hCG injection, respectively, from F1 (C57BL/6 × CBA/H) crosses on superovulation. Human H3.1(Santenard et al. 2010; aa 1 to 135), H3.2 (aa 1 to 135), H3.3 (Santenard et al. 2010), and H2A (HIST1H2AK) cDNAs were subcloned into pRN3P plasmid and corresponding mRNAs were transcribed in vitro, as described previously (Santenard et al. 2010). The H3.2 plasmid was generated by mutating the H3.1 construct. 1-2 pl of corresponding mRNAs at 230 ng/μl were microinjected. Embryos were then cultured in KSOM medium at 37ºC and 5% $CO_2$ until appropriate stage and were subject to FRAP analysis. Embryos were subsequently placed back in the incubator, allowed to develop to the blastocyst stage and developmental progression was scored on the 3$^{rd}$ day. All fusions were cloned with EGFP in C-terminal and all plasmids have identical 3' and 5'UTRs. For the FRAP analysis in blastocysts, the levels of GFP in the blastocyst were too noisy when microinjection was performed in the zygote. Thus, to overcome this limitation, both blastomeres of 2-cell stage embryos, collected at 45 hphCG, were injected with identical concentrations of mRNA. We previously determined that recovery rates are independent of protein levels (see Supplementary Figure S3). For the CARM1 double microinjection experiments, zygotes were injected with appropriate mRNAs 18 h post-hCG and cultured until the late 2-cell stage (46 h post-hCG), at which point one of the blastomeres was injected with HA.CARM1 mRNA (0.8 μg/μL) with mRFP mRNA as tracer (Torres-Padilla et al. 2007). Embryos were cultured until the 8-cell stage and double-positive embryos were subject to FRAP. In each embryo, one H3.1-GFP+/RFP- and one H3.1-GFP+/RFP+ blastomere was analysed. We have checked that the presence of RFP does not influence the GFP recovery curves (not shown). To verify the incorporation of histones into chromatin, zygotes were injected with H3.1, H3.2 and H2A-GFP mRNAs, as described and embryos were fixed in mitosis (48-50 h post-hCG). Fixed embryos were mounted in Vectashield (Vector Laboratories) containing 4'-6-Diamidino-2-phenylindole (DAPI) for visualizing DNA. Furthermore, H2A, H3.1 and H3.2-positive 2-cell stage embryos were subject to Triton pre-extraction, as described (Hajkova et al. 2010), fixed, mounted, and GFP signal was analysed by confocal microscopy. Note that it is known that the inside of the NLBs tends to accumulate non-incorporated histones or

overexpressed proteins. Therefore, we systematically avoided the NLBs during our FRAP experiments.

**Immunostaining**

ES cells were fixed with 4% paraformaldehyde in PBS for 20 min at room temperature. After washing with PBS, cells were permeabilized with 0.5% TritonX-100 in PBS for 10 min and then incubated in blocking solution (0.2% BSA in PBS) for 30 min. Primary antibody used was Oct4 (611202, BD Phamingen). After incubation in blocking solution containing primary antibody for 1 hour, cells were washed three times with 0.01% TritonX-100 in PBS for 5 min each and then incubated in blocking solution containing secondary antibody labeled with Cy3 (Jackson lmmunoResearch Laboratory). After washing with PBS, mounting was done in Vectashield (Vector Labs).

**Microscopy**

All experiments were performed using a Leica SP2 confocal microscope and at 37ºC using a 63.0 x 1.4 oil objective. For FRAP, embryos were placed in drops of M2 medium on a glass bottom dish. A rectangular region of interest of 2.28 $\mu m^2$ was chosen randomly within a nucleus avoiding the nucleolar-like bodies and the surrounding heterochromatin regions and was subject to FRAP. Ten prebleach frames were acquired followed by 2 bleach pulses without acquisition. Recovery of fluorescence was followed during 60 seconds, with 1 frame/second. The raw data was processed with Fiji software (ImageJ). All analysis was done on background-subtracted values, using EasyFRAP software (Rapsomaniki et al. 2012). Briefly, the signal of the bleached region was normalised to its prebleach value, which was set to 1. The fluorescence intensity of the whole nucleus at each timepoint was used to correct the decrease in signal intensity in the ROI during the imaging process. The obtained curves were normalized using the Full-scale normalization method so that the first postbleach frame was set to zero. Normalized curves were then subject to curve fitting. For fixed samples, confocal microscopy was performed using a 63x oil objective on Leica SP2 AOBS MP inverted microscope. Z-sections were taken every 1 μm.

**Curve fitting and statistical analysis**

Experimentally obtained and normalized recovery curves were fit using Prism6 software (GraphPad Software). Two-phase exponential association equation (Y=Ymax1*(1-e(-K1*X)) + Ymax2*(1-e(-K2*X)) was used to obtain mobile fractions and reaction rates, as this has been previously described to be appropriate for nuclear proteins (Phair and Misteli 2000). Accordingly, throughout the manuscript, Ymax1 values are used for mobile fraction estimation, as they reflect the steady-state protein pool, unless otherwise stated. However, all the Ymax1 and Ymax2 and their statistical comparisons are shown in the Supplementary Information. All the fit data are presented as mean ± S.E.M. Statistical analysis on mobile fractions between different stages was performed using and QuickCalcs software (GraphPad Software). Unpaired t-test was used for comparing two groups.

**Inhibitor treatment**

To address if histone mobility is regulated trough the action of the G9a histone methyltransferase or through histone acetylation, zygotes were collected as detailed above, microinjected with H2A-GFP or H3.1-GFP mRNA and allowed to develop till the 8-cell stage. Embryos were then treated with TSA (100 nM) for 2 hours to inhibit HDAC activity (Ma et al. 2001; Maalouf et al. 2009) or BIX-01294 (4.1 mM) for 4 hours to inhibit G9a (Kubicek et al. 2007), after which they were subject to FRAP as above. Control embryos were treated with vehicule (DMSO) and subject to FRAP under identical conditions in parallel. After FRAP analysis, embryos were fixed as described (Torres-Padilla et al. 2006) and the effect of inhibitors was verified by immunostaining. Antibodies used were: anti-H4K8,12ac (kindly provided by M. Oulad-Abdelghani, IGBMC) and anti-H3K9me2 (Upstate 07-441), at 1:200 dilution.

**Electron microscopy**

Embryos at the 2-cell (n=3) and 8-cell (n=3) stages were collected after natural matings of B6CBAF1/J mice. Embryos were fixed in 2% formaldehyde + 2,5% glutaraldehyde in 0.1M cacodylate buffer for 2h at 37°C, postfixed 1h at 4°C in 1% osmium tetroxide and *en bloc* stained with 1% uranyl acetate for 1h at 4°C. Samples were then dehydrated in graded ethanol solutions (50%, 70%, 90%, 100%) to be then infiltrated with epoxy resin by a graded series of dilutions (30%, 70%, 100%). Due to the size of the embryos, they were flat embedded in a

sandwich of Aclar (200$\mu$m) in order to be observed using binoculars. Ultrathin sections (70 nm) were performed using an ultracut UCT ultramicrotome (Leica Microsystems, Vienna, Austria) and mounted on pioloform coated slot grids to avoid crossing mesh in the nucleus. They were then stained for 20 minutes with uranyl acetate and 5 minutes with lead citrate and observed with a transmission electron microscope (CM12, Philips; FEI Electron Optics, Eindhoven, the Netherlands) operated at 80kV. Images were acquired using an Orius 1000 ccd camera (Gatan, Pleasanton, CA). MEFs (DMEM 1g/ml + 10% FCS + gentamycin) were fixed and treated as described above (n>40).

**Quantification of electron dense regions from TEM micrographs.**

The evolution of heterochromatin compaction between 2-cell and 8-cell embryos was quantified by comparing the relative areas of electron-dense (ED) regions in transmission electron microscopy (TEM) images inside the nucleus. Assuming the separability of ED and non-ED regions into two classes, these regions can be classified by thresholding methods. To ensure a proper classification, the illumination bias of TEM images was corrected using an automatic method based on intensity gradients and a bivariate polynomial modeling (Tasdizen et al. 2008) prior to the classification procedure. To define a proper region of interest (ROI) corresponding to the nucleus without the nucleolus or the nucleolar-like bodies (Supplementary Figure S8a) the classification task was performed using three steps. First, the boundaries of the nucleus were estimated. Because the homogeneity of the intensities inside and outside the nucleus and the poor boundary definition precluded the use of an automatic method, this step was done manually. Secondly, the area occupied by the nucleolus was removed based on two observations i) the nucleoli are large ED regions in TEM images with relatively smooth edges (in contrast with heterochromatin) and ii) the nucleoli are separable from the background of the nucleus (the histogram is bimodal). These two parameters allowed the automatic segmentation of the nucleoli based on a minimum thresholding (Prewitt and Mendelsohn 1966) followed by a morphological opening in order to remove remaining small ED regions (Supplementary Figure S8b). Finally, the third step was to classify ED/non-ED regions from the ROI defined by the nucleus minus the nucleoli using the isodata thresholding method (Ridler and Calvard 1978), which resulted in the segmentation of ED and non-ED regions (Mask, Figure 4b). Subsequently, the proportion of ED area over the whole ROI area was computed as a percentage. The whole procedure was

implemented as a macro of ImageJ. The thresholding methods and the morphological opening used in the experiments are the ImageJ implementation. The minimum and isodata thresholding procedures correspond to *Minimum* and *Default* methods of *Auto global thresholding* menu. The illumination bias correction has been implemented as a plugin of ImageJ.

**ES cell culture and generation of 2C::tdTomato MuERVL reporter cell line**

Mouse E14 ES cell line was cultured without feeders on gelatin-coated glass-bottom dishes (MatTek) in DMEM with GlutaMax (Invitrogen) containing 15% FCS, LIF, non essential aminoacids, penicillin/streptomycine, and 0.1 mM 2-mercaptoethanol supplemented with 3 $\mu$M CHIR9901 and 1 $\mu$M PD0325901. The 2C::tdTomato plasmid (addgene) (Macfarlan et al. 2012) was transfected into E14 ES cells by Lipofectamine 2000 and cells were selected with 200µg/mL hygromycin. After selection, several colonies were picked and the clones in which tdTomato was expressed in a small proportion of cells (Macfarlan et al. 2012) were chosen for further experiments. For FRAP experiments, cells were transiently transfected with H3.1-GFP or H2A-GFP plamids using Lipofectamine 2000 (Invitrogen) according to manufacturer's instructions. The H3.1-EGFP plasmid was constructed by inserting the human H3.1 cDNA (Santenard et al. 2010) into the pEGFP-N2 plasmid (Clonetech). FRAP was performed 24 h after transfection on tdTomato+/GFP+ as well as control (tdTomato-/GFP+) cells.

## References for Supplementary Methods and Figures


Hajkova P, Jeffries SJ, Lee C, Miller N, Jackson SP, Surani MA. 2010. Genome-wide reprogramming in the mouse germ line entails the base excision repair pathway. *Science* **329**: 78-82.

Kubicek S, O'Sullivan RJ, August EM, Hickey ER, Zhang Q, Teodoro ML, Rea S, Mechtler K, Kowalski JA, Homon CA, Kelly TA, Jenuwein T. 2007. Reversal of H3K9me2 by a small-molecule inhibitor for the G9a histone methyltransferase. Mol Cell **25(3)**:473-81.

Ma J, Svoboda P, Schultz RM, Stein P. 2001. Regulation of Zygotic Gene Activation in the Preimplantation Mouse Embryo: Global Activation and Repression of Gene Expression. Biol Reprod **64:** 1713-1721

Maalouf WE, Liu Z, Brochard V, Renard JP, Debey P, Beaujean N, Zink D. 2009. Trichostatin A treatment of cloned mouse embryos improves constitutive heterochromatin remodeling as well as developmental potential to term. BMC Dev Biol. **11:**9-11.

Macfarlan TS, Gifford WD, Driscoll S, Lettieri K, Rowe HM, Bonanomi D, Firth A, Singer O, Trono D, Pfaff SL. 2012. Embryonic stem cell potency fluctuates with endogenous retrovirus activity. *Nature* **487**: 57-63.

Phair RD, Misteli T. 2000. High mobility of proteins in the mammalian cell nucleus. *Nature* **404**: 604-609.

Prewitt JM, Mendelsohn ML. 1966. The analysis of cell images. *Ann N Y Acad Sci* **128**: 1035-1053.

Rapsomaniki MA, Kotsantis P, Symeonidou IE, Giakoumakis NN, Taraviras S, Lygerou Z. 2012. easyFRAP: an interactive, easy-to-use tool for qualitative and quantitative analysis of FRAP data. *Bioinformatics* **28**: 1800-1801.

Ridler TW, Calvard S. 1978. Picture thresholding using an iterative selection method. in *IEEE Transactions on Systems, Man and Cybernetics* (ed. IEEE), pp. 630-632.

Santenard A, Ziegler-Birling C, Koch M, Tora L, Bannister AJ, Torres-Padilla ME. 2010. Heterochromatin formation in the mouse embryo requires critical residues of the histone variant H3.3. *Nat Cell Biol* **12**: 853-862.

Tasdizen T, Jurrus E, Whitaker RT. 2008. Non-uniform illumination correction in transmission electron microscopy. in *MICCAI Workshop on Microscopy Image Analysis with Applications in Biology*, pp. 5-6.

Torres-Padilla ME, Parfitt DE, Kouzarides T, Zernicka-Goetz M. 2007. Histone arginine methylation regulates pluripotency in the early mouse embryo. *Nature* **445**: 214-218.

**Supplementary Table S1. Estimated mobile fractions for histones-GFP at the 2-cell and 8-cell stage**
Mobile fractions (Ymax1 values) are displayed in percentage and are the average ± S.E. of the indicated number of nuclei analysed. For reference, the Ymax2 value is also shown.

| | 2-cell | 8-cell |
|---|---|---|
| **H2A-GFP** | 29.36 ± 3.24<br>n=18<br>*(Ymax2= 12.62 ± 2.9)* | 8.33 ± 2.9<br>n=19<br>*(Ymax2= 9.58 ± 4.1)* |
| **H3.1-GFP** | 23.7± 4.97<br>n=20<br>*(Ymax2= 43.18 ± 5.33)* | 4.98 ± 4.81<br>n=23<br>*(Ymax2= 9.95 ± 2.15)* |
| **H3.2-GFP** | 25.19 ± 4.29<br>n=17<br>*(Ymax2= 38.97 ± 4.75)* | 4.99 ± 0.9<br>n=17<br>*(Ymax2= 3.36 ± 1.2)* |
| **H3.3-GFP** | 10.16 ± 7.88<br>n=18<br>*(Ymax2= 13.59 ± 2.5)* | 5.84 ± 2.03<br>n=17<br>*(Ymax2= 9.48 ± 2.27)* |

**Supplementary Table S2. Recovery Kinetics (K values) of GFP-tagged histones during early embryogenesis**

| K values | 2-cell | 8-cell | ICM | TE |
|---|---|---|---|---|
| **H2A-GFP** | Fast: 1.93±2.1<br>Slow: 0.09± 0.01 | Fast: 0.45 ± 0.17<br>Slow: 0.08 ± 0.02 | n/d | n/d |
| **H3.1-GFP** | Fast: 0.65 ± 0.08<br>Slow: 0.09 ± 0.01 | Fast: 0.55 ± 0.14<br>Slow: 0.02 ± 0.02 | Fast: 1.61 ±1.5<br>Slow: 0.005±0.01 | 0.0007 ± 2.04e-05 |
| **H3.2-GFP** | Fast: 0.63 ± 0.08<br>Slow: 0.08 ± 0.01 | Fast: 0.97 ± 1.12<br>Slow: 0.04 ± 0.02 | n/d | n/d |
| **H3.3-GFP** | Fast: 0.45 ± 0.13<br>Slow: 0.02 ± 0.02 | Fast: 0.54 ± 0.15<br>Slow: 0.03 ± 0.02 | n/d | n/d |

*n/d: not determined.
**Recovery curves for the indicated GFP-fused histones were fit into a two-phase exponential association equation (Y=Ymax1*(1-exp(-K1*X)) + Ymax2*(1-exp(-K2*X)) to calculate reaction rates (K values ± SEM). Both slow (K1) and fast (K2) recovery rates (±SEM) are shown. FRAP recovery curves for H3.1-GFP in the TE were fit into a linear equation and the slope (corresponding to the reaction rate) is indicated

**Supplementary Table S3. Statistical comparison between mobility of different histones at the 2-cell and 8-cell stage using unpaired *t*-test (p-values are indicated).**
The mobile fraction analysed refers to the **Ymax1**

| | H2A-GFP 2-cell | H2A-GFP 8-cell | H3.1-GFP 2-cell | H3.1-GFP 8-cell | H3.2-GFP 2-cell | H3.2-GFP 8-cell | H3.3-GFP 2-cell | H3.3-GFP 8-cell |
|---|---|---|---|---|---|---|---|---|
| **H2A-GFP 2-cell** | | p<0.0001 | p=0.337 | p=0.0003 | p=0.44 | p<0.0001 | p=0.027 | p<0.0001 |
| **H2A-GFP 8-cell** | p<0.0001 | | p=0.0154 | p=0.599 | p=0.0027 | p=0.279 | p=0.828 | p= 0.486 |
| **H3.1-GFP 2-cell** | p=0.337 | p=0.0154 | | p=0.0101 | p=0.82 | p=0.0016 | p=0.143 | p=0.0036 |
| **H3.1-GFP 8-cell** | p=0.0003 | p=0.599 | p=0.0101 | | p=0.0043 | p=0.998 | p=0.5584 | p= 0.884 |
| **H3.2-GFP 2-cell** | p=0.44 | p=0.0027 | p=0.82 | p=0.0043 | | p<0.0001 | p=0.1036 | p=0.0003 |
| **H3.2-GFP 8-cell** | p<0.0001 | p=0.279 | p=0.0016 | p=0.998 | p<0.0001 | | p=0.519 | p= 0.704 |
| **H3.3-GFP 2-cell** | p=0.027 | p=0.828 | p=0.143 | p=0.5584 | p=0.0036 | p=0.519 | | p=0.599 |
| **H3.3-GFP 8-cell** | p<0.0001 | p= 0.486 | p=0.0036 | p=0.884 | p=0.0003 | p= 0.704 | p=0.599 | |

**Supplementary Table S4. Statistical comparison between mobility of different histones at the 2-cell and 8-cell stage using unpaired *t*-test (p-values are indicated).**
The mobile fraction analysed refers to the **Ymax2**

| | H2A-GFP 2-cell | H2A-GFP 8-cell | H3.1-GFP 2-cell | H3.1-GFP 8-cell | H3.2-GFP 2-cell | H3.2-GFP 8-cell | H3.3-GFP 2-cell | H3.3-GFP 8-cell |
|---|---|---|---|---|---|---|---|---|
| **H2A-GFP 2-cell** | | p=0.545 | p<0.0001 | p=0.454 | p<0.0001 | p=0.0068 | p=0.802 | p=0.403 |
| **H2A-GFP 8-cell** | p=0.545 | | p<0.0001 | p=0.932 | p<0.0001 | p=0.151 | p=0.409 | p= 0.983 |
| **H3.1-GFP 2-cell** | p<0.0001 | p<0.0001 | | p<0.0001 | p=0.565 | p<0.0001 | p<0.0001 | p<0.0001 |
| **H3.1-GFP 8-cell** | p=0.454 | p=0.932 | p<0.0001 | | p<0.0001 | p=0.019 | p= 0.276 | p= 0.883 |
| **H3.2-GFP 2-cell** | p<0.0001 | p<0.0001 | p=0.565 | p<0.0001 | | p<0.0001 | p<0.0001 | p<0.0001 |
| **H3.2-GFP 8-cell** | p=0.0068 | p=0.151 | p<0.0001 | p=0.019 | p<0.0001 | | p=0.0008 | p= 0.023 |
| **H3.3-GFP 2-cell** | p=0.802 | p=0.409 | p<0.0001 | p=0.276 | p<0.0001 | p=0.0008 | | p=0.232 |
| **H3.3-GFP 8-cell** | p=0.403 | p= 0.983 | p<0.0001 | p=0.884 | p<0.0001 | p= 0.023 | p=0.232 | |

**Supplementary Table S5. Estimated mobile fractions for H3.1-GFP and H2A-GFP at the 8-cell stage after treatment with TSA and BIX-01294**

Mobile fractions of fast (F) and slow (S) recovery phases (Ymax2 and Ymax1 values, respectively) and the corresponding K1 and K2 values are displayed in percentage and are the average ± S.E. of the indicated number of nuclei analysed.

| | **8-cell DMSO** | **8-cell TSA** | **8-cell BIX01294** |
|---|---|---|---|
| **H2A-GFP** | 6.5 ± 1.6<br>n=18<br>*(Ymax2= 6.9 ± 1.7)* | 7.29 ± 0.8<br>n=14<br>*(Ymax2= 7.26 ± 0.8)* | 7.4 ± 1.7<br>n=10<br>*(Ymax2= 10.4 ± 2)* |
| **H3.1-GFP** | 5.0± 0.71<br>n=27<br>*(Ymax2= 5.8 ± 0.88)* | 4.8 ± 0.7<br>n=16<br>*(Ymax2= 6.3 ± 1.03)* | 6.14 ± 9.7<br>n=13<br>*(Ymax2= 5.2 ± 9.7)* |
| **H2A-GFP** | K1=0.08 ± 0.03<br>K2=0.66 ± 0.31<br>n=18 | K1=0.03 ± 0.01<br>K2=0.73 ± 0.23<br>n=14 | K1=0.06 ± 0.02<br>K2=0.52 ± 0.16<br>n=10 |
| **H3.1-GFP** | K1=0.06 ± 0.01<br>K2=0.87 ± 0.35<br>n=27 | K1=0.05 ± 0.02<br>K2=0.83 ± 0.36<br>n=16 | K1=0.21 ± 0.19<br>K2=0.71 ± 1.08<br>n=13 |

**Supplementary Table S6. Estimated mobile fractions for H3.1-GFP at the 8-cell stage after lineage allocation upon CARM1 expression.**

Mobile fractions of fast (F) and slow (S) recovery phases (Ymax2 and Ymax1 values, respectively) are displayed in percentage and are the average ± S.E. of the indicated number of nuclei analysed.

| | **CARM1+** | **CARM1-** | **CARM1 CD+** |
|---|---|---|---|
| **H3.1-GFP** | (F) 14.43 ± 3.3<br>(S) 7.36 ± 2.9<br>n=20 | (F) 7.7 ± 2.2<br>(S) 5.44 ± 1.7<br>n=19 | (F) 7.68 ± 1.68<br>(S) 4.20 ± 1.78<br>n=16 |

# Discussion and Conclusion

Preimplantation development is the first step in a series of morphogenetic events that occur during the development of a new individual. Two highly differentiated cells, the gametes, give rise to a totipotent cell, the zygote, in which a new developmental program has to be set up. For development to initiate correctly, the chromatin of both gametes has to be remodeled. The chromatin environment and specifically heterochromatin modifications are markers that allow us to study remodeling events in preimplantation embryos.

In the first part of this manuscript, we have used the lack of H4K20 tri-methylation, a marker of constitutive heterochromatin, in the embryo to study the functional relevance of the removal of this mark endogenously. The ectopic expression of SUV4-20h1 and SUV4-20h2 showed different abilities *in vivo* to tri-methylate H4K20. Specifically, SUV4-20h2 had a higher methyl-transferase activity to generate H4K20me3. In preimplantation embryos, *Suv4-20h2* is maternally inherited but quickly degraded and not expressed by the embryo until peri-implantation. Because of the observed lethality in *Suv4-20h2*-injected zygotes, we hypothesize that the endogenous silencing of *Suv4-20h2* is probably required for preimplantation development to proceed normally. A potential future development of this work, which is currently a caveat, is the absence of data on the levels of the endogenous SUV4-20h1 and SUV4-20h2 proteins themselves. Unfortunately, there are no antibodies available for immunostainings to conclude on the absence of the methyl-transferases *in vivo*, but our experiments with exogenously expressed proteins strongly suggest that if these proteins were expressed in the embryo the levels of H4K20me3 would not be undetectable. Similarly, the expression of *Phf-2*, an *in vitro* demethylase of H4K20me3, is similar to the pattern of expression of maternally inherited genes in the embryo. However, PHF-2 is present throughout preimplantation development. Therefore, a knock-down approach of *Phf-2* in the oocyte (prior to fertilization) is necessary to fully establish whether the absence of H4K20me3 is a combinatorial consequence of the lack of *Suv4-20h2* expression and an active demethylation process by PHF-2 or another demethylase.

The effects of the ectopic-expression in mouse embryos contrast with the overexpression of *Xenopus XSuv4-20h1* and *XSuv4-20h2* in *Xenopus laevis* two-cell stage embryos (Nicetto et al. 2013). While the depletion of *XSuv4-20h1* and *XSuv4-20h2*, via morpholino injection, caused

defects in eye and melanophore development, the overexpression of *XSuv4-20h1* and *XSuv4-20h2* did not result in embryonic lethality. In contrast, KO of *Suv4-20h1* and *Suv4-20h2* in mice only caused post-natal lethality and did not affect development (Schotta et al. 2008). It seems that evolutionarily, SUV4-20s are required in *Xenopus laevis* development while being deleterious to preimplantation development in *Mus musculus*. Additionally, mouse and frog SUV4-20 proteins share 88% identity in the SET domain and ectopic expression of both *XSuv4-20h1* or *XSuv4-20h2* resulted in an increase in H4K20me3 and H4K20me2 without any obvious deleterious effect on the cell cycle. This indicates that either the increase in H4K20me3 is interpreted differently or that the readers of this mark are different between these two species since the SUV4-20s are highly conserved. I would be personally curious to test whether XSUV4-20h1 or XSUV4-20h2 would cause the same effects as the murine SUV4-20h2 in mouse preimplantation development. However, we can speculate that the most likely outcome would be embryonic arrest as long as XSUV4-20h1 or XSUV4-20h2 are able to tri-methylate H4K20 in the mouse embryo, since our data show that the preimplantation arrest is dependent on the SUV4-20h2 histone methyl-transferase activity.

Although we tried to study the effects of the ectopic expression of *Suv4-20h1* and *Suv4-20h2* on H4K20me2, we were not able to consistently detect a signal in IF, thus we are not able to rule out a role of H4K20me2 in the SUV4-20H2-induced arrest. However, it seems highly likely that SUV4-20H1 mediates H4K20 dimethylation because of the observed decrease in H4K20me1 and very mild increase in H4K20me3 at the 2-cell stage. If it is confirmed that SUV4-20H1 generates H4K20me2 in the embryo, then this rules out an effect of H4K20me2 on S-phase arrest and development block in *Suv4-20h2*-expressing embryos. Indeed, a previous report has indicated that upon hydroxyurea treatment HCT116 cells exhibited an increase in H4K20me3 levels and a decrease in H4K20me2 upon ATR activation (Hajdu et al. 2011), suggesting that the existence of a link between H4K20me3 levels and the activation of the ATR pathway, which we confirmed. H4K20me3 levels were also shown to increase upon DNA double-stand break (DSB) (Pei et al. 2011). It is not possible to conclude as to how cells are able to interpret the H4K20me3 mark into a signal for either ATR activation or DSB-pathway repair, since both pathways require different machineries. In the embryos, it seems that H4K20me3 activates primarily the ATR pathway, although we still need to verify that the ATM or DNA-PK pathways are not also involved by using

specific inhibitors of both pathway and verifying that they do not also rescue embryonic development.

In *Mus musculus*, the BAH domain of ORC1 can bind to all levels of H4K20 methylation (Kuo et al. 2012), we can hypothesize that perturbation of the levels of H4K20me3 would lead to an defect in origin licensing during the formation of the pre-Replication Complex (pre-RC). If the pre-RC can bind to chromatin regardless of the levels of H4K20me3 and license the origins, it is not known whether the subsequent steps (primase loading, nucleotide incorporation…) of replication can proceed normally. Once the origins are licensed, RPA (Replication protein A) binds to the ssDNA which has been shown to be enough to activate ATR *in vitro*, although *in vivo* ATR is not immediately activated and requires a more potent signal. Such a signal could be a result of multiple origins being initiated at the same time because of interactions between ORC and H4K20me3 leading to an accumulation of RPA at ssDNAs and activation of ATR. Additionally, once the cell senses that the ATR pathway is functional, it can activate dormant origins to catch up and finish replication in a timely manner, this could explain our observation of continuous EdU incorporation during late S-phase in zygote and 2-cell stage embryos, with high levels of H4K20me3 resulting from SUV4-20H2 expression. By using an ATR inhibitor, we were able to partially rescue the developmental phenotype, suggesting that other factors might be involved. Furthermore, it remains to be verified whether ATR inhibition also affects H4K20me3 levels upon treatment.

The global gene expression data obtained by pulsing EU incorporation during EGA, allowed us to conclude that there is a reduction in the percentage of embryos that are actively transcribing upon *Suv4-20h2* expression. However, we are not able to conclude whether this effect on transcription contributes to the embryonic arrest. To this effect, we will need to analyze expression of genes that are necessary for developmental progression at the zygote and 2-cell stage. We can also verify that the activation of the S-phase checkpoint does not lead to a direct effect on transcription, by analyzing embryos that were treated with ATRi and compare their levels of gene expression to untreated embryos in a *Suv4-20h2*-expressing background. It was previously reported that deposition of H4K20me3 through SUV4-20H2 causes RNA Pol II pausing and represses gene

expression in transformed cell lines by blocking H4K16ac (Kapoor-Vazirani, Kagey, and Vertino 2011). Given that we measured a slight decrease, but not a complete loss, of global gene expression, we can conclude that the increased levels of H4K20me3 do not completely block transcription indicating that this increase can be overcome by the transcription machinery in preimplantation embryos. We still need to verify whether H4K16ac is affected in *Suv4-20h2*-embryos to rule out competition between the two marks and to verify that the reduction in global gene expression is not a consequence of a decrease in H4K16ac.

Finally, another remaining unresolved question is what happens to H3K64me3 upon ectopic expression of *Suv4-20h2*. In somatic cells, depletion of both *Suv4-20h1* and *Suv4-20h2* reduces H4K20me3 levels, but not H3K64me3, therefore it was concluded that H3K64me3 levels were independent of H4K20me3. However, embryos expressing *Suv4-20h2*, showed a marked increase in H3K64me3 and H4K20me3. This observation could indicate that the *de novo* establishment of both marks is linked during embryogenesis. Additionally, since H3K64me3 and H4K20me3 exhibit the same dynamics during development this suggests that their levels could be controlled by the same mechanism during preimplantation development. Because of the absence of H3K64me3 in the *Suv4-20h2mut*-injected embryos we can postulate that the concomitant H4K20me3 increase is required for the *de novo* establishment of H3K64me3 in embryos.

The second part of this work focused on facultative heterochromatin and more specifically on H2AK119ub (H2Au) and on members of the non-canonical PRC1 which catalyzes this modification. Our data show that H2Au is present throughout preimplantation development and shows different patterns at the zygote and blastocyst stages. In the zygote, H2Au dynamically changes its levels and localization during the Pronuclear progression. Upon fertilization, H2Au is enriched on both parental chromatin, but becomes reduced and mainly localized on the maternal chromatin by PN5. These dynamics suggests that H2A ubiquitylation might be important upon protamine exchange after fertilization and is lost during nuclear reprogramming of the paternal chromatin. The loss of the modification seems to take place mainly on the parental chromatin, but it is not known if it is due to histone exchange or active de-ubiquitylation. We did not detect an asymmetric localization of H2Au at the 2-cell stage, showing that the asymmetry is unique to the

zygote stage and suggesting that facultative heterochromatin on the parental chromatin has established similar signatures by 2-cell stage. At the blastocyst stage, H2Au showed a foci enrichment in trophectodermal (TE) lineage in half of the observed embryos correlating with the percentage of female blastocysts and X inactivation in TE lineage. Interestingly, none of the studied ncPRC1 proteins (detailed below) showed a similar enrichment pattern at the blastocyst stage, indicating that these proteins might not be involved in the recruitment of PRC1 to X inactivation sites at the blastocyst stage and suggesting that non-canonical and canonical members of PRC1 are not key players in this silencing.

The canonical PRC1 complex has been studied during preimplantation development and previous reports have shown that CBX2 was the main partner of RING1B, the catalytic member of PRC1 (Puschendorf et al. 2008). However, KD of *Ring1a/Ring1b* led to a 2-cell stage block, whereas *Cbx2* KO was not lethal. This has led us to wonder if the members of the non-canonical PRC1, which have not been studied during preimplantation development, play a role in the recruitment and regulation of PRC1 after fertilization. Thus, we observed that RYBP and its homologue YAF-2 associate with RING1, have different patterning during preimplantation development and might play different roles. RYBP was highly detected after the 4-cell stages, while YAF-2 was highly present before the 2-cell stage. Double knock-out of *Rybp* and *Yaf2* in ES cells showed no synergistic effects which suggested potential independent functions (Hisada et al. 2012), if this is the case we could assume that it is exemplified by the exclusion in the levels of both proteins during preimplantation development. If they have different functions and both compete for access to bind to the finite amount of RING1 available, then this could be a mechanism to control which protein associates with RING1 and thus controls the downstream targeting of ncPRC1. Conditional KO of *Rybp* in ES cells leads to derepression of retro-elements which are known to be expressed at the 2-cell stage. Correspondingly, the levels of RYBP were very low at the 2-cell stage during the expression of these retro- elements. The levels of RYBP increased at the 4-cell stage while expression of retro- elements is known to become reduced. This observation suggests the existence of window of opportunity at the 2-cell stage for the expression of retro-elements while RYBP is not present. To verify whether RYBP is involved in the silencing of retro-elements, we suggest either a KD of *Rybp* in the embryos to prolong the expression of these

elements or an ectopic expression in the zygote and at the 2-cell stage that could lead to the silencing of the retro-elements.

L3MBTL2, which is in complex with RYBP/YAF-2 and RING1, was detected throughout preimplantation development, while L3MBTL1, one of its homologues, formed foci at the morula stage, just before formation of H2AK119ub foci at X-inactivation sites in the blastocyst. It was shown that both L3MBTL2 and L3MBTL1 could compact chromatin *in vitro*. However, it is known (others and our EM data) that the embryonic chromatin structure is atypical and lacks chromatin compaction at the zygote and 2-cell stage. This leads us to postulate that both proteins are not able to compact chromatin in the early steps of preimplantation development although all the members of the ncPRC1 are present at these stages. Therefore, their pattern of expression suggests other potential functions during preimplantation development that can be validated through KD approaches to determine their contribution to facultative heterochromatin *de novo* establishment in preimplantation development.

The third and final chapter of this work involved studying the global pattern of embryonic chromatin ultrastructure. Transmission electron microscopy (TEM) has been used to visualize chromatin structure in somatic cells, and electron density has been applied to gauge chromatin compaction. Because of the previously described changes to the chromatin landscape that is observed in preimplantation embryos, we used TEM to study the state of endogenous chromatin compaction in the embryos. Electron density increased significantly between the 2- and 8-cell stages and correlated with a reduction in histone dynamics and nuclear reorganization. Thus, this method can be used to gauge the state chromatin compaction. This method will be further applied to test whether heterochromatin modifications correlate to chromatin compaction *in vivo* and whether chromatin modifiers can affect chromatin compaction *in vivo*. We can also use this method to study the differences in chromatin landscape between the paternal and maternal chromatin at the zygote stage. Although we successfully measured chromatin compaction and histone dynamics, we were able to make a correlation between the two events without indicating if they are both directly linked or if one can affect the other. This caveat could be addressed by either forcing the chromatin to compact (similarly to *in vitro* experiments to study the compaction of reconstituted nucleosomes)

using ectopic expression methods of known *in vitro* chromatin compactors or by destabilizing histone incorporation and nucleosome spacing (by KD of histone chaperones or histone variants) and check if electron density is affected in the embryo.

In Conclusion, this work has focused on studying different facets of heterochromatin during preimplantation development and has contributed to improve our understanding of some of the mechanisms involved in heterochromatin reorganization. As we have answered some of the questions asked, many new questions have arisen and future work will be needed to further our knowledge of the underlying mechanisms.

# Bibliographic references


Adenot, P. G., Y. Mercier, J. P. Renard, and E. M. Thompson. 1997. 'Differential H4 acetylation of paternal and maternal chromatin precedes DNA replication and differential transcriptional activity in pronuclei of 1-cell mouse embryos', *Development*, 124: 4615-25.

Akasaka, T., M. Kanno, R. Balling, M. A. Mieza, M. Taniguchi, and H. Koseki. 1996. 'A role for mel-18, a Polycomb group-related vertebrate gene, during theanteroposterior specification of the axial skeleton', *Development*, 122: 1513-22.

Alberts B., Johnson I., Lewis J., Raff M., Roberts K., Walter P. 2002. *Molecular Biology of the Cell. 4th edition.*

.

Anglana, Mauro, Françoise Apiou, Aaron Bensimon, and Michelle Debatisse. 2003. 'Dynamics of DNA Replication in Mammalian Somatic Cells', *Cell*, 114: 385-94.

Aoki, F., D. M. Worrad, and R. M. Schultz. 1997. 'Regulation of transcriptional activity during the first and second cell cycles in the preimplantation mouse embryo', *Developmental biology*, 181: 296-307.

Arney, K. L., S. Bao, A. J. Bannister, T. Kouzarides, and M. A. Surani. 2002. 'Histone methylation defines epigenetic asymmetry in the mouse zygote', *Int J Dev Biol*, 46: 317-20.

Arrigoni, R., S. L. Alam, J. A. Wamstad, V. J. Bardwell, W. I. Sundquist, and N. Schreiber-Agus. 2006. 'The Polycomb-associated protein Rybp is a ubiquitin binding protein', *FEBS Lett*, 580: 6233-41.

Azuara, V., P. Perry, S. Sauer, M. Spivakov, H. F. Jorgensen, R. M. John, M. Gouti, M. Casanova, G. Warnes, M. Merkenschlager, and A. G. Fisher. 2006. 'Chromatin signatures of pluripotent cell lines', *Nature cell biology*, 8: 532-8.

Bannister, A. J., P. Zegerman, J. F. Partridge, E. A. Miska, J. O. Thomas, R. C. Allshire, and T. Kouzarides. 2001. 'Selective recognition of methylated lysine 9 on histone H3 by the HP1 chromo domain', *Nature*, 410: 120-4.

Barlow, J. H., R. B. Faryabi, E. Callen, N. Wong, A. Malhowski, H. T. Chen, G. Gutierrez-Cruz, H. W. Sun, P. McKinnon, G. Wright, R. Casellas, D. F. Robbiani, L. Staudt, O. Fernandez-Capetillo, and A. Nussenzweig. 2013. 'Identification of early replicating fragile sites that contribute to genome instability', *Cell*, 152: 620-32.

Barski, A., S. Cuddapah, K. Cui, T. Y. Roh, D. E. Schones, Z. Wang, G. Wei, I. Chepelev, and K. Zhao. 2007. 'High-resolution profiling of histone methylations in the human genome', *Cell*, 129: 823-37.

Bartek, J., and J. Lukas. 2003. 'Chk1 and Chk2 kinases in checkpoint control and cancer', *Cancer Cell*, 3: 421-9.

Beck, D. B., A. Burton, H. Oda, C. Ziegler-Birling, M. E. Torres-Padilla, and D. Reinberg. 2012. 'The role of PR-Set7 in replication licensing depends on Suv4-20h', *Genes & development*, 26: 2580-9.

Beisel, C., and R. Paro. 2011. 'Silencing chromatin: comparing modes and mechanisms', *Nature reviews. Genetics*, 12: 123-35.

Belmont, A. S. 2006. 'Mitotic chromosome structure and condensation', *Curr Opin Cell Biol*, 18: 632-8.

Bensaude, O., C. Babinet, M. Morange, and F. Jacob. 1983. 'Heat shock proteins, first major products of zygotic gene activity in mouse embryo', *Nature*, 305: 331-3.

Benson, L. J., Y. Gu, T. Yakovleva, K. Tong, C. Barrows, C. L. Strack, R. G. Cook, C. A. Mizzen, and A. T. Annunziato. 2006. 'Modifications of H3 and H4 during chromatin replication, nucleosome assembly, and histone exchange', *J Biol Chem*, 281: 9287-96.

Benveniste, D., H. J. Sonntag, G. Sanguinetti, and D. Sproul. 2014. 'Transcription factor binding predicts histone modifications in human cell lines', *Proceedings of the National Academy of Sciences of the United States of America*, 111: 13367-72.

Bermejo, R., T. Capra, R. Jossen, A. Colosio, C. Frattini, W. Carotenuto, A. Cocito, Y. Doksani, H. Klein, B. Gomez-Gonzalez, A. Aguilera, Y. Katou, K. Shirahige, and M. Foiani. 2011. 'The replication checkpoint protects fork stability by releasing transcribed genes from nuclear pores', *Cell*, 146: 233-46.

Bermejo, R., M. S. Lai, and M. Foiani. 2012. 'Preventing replication stress to maintain genome stability: resolving conflicts between replication and transcription', *Molecular cell*, 45: 710-8.

Bernstein, B. E., T. S. Mikkelsen, X. Xie, M. Kamal, D. J. Huebert, J. Cuff, B. Fry, A. Meissner, M. Wernig, K. Plath, R. Jaenisch, A. Wagschal, R. Feil, S. L. Schreiber, and E. S. Lander. 2006. 'A bivalent chromatin structure marks key developmental genes in embryonic stem cells', *Cell*, 125: 315-26.

Bernstein, E., E. M. Duncan, O. Masui, J. Gil, E. Heard, and C. D. Allis. 2006. 'Mouse polycomb proteins bind differentially to methylated histone H3 and RNA and are enriched in facultative heterochromatin', *Mol Cell Biol*, 26: 2560-9.

Bester, A. C., M. Roniger, Y. S. Oren, M. M. Im, D. Sarni, M. Chaoat, A. Bensimon, G. Zamir, D. S. Shewach, and B. Kerem. 2011. 'Nucleotide deficiency promotes genomic instability in early stages of cancer development', *Cell*, 145: 435-46.

Black, J. C., A. Allen, C. Van Rechem, E. Forbes, M. Longworth, K. Tschop, C. Rinehart, J. Quiton, R. Walsh, A. Smallwood, N. J. Dyson, and J. R. Whetstine. 2010. 'Conserved antagonism between JMJD2A/KDM4A and HP1gamma during cell cycle progression', *Molecular cell*, 40: 736-48.

Black, J. C., A. L. Manning, C. Van Rechem, J. Kim, B. Ladd, J. Cho, C. M. Pineda, N. Murphy, D. L. Daniels, C. Montagna, P. W. Lewis, K. Glass, C. D. Allis, N. J. Dyson, G. Getz, and J. R. Whetstine. 2013. 'KDM4A lysine demethylase induces site-specific copy gain and rereplication of regions amplified in tumors', *Cell*, 154: 541-55.

Blackledge, N. P., A. M. Farcas, T. Kondo, H. W. King, J. F. McGouran, L. L. Hanssen, S. Ito, S. Cooper, K. Kondo, Y. Koseki, T. Ishikura, H. K. Long, T. W. Sheahan, N. Brockdorff, B. M. Kessler, H. Koseki, and R. J. Klose. 2014. 'Variant PRC1 complex-dependent H2A ubiquitylation drives PRC2 recruitment and polycomb domain formation', *Cell*, 157: 1445-59.

Bochkarev, A., R. A. Pfuetzner, A. M. Edwards, and L. Frappier. 1997. 'Structure of the single-stranded-DNA-binding domain of replication protein A bound to DNA', *Nature*, 385: 176-81.

Bolton, V. N., P. J. Oades, and M. H. Johnson. 1984. 'The relationship between cleavage, DNA replication, and gene expression in the mouse 2-cell embryo', *Journal of embryology and experimental morphology*, 79: 139-63.

Bonasio, R., E. Lecona, V. Narendra, P. Voigt, F. Parisi, Y. Kluger, and D. Reinberg. 2014. 'Interactions with RNA direct the Polycomb group protein SCML2 to chromatin where it represses target genes', *eLife*, 3: e02637.

Bornemann, D., E. Miller, and J. Simon. 1996. 'The Drosophila Polycomb group gene Sex comb on midleg (Scm) encodes a zinc finger protein with similarity to polyhomeotic protein', *Development*, 122: 1621-30.

Botuyan, M. V., J. Lee, I. M. Ward, J. E. Kim, J. R. Thompson, J. Chen, and G. Mer. 2006. 'Structural basis for the methylation state-specific recognition of histone H4-K20 by 53BP1 and Crb2 in DNA repair', *Cell*, 127: 1361-73.

Bouniol, C., E. Nguyen, and P. Debey. 1995. 'Endogenous transcription occurs at the 1-cell stage in the mouse embryo', *Exp Cell Res*, 218: 57-62.

Boyer, L. A., K. Plath, J. Zeitlinger, T. Brambrink, L. A. Medeiros, T. I. Lee, S. S. Levine, M. Wernig, A. Tajonar, M. K. Ray, G. W. Bell, A. P. Otte, M. Vidal, D. K. Gifford, R. A. Young, and R. Jaenisch. 2006. 'Polycomb complexes repress developmental regulators in murine embryonic stem cells', *Nature*, 441: 349-53.

Branco, M. R., M. King, V. Perez-Garcia, A. B. Bogutz, M. Caley, E. Fineberg, L. Lefebvre, S. J. Cook, W. Dean, M. Hemberger, and W. Reik. 2016. 'Maternal DNA Methylation Regulates Early Trophoblast Development', *Developmental cell*, 36: 152-63.

Brookes, E., I. de Santiago, D. Hebenstreit, K. J. Morris, T. Carroll, S. Q. Xie, J. K. Stock, M. Heidemann, D. Eick, N. Nozaki, H. Kimura, J. Ragoussis, S. A. Teichmann, and A. Pombo. 2012. 'Polycomb associates genome-wide with a specific RNA polymerase II variant, and regulates metabolic genes in ESCs', *Cell stem cell*, 10: 157-70.

Brown, E. J., and D. Baltimore. 2000. 'ATR disruption leads to chromosomal fragmentation and early embryonic lethality', *Genes & development*, 14: 397-402.

Brown, J. L., D. Mucci, M. Whiteley, M. L. Dirksen, and J. A. Kassis. 1998. 'The Drosophila Polycomb group gene pleiohomeotic encodes a DNA binding protein with homology to the transcription factor YY1', *Molecular cell*, 1: 1057-64.

Brownell, J. E., J. Zhou, T. Ranalli, R. Kobayashi, D. G. Edmondson, S. Y. Roth, and C. D. Allis. 1996. 'Tetrahymena histone acetyltransferase A: a homolog to yeast Gcn5p linking histone acetylation to gene activation', *Cell*, 84: 843-51.

Buchmann, A. M., J. R. Skaar, and J. A. DeCaprio. 2004. 'Activation of a DNA damage checkpoint response in a TAF1-defective cell line', *Mol Cell Biol*, 24: 5332-9.

Burton, A., and M. E. Torres-Padilla. 2014. 'Chromatin dynamics in the regulation of cell fate allocation during early embryogenesis', *Nature reviews. Molecular cell biology*, 15: 723-34.

Byun, T. S., M. Pacek, M. C. Yee, J. C. Walter, and K. A. Cimprich. 2005. 'Functional uncoupling of MCM helicase and DNA polymerase activities activates the ATR-dependent checkpoint', *Genes & development*, 19: 1040-52.

Cao, R., L. Wang, H. Wang, L. Xia, H. Erdjument-Bromage, P. Tempst, R. S. Jones, and Y. Zhang. 2002. 'Role of histone H3 lysine 27 methylation in Polycomb-group silencing', *Science*, 298: 1039-43.

Cao, R., and Y. Zhang. 2004. 'SUZ12 is required for both the histone methyltransferase activity and the silencing function of the EED-EZH2 complex', *Molecular cell*, 15: 57-67.

Capasso, H., C. Palermo, S. Wan, H. Rao, U. P. John, M. J. O'Connell, and N. C. Walworth. 2002. 'Phosphorylation activates Chk1 and is required for checkpoint-mediated cell cycle arrest', *J Cell Sci*, 115: 4555-64.

Casas-Delucchi, C. S., and M. C. Cardoso. 2011. 'Epigenetic control of DNA replication dynamics in mammals', *Nucleus*, 2: 370-82.

Casper, A. M., P. Nghiem, M. F. Arlt, and T. W. Glover. 2002. 'ATR regulates fragile site stability', *Cell*, 111: 779-89.

Caterino, T. L., and J. J. Hayes. 2007. 'Chromatin structure depends on what's in the nucleosome's pocket', *Nature structural & molecular biology*, 14: 1056-8.

Cayrou, C., P. Coulombe, A. Vigneron, S. Stanojcic, O. Ganier, I. Peiffer, E. Rivals, A. Puy, S. Laurent-Chabalier, R. Desprat, and M. Mechali. 2011. 'Genome-scale analysis of metazoan replication origins reveals their organization in specific but flexible sites defined by conserved features', *Genome Res*, 21: 1438-49.

Celeste, A., O. Fernandez-Capetillo, M. J. Kruhlak, D. R. Pilch, D. W. Staudt, A. Lee, R. F. Bonner, W. M. Bonner, and A. Nussenzweig. 2003. 'Histone H2AX phosphorylation is dispensable for the initial recognition of DNA breaks', *Nature cell biology*, 5: 675-9.

Celeste, A., S. Petersen, P. J. Romanienko, O. Fernandez-Capetillo, H. T. Chen, O. A. Sedelnikova, B. Reina-San-Martin, V. Coppola, E. Meffre, M. J. Difilippantonio, C. Redon, D. R. Pilch, A. Olaru, M. Eckhaus, R. D. Camerini-Otero, L. Tessarollo, F. Livak, K. Manova, W. M. Bonner, M. C. Nussenzweig, and A. Nussenzweig. 2002. 'Genomic instability in mice lacking histone H2AX', *Science*, 296: 922-7.

Chen, D., J. Zhang, M. Li, E. R. Rayburn, H. Wang, and R. Zhang. 2009. 'RYBP stabilizes p53 by modulating MDM2', *EMBO reports*, 10: 166-72.

Chen, M. S., C. E. Ryan, and H. Piwnica-Worms. 2003. 'Chk1 kinase negatively regulates mitotic function of Cdc25A phosphatase through 14-3-3 binding', *Mol Cell Biol*, 23: 7488-97.

Ciccia, A., and S. J. Elledge. 2010. 'The DNA damage response: making it safe to play with knives', *Molecular cell*, 40: 179-204.

Cifuentes-Rojas, C., A. J. Hernandez, K. Sarma, and J. T. Lee. 2014. 'Regulatory interactions between RNA and polycomb repressive complex 2', *Molecular cell*, 55: 171-85.

Cimprich, K. A., and D. Cortez. 2008. 'ATR: an essential regulator of genome integrity', *Nature reviews. Molecular cell biology*, 9: 616-27.

Clarke, C. A., and P. R. Clarke. 2005. 'DNA-dependent phosphorylation of Chk1 and Claspin in a human cell-free system', *Biochem J*, 388: 705-12.

Collins, N., R. A. Poot, I. Kukimoto, C. Garcia-Jimenez, G. Dellaire, and P. D. Varga-Weisz. 2002. 'An ACF1-ISWI chromatin-remodeling complex is required for DNA replication through heterochromatin', *Nature genetics*, 32: 627-32.

Congdon, L. M., S. I. Houston, C. S. Veerappan, T. M. Spektor, and J. C. Rice. 2010. 'PR-Set7-mediated monomethylation of histone H4 lysine 20 at specific genomic regions induces transcriptional repression', *J Cell Biochem*, 110: 609-19.

Cook, P. R. 1995. 'A chromomeric model for nuclear and chromosome structure', *J Cell Sci*, 108 ( Pt 9): 2927-35.

Cooper, S., M. Dienstbier, R. Hassan, L. Schermelleh, J. Sharif, N. P. Blackledge, V. De Marco, S. Elderkin, H. Koseki, R. Klose, A. Heger, and N. Brockdorff. 2014. 'Targeting polycomb to pericentric heterochromatin in embryonic stem cells reveals a role for H2AK119u1 in PRC2 recruitment', *Cell reports*, 7: 1456-70.

Core, N., S. Bel, S. J. Gaunt, M. Aurrand-Lions, J. Pearce, A. Fisher, and M. Djabali. 1997. 'Altered cellular proliferation and mesoderm patterning in Polycomb-M33-deficient mice', *Development*, 124: 721-9.

Cortez, D., G. Glick, and S. J. Elledge. 2004. 'Minichromosome maintenance proteins are direct targets of the ATM and ATR checkpoint kinases', *Proceedings of the National Academy of Sciences of the United States of America*, 101: 10078-83.

Cortez, D., S. Guntuku, J. Qin, and S. J. Elledge. 2001. 'ATR and ATRIP: partners in checkpoint signaling', *Science*, 294: 1713-6.

Creyghton, M. P., A. W. Cheng, G. G. Welstead, T. Kooistra, B. W. Carey, E. J. Steine, J. Hanna, M. A. Lodato, G. M. Frampton, P. A. Sharp, L. A. Boyer, R. A. Young, and R. Jaenisch. 2010. 'Histone H3K27ac separates active from poised enhancers and predicts developmental state', *Proceedings of the National Academy of Sciences of the United States of America*, 107: 21931-6.

da Rocha, S. T., V. Boeva, M. Escamilla-Del-Arenal, K. Ancelin, C. Granier, N. R. Matias, S. Sanulli, J. Chow, E. Schulz, C. Picard, S. Kaneko, K. Helin, D. Reinberg, A. F. Stewart, A. Wutz, R. Margueron, and E. Heard. 2014. 'Jarid2 Is Implicated in the Initial Xist-Induced Targeting of PRC2 to the Inactive X Chromosome', *Molecular cell*, 53: 301-16.

Dalgaard, J. Z. 2012. 'Causes and consequences of ribonucleotide incorporation into nuclear DNA', *Trends Genet*, 28: 592-7.

Daujat, S., T. Weiss, F. Mohn, U. C. Lange, C. Ziegler-Birling, U. Zeissler, M. Lappe, D. Schubeler, M. E. Torres-Padilla, and R. Schneider. 2009. 'H3K64 trimethylation marks heterochromatin and is dynamically remodeled during developmental reprogramming', *Nature structural & molecular biology*, 16: 777-81.

Davidovich, C., L. Zheng, K. J. Goodrich, and T. R. Cech. 2013. 'Promiscuous RNA binding by Polycomb repressive complex 2', *Nature structural & molecular biology*, 20: 1250-7.

de Klein, A., M. Muijtjens, R. van Os, Y. Verhoeven, B. Smit, A. M. Carr, A. R. Lehmann, and J. H. Hoeijmakers. 2000. 'Targeted disruption of the cell-cycle checkpoint gene ATR leads to early embryonic lethality in mice', *Current biology : CB*, 10: 479-82.

de Napoles, M., J. E. Mermoud, R. Wakao, Y. A. Tang, M. Endoh, R. Appanah, T. B. Nesterova, J. Silva, A. P. Otte, M. Vidal, H. Koseki, and N. Brockdorff. 2004. 'Polycomb group proteins Ring1A/B link ubiquitylation of histone H2A to heritable gene silencing and X inactivation', *Developmental cell*, 7: 663-76.

del Mar Lorente, M., C. Marcos-Gutierrez, C. Perez, J. Schoorlemmer, A. Ramirez, T. Magin, and M. Vidal. 2000. 'Loss- and gain-of-function mutations show a polycomb group function for Ring1A in mice', *Development*, 127: 5093-100.

Derheimer, F. A., H. M. O'Hagan, H. M. Krueger, S. Hanasoge, M. T. Paulsen, and M. Ljungman. 2007. 'RPA and ATR link transcriptional stress to p53', *Proceedings of the National Academy of Sciences of the United States of America*, 104: 12778-83.

Durrin, L. K., R. K. Mann, P. S. Kayne, and M. Grunstein. 1991. 'Yeast histone H4 N-terminal sequence is required for promoter activation in vivo', *Cell*, 65: 1023-31.

El Messaoudi-Aubert, S., J. Nicholls, G. N. Maertens, S. Brookes, E. Bernstein, and G. Peters. 2010. 'Role for the MOV10 RNA helicase in polycomb-mediated repression of the INK4a tumor suppressor', *Nature structural & molecular biology*, 17: 862-8.

Ellison, V., and B. Stillman. 2003. 'Biochemical characterization of DNA damage checkpoint complexes: clamp loader and clamp complexes with specificity for 5' recessed DNA', *PLoS biology*, 1: E33.

Endoh, M., T. A. Endo, T. Endoh, Y. Fujimura, O. Ohara, T. Toyoda, A. P. Otte, M. Okano, N. Brockdorff, M. Vidal, and H. Koseki. 2008. 'Polycomb group proteins Ring1A/B are functionally linked to the core transcriptional regulatory circuitry to maintain ES cell identity', *Development*, 135: 1513-24.

Erhardt, S., I. H. Su, R. Schneider, S. Barton, A. J. Bannister, L. Perez-Burgos, T. Jenuwein, T. Kouzarides, A. Tarakhovsky, and M. A. Surani. 2003. 'Consequences of the depletion of zygotic and embryonic enhancer of zeste 2 during preimplantation mouse development', *Development*, 130: 4235-48.

Erkek, S., M. Hisano, C. Y. Liang, M. Gill, R. Murr, J. Dieker, D. Schubeler, J. van der Vlag, M. B. Stadler, and A. H. Peters. 2013. 'Molecular determinants of nucleosome retention at CpG-rich sequences in mouse spermatozoa', *Nature structural & molecular biology*, 20: 868-75.

Eskeland, R., M. Leeb, G. R. Grimes, C. Kress, S. Boyle, D. Sproul, N. Gilbert, Y. Fan, A. I. Skoultchi, A. Wutz, and W. A. Bickmore. 2010. 'Ring1B compacts chromatin structure and represses gene expression independent of histone ubiquitination', *Molecular cell*, 38: 452-64.

Fadloun, A., A. Eid, and M. E. Torres-Padilla. 2013. 'Mechanisms and dynamics of heterochromatin formation during Mammalian development: closed paths and open questions', *Curr Top Dev Biol*, 104: 1-45.

Fang, J., T. Chen, B. Chadwick, E. Li, and Y. Zhang. 2004. 'Ring1b-mediated H2A ubiquitination associates with inactive X chromosomes and is involved in initiation of X inactivation', *J Biol Chem*, 279: 52812-5.

Fanning, E., V. Klimovich, and A. R. Nager. 2006. 'A dynamic model for replication protein A (RPA) function in DNA processing pathways', *Nucleic acids research*, 34: 4126-37.

Farcas, A. M., N. P. Blackledge, I. Sudbery, H. K. Long, J. F. McGouran, N. R. Rose, S. Lee, D. Sims, A. Cerase, T. W. Sheahan, H. Koseki, N. Brockdorff, C. P. Ponting, B. M. Kessler, and R. J. Klose. 2012. 'KDM2B links the Polycomb Repressive Complex 1 (PRC1) to recognition of CpG islands', *eLife*, 1: e00205.

Faust, C., A. Schumacher, B. Holdener, and T. Magnuson. 1995. 'The eed mutation disrupts anterior mesoderm production in mice', *Development*, 121: 273-85.

Ferrari, K. J., A. Scelfo, S. Jammula, A. Cuomo, I. Barozzi, A. Stutzer, W. Fischle, T. Bonaldi, and D. Pasini. 2014. 'Polycomb-dependent H3K27me1 and H3K27me2 regulate active transcription and enhancer fidelity', *Molecular cell*, 53: 49-62.

Finch, J. T., and A. Klug. 1976. 'Solenoidal Model for Superstructure in Chromatin', *Proceedings of the National Academy of Sciences of the United States of America*, 73: 1897-901.

Flach, G., M. H. Johnson, P. R. Braude, R. A. Taylor, and V. N. Bolton. 1982. 'The transition from maternal to embryonic control in the 2-cell mouse embryo', *The EMBO journal*, 1: 681-6.

Forzati, F., A. Federico, P. Pallante, A. Abbate, F. Esposito, U. Malapelle, R. Sepe, G. Palma, G. Troncone, M. Scarfo, C. Arra, M. Fedele, and A. Fusco. 2012. 'CBX7 is a tumor suppressor in mice and humans', *J Clin Invest*, 122: 612-23.

Fraga, M. F., E. Ballestar, A. Villar-Garea, M. Boix-Chornet, J. Espada, G. Schotta, T. Bonaldi, C. Haydon, S. Ropero, K. Petrie, N. G. Iyer, A. Perez-Rosado, E. Calvo, J. A. Lopez, A. Cano, M. J. Calasanz, D. Colomer, M. A. Piris, N. Ahn, A. Imhof, C. Caldas, T. Jenuwein, and M. Esteller. 2005. 'Loss of acetylation at Lys16 and trimethylation at Lys20 of histone H4 is a common hallmark of human cancer', *Nature genetics*, 37: 391-400.

Francis, N. J., R. E. Kingston, and C. L. Woodcock. 2004. 'Chromatin compaction by a polycomb group protein complex', *Science*, 306: 1574-7.

Gambus, A., R. C. Jones, A. Sanchez-Diaz, M. Kanemaki, F. van Deursen, R. D. Edmondson, and K. Labib. 2006. 'GINS maintains association of Cdc45 with MCM in replisome progression complexes at eukaryotic DNA replication forks', *Nature cell biology*, 8: 358-66.

Gao, Z., J. Zhang, R. Bonasio, F. Strino, A. Sawai, F. Parisi, Y. Kluger, and D. Reinberg. 2012. 'PCGF homologs, CBX proteins, and RYBP define functionally distinct PRC1 family complexes', *Molecular cell*, 45: 344-56.

Garcia, E., C. Marcos-Gutierrez, M. del Mar Lorente, J. C. Moreno, and M. Vidal. 1999. 'RYBP, a new repressor protein that interacts with components of the mammalian Polycomb complex, and with the transcription factor YY1', *The EMBO journal*, 18: 3404-18.

Ge, X. Q., D. A. Jackson, and J. J. Blow. 2007. 'Dormant origins licensed by excess Mcm2-7 are required for human cells to survive replicative stress', *Genes & development*, 21: 3331-41.

Gearhart, M. D., C. M. Corcoran, J. A. Wamstad, and V. J. Bardwell. 2006. 'Polycomb group and SCF ubiquitin ligases are found in a novel BCOR complex that is recruited to BCL6 targets', *Mol Cell Biol*, 26: 6880-9.

Gehani, S. S., S. Agrawal-Singh, N. Dietrich, N. S. Christophersen, K. Helin, and K. Hansen. 2010. 'Polycomb group protein displacement and gene activation through MSK-dependent H3K27me3S28 phosphorylation', *Molecular cell*, 39: 886-900.

Gil, J., D. Bernard, D. Martinez, and D. Beach. 2004. 'Polycomb CBX7 has a unifying role in cellular lifespan', *Nature cell biology*, 6: 67-72.

Gilbert, D. M. 2007. 'Replication origin plasticity, Taylor-made: inhibition vs recruitment of origins under conditions of replication stress', *Chromosoma*, 116: 341-7.

Groth, A., W. Rocha, A. Verreault, and G. Almouzni. 2007. 'Chromatin challenges during DNA replication and repair', *Cell*, 128: 721-33.

Guo, Y., N. Nady, C. Qi, A. Allali-Hassani, H. Zhu, P. Pan, M. A. Adams-Cioaba, M. F. Amaya, A. Dong, M. Vedadi, M. Schapira, R. J. Read, C. H. Arrowsmith, and J. Min. 2009. 'Methylation-state-specific recognition of histones by the MBT repeat protein L3MBTL2', *Nucleic acids research*, 37: 2204-10.

Guo, Z., A. Kumagai, S. X. Wang, and W. G. Dunphy. 2000. 'Requirement for Atr in phosphorylation of Chk1 and cell cycle regulation in response to DNA replication blocks and UV-damaged DNA in Xenopus egg extracts', *Genes & development*, 14: 2745-56.

Hajdu, I., A. Ciccia, S. M. Lewis, and S. J. Elledge. 2011. 'Wolf-Hirschhorn syndrome candidate 1 is involved in the cellular response to DNA damage', *Proceedings of the National Academy of Sciences of the United States of America*, 108: 13130-4.

Hammoud, S. S., D. A. Nix, H. Zhang, J. Purwar, D. T. Carrell, and B. R. Cairns. 2009. 'Distinctive chromatin in human sperm packages genes for embryo development', *Nature*, 460: 473-8.

Hanada, K., M. Budzowska, S. L. Davies, E. van Drunen, H. Onizawa, H. B. Beverloo, A. Maas, J. Essers, I. D. Hickson, and R. Kanaar. 2007. 'The structure-specific endonuclease Mus81 contributes to replication restart by generating double-strand DNA breaks', *Nature structural & molecular biology*, 14: 1096-104.

Hasegawa, K., H. S. Sin, S. Maezawa, T. J. Broering, A. V. Kartashov, K. G. Alavattam, Y. Ichijima, F. Zhang, W. C. Bacon, K. D. Greis, P. R. Andreassen, A. Barski, and S. H. Namekawa. 2015. 'SCML2 establishes the male germline epigenome through regulation of histone H2A ubiquitination', *Developmental cell*, 32: 574-88.

Hassepass, I., R. Voit, and I. Hoffmann. 2003. 'Phosphorylation at serine 75 is required for UV-mediated degradation of human Cdc25A phosphatase at the S-phase checkpoint', *J Biol Chem*, 278: 29824-9.

Hayashi, M., Y. Katou, T. Itoh, A. Tazumi, Y. Yamada, T. Takahashi, T. Nakagawa, K. Shirahige, and H. Masukata. 2007. 'Genome-wide localization of pre-RC sites and identification of replication origins in fission yeast', *The EMBO journal*, 26: 1327-39.

He, J., L. Shen, M. Wan, O. Taranova, H. Wu, and Y. Zhang. 2013. 'Kdm2b maintains murine embryonic stem cell status by recruiting PRC1 complex to CpG islands of developmental genes', *Nature cell biology*, 15: 373-84.

Helmrich, A., M. Ballarino, E. Nudler, and L. Tora. 2013. 'Transcription-replication encounters, consequences and genomic instability', *Nature structural & molecular biology*, 20: 412-8.

Hemberger, M., W. Dean, and W. Reik. 2009. 'Epigenetic dynamics of stem cells and cell lineage commitment: digging Waddington's canal', *Nature reviews. Molecular cell biology*, 10: 526-37.

Hisada, K., C. Sanchez, T. A. Endo, M. Endoh, M. Roman-Trufero, J. Sharif, H. Koseki, and M. Vidal. 2012. 'RYBP represses endogenous retroviruses and preimplantation- and germ line-specific genes in mouse embryonic stem cells', *Mol Cell Biol*, 32: 1139-49.

Hisano, M., S. Erkek, S. Dessus-Babus, L. Ramos, M. B. Stadler, and A. H. Peters. 2013. 'Genome-wide chromatin analysis in mature mouse and human spermatozoa', *Nat Protoc*, 8: 2449-70.

Hoek, M., and B. Stillman. 2003. 'Chromatin assembly factor 1 is essential and couples chromatin assembly to DNA replication in vivo', *Proceedings of the National Academy of Sciences of the United States of America*, 100: 12183-8.

Hogan, B. L., R. Beddington, F. Costantini, and E. Lacy. 1994. *Manipulating the Mouse Embryo* (Cold Spring Harbor Laboratory Press).

Horowitz, R. A., D. A. Agard, J. W. Sedat, and C. L. Woodcock. 1994. 'The 3-Dimensional Architecture of Chromatin in-Situ - Electron Tomography Reveals Fibers Composed of a Continuously Variable Zigzag Nucleosomal Ribbon', *Journal of Cell Biology*, 125: 1-10.

Houston, S. I., K. J. McManus, M. M. Adams, J. K. Sims, P. B. Carpenter, M. J. Hendzel, and J. C. Rice. 2008. 'Catalytic function of the PR-Set7 histone H4 lysine 20 monomethyltransferase is essential for mitotic entry and genomic stability', *J Biol Chem*, 283: 19478-88.

Huberman, J. A., and A. D. Riggs. 1966. 'Autoradiography of chromosomal DNA fibers from Chinese hamster cells', *Proceedings of the National Academy of Sciences of the United States of America*, 55: 599-606.

Illingworth, R. S., M. Moffat, A. R. Mann, D. Read, C. J. Hunter, M. M. Pradeepa, I. R. Adams, and W. A. Bickmore. 2015. 'The E3 ubiquitin ligase activity of RING1B is not essential for early mouse development', *Genes & development*, 29: 1897-902.

Jachowicz, J. W., A. Santenard, A. Bender, J. Muller, and M. E. Torres-Padilla. 2013. 'Heterochromatin establishment at pericentromeres depends on nuclear position', *Genes & development*, 27: 2427-32.

Jackson, D. A., and A. Pombo. 1998. 'Replicon clusters are stable units of chromosome structure: evidence that nuclear organization contributes to the efficient activation and propagation of S phase in human cells', *J Cell Biol*, 140: 1285-95.

Jackson, V. 1988. 'Deposition of newly synthesized histones: hybrid nucleosomes are not tandemly arranged on daughter DNA strands', *Biochemistry*, 27: 2109-20.

Jermann, P., L. Hoerner, L. Burger, and D. Schubeler. 2014. 'Short sequences can efficiently recruit histone H3 lysine 27 trimethylation in the absence of enhancer activity and DNA methylation', *Proceedings of the National Academy of Sciences of the United States of America*, 111: E3415-21.

Jones, R. S., and W. M. Gelbart. 1990. 'Genetic analysis of the enhancer of zeste locus and its role in gene regulation in Drosophila melanogaster', *Genetics*, 126: 185-99.

Jorgensen, S., I. Elvers, M. B. Trelle, T. Menzel, M. Eskildsen, O. N. Jensen, T. Helleday, K. Helin, and C. S. Sorensen. 2007. 'The histone methyltransferase SET8 is required for S-phase progression', *J Cell Biol*, 179: 1337-45.

Jung, J., T. G. Kim, G. E. Lyons, H. R. Kim, and Y. Lee. 2005. 'Jumonji regulates cardiomyocyte proliferation via interaction with retinoblastoma protein', *J Biol Chem*, 280: 30916-23.

Kalantry, S., K. C. Mills, D. Yee, A. P. Otte, B. Panning, and T. Magnuson. 2006. 'The Polycomb group protein Eed protects the inactive X-chromosome from differentiation-induced reactivation', *Nature cell biology*, 8: 195-202.

Kalb, R., S. Latwiel, H. I. Baymaz, P. W. Jansen, C. W. Muller, M. Vermeulen, and J. Muller. 2014. 'Histone H2A monoubiquitination promotes histone H3 methylation in Polycomb repression', *Nature structural & molecular biology*, 21: 569-71.

Kalenik, J. L., D. Chen, M. E. Bradley, S. J. Chen, and T. C. Lee. 1997. 'Yeast two-hybrid cloning of a novel zinc finger protein that interacts with the multifunctional transcription factor YY1', *Nucleic acids research*, 25: 843-9.

Kaneko, S., R. Bonasio, R. Saldana-Meyer, T. Yoshida, J. Son, K. Nishino, A. Umezawa, and D. Reinberg. 2014. 'Interactions between JARID2 and noncoding RNAs regulate PRC2 recruitment to chromatin', *Molecular cell*, 53: 290-300.

Kaneko, S., J. Son, R. Bonasio, S. S. Shen, and D. Reinberg. 2014. 'Nascent RNA interaction keeps PRC2 activity poised and in check', *Genes & development*, 28: 1983-8.

Kaneko, S., J. Son, S. S. Shen, D. Reinberg, and R. Bonasio. 2013. 'PRC2 binds active promoters and contacts nascent RNAs in embryonic stem cells', *Nature structural & molecular biology*, 20: 1258-64.

Kapoor-Vazirani, P., J. D. Kagey, and P. M. Vertino. 2011. 'SUV420H2-mediated H4K20 trimethylation enforces RNA polymerase II promoter-proximal pausing by blocking hMOF-dependent H4K16 acetylation', *Mol Cell Biol*, 31: 1594-609.

Kasahara, K., H. Goto, M. Enomoto, Y. Tomono, T. Kiyono, and M. Inagaki. 2010. '14-3-3gamma mediates Cdc25A proteolysis to block premature mitotic entry after DNA damage', *The EMBO journal*, 29: 2802-12.

Kayne, P. S., U. J. Kim, M. Han, J. R. Mullen, F. Yoshizaki, and M. Grunstein. 1988. 'Extremely conserved histone H4 N terminus is dispensable for growth but essential for repressing the silent mating loci in yeast', *Cell*, 55: 27-39.

Khalil, A. M., M. Guttman, M. Huarte, M. Garber, A. Raj, D. Rivea Morales, K. Thomas, A. Presser, B. E. Bernstein, A. van Oudenaarden, A. Regev, E. S. Lander, and J. L. Rinn. 2009. 'Many human large intergenic noncoding RNAs associate with chromatin-modifying complexes and affect gene expression', *Proceedings of the National Academy of Sciences of the United States of America*, 106: 11667-72.

Khurana, S., and P. Oberdoerffer. 2015. 'Replication Stress: A Lifetime of Epigenetic Change', *Genes (Basel)*, 6: 858-77.

Kim, H., K. Kang, and J. Kim. 2009. 'AEBP2 as a potential targeting protein for Polycomb Repression Complex PRC2', *Nucleic acids research*, 37: 2940-50.

Koga, H., S. Matsui, T. Hirota, S. Takebayashi, K. Okumura, and H. Saya. 1999. 'A human homolog of Drosophila lethal(3)malignant brain tumor (l(3)mbt) protein associates with condensed mitotic chromosomes', *Oncogene*, 18: 3799-809.

Kourmouli, N., P. Jeppesen, S. Mahadevhaiah, P. Burgoyne, R. Wu, D. M. Gilbert, S. Bongiorni, G. Prantera, L. Fanti, S. Pimpinelli, W. Shi, R. Fundele, and P. B. Singh. 2004. 'Heterochromatin and tri-methylated lysine 20 of histone H4 in animals', *J Cell Sci*, 117: 2491-501.

Kouzarides, T. 2007. 'Chromatin modifications and their function', *Cell*, 128: 693-705.

Ku, M., R. P. Koche, E. Rheinbay, E. M. Mendenhall, M. Endoh, T. S. Mikkelsen, A. Presser, C. Nusbaum, X. Xie, A. S. Chi, M. Adli, S. Kasif, L. M. Ptaszek, C. A. Cowan, E. S. Lander, H. Koseki, and B. E. Bernstein. 2008. 'Genomewide analysis of PRC1 and PRC2 occupancy identifies two classes of bivalent domains', *PLoS genetics*, 4: e1000242.

Kumagai, A., J. Lee, H. Y. Yoo, and W. G. Dunphy. 2006. 'TopBP1 activates the ATR-ATRIP complex', *Cell*, 124: 943-55.

Kuo, A. J., J. Song, P. Cheung, S. Ishibe-Murakami, S. Yamazoe, J. K. Chen, D. J. Patel, and O. Gozani. 2012. 'The BAH domain of ORC1 links H4K20me2 to DNA replication licensing and Meier-Gorlin syndrome', *Nature*, 484: 115-9.

Lachner, M., D. O'Carroll, S. Rea, K. Mechtler, and T. Jenuwein. 2001. 'Methylation of histone H3 lysine 9 creates a binding site for HP1 proteins', *Nature*, 410: 116-20.

Landeira, D., S. Sauer, R. Poot, M. Dvorkina, L. Mazzarella, H. F. Jorgensen, C. F. Pereira, M. Leleu, F. M. Piccolo, M. Spivakov, E. Brookes, A. Pombo, C. Fisher, W. C. Skarnes, T. Snoek, K. Bezstarosti, J. Demmers, R. J. Klose, M. Casanova, L. Tavares, N. Brockdorff, M. Merkenschlager, and A. G. Fisher. 2010. 'Jarid2 is a PRC2 component in embryonic stem cells required for multi-lineage differentiation and recruitment of PRC1 and RNA Polymerase II to developmental regulators', *Nature cell biology*, 12: 618-24.

Lange, U. C., S. Siebert, M. Wossidlo, T. Weiss, C. Ziegler-Birling, J. Walter, M. E. Torres-Padilla, S. Daujat, and R. Schneider. 2013. 'Dissecting the role of H3K64me3 in mouse pericentromeric heterochromatin', *Nature communications*, 4: 2233.

Latreille, D., L. Bluy, M. Benkirane, and R. E. Kiernan. 2014. 'Identification of histone 3 variant 2 interacting factors', *Nucleic acids research*, 42: 3542-50.

Lau, P. N., and P. Cheung. 2011. 'Histone code pathway involving H3 S28 phosphorylation and K27 acetylation activates transcription and antagonizes polycomb silencing', *Proceedings of the National Academy of Sciences of the United States of America*, 108: 2801-6.

Lebofsky, R., R. Heilig, M. Sonnleitner, J. Weissenbach, and A. Bensimon. 2006. 'DNA replication origin interference increases the spacing between initiation events in human cells', *Molecular biology of the cell*, 17: 5337-45.

Lecona, E., V. Narendra, and D. Reinberg. 2015. 'USP7 cooperates with SCML2 to regulate the activity of PRC1', *Mol Cell Biol*, 35: 1157-68.

Lecona, E., L. A. Rojas, R. Bonasio, A. Johnston, O. Fernandez-Capetillo, and D. Reinberg. 2013. 'Polycomb protein SCML2 regulates the cell cycle by binding and modulating CDK/CYCLIN/p21 complexes', *PLoS biology*, 11: e1001737.

Lee, J., A. Kumagai, and W. G. Dunphy. 2001. 'Positive regulation of Wee1 by Chk1 and 14-3-3 proteins', *Molecular biology of the cell*, 12: 551-63.

Lee, T. I., R. G. Jenner, L. A. Boyer, M. G. Guenther, S. S. Levine, R. M. Kumar, B. Chevalier, S. E. Johnstone, M. F. Cole, K. Isono, H. Koseki, T. Fuchikami, K. Abe, H. L. Murray, J. P. Zucker, B. Yuan, G. W. Bell, E. Herbolsheimer, N. M. Hannett, K. Sun, D. T. Odom, A. P. Otte, T. L. Volkert, D. P. Bartel, D. A.

Melton, D. K. Gifford, R. Jaenisch, and R. A. Young. 2006. 'Control of developmental regulators by Polycomb in human embryonic stem cells', *Cell*, 125: 301-13.

Leeb, M., D. Pasini, M. Novatchkova, M. Jaritz, K. Helin, and A. Wutz. 2010. 'Polycomb complexes act redundantly to repress genomic repeats and genes', *Genes & development*, 24: 265-76.

Lesch, B. J., G. A. Dokshin, R. A. Young, J. R. McCarrey, and D. C. Page. 2013. 'A set of genes critical to development is epigenetically poised in mouse germ cells from fetal stages through completion of meiosis', *Proceedings of the National Academy of Sciences of the United States of America*, 110: 16061-6.

Letessier, A., G. A. Millot, S. Koundrioukoff, A. M. Lachages, N. Vogt, R. S. Hansen, B. Malfoy, O. Brison, and M. Debatisse. 2011. 'Cell-type-specific replication initiation programs set fragility of the FRA3B fragile site', *Nature*, 470: 120-3.

Levine, S. S., A. Weiss, H. Erdjument-Bromage, Z. Shao, P. Tempst, and R. E. Kingston. 2002. 'The core of the polycomb repressive complex is compositionally and functionally conserved in flies and humans', *Mol Cell Biol*, 22: 6070-8.

Lewis, P. W., S. J. Elsaesser, K. M. Noh, S. C. Stadler, and C. D. Allis. 2010. 'Daxx is an H3.3-specific histone chaperone and cooperates with ATRX in replication-independent chromatin assembly at telomeres', *Proceedings of the National Academy of Sciences of the United States of America*, 107: 14075-80.

Li, M., C. L. Brooks, N. Kon, and W. Gu. 2004. 'A dynamic role of HAUSP in the p53-Mdm2 pathway', *Molecular cell*, 13: 879-86.

Liu, B., Y. F. Liu, Y. R. Du, A. N. Mardaryev, W. Yang, H. Chen, Z. M. Xu, C. Q. Xu, X. R. Zhang, V. A. Botchkarev, Y. Zhang, and G. L. Xu. 2013. 'Cbx4 regulates the proliferation of thymic epithelial cells and thymus function', *Development*, 140: 780-8.

Liu, Q., S. Guntuku, X. S. Cui, S. Matsuoka, D. Cortez, K. Tamai, G. Luo, S. Carattini-Rivera, F. DeMayo, A. Bradley, L. A. Donehower, and S. J. Elledge. 2000. 'Chk1 is an essential kinase that is regulated by Atr and required for the G(2)/M DNA damage checkpoint', *Genes & development*, 14: 1448-59.

Lorch, Y., J. W. LaPointe, and R. D. Kornberg. 1992. 'Initiation on chromatin templates in a yeast RNA polymerase II transcription system', *Genes & development*, 6: 2282-7.

Loughlin, F. E., R. E. Mansfield, P. M. Vaz, A. P. McGrath, S. Setiyaputra, R. Gamsjaeger, E. S. Chen, B. J. Morris, J. M. Guss, and J. P. Mackay. 2009. 'The zinc fingers of the SR-like protein ZRANB2 are single-stranded RNA-binding domains that recognize 5' splice site-like sequences', *Proceedings of the National Academy of Sciences of the United States of America*, 106: 5581-6.

Loyola, A., T. Bonaldi, D. Roche, A. Imhof, and G. Almouzni. 2006. 'PTMs on H3 variants before chromatin assembly potentiate their final epigenetic state', *Molecular cell*, 24: 309-16.

Luger, K., A. W. Mader, R. K. Richmond, D. F. Sargent, and T. J. Richmond. 1997. 'Crystal structure of the nucleosome core particle at 2.8 A resolution', *Nature*, 389: 251-60.

Lukas, C., J. Bartkova, L. Latella, J. Falck, N. Mailand, T. Schroeder, M. Sehested, J. Lukas, and J. Bartek. 2001. 'DNA damage-activated kinase Chk2 is independent of proliferation or differentiation yet correlates with tissue biology', *Cancer Res*, 61: 4990-3.

Lutzmann, M., and M. Mechali. 2008. 'MCM9 binds Cdt1 and is required for the assembly of prereplication complexes', *Molecular cell*, 31: 190-200.

Ma, X. J., J. Wu, B. A. Altheim, M. C. Schultz, and M. Grunstein. 1998. 'Deposition-related sites K5/K12 in histone H4 are not required for nucleosome deposition in yeast', *Proceedings of the National Academy of Sciences of the United States of America*, 95: 6693-8.

MacDougall, C. A., T. S. Byun, C. Van, M. C. Yee, and K. A. Cimprich. 2007. 'The structural determinants of checkpoint activation', *Genes & development*, 21: 898-903.

Maenner, S., M. Blaud, L. Fouillen, A. Savoye, V. Marchand, A. Dubois, S. Sanglier-Cianferani, A. Van Dorsselaer, P. Clerc, P. Avner, A. Visvikis, and C. Branlant. 2010. '2-D structure of the A region of Xist RNA and its implication for PRC2 association', *PLoS biology*, 8: e1000276.

Maertens, G. N., S. El Messaoudi-Aubert, S. Elderkin, K. Hiom, and G. Peters. 2010. 'Ubiquitin-specific proteases 7 and 11 modulate Polycomb regulation of the INK4a tumour suppressor', *The EMBO journal*, 29: 2553-65.

Mahaney, B. L., K. Meek, and S. P. Lees-Miller. 2009. 'Repair of ionizing radiation-induced DNA double-strand breaks by non-homologous end-joining', *Biochem J*, 417: 639-50.

Majka, J., A. Niedziela-Majka, and P. M. Burgers. 2006. 'The checkpoint clamp activates Mec1 kinase during initiation of the DNA damage checkpoint', *Molecular cell*, 24: 891-901.

Margueron, R., G. Li, K. Sarma, A. Blais, J. Zavadil, C. L. Woodcock, B. D. Dynlacht, and D. Reinberg. 2008. 'Ezh1 and Ezh2 maintain repressive chromatin through different mechanisms', *Molecular cell*, 32: 503-18.

Margueron, R., and D. Reinberg. 2011a. 'The Polycomb complex PRC2 and its mark in life', *Nature*, 469: 343-9.

Margueron, Raphael, and Danny Reinberg. 2011b. 'The Polycomb complex PRC2 and its mark in life', *Nature*, 469: 343-49.

Martin, C., N. Beaujean, V. Brochard, C. Audouard, D. Zink, and P. Debey. 2006. 'Genome restructuring in mouse embryos during reprogramming and early development', *Developmental biology*, 292: 317-32.

Martin, C., and Y. Zhang. 2005. 'The diverse functions of histone lysine methylation', *Nature reviews. Molecular cell biology*, 6: 838-49.

Marzluff, W. F., P. Gongidi, K. R. Woods, J. Jin, and L. J. Maltais. 2002. 'The human and mouse replication-dependent histone genes', *Genomics*, 80: 487-98.

Matsuoka, S., M. Huang, and S. J. Elledge. 1998. 'Linkage of ATM to cell cycle regulation by the Chk2 protein kinase', *Science*, 282: 1893-7.

Maya-Mendoza, A., E. Petermann, D. A. Gillespie, K. W. Caldecott, and D. A. Jackson. 2007. 'Chk1 regulates the density of active replication origins during the vertebrate S phase', *The EMBO journal*, 26: 2719-31.

McGinty, R. K., R. C. Henrici, and S. Tan. 2014. 'Crystal structure of the PRC1 ubiquitylation module bound to the nucleosome', *Nature*, 514: 591-6.

McIntosh, D., and J. J. Blow. 2012. 'Dormant origins, the licensing checkpoint, and the response to replicative stresses', *Cold Spring Harb Perspect Biol*, 4.

McMurray, C. T. 2010. 'Mechanisms of trinucleotide repeat instability during human development', *Nature reviews. Genetics*, 11: 786-99.

Mechali, M. 2010. 'Eukaryotic DNA replication origins: many choices for appropriate answers', *Nature reviews. Molecular cell biology*, 11: 728-38.

Mechali, M., K. Yoshida, P. Coulombe, and P. Pasero. 2013. 'Genetic and epigenetic determinants of DNA replication origins, position and activation', *Current opinion in genetics & development*, 23: 124-31.

Meek, K., V. Dang, and S. P. Lees-Miller. 2008. 'DNA-PK: the means to justify the ends?', *Adv Immunol*, 99: 33-58.

Mendenhall, E. M., R. P. Koche, T. Truong, V. W. Zhou, B. Issac, A. S. Chi, M. Ku, and B. E. Bernstein. 2010. 'GC-rich sequence elements recruit PRC2 in mammalian ES cells', *PLoS genetics*, 6: e1001244.

Meselson, M., and F. W. Stahl. 1958. 'The Replication of DNA in Escherichia Coli', *Proceedings of the National Academy of Sciences of the United States of America*, 44: 671-82.

Mikkelsen, T. S., M. Ku, D. B. Jaffe, B. Issac, E. Lieberman, G. Giannoukos, P. Alvarez, W. Brockman, T. K. Kim, R. P. Koche, W. Lee, E. Mendenhall, A. O'Donovan, A. Presser, C. Russ, X. Xie, A. Meissner, M.

Wernig, R. Jaenisch, C. Nusbaum, E. S. Lander, and B. E. Bernstein. 2007. 'Genome-wide maps of chromatin state in pluripotent and lineage-committed cells', *Nature*, 448: 553-60.

Moazed, D., and P. H. O'Farrell. 1992. 'Maintenance of the engrailed expression pattern by Polycomb group genes in Drosophila', *Development*, 116: 805-10.

Mochizuki, K., M. Tachibana, M. Saitou, Y. Tokitake, and Y. Matsui. 2012. 'Implication of DNA demethylation and bivalent histone modification for selective gene regulation in mouse primordial germ cells', *PloS one*, 7: e46036.

Molinari, M., C. Mercurio, J. Dominguez, F. Goubin, and G. F. Draetta. 2000. 'Human Cdc25 A inactivation in response to S phase inhibition and its role in preventing premature mitosis', *EMBO reports*, 1: 71-9.

Montellier, E., F. Boussouar, S. Rousseaux, K. Zhang, T. Buchou, F. Fenaille, H. Shiota, A. Debernardi, P. Hery, S. Curtet, M. Jamshidikia, S. Barral, H. Holota, A. Bergon, F. Lopez, P. Guardiola, K. Pernet, J. Imbert, C. Petosa, M. Tan, Y. Zhao, M. Gerard, and S. Khochbin. 2013. 'Chromatin-to-nucleoprotamine transition is controlled by the histone H2B variant TH2B', *Genes & development*, 27: 1680-92.

Montini, E., G. Buchner, C. Spalluto, G. Andolfi, A. Caruso, J. T. den Dunnen, D. Trump, M. Rocchi, A. Ballabio, and B. Franco. 1999. 'Identification of SCML2, a second human gene homologous to the Drosophila sex comb on midleg (Scm): A new gene cluster on Xp22', *Genomics*, 58: 65-72.

Morey, L., L. Aloia, L. Cozzuto, S. A. Benitah, and L. Di Croce. 2013. 'RYBP and Cbx7 define specific biological functions of polycomb complexes in mouse embryonic stem cells', *Cell reports*, 3: 60-9.

Morey, L., G. Pascual, L. Cozzuto, G. Roma, A. Wutz, S. A. Benitah, and L. Di Croce. 2012. 'Nonoverlapping functions of the Polycomb group Cbx family of proteins in embryonic stem cells', *Cell stem cell*, 10: 47-62.

Murzina, N., A. Verreault, E. Laue, and B. Stillman. 1999. 'Heterochromatin dynamics in mouse cells: interaction between chromatin assembly factor 1 and HP1 proteins', *Molecular cell*, 4: 529-40.

Nakatani, T., K. Yamagata, T. Kimura, M. Oda, H. Nakashima, M. Hori, Y. Sekita, T. Arakawa, T. Nakamura, and T. Nakano. 2015. 'Stella preserves maternal chromosome integrity by inhibiting 5hmC-induced gammaH2AX accumulation', *EMBO reports*, 16: 582-9.

Neira, J. L., M. Roman-Trufero, L. M. Contreras, J. Prieto, G. Singh, F. N. Barrera, M. L. Renart, and M. Vidal. 2009. 'The transcriptional repressor RYBP is a natively unfolded protein which folds upon binding to DNA', *Biochemistry*, 48: 1348-60.

Nekrasov, M., T. Klymenko, S. Fraterman, B. Papp, K. Oktaba, T. Kocher, A. Cohen, H. G. Stunnenberg, M. Wilm, and J. Muller. 2007. 'Pcl-PRC2 is needed to generate high levels of H3-K27 trimethylation at Polycomb target genes', *The EMBO journal*, 26: 4078-88.

Nekrasov, M., B. Wild, and J. Muller. 2005. 'Nucleosome binding and histone methyltransferase activity of Drosophila PRC2', *EMBO reports*, 6: 348-53.

Ng, J. H., V. Kumar, M. Muratani, P. Kraus, J. C. Yeo, L. P. Yaw, K. Xue, T. Lufkin, S. Prabhakar, and H. H. Ng. 2013. 'In vivo epigenomic profiling of germ cells reveals germ cell molecular signatures', *Developmental cell*, 24: 324-33.

Nguyen, C. D., R. E. Mansfield, W. Leung, P. M. Vaz, F. E. Loughlin, R. P. Grant, and J. P. Mackay. 2011. 'Characterization of a family of RanBP2-type zinc fingers that can recognize single-stranded RNA', *J Mol Biol*, 407: 273-83.

Nicetto, D., M. Hahn, J. Jung, T. D. Schneider, T. Straub, R. David, G. Schotta, and R. A. Rupp. 2013. 'Suv4-20h histone methyltransferases promote neuroectodermal differentiation by silencing the pluripotency-associated Oct-25 gene', *PLoS genetics*, 9: e1003188.

Nishioka, K., J. C. Rice, K. Sarma, H. Erdjument-Bromage, J. Werner, Y. Wang, S. Chuikov, P. Valenzuela, P. Tempst, R. Steward, J. T. Lis, C. D. Allis, and D. Reinberg. 2002. 'PR-Set7 is a nucleosome-specific

methyltransferase that modifies lysine 20 of histone H4 and is associated with silent chromatin', *Molecular cell*, 9: 1201-13.

Norio, P., S. Kosiyatrakul, Q. Yang, Z. Guan, N. M. Brown, S. Thomas, R. Riblet, and C. L. Schildkraut. 2005. 'Progressive activation of DNA replication initiation in large domains of the immunoglobulin heavy chain locus during B cell development', *Molecular cell*, 20: 575-87.

O'Carroll, D., S. Erhardt, M. Pagani, S. C. Barton, M. A. Surani, and T. Jenuwein. 2001. 'The polycomb-group gene Ezh2 is required for early mouse development', *Mol Cell Biol*, 21: 4330-6.

O'Connell, M. J., J. M. Raleigh, H. M. Verkade, and P. Nurse. 1997. 'Chk1 is a wee1 kinase in the G2 DNA damage checkpoint inhibiting cdc2 by Y15 phosphorylation', *The EMBO journal*, 16: 545-54.

O'Keefe, R. T., S. C. Henderson, and D. L. Spector. 1992. 'Dynamic organization of DNA replication in mammalian cell nuclei: spatially and temporally defined replication of chromosome-specific alpha-satellite DNA sequences', *J Cell Biol*, 116: 1095-110.

O'Loghlen, A., A. M. Munoz-Cabello, A. Gaspar-Maia, H. A. Wu, A. Banito, N. Kunowska, T. Racek, H. N. Pemberton, P. Beolchi, F. Lavial, O. Masui, M. Vermeulen, T. Carroll, J. Graumann, E. Heard, N. Dillon, V. Azuara, A. P. Snijders, G. Peters, E. Bernstein, and J. Gil. 2012. 'MicroRNA regulation of Cbx7 mediates a switch of Polycomb orthologs during ESC differentiation', *Cell stem cell*, 10: 33-46.

Oda, H., M. R. Hubner, D. B. Beck, M. Vermeulen, J. Hurwitz, D. L. Spector, and D. Reinberg. 2010. 'Regulation of the histone H4 monomethylase PR-Set7 by CRL4(Cdt2)-mediated PCNA-dependent degradation during DNA damage', *Molecular cell*, 40: 364-76.

Oda, H., I. Okamoto, N. Murphy, J. Chu, S. M. Price, M. M. Shen, M. E. Torres-Padilla, E. Heard, and D. Reinberg. 2009. 'Monomethylation of histone H4-lysine 20 is involved in chromosome structure and stability and is essential for mouse development', *Mol Cell Biol*, 29: 2278-95.

Olins, A. L., and D. E. Olins. 1974. 'Spheroid chromatin units (v bodies)', *Science*, 183: 330-2.

Oudet, P., M. Grossbellard, and P. Chambon. 1975. 'Electron-Microscopic and Biochemical Evidence That Chromatin Structure Is a Repeating Unit', *Cell*, 4: 281-300.

Ozeri-Galai, E., M. Schwartz, A. Rahat, and B. Kerem. 2008. 'Interplay between ATM and ATR in the regulation of common fragile site stability', *Oncogene*, 27: 2109-17.

Pacek, M., and J. C. Walter. 2004. 'A requirement for MCM7 and Cdc45 in chromosome unwinding during eukaryotic DNA replication', *The EMBO journal*, 23: 3667-76.

Pak, D. T., M. Pflumm, I. Chesnokov, D. W. Huang, R. Kellum, J. Marr, P. Romanowski, and M. R. Botchan. 1997. 'Association of the origin recognition complex with heterochromatin and HP1 in higher eukaryotes', *Cell*, 91: 311-23.

Pandey, R. R., T. Mondal, F. Mohammad, S. Enroth, L. Redrup, J. Komorowski, T. Nagano, D. Mancini-Dinardo, and C. Kanduri. 2008. 'Kcnq1ot1 antisense noncoding RNA mediates lineage-specific transcriptional silencing through chromatin-level regulation', *Molecular cell*, 32: 232-46.

Pasero, P., and S. M. Gasser. 2002. 'In vitro DNA replication assays in yeast extracts', *Methods Enzymol*, 351: 184-99.

Pasini, D., A. P. Bracken, J. B. Hansen, M. Capillo, and K. Helin. 2007. 'The polycomb group protein Suz12 is required for embryonic stem cell differentiation', *Mol Cell Biol*, 27: 3769-79.

Pasini, D., A. P. Bracken, M. R. Jensen, E. Lazzerini Denchi, and K. Helin. 2004. 'Suz12 is essential for mouse development and for EZH2 histone methyltransferase activity', *The EMBO journal*, 23: 4061-71.

Pasini, D., P. A. Cloos, J. Walfridsson, L. Olsson, J. P. Bukowski, J. V. Johansen, M. Bak, N. Tommerup, J. Rappsilber, and K. Helin. 2010. 'JARID2 regulates binding of the Polycomb repressive complex 2 to target genes in ES cells', *Nature*, 464: 306-10.

Passarge, E. 1979. 'Emil Heitz and the concept of heterochromatin: longitudinal chromosome differentiation was recognized fifty years ago', *Am J Hum Genet*, 31: 106-15.

Patterson, J. T., and H. J. Muller. 1930. 'Are "Progressive" Mutations Produced by X-Rays?', *Genetics*, 15: 495-577.

Pei, H., L. Zhang, K. Luo, Y. Qin, M. Chesi, F. Fei, P. L. Bergsagel, L. Wang, Z. You, and Z. Lou. 2011. 'MMSET regulates histone H4K20 methylation and 53BP1 accumulation at DNA damage sites', *Nature*, 470: 124-8.

Pelegri, F., and R. Lehmann. 1994. 'A role of polycomb group genes in the regulation of gap gene expression in Drosophila', *Genetics*, 136: 1341-53.

Peng, C. Y., P. R. Graves, R. S. Thoma, Z. Wu, A. S. Shaw, and H. Piwnica-Worms. 1997. 'Mitotic and G2 checkpoint control: regulation of 14-3-3 protein binding by phosphorylation of Cdc25C on serine-216', *Science*, 277: 1501-5.

Petermann, E., A. Maya-Mendoza, G. Zachos, D. A. Gillespie, D. A. Jackson, and K. W. Caldecott. 2006. 'Chk1 requirement for high global rates of replication fork progression during normal vertebrate S phase', *Mol Cell Biol*, 26: 3319-26.

Petermann, E., M. Woodcock, and T. Helleday. 2010. 'Chk1 promotes replication fork progression by controlling replication initiation', *Proceedings of the National Academy of Sciences of the United States of America*, 107: 16090-5.

Peters, A. H., D. O'Carroll, H. Scherthan, K. Mechtler, S. Sauer, C. Schofer, K. Weipoltshammer, M. Pagani, M. Lachner, A. Kohlmaier, S. Opravil, M. Doyle, M. Sibilia, and T. Jenuwein. 2001. 'Loss of the Suv39h histone methyltransferases impairs mammalian heterochromatin and genome stability', *Cell*, 107: 323-37.

Pirity, M. K., J. Locker, and N. Schreiber-Agus. 2005. 'Rybp/DEDAF is required for early postimplantation and for central nervous system development', *Mol Cell Biol*, 25: 7193-202.

Plath, K., J. Fang, S. K. Mlynarczyk-Evans, R. Cao, K. A. Worringer, H. Wang, C. C. de la Cruz, A. P. Otte, B. Panning, and Y. Zhang. 2003. 'Role of histone H3 lysine 27 methylation in X inactivation', *Science*, 300: 131-5.

Poli, J., O. Tsaponina, L. Crabbe, A. Keszthelyi, V. Pantesco, A. Chabes, A. Lengronne, and P. Pasero. 2012. 'dNTP pools determine fork progression and origin usage under replication stress', *The EMBO journal*, 31: 883-94.

Poot, R. A., L. Bozhenok, D. L. van den Berg, S. Steffensen, F. Ferreira, M. Grimaldi, N. Gilbert, J. Ferreira, and P. D. Varga-Weisz. 2004. 'The Williams syndrome transcription factor interacts with PCNA to target chromatin remodelling by ISWI to replication foci', *Nature cell biology*, 6: 1236-44.

Posfai, E., R. Kunzmann, V. Brochard, J. Salvaing, E. Cabuy, T. C. Roloff, Z. Liu, M. Tardat, M. van Lohuizen, M. Vidal, N. Beaujean, and A. H. Peters. 2012. 'Polycomb function during oogenesis is required for mouse embryonic development', *Genes & development*, 26: 920-32.

Probst, A. V., F. Santos, W. Reik, G. Almouzni, and W. Dean. 2007. 'Structural differences in centromeric heterochromatin are spatially reconciled on fertilisation in the mouse zygote', *Chromosoma*, 116: 403-15.

Puschendorf, M., R. Terranova, E. Boutsma, X. Mao, K. Isono, U. Brykczynska, C. Kolb, A. P. Otte, H. Koseki, S. H. Orkin, M. van Lohuizen, and A. H. Peters. 2008. 'PRC1 and Suv39h specify parental asymmetry at constitutive heterochromatin in early mouse embryos', *Nature genetics*, 40: 411-20.

Qin, J., W. A. Whyte, E. Anderssen, E. Apostolou, H. H. Chen, S. Akbarian, R. T. Bronson, K. Hochedlinger, S. Ramaswamy, R. A. Young, and H. Hock. 2012. 'The polycomb group protein L3mbtl2 assembles an atypical PRC1-family complex that is essential in pluripotent stem cells and early development', *Cell stem cell*, 11: 319-32.

Rajasekhar, V. K., and M. Begemann. 2007. 'Concise review: roles of polycomb group proteins in development and disease: a stem cell perspective', *Stem cells*, 25: 2498-510.

Rea, S., F. Eisenhaber, D. O'Carroll, B. D. Strahl, Z. W. Sun, M. Schmid, S. Opravil, K. Mechtler, C. P. Ponting, C. D. Allis, and T. Jenuwein. 2000. 'Regulation of chromatin structure by site-specific histone H3 methyltransferases', *Nature*, 406: 593-9.

Remus, D., F. Beuron, G. Tolun, J. D. Griffith, E. P. Morris, and J. F. Diffley. 2009. 'Concerted loading of Mcm2-7 double hexamers around DNA during DNA replication origin licensing', *Cell*, 139: 719-30.

Rice, J. C., K. Nishioka, K. Sarma, R. Steward, D. Reinberg, and C. D. Allis. 2002. 'Mitotic-specific methylation of histone H4 Lys 20 follows increased PR-Set7 expression and its localization to mitotic chromosomes', *Genes & development*, 16: 2225-30.

Riising, E. M., I. Comet, B. Leblanc, X. Wu, J. V. Johansen, and K. Helin. 2014. 'Gene silencing triggers polycomb repressive complex 2 recruitment to CpG islands genome wide', *Molecular cell*, 55: 347-60.

Rinn, J. L., M. Kertesz, J. K. Wang, S. L. Squazzo, X. Xu, S. A. Brugmann, L. H. Goodnough, J. A. Helms, P. J. Farnham, E. Segal, and H. Y. Chang. 2007. 'Functional demarcation of active and silent chromatin domains in human HOX loci by noncoding RNAs', *Cell*, 129: 1311-23.

Roberts, S. A., N. Strande, M. D. Burkhalter, C. Strom, J. M. Havener, P. Hasty, and D. A. Ramsden. 2010. 'Ku is a 5'-dRP/AP lyase that excises nucleotide damage near broken ends', *Nature*, 464: 1214-7.

Rugg-Gunn, P. J., B. J. Cox, A. Ralston, and J. Rossant. 2010. 'Distinct histone modifications in stem cell lines and tissue lineages from the early mouse embryo', *Proceedings of the National Academy of Sciences of the United States of America*, 107: 10783-90.

Sakaue, M., H. Ohta, Y. Kumaki, M. Oda, Y. Sakaide, C. Matsuoka, A. Yamagiwa, H. Niwa, T. Wakayama, and M. Okano. 2010. 'DNA methylation is dispensable for the growth and survival of the extraembryonic lineages', *Current biology : CB*, 20: 1452-7.

Sanchez, C., I. Sanchez, J. A. Demmers, P. Rodriguez, J. Strouboulis, and M. Vidal. 2007. 'Proteomics analysis of Ring1B/Rnf2 interactors identifies a novel complex with the Fbxl10/Jhdm1B histone demethylase and the Bcl6 interacting corepressor', *Mol Cell Proteomics*, 6: 820-34.

Sanchez, Y., C. Wong, R. S. Thoma, R. Richman, Z. Wu, H. Piwnica-Worms, and S. J. Elledge. 1997. 'Conservation of the Chk1 checkpoint pathway in mammals: linkage of DNA damage to Cdk regulation through Cdc25', *Science*, 277: 1497-501.

Sanders, S. L., M. Portoso, J. Mata, J. Bahler, R. C. Allshire, and T. Kouzarides. 2004. 'Methylation of histone H4 lysine 20 controls recruitment of Crb2 to sites of DNA damage', *Cell*, 119: 603-14.

Santenard, A., C. Ziegler-Birling, M. Koch, L. Tora, A. J. Bannister, and M. E. Torres-Padilla. 2010. 'Heterochromatin formation in the mouse embryo requires critical residues of the histone variant H3.3', *Nature cell biology*, 12: 853-62.

Santos, F., A. H. Peters, A. P. Otte, W. Reik, and W. Dean. 2005. 'Dynamic chromatin modifications characterise the first cell cycle in mouse embryos', *Developmental biology*, 280: 225-36.

Sasaki, T., S. Ramanathan, Y. Okuno, C. Kumagai, S. S. Shaikh, and D. M. Gilbert. 2006. 'The Chinese hamster dihydrofolate reductase replication origin decision point follows activation of transcription and suppresses initiation of replication within transcription units', *Mol Cell Biol*, 26: 1051-62.

Saurin, A. J., C. Shiels, J. Williamson, D. P. Satijn, A. P. Otte, D. Sheer, and P. S. Freemont. 1998. 'The human polycomb group complex associates with pericentromeric heterochromatin to form a novel nuclear domain', *J Cell Biol*, 142: 887-98.

Savitsky, K., A. Bar-Shira, S. Gilad, G. Rotman, Y. Ziv, L. Vanagaite, D. A. Tagle, S. Smith, T. Uziel, S. Sfez, M. Ashkenazi, I. Pecker, M. Frydman, R. Harnik, S. R. Patanjali, A. Simmons, G. A. Clines, A. Sartiel, R. A. Gatti, L. Chessa, O. Sanal, M. F. Lavin, N. G. Jaspers, A. M. Taylor, C. F. Arlett, T. Miki, S. M. Weissman, M. Lovett, F. S. Collins, and Y. Shiloh. 1995. 'A single ataxia telangiectasia gene with a product similar to PI-3 kinase', *Science*, 268: 1749-53.

Schmitges, F. W., A. B. Prusty, M. Faty, A. Stutzer, G. M. Lingaraju, J. Aiwazian, R. Sack, D. Hess, L. Li, S. Zhou, R. D. Bunker, U. Wirth, T. Bouwmeester, A. Bauer, N. Ly-Hartig, K. Zhao, H. Chan, J. Gu, H.

Gut, W. Fischle, J. Muller, and N. H. Thoma. 2011. 'Histone methylation by PRC2 is inhibited by active chromatin marks', *Molecular cell*, 42: 330-41.

Schmitt, E., R. Boutros, C. Froment, B. Monsarrat, B. Ducommun, and C. Dozier. 2006. 'CHK1 phosphorylates CDC25B during the cell cycle in the absence of DNA damage', *J Cell Sci*, 119: 4269-75.

Schneider, A. C., L. C. Heukamp, S. Rogenhofer, G. Fechner, P. J. Bastian, A. von Ruecker, S. C. Muller, and J. Ellinger. 2011. 'Global histone H4K20 trimethylation predicts cancer-specific survival in patients with muscle-invasive bladder cancer', *BJU Int*, 108: E290-6.

Schoeftner, S., A. K. Sengupta, S. Kubicek, K. Mechtler, L. Spahn, H. Koseki, T. Jenuwein, and A. Wutz. 2006. 'Recruitment of PRC1 function at the initiation of X inactivation independent of PRC2 and silencing', *The EMBO journal*, 25: 3110-22.

Schotta, G., M. Lachner, K. Sarma, A. Ebert, R. Sengupta, G. Reuter, D. Reinberg, and T. Jenuwein. 2004. 'A silencing pathway to induce H3-K9 and H4-K20 trimethylation at constitutive heterochromatin', *Genes & development*, 18: 1251-62.

Schotta, G., R. Sengupta, S. Kubicek, S. Malin, M. Kauer, E. Callen, A. Celeste, M. Pagani, S. Opravil, I. A. De La Rosa-Velazquez, A. Espejo, M. T. Bedford, A. Nussenzweig, M. Busslinger, and T. Jenuwein. 2008. 'A chromatin-wide transition to H4K20 monomethylation impairs genome integrity and programmed DNA rearrangements in the mouse', *Genes & development*, 22: 2048-61.

Schuettengruber, B., M. Ganapathi, B. Leblanc, M. Portoso, R. Jaschek, B. Tolhuis, M. van Lohuizen, A. Tanay, and G. Cavalli. 2009. 'Functional anatomy of polycomb and trithorax chromatin landscapes in Drosophila embryos', *PLoS biology*, 7: e13.

Schuettengruber, B., N. Oded Elkayam, T. Sexton, M. Entrevan, S. Stern, A. Thomas, E. Yaffe, H. Parrinello, A. Tanay, and G. Cavalli. 2014. 'Cooperativity, specificity, and evolutionary stability of Polycomb targeting in Drosophila', *Cell reports*, 9: 219-33.

Schwartz, Y. B., and V. Pirrotta. 2007. 'Polycomb silencing mechanisms and the management of genomic programmes', *Nature reviews. Genetics*, 8: 9-22.

———. 2013. 'A new world of Polycombs: unexpected partnerships and emerging functions', *Nature reviews. Genetics*, 14: 853-64.

Seki, Y., M. Yamaji, Y. Yabuta, M. Sano, M. Shigeta, Y. Matsui, Y. Saga, M. Tachibana, Y. Shinkai, and M. Saitou. 2007. 'Cellular dynamics associated with the genome-wide epigenetic reprogramming in migrating primordial germ cells in mice', *Development*, 134: 2627-38.

Sequeira-Mendes, J., R. Diaz-Uriarte, A. Apedaile, D. Huntley, N. Brockdorff, and M. Gomez. 2009. 'Transcription initiation activity sets replication origin efficiency in mammalian cells', *PLoS genetics*, 5: e1000446.

Shao, Z., F. Raible, R. Mollaaghababa, J. R. Guyon, C. T. Wu, W. Bender, and R. E. Kingston. 1999. 'Stabilization of chromatin structure by PRC1, a Polycomb complex', *Cell*, 98: 37-46.

Shen, X., W. Kim, Y. Fujiwara, M. D. Simon, Y. Liu, M. R. Mysliwiec, G. C. Yuan, Y. Lee, and S. H. Orkin. 2009. 'Jumonji modulates polycomb activity and self-renewal versus differentiation of stem cells', *Cell*, 139: 1303-14.

Shen, X., Y. Liu, Y. J. Hsu, Y. Fujiwara, J. Kim, X. Mao, G. C. Yuan, and S. H. Orkin. 2008. 'EZH1 mediates methylation on histone H3 lysine 27 and complements EZH2 in maintaining stem cell identity and executing pluripotency', *Molecular cell*, 32: 491-502.

Shen, Z., K. M. Sathyan, Y. Geng, R. Zheng, A. Chakraborty, B. Freeman, F. Wang, K. V. Prasanth, and S. G. Prasanth. 2010. 'A WD-repeat protein stabilizes ORC binding to chromatin', *Molecular cell*, 40: 99-111.

Shibahara, K., and B. Stillman. 1999. 'Replication-dependent marking of DNA by PCNA facilitates CAF-1-coupled inheritance of chromatin', *Cell*, 96: 575-85.

Shrivastav, M., L. P. De Haro, and J. A. Nickoloff. 2008. 'Regulation of DNA double-strand break repair pathway choice', *Cell research*, 18: 134-47.

Sidoli, S., V. Schwammle, C. Ruminowicz, T. A. Hansen, X. Wu, K. Helin, and O. N. Jensen. 2014. 'Middle-down hybrid chromatography/tandem mass spectrometry workflow for characterization of combinatorial post-translational modifications in histones', *Proteomics*, 14: 2200-11.

Simon, J. A., and R. E. Kingston. 2009. 'Mechanisms of polycomb gene silencing: knowns and unknowns', *Nature reviews. Molecular cell biology*, 10: 697-708.

Simon, J., A. Chiang, W. Bender, M. J. Shimell, and M. O'Connor. 1993. 'Elements of the Drosophila bithorax complex that mediate repression by Polycomb group products', *Developmental biology*, 158: 131-44.

Sims, J. K., S. I. Houston, T. Magazinnik, and J. C. Rice. 2006. 'A trans-tail histone code defined by monomethylated H4 Lys-20 and H3 Lys-9 demarcates distinct regions of silent chromatin', *J Biol Chem*, 281: 12760-6.

Sing, A., D. Pannell, A. Karaiskakis, K. Sturgeon, M. Djabali, J. Ellis, H. D. Lipshitz, and S. P. Cordes. 2009. 'A vertebrate Polycomb response element governs segmentation of the posterior hindbrain', *Cell*, 138: 885-97.

Sirbu, B. M., F. B. Couch, J. T. Feigerle, S. Bhaskara, S. W. Hiebert, and D. Cortez. 2011. 'Analysis of protein dynamics at active, stalled, and collapsed replication forks', *Genes & development*, 25: 1320-7.

Smits, V. A., P. M. Reaper, and S. P. Jackson. 2006. 'Rapid PIKK-dependent release of Chk1 from chromatin promotes the DNA-damage checkpoint response', *Current biology : CB*, 16: 150-9.

Sobel, R. E., R. G. Cook, C. A. Perry, A. T. Annunziato, and C. D. Allis. 1995. 'Conservation of deposition-related acetylation sites in newly synthesized histones H3 and H4', *Proceedings of the National Academy of Sciences of the United States of America*, 92: 1237-41.

Sogo, J. M., M. Lopes, and M. Foiani. 2002. 'Fork reversal and ssDNA accumulation at stalled replication forks owing to checkpoint defects', *Science*, 297: 599-602.

Sogo, J. M., H. Stahl, T. Koller, and R. Knippers. 1986. 'Structure of replicating simian virus 40 minichromosomes. The replication fork, core histone segregation and terminal structures', *J Mol Biol*, 189: 189-204.

Sorensen, C. S., R. G. Syljuasen, J. Falck, T. Schroeder, L. Ronnstrand, K. K. Khanna, B. B. Zhou, J. Bartek, and J. Lukas. 2003. 'Chk1 regulates the S phase checkpoint by coupling the physiological turnover and ionizing radiation-induced accelerated proteolysis of Cdc25A', *Cancer Cell*, 3: 247-58.

Southall, S. M., N. B. Cronin, and J. R. Wilson. 2014. 'A novel route to product specificity in the Suv4-20 family of histone H4K20 methyltransferases', *Nucleic acids research*, 42: 661-71.

Stender, J. D., G. Pascual, W. Liu, M. U. Kaikkonen, K. Do, N. J. Spann, M. Boutros, N. Perrimon, M. G. Rosenfeld, and C. K. Glass. 2012. 'Control of proinflammatory gene programs by regulated trimethylation and demethylation of histone H4K20', *Molecular cell*, 48: 28-38.

Stielow, C., B. Stielow, F. Finkernagel, M. Scharfe, M. Jarek, and G. Suske. 2014. 'SUMOylation of the polycomb group protein L3MBTL2 facilitates repression of its target genes', *Nucleic acids research*, 42: 3044-58.

Stokes, M. P., R. Van Hatten, H. D. Lindsay, and W. M. Michael. 2002. 'DNA replication is required for the checkpoint response to damaged DNA in Xenopus egg extracts', *J Cell Biol*, 158: 863-72.

Strahl, B. D., and C. D. Allis. 2000. 'The language of covalent histone modifications', *Nature*, 403: 41-5.

Su, I. H., A. Basavaraj, A. N. Krutchinsky, O. Hobert, A. Ullrich, B. T. Chait, and A. Tarakhovsky. 2003. 'Ezh2 controls B cell development through histone H3 methylation and Igh rearrangement', *Nat Immunol*, 4: 124-31.

Surani, M. A., K. Hayashi, and P. Hajkova. 2007. 'Genetic and epigenetic regulators of pluripotency', *Cell*, 128: 747-62.

Szilard, R. K., P. E. Jacques, L. Laramee, B. Cheng, S. Galicia, A. R. Bataille, M. Yeung, M. Mendez, M. Bergeron, F. Robert, and D. Durocher. 2010. 'Systematic identification of fragile sites via genome-wide location analysis of gamma-H2AX', *Nature structural & molecular biology*, 17: 299-305.

Tagami, H., D. Ray-Gallet, G. Almouzni, and Y. Nakatani. 2004. 'Histone H3.1 and H3.3 complexes mediate nucleosome assembly pathways dependent or independent of DNA synthesis', *Cell*, 116: 51-61.

Takai, H., K. Naka, Y. Okada, M. Watanabe, N. Harada, S. Saito, C. W. Anderson, E. Appella, M. Nakanishi, H. Suzuki, K. Nagashima, H. Sawa, K. Ikeda, and N. Motoyama. 2002. 'Chk2-deficient mice exhibit radioresistance and defective p53-mediated transcription', *The EMBO journal*, 21: 5195-205.

Takebayashi, S. I., E. M. Manders, H. Kimura, H. Taguchi, and K. Okumura. 2001. 'Mapping sites where replication initiates in mammalian cells using DNA fibers', *Exp Cell Res*, 271: 263-8.

Takeuchi, T., Y. Yamazaki, Y. Katoh-Fukui, R. Tsuchiya, S. Kondo, J. Motoyama, and T. Higashinakagawa. 1995. 'Gene trap capture of a novel mouse gene, jumonji, required for neural tube formation', *Genes & development*, 9: 1211-22.

Tan, B. C., C. T. Chien, S. Hirose, and S. C. Lee. 2006. 'Functional cooperation between FACT and MCM helicase facilitates initiation of chromatin DNA replication', *The EMBO journal*, 25: 3975-85.

Tardat, M., M. Albert, R. Kunzmann, Z. Liu, L. Kaustov, R. Thierry, S. Duan, U. Brykczynska, C. H. Arrowsmith, and A. H. Peters. 2015. 'Cbx2 targets PRC1 to constitutive heterochromatin in mouse zygotes in a parent-of-origin-dependent manner', *Molecular cell*, 58: 157-71.

Tardat, M., J. Brustel, O. Kirsh, C. Lefevbre, M. Callanan, C. Sardet, and E. Julien. 2010. 'The histone H4 Lys 20 methyltransferase PR-Set7 regulates replication origins in mammalian cells', *Nature cell biology*, 12: 1086-93.

Tardat, M., R. Murr, Z. Herceg, C. Sardet, and E. Julien. 2007. 'PR-Set7-dependent lysine methylation ensures genome replication and stability through S phase', *J Cell Biol*, 179: 1413-26.

Tartof, K. D., C. Hobbs, and M. Jones. 1984. 'A structural basis for variegating position effects', *Cell*, 37: 869-78.

Tavares, L., E. Dimitrova, D. Oxley, J. Webster, R. Poot, J. Demmers, K. Bezstarosti, S. Taylor, H. Ura, H. Koide, A. Wutz, M. Vidal, S. Elderkin, and N. Brockdorff. 2012. 'RYBP-PRC1 complexes mediate H2A ubiquitylation at polycomb target sites independently of PRC2 and H3K27me3', *Cell*, 148: 664-78.

Taylor, J. H. 1959. 'Autoradiographic Studies of Nucleic Acids and Proteins During Meiosis in Lilium Longiflorum', *American Journal of Botany*, 46: 477-84.

———. 1977. 'Increase in DNA replication sites in cells held at the beginning of S phase', *Chromosoma*, 62: 291-300.

Taylor, J. H., P. S. Woods, and W. L. Hughes. 1957. 'The Organization and Duplication of Chromosomes as Revealed by Autoradiographic Studies Using Tritium-Labeled Thymidinee', *Proceedings of the National Academy of Sciences of the United States of America*, 43: 122-8.

Tie, F., C. A. Stratton, R. L. Kurzhals, and P. J. Harte. 2007. 'The N terminus of Drosophila ESC binds directly to histone H3 and is required for E(Z)-dependent trimethylation of H3 lysine 27', *Mol Cell Biol*, 27: 2014-26.

Tomizawa, J., and G. Selzer. 1979. 'Initiation of DNA synthesis in Escherichia coli', *Annu Rev Biochem*, 48: 999-1034.

Torres-Padilla, M. E., A. J. Bannister, P. J. Hurd, T. Kouzarides, and M. Zernicka-Goetz. 2006. 'Dynamic distribution of the replacement histone variant H3.3 in the mouse oocyte and preimplantation embryos', *Int J Dev Biol*, 50: 455-61.

Trenz, K., A. Errico, and V. Costanzo. 2008. 'Plx1 is required for chromosomal DNA replication under stressful conditions', *The EMBO journal*, 27: 876-85.

Trojer, P., A. R. Cao, Z. Gao, Y. Li, J. Zhang, X. Xu, G. Li, R. Losson, H. Erdjument-Bromage, P. Tempst, P. J. Farnham, and D. Reinberg. 2011. 'L3MBTL2 protein acts in concert with PcG protein-mediated

monoubiquitination of H2A to establish a repressive chromatin structure', *Molecular cell*, 42: 438-50.

Trojer, P., G. Li, R. J. Sims, 3rd, A. Vaquero, N. Kalakonda, P. Boccuni, D. Lee, H. Erdjument-Bromage, P. Tempst, S. D. Nimer, Y. H. Wang, and D. Reinberg. 2007. 'L3MBTL1, a histone-methylation-dependent chromatin lock', *Cell*, 129: 915-28.

Trujillo, K. M., and M. A. Osley. 2012. 'A role for H2B ubiquitylation in DNA replication', *Molecular cell*, 48: 734-46.

Tsai, M. C., O. Manor, Y. Wan, N. Mosammaparast, J. K. Wang, F. Lan, Y. Shi, E. Segal, and H. Y. Chang. 2010. 'Long noncoding RNA as modular scaffold of histone modification complexes', *Science*, 329: 689-93.

Tschiersch, B., A. Hofmann, V. Krauss, R. Dorn, G. Korge, and G. Reuter. 1994. 'The protein encoded by the Drosophila position-effect variegation suppressor gene Su(var)3-9 combines domains of antagonistic regulators of homeotic gene complexes', *The EMBO journal*, 13: 3822-31.

Valk-Lingbeek, M. E., S. W. Bruggeman, and M. van Lohuizen. 2004. 'Stem cells and cancer; the polycomb connection', *Cell*, 118: 409-18.

Vandamme, J., P. Volkel, C. Rosnoblet, P. Le Faou, and P. O. Angrand. 2011. 'Interaction proteomics analysis of polycomb proteins defines distinct PRC1 complexes in mammalian cells', *Mol Cell Proteomics*, 10: M110 002642.

Varambally, S., S. M. Dhanasekaran, M. Zhou, T. R. Barrette, C. Kumar-Sinha, M. G. Sanda, D. Ghosh, K. J. Pienta, R. G. Sewalt, A. P. Otte, M. A. Rubin, and A. M. Chinnaiyan. 2002. 'The polycomb group protein EZH2 is involved in progression of prostate cancer', *Nature*, 419: 624-9.

Vastenhouw, N. L., Y. Zhang, I. G. Woods, F. Imam, A. Regev, X. S. Liu, J. Rinn, and A. F. Schier. 2010. 'Chromatin signature of embryonic pluripotency is established during genome activation', *Nature*, 464: 922-6.

Vermeulen, M., H. C. Eberl, F. Matarese, H. Marks, S. Denissov, F. Butter, K. K. Lee, J. V. Olsen, A. A. Hyman, H. G. Stunnenberg, and M. Mann. 2010. 'Quantitative interaction proteomics and genome-wide profiling of epigenetic histone marks and their readers', *Cell*, 142: 967-80.

Voigt, P., G. LeRoy, W. J. Drury, 3rd, B. M. Zee, J. Son, D. B. Beck, N. L. Young, B. A. Garcia, and D. Reinberg. 2012. 'Asymmetrically modified nucleosomes', *Cell*, 151: 181-93.

Voncken, J. W., B. A. Roelen, M. Roefs, S. de Vries, E. Verhoeven, S. Marino, J. Deschamps, and M. van Lohuizen. 2003. 'Rnf2 (Ring1b) deficiency causes gastrulation arrest and cell cycle inhibition', *Proceedings of the National Academy of Sciences of the United States of America*, 100: 2468-73.

Wachter, E., T. Quante, C. Merusi, A. Arczewska, F. Stewart, S. Webb, and A. Bird. 2014. 'Synthetic CpG islands reveal DNA sequence determinants of chromatin structure', *eLife*, 3: e03397.

Wang, L., J. L. Brown, R. Cao, Y. Zhang, J. A. Kassis, and R. S. Jones. 2004. 'Hierarchical recruitment of polycomb group silencing complexes', *Molecular cell*, 14: 637-46.

Wang, R., A. B. Taylor, B. Z. Leal, L. V. Chadwell, U. Ilangovan, A. K. Robinson, V. Schirf, P. J. Hart, E. M. Lafer, B. Demeler, A. P. Hinck, D. G. McEwen, and C. A. Kim. 2010. 'Polycomb group targeting through different binding partners of RING1B C-terminal domain', *Structure*, 18: 966-75.

Ward, I. M., and J. Chen. 2001. 'Histone H2AX is phosphorylated in an ATR-dependent manner in response to replicational stress', *J Biol Chem*, 276: 47759-62.

Weintraub, H., and M. Groudine. 1976. 'Chromosomal subunits in active genes have an altered conformation', *Science*, 193: 848-56.

Wilkinson, F., H. Pratt, and M. L. Atchison. 2010. 'PcG recruitment by the YY1 REPO domain can be mediated by Yaf2', *J Cell Biochem*, 109: 478-86.

Williams, R. S., J. S. Williams, and J. A. Tainer. 2007. 'Mre11-Rad50-Nbs1 is a keystone complex connecting DNA repair machinery, double-strand break signaling, and the chromatin template', *Biochem Cell Biol*, 85: 509-20.

Wilsker, D., E. Petermann, T. Helleday, and F. Bunz. 2008. 'Essential function of Chk1 can be uncoupled from DNA damage checkpoint and replication control', *Proceedings of the National Academy of Sciences of the United States of America*, 105: 20752-7.

Wismar, J., T. Loffler, N. Habtemichael, O. Vef, M. Geissen, R. Zirwes, W. Altmeyer, H. Sass, and E. Gateff. 1995. 'The Drosophila melanogaster tumor suppressor gene lethal(3)malignant brain tumor encodes a proline-rich protein with a novel zinc finger', *Mechanisms of development*, 53: 141-54.

Wongtawan, T., J. E. Taylor, K. A. Lawson, I. Wilmut, and S. Pennings. 2011. 'Histone H4K20me3 and HP1alpha are late heterochromatin markers in development, but present in undifferentiated embryonic stem cells', *Journal of Cell Science*, 124: 1878-90.

Woo, C. J., P. V. Kharchenko, L. Daheron, P. J. Park, and R. E. Kingston. 2010. 'A region of the human HOXD cluster that confers polycomb-group responsiveness', *Cell*, 140: 99-110.

Woodcock, C. L. F., L. L. Y. Frado, and J. B. Rattner. 1984. 'The Higher-Order Structure of Chromatin - Evidence for a Helical Ribbon Arrangement', *Journal of Cell Biology*, 99: 42-52.

Woodward, A. M., T. Gohler, M. G. Luciani, M. Oehlmann, X. Ge, A. Gartner, D. A. Jackson, and J. J. Blow. 2006. 'Excess Mcm2-7 license dormant origins of replication that can be used under conditions of replicative stress', *J Cell Biol*, 173: 673-83.

Wu, X., J. V. Johansen, and K. Helin. 2013. 'Fbxl10/Kdm2b recruits polycomb repressive complex 1 to CpG islands and regulates H2A ubiquitylation', *Molecular cell*, 49: 1134-46.

Wyrick, J. J., F. C. Holstege, E. G. Jennings, H. C. Causton, D. Shore, M. Grunstein, E. S. Lander, and R. A. Young. 1999. 'Chromosomal landscape of nucleosome-dependent gene expression and silencing in yeast', *Nature*, 402: 418-21.

Xi, H., Y. Yu, Y. Fu, J. Foley, A. Halees, and Z. Weng. 2007. 'Analysis of overrepresented motifs in human core promoters reveals dual regulatory roles of YY1', *Genome Res*, 17: 798-806.

Xu, J., J. A. Watts, S. D. Pope, P. Gadue, M. Kamps, K. Plath, K. S. Zaret, and S. T. Smale. 2009. 'Transcriptional competence and the active marking of tissue-specific enhancers by defined transcription factors in embryonic and induced pluripotent stem cells', *Genes & development*, 23: 2824-38.

Yap, K. L., S. Li, A. M. Munoz-Cabello, S. Raguz, L. Zeng, S. Mujtaba, J. Gil, M. J. Walsh, and M. M. Zhou. 2010. 'Molecular interplay of the noncoding RNA ANRIL and methylated histone H3 lysine 27 by polycomb CBX7 in transcriptional silencing of INK4a', *Molecular cell*, 38: 662-74.

Yokoyama, Y., A. Matsumoto, M. Hieda, Y. Shinchi, E. Ogihara, M. Hamada, Y. Nishioka, H. Kimura, K. Yoshidome, M. Tsujimoto, and N. Matsuura. 2014. 'Loss of histone H4K20 trimethylation predicts poor prognosis in breast cancer and is associated with invasive activity', *Breast Cancer Res*, 16: R66.

Yoo, H. Y., A. Kumagai, A. Shevchenko, A. Shevchenko, and W. G. Dunphy. 2004. 'Adaptation of a DNA replication checkpoint response depends upon inactivation of Claspin by the Polo-like kinase', *Cell*, 117: 575-88.

Yuan, W., M. Xu, C. Huang, N. Liu, S. Chen, and B. Zhu. 2011. 'H3K36 methylation antagonizes PRC2-mediated H3K27 methylation', *J Biol Chem*, 286: 7983-9.

Zeman, M. K., and K. A. Cimprich. 2014. 'Causes and consequences of replication stress', *Nature cell biology*, 16: 2-9.

Zhang, Y. W., D. M. Otterness, G. G. Chiang, W. Xie, Y. C. Liu, F. Mercurio, and R. T. Abraham. 2005. 'Genotoxic stress targets human Chk1 for degradation by the ubiquitin-proteasome pathway', *Molecular cell*, 19: 607-18.

Zhao, H., and H. Piwnica-Worms. 2001. 'ATR-mediated checkpoint pathways regulate phosphorylation and activation of human Chk1', *Mol Cell Biol*, 21: 4129-39.

Zhao, H., J. L. Watkins, and H. Piwnica-Worms. 2002. 'Disruption of the checkpoint kinase 1/cell division cycle 25A pathway abrogates ionizing radiation-induced S and G2 checkpoints', *Proceedings of the National Academy of Sciences of the United States of America*, 99: 14795-800.

Zhao, J., T. K. Ohsumi, J. T. Kung, Y. Ogawa, D. J. Grau, K. Sarma, J. J. Song, R. E. Kingston, M. Borowsky, and J. T. Lee. 2010. 'Genome-wide identification of polycomb-associated RNAs by RIP-seq', *Molecular cell*, 40: 939-53.

Zhao, J., B. K. Sun, J. A. Erwin, J. J. Song, and J. T. Lee. 2008. 'Polycomb proteins targeted by a short repeat RNA to the mouse X chromosome', *Science*, 322: 750-6.

Ziegler-Birling, C., A. Helmrich, L. Tora, and M. E. Torres-Padilla. 2009. 'Distribution of p53 binding protein 1 (53BP1) and phosphorylated H2A.X during mouse preimplantation development in the absence of DNA damage', *Int J Dev Biol*, 53: 1003-11.

Zou, L., and S. J. Elledge. 2003. 'Sensing DNA damage through ATRIP recognition of RPA-ssDNA complexes', *Science*, 300: 1542-8.

André EID

# Mechanisms of cell fate and chromatin plasticity during early mouse embryogenesis


## Résumé

La chromatine embryonnaire subit des changements nécessaires pour l'établissement d'un nouveau programme développemental. Ce travail a étudié l'organisation de l'hétérochromatine au cours du développement sous trois facettes. La première étant celle de d'hétérochromatine constitutive, à travers, l'établissement forcé de la marque H4K20me3 qui provoque un arrêt du développement préimplantatoire. Ce phénotype dépend spécifiquement de l'activité de la methyltransferase SUV4-20h2 et induit l'activation de la voie de signalisation ATR qui bloque la phase de réplication. En deuxième partie, l'hétérochromatine facultative a été le sujet d'une analyse de l'expression des protéines du complexe non-canonique PRC1 et de la modification H2AK119ub qui en résulte. Finalement, une analyse de la chromatine embryonnaire a été mise en place et a permis la détection des changements de niveau de compaction au cours du développement préimplantatoire.


Mots clés : hétérochromatine facultative et constitutive, développement préimplantatoire, ATR, réplication, compaction.


## Résumé en anglais

Embryonic chromatin undergoes necessary changes to establish a new developmental program. This work has addressed the organization of heterochromatin in preimplantation embryos from three angles. The first part probed the absence of constitutive heterochromatin by forcing the establishment of the H4K20me3 mark which results in an embryonic arrest prior to the 2-cell stage. This phenotype is due to the specific histone methyl-transferase activity of SUV4-20h2 and is induced by ATR activation which blocks replication. In the second part, facultative heterochromatin was studied by analyzing the levels of several members of the non-canonical PRC1 complex as well as the resultant modification H2AK119ub. Finally, an analysis of the embryonic chromatin was set up and allowed for the measurement of changes in the chromatin openness during preimplantation development.


Key words: Facultative and constitutive heterochromatin, preimplantation development, ATR, replication, compaction.